

Aerobic Ruthenium-Catalyzed C–H Activations

Dissertation

for the award of the degree

“Doctor rerum naturalium”

of the Georg-August-Universität Göttingen

within the doctoral program of chemistry

of the Georg-August University School of Science (GAUSS)

Submitted by

Alexander Bechtoldt

From Frankfurt am Main, Germany



Göttingen, 2018

Thesis Committee

Prof. Dr. Lutz Ackermann, Institute of Organic and Biomolecular Chemistry

Prof. Dr. Konrad Koszinowski, Institute of Organic and Biomolecular Chemistry

Members of the Examination Board

Reviewer: Prof. Dr. Lutz Ackermann, Institute of Organic and Biomolecular Chemistry

Second Reviewer: Prof. Dr. Konrad Koszinowski, Institute of Organic and Biomolecular Chemistry

Further Members of the Examination Board

Prof. Dr. Dietmar Stalke, Institute of Inorganic Chemistry

Prof. Dr. Manuel Alcarazo, Institute of Organic and Biomolecular Chemistry

Dr. Franziska Thomas, Institute of Organic and Biomolecular Chemistry

Dr. Max Hansmann, Institute of Organic and Biomolecular Chemistry

Date of the oral examination: 17.08.2018

Contents

1	Introduction.....	1
1.1	Transition Metal-Catalyzed C–H Functionalizations.....	1
1.2	C–H Activation by Chelation Assistance.....	6
1.3	Ruthenium Catalyzed C–H Functionalization	9
1.4	Ruthenium-Catalyzed Twofold C–H Activation Between Benzoic Acids and Acrylic Esters.....	12
1.5	Carboxylic Acid as a Traceless Directing Group.....	15
1.6	Hydrogen Isotope Exchange Reactions (HIE) for Isotopic Labeling	18
1.7	Renewable Hydrocarbons in Organic Synthesis	22
2	Objectives.....	25
3	Results and Discussion.....	27
3.1	Ruthenium(II)-Oxidase Catalyzed Twofold C–H Alkenylation with Oxygen as the Sole Oxidant.....	27
3.1.1	Optimization Studies for Ruthenium(II)-Oxidase in Traditional Solvents.....	27
3.1.2	Scope of Ruthenium(II)-Oxidase Catalyzed Formation of Phthalides	30
3.1.3	Optimization Studies for Ruthenium(II)-Oxidase in Renewable Solvents.....	36
3.1.4	Scope of Ruthenium(II)-Oxidase in Biomass Derived γ -Valerolactone.....	39
3.1.5	Evaluation of Ruthenium(II)-Oxidase Reactivity in Flow.....	48
3.1.6	Kinetic and Mechanistic Studies.....	53
3.1.6.1	Oxygen Uptake Study and Investigation of the Oxidation Mode	53
3.1.6.2	Labeled Oxygen Study	55
3.1.6.3	Kinetic Isotope Effect (KIE) Studies	56
3.1.6.4	Synthesis of Reaction Intermediates	61
3.1.6.5	Proposed catalytic cycle	70
3.2	Ruthenium(II)-Catalyzed Decarboxylative Alkenylation/Alkylation of Benzoic Acids	72
3.2.1	Optimization Studies.....	72
3.2.2	Scope of the Decarboxylative Alkenylation	78
3.2.3	KIE and CO ₂ Evolution Studies.....	83
3.2.4	Mechanistic and Kinetic Studies of Ruthenium(II)-Catalyzed Decarboxylative Alkylation	86
3.3	Ruthenium(II)-Catalyzed Hydrogen Isotope Exchange on Acrylic Esters	90
3.3.1	Optimization of the Hydrogen Isotope Exchange on Acrylic Esters.....	90

3.3.2	Scope for Hydrogen Isotope Exchange Labeling on Acrylic Esters.....	94
3.3.3	Kinetic Studies and Catalyst Investigations.....	100
3.3.4	Scale-Up and Synthetic Applications of Deuterated Acrylates.....	102
4	Summary and Outlook	105
5	Experimental Section	108
5.1	General Remarks.....	108
5.2	Representative Procedures	112
5.2.1	Representative Procedure A: Ruthenium(II)-Catalyzed Oxidative Alkenylation of Benzoic Acids in <i>n</i> -Butanol.....	112
5.2.2	Representative Procedure B: Ruthenium(II)-Catalyzed Oxidative Alkenylation of Benzoic Acids in γ -Valerolactone	112
5.2.3	Representative Procedure C: Ruthenium(II)-Catalyzed Decarboxylative Alkenylation of Benzoic Acids.....	112
5.2.4	Representative Procedure D: Ruthenium(II)-Catalyzed Deuteration of Acrylic Esters	113
5.2.5	Representative Procedure E: Ruthenium(II)-Catalyzed Deuteration of Acrylic Esters in C ₆ D ₆	113
5.3	Experimental Procedures and Analytical Data	114
5.3.1	Ruthenium(II)-Oxidase C–H Alkenylation of Benzoic Acids.....	114
5.3.1.1	Experimental Data for the Synthesis of Phthalides	114
5.3.1.2	Kinetic and Mechanistic Studies	147
5.3.1.3	Synthesis of Reaction Intermediates	161
5.3.2	Data for the Ruthenium(II) Decarboxylative Alkenylation of Benzoic Acids	169
5.3.2.1	Data of Alkenylated Arenes	169
5.3.2.2	Additional Studies for the Decarboxylative Alkenylation of Benzoic Acids	185
5.3.2.3	Studies for the Decarboxylative Alkylation of Benzoic Acids	189
5.3.3	Data for the Ruthenium(II)-Catalyzed Deuteration of Acrylic Esters	196
5.3.3.1	Data of Deuterium Labeled Compounds.....	196
5.3.3.2	Kinetic Study for the Deuterium Labelling Reaction.....	212
5.3.3.3	Synthesis of 107	217
5.3.3.4	Synthesis of Deuterium Labeled Compounds.....	218
5.3.4	Synthesis of Deuterated Benzoic Acids.....	222
5.4	Data for X-Ray Diffraction Measurements.....	228

6	References	232
	Acknowledgements	241
	Curriculum Vitae	243

Abbreviations

List of Abbreviations

Ac	acetyl
Ad	adamantyl
Alk	alkyl
AMLA	ambiphilic metal-ligand activation
ATR	Attenuated total reflectance
BA	benzoic acid
BIES	base assisted internal electrophilic substitution
Bn	benzyl
Bphen	4,7-diphenyl-1,10-phenanthroline
Bu	butyl
cat	catalytic
CMD	concerted metalation-deprotonation
cod	1,5-cyclooctadiene
Cp*	1,2,3,4,5-pentamethylcyclopentadiene
Cy	cyclohexyl
DCE	1,2-dichloroethane
DCM	dichloromethane
DMF	<i>N,N</i> -dimethylformamide
DMAP	4-(diethylamino)pyridine
DMSO	dimethylsulfoxide
δ	<i>chemical shift</i>

Abbreviations

EDG	electron donating group
EI	electron ionization
Et	ethyl
EWG	electron withdrawing group
FG	functional group
FTICR	fourier transform ion cyclotron resonance
GC-MS	gas chromatography-mass spectrometry
GVL	γ -valerolactone
Hept	heptyl
HMF	5-hydroxymethylfurfural
HRMS	high resolution mass spectrometry
Int	intermediate
IES	internal electrophilic substitution
IR	infrared
<i>J</i>	coupling constant (NMR)
KIE	kinetic isotope effect
L	ligand
M	metal
Mes	2,4,6-trimethylphenyl
Me	methyl
Ms	mesyl, methylsulfonyl
<i>m</i>	<i>meta</i>

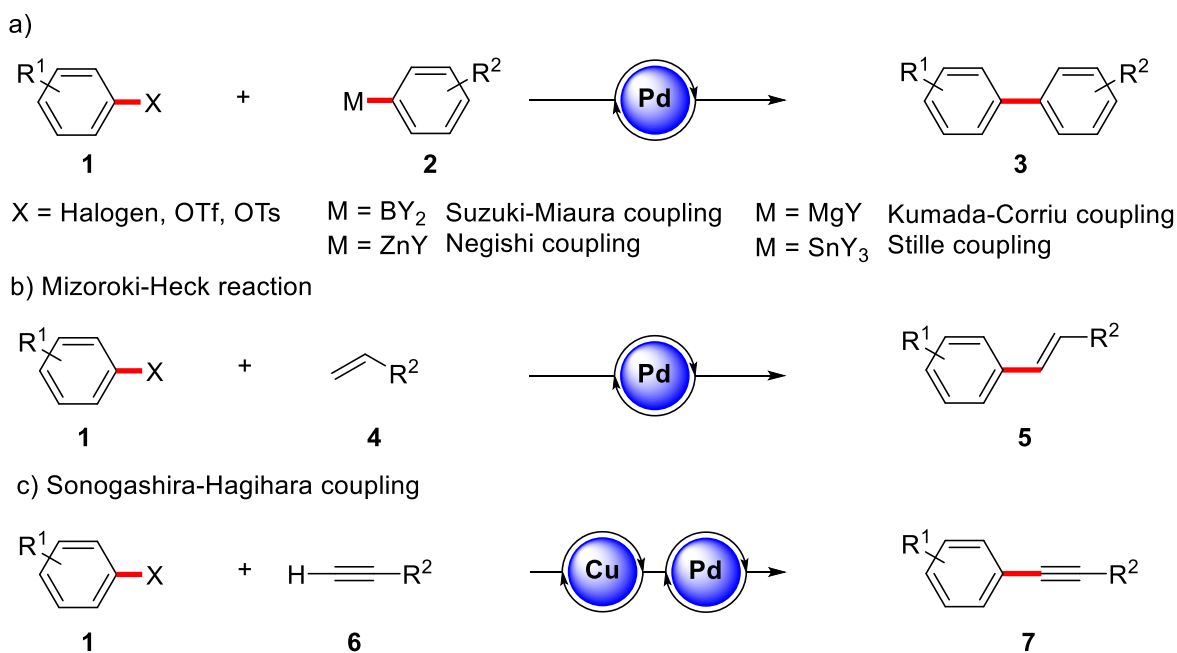
Abbreviations

M. p.	melting point
NBS	<i>N</i> -bromosuccinimide
NMP	<i>N</i> -methyl-2-pyrrolidinone
NMR	nuclear magnetic resonance
ORTEP	Oak Ridge Thermal Ellipsoid Plot
PEG	polyethylene glycole
Ph	phenyl
phen	1,10-phenanthroline
PIDA	(bisacetoxiodo)benzene
PIFA	[bis(trifluoracetoxo)iodo]benzene
ppm	parts per milion
ppb	parts per bilion
py	pyridine
SPO	secondary phosphine oxide
THF	tetrahydrofurane
TLC	thin layer chromatography
TOF	time of flight
TON	turnover number
TS	transition state
Ts	tosyl, 4-toluolsulfonyl

1 Introduction

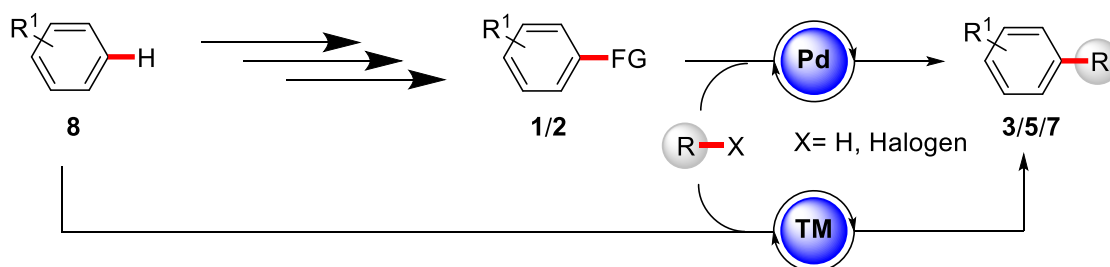
1.1 Transition Metal-Catalyzed C–H Functionalizations

Substituted arenes are key building blocks in living organisms, pharmaceutical compounds and functional materials, such as optoelectronic devices. Traditionally, there have been several ways to functionalize arenes with alkyl groups and heteroatoms, while the synthesis of arene–arene bonds was challenging and conjoined to several limitations. The discovery and development of nickel- and palladium-catalyzed cross-coupling reactions opened new possibilities for the formation of C–C and C–heteroatom bonds.^[1] This class of broadly applicable reactions offered the possibility for the selective formation of a bond between electron-deficient and electron-rich arenes, alkenes or alkynes. As electrophilic arenes halogen-, triflate- or tosylate-substituted arenes are suitable, while as nucleophilic coupling partner several organometallic reagents are applicable. The most important are boronic acids and esters (Suzuki-Miyaura coupling),^[2] organozinc compounds (Negishi coupling),^[3] Grignard reagents (Kumada-Corriu coupling)^[4] and organostannanes (Stille coupling).^[5] In addition to these biaryl forming reactions, alkenylation (Mizoroki-Heck reaction)^[6] and alkynylation reactions (Sonogashira-Hagihara coupling)^[7] are well established. The general reaction structure and the most common organometallic reagents are depicted in Scheme 1.



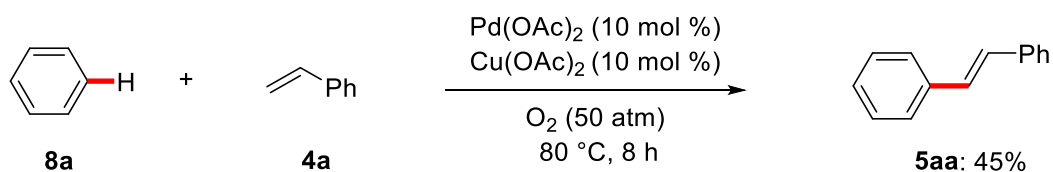
Scheme 1: Selected palladium-catalyzed cross-coupling reactions.

In 2010, the Nobel prize in chemistry was awarded to Richard F. Heck, Ei-Ichi Negishi and Akira Suzuki, for the development of palladium-catalyzed cross-coupling reactions.^[8] Recent publications showed these reactions to work at incredibly low catalyst loadings in the range of parts per billion (ppb) and turn over numbers (TON) of higher than 10^6 .^[9] Despite this groundbreaking improvement of the organic chemist's toolbox, cross-coupling reactions have the general drawback that prefunctionalization of the substrates is needed.^[10] Considering the overall process from the bulk chemical to the fine chemical product, these prefunctionalizations are accompanied by the use of stoichiometric reagents, byproducts and solvents, diminishing the overall step and atom economy. Therefore it would be highly attractive to substitute the prefunctionalization of one or both coupling partners by the direct functionalization of C–H bonds (Scheme 2).



Scheme 2: Cross-coupling and C–H activation approaches.

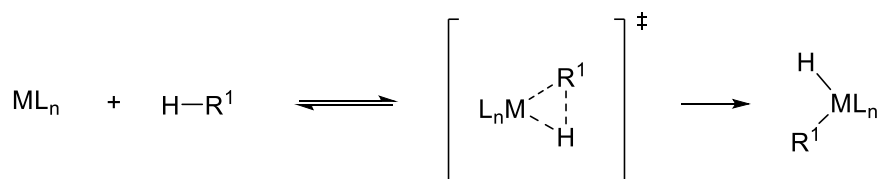
An early example of a catalytic C–H functionalization reaction that does not rely on prefunctionalized arenes was already reported in 1969, before the discovery of cross-coupling reactions.^[11] In their pioneering work, Yuzo Fujiwara and Ychiro Moritani were able to perform an oxidative alkenylation reaction of benzene with styrene to generate stilbene (**5aa**) in a formal dehydrogenative coupling (Scheme 3).



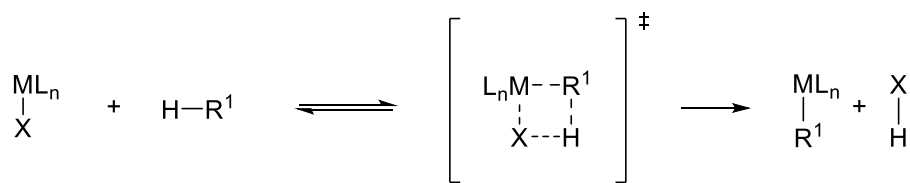
Scheme 3: Fujiwara-Moritani reaction.

The former prefunctionalization and oxidative addition process was replaced by a catalytic C–H metalation keystone. Based on the metal catalyst and oxidation state, several mechanisms for the activation of C–H bonds have been widely accepted (Scheme 4):^[10, 12] a) oxidative addition for low valent, electron-rich late transition metals; b) σ -bond metathesis for early transition metals and lanthanoids; c) 1,2-addition to unsaturated M=X bonds; d) electrophilic substitution with late transition metals in higher oxidation states; and e) base assisted deprotonation, using internal carboxylate or secondary phosphine oxide (SPO) ligands.

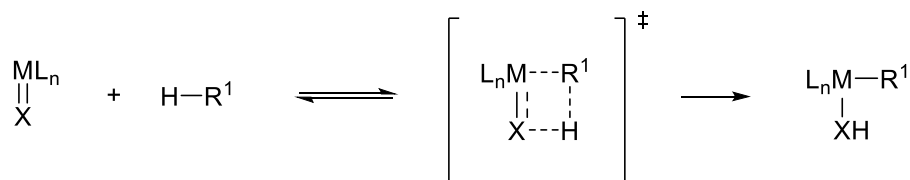
(a) oxidative addition



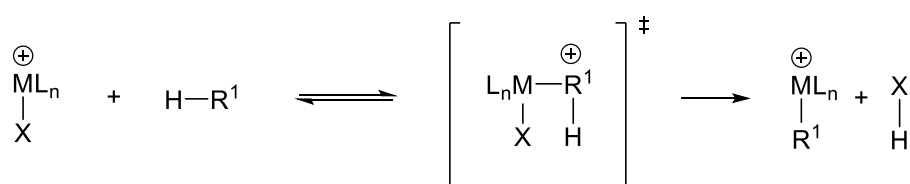
(b) σ -bond metathesis



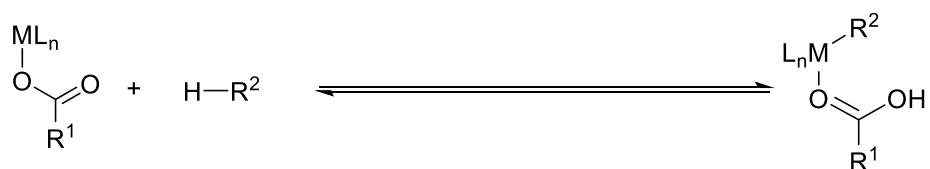
(c) 1,2-addition



(d) electrophilic substitution

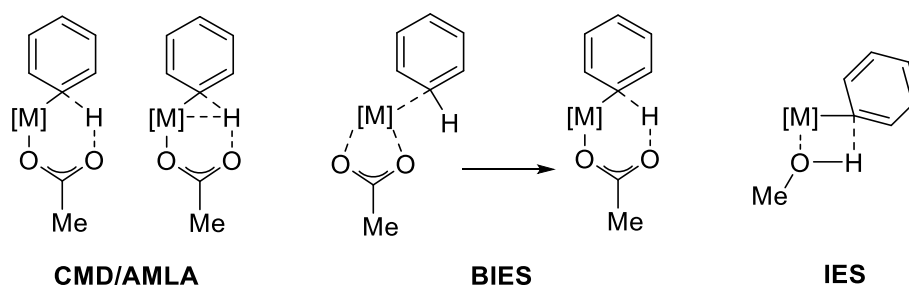


(e) base-assisted metalation



Scheme 4: Possible mechanistic pathways for the activation of C–H bonds.

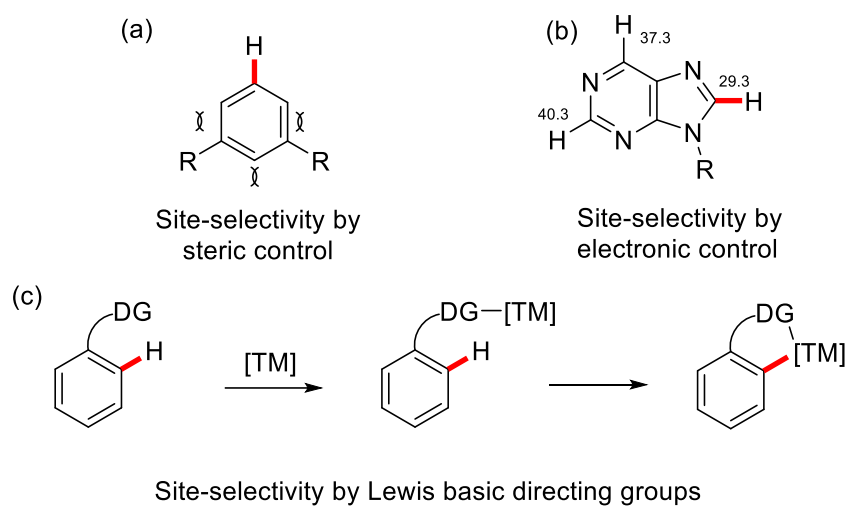
The redoxneutral base-assisted metalation is a common process for the majority of C–H activation reactions.^[10] Depending on the transition state geometry several mechanisms for the metalation step have been proposed (Scheme 5). The independently disclosed concerted metalation deprotonation (CMD)^[13] and the ambiphilic metal ligand activation (AMLA)^[14] pathways are characteristic for a six membered transition states, which can be stabilized by agostic metal hydrogen interactions. Electron-rich arenes preferentially react in a base-assisted internal electrophilic substitution (BIES) type mechanism, which is distinguished by a precoordination of the catalyst by the unsaturated *ipso*-carbon atom prior to the deprotonation step.^[15] Moreover, alkoxylate- and hydroxylate-assisted metalations occur *via* a four membered transition state in an internal electrophilic substitution (IES) mechanism.^[16]



Scheme 5: Transition states for the base assisted deprotonation of benzene.

One major challenge of direct C–H activation strategies is to distinguish between several C–H bonds to achieve a selective functionalization at the desired position.^[17] Three main strategies have been identified to achieve site-selectivity. Substituents at the arene, especially when they are bulky, could be used to block adjacent positions (Scheme 6, a). Besides sterical control, site-selectivity could be achieved making use of the electronic structure of the substrate. This approach functionalizes the most acidic position, as depicted at the pK_a values of purine (b).^[18] Lewis-basic groups at the substrates could be used as directing groups, which coordinate transition metal complexes and direct them to a certain position (c).^[17]

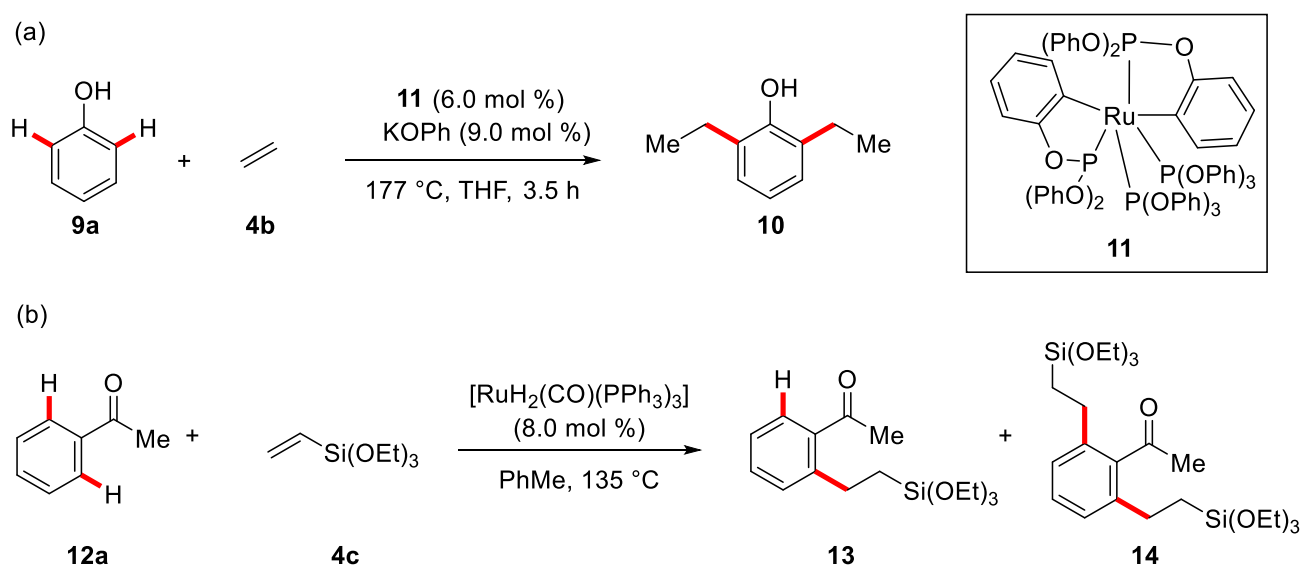
Introduction



Scheme 6: Strategies to achieve site-selectivity in C–H activation.

1.2 C–H Activation by Chelation Assistance

The C–H bond is an ubiquitous structural motif in organic molecules. Therefore, strategies to achieve site-selectivity are important, when C–H bonds should be activated and functionalized directly by transition metal catalysis. One option is the use of Lewis-basic groups that lead the catalyst to a certain position, thereby multiplying the effective concentration of the catalyst at that position. In 1986, Larry N. Lewis and Joanne F. Smith demonstrated this concept on the deuteration and alkylation of phenol, using a transient phosphite directing group and catalytic amounts of complex **11** (Table 1),^[19] which was previously described by Parshall *et al.*^[20] In 1993, Murai and Chatani used this directing group approach for the hydroarylation of alkenes by ruthenium-catalysis (b). In their report, they were able to control between the mono- and the dialkylated products (**13** and **14**) by simply changing the substrate ratios.^[21]

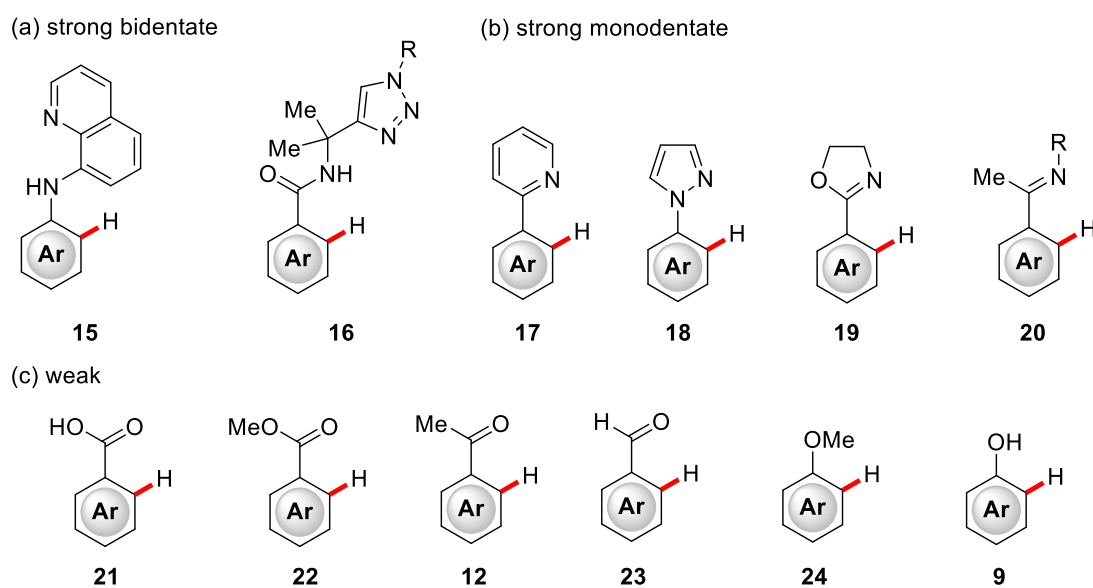


Entry	Equiv (12a)	Equiv (4c)	Yield (13) [%]	Yield (14) [%]
1	1.0	1.0	75	8
2	1.0	3.0	< 1	94

Table 1: Pioneering hydroarylation reactions by a) Lewis & Smith and b) Murai & Chatani.

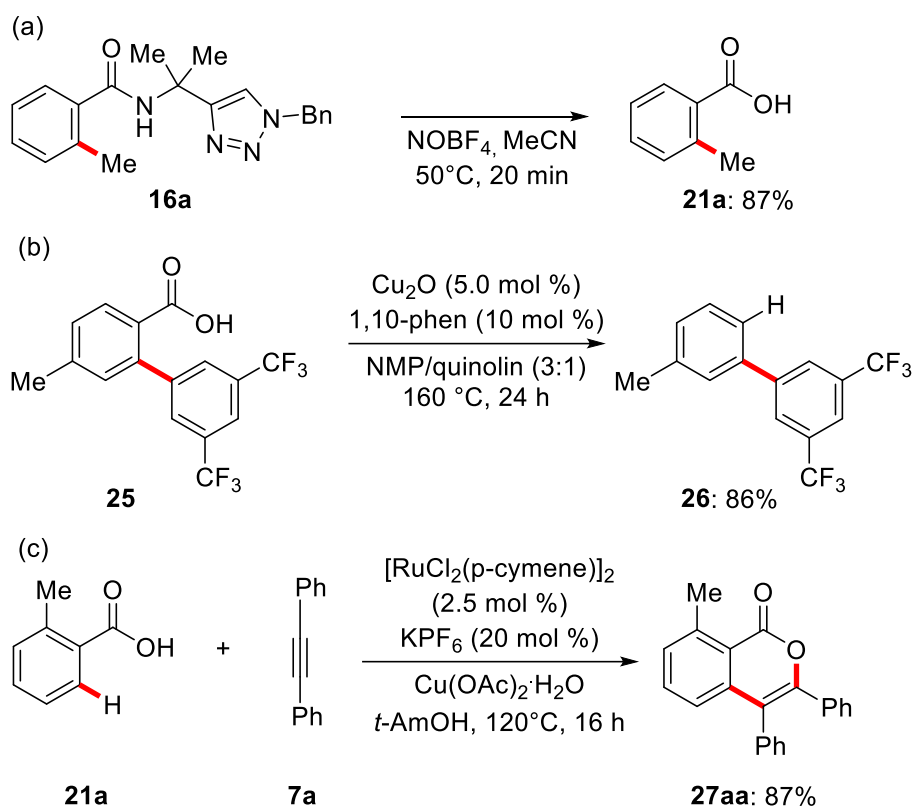
A plenty of Lewis-basic groups are known to act as a directing group. They can be grouped according to their coordination behaviour in strongly and weakly coordinating directing groups.^[22] While strongly coordinating directing groups coordinate the transition metal *via* strong σ -donating

phosphorous or nitrogen atoms, the term weakly coordinating directing group is used for a directing group, that coordinates by weak σ -donating oxygen atoms. Strongly coordinating directing groups can be differentiated in bidentate, such as 8-aminoquinoline^[23] or the triazole-based directing group TAM^[24] (Scheme 7, a) and monodentate directing groups,^[25] like 2-pyridin, 1-pyrazole, 2-oxazolin or ketimines (b). Commonly used weakly coordinating directing groups are carboxylic acids, esters, ketones, aldehydes, ethers or hydroxyl groups (c).^[22a]



Scheme 7: Representative examples of directing groups.

Since the employed directing group is usually not part of the target molecule the *post*-synthetic transformation of these groups is an important issue. Scheme 8 shows selected examples for *post*-synthetic modifications: (a) conversion of the triazole based directing group TAM to a carboxylic acid by oxidation with NOBF_4 ;^[26] (b) traceless removal of the carboxylic acid directing group by copper(I)-catalyzed protodecarboxylation;^[27] (c) annulative introduction of the carboxylic acid directing group into the targeted *iso*-coumarine structure.^[28]



Scheme 8: *post*-Functionalization of directing groups by (a) removal, (b) traceless removal (c) direct incorporation to the target molecule.

In contrast to the advanced development of C–H functionalization methods for strongly coordinating directing groups, weakly coordinating directing groups are privileged substrates for the majority of transformations. A *plethora* of structural motifs are commercially available at reasonable prices and often accessible from natural feedstocks. In addition, methods for *post*-synthetic modifications are well developed, providing possibilities to build up structural diversity.

1.3 Ruthenium Catalyzed C–H Functionalization

Since Lewis and Smith reported the catalytic addition of ethylene to phenol in 1986,^[19a] ruthenium complexes have emerged as a general class of catalysts for the functionalization of arenes. For the activation of C–H bonds, complexes of the type (arene)RuCl₂-dimers as versatile precursors or well-defined arene ruthenium biscarboxylates have shown to be a powerful class of catalysts.^[29] Compared to other 4d and 5d transition metals associated to C–H activation, the price of ruthenium is constantly low, making it economically attractive. Table 2 shows commonly used second and third row transition metals for the activation of C–H bonds together with their prices and typical catalysts or precursors. It is noteworthy, that complexes of the 3d transition metals cobalt,^[30] iron^[31] and manganese^[32] have recently shown to be powerful tools for C–H functionalization, but especially the use of weakly coordinating directing groups remains challenging for 3d metals.

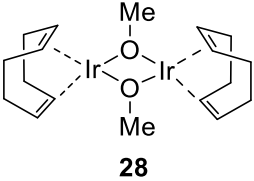
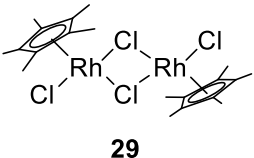
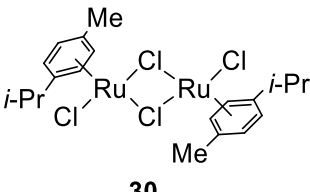
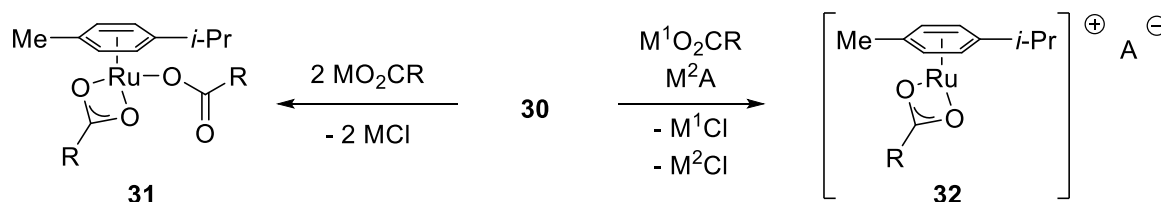
Metal	USD per fine ounce	USD per mol	Typical catalysts and precursors
Iridium	1375	8488	 28
Palladium	1009	3439	Pd(OAc) ₂ , PdCl ₂ , Pd(acac) ₂
Rhodium	2240	7418	 29
Ruthenium	250	812	 30

Table 2: Transition metals, their prices and typical precursors commonly used in C–H activation.^[33]

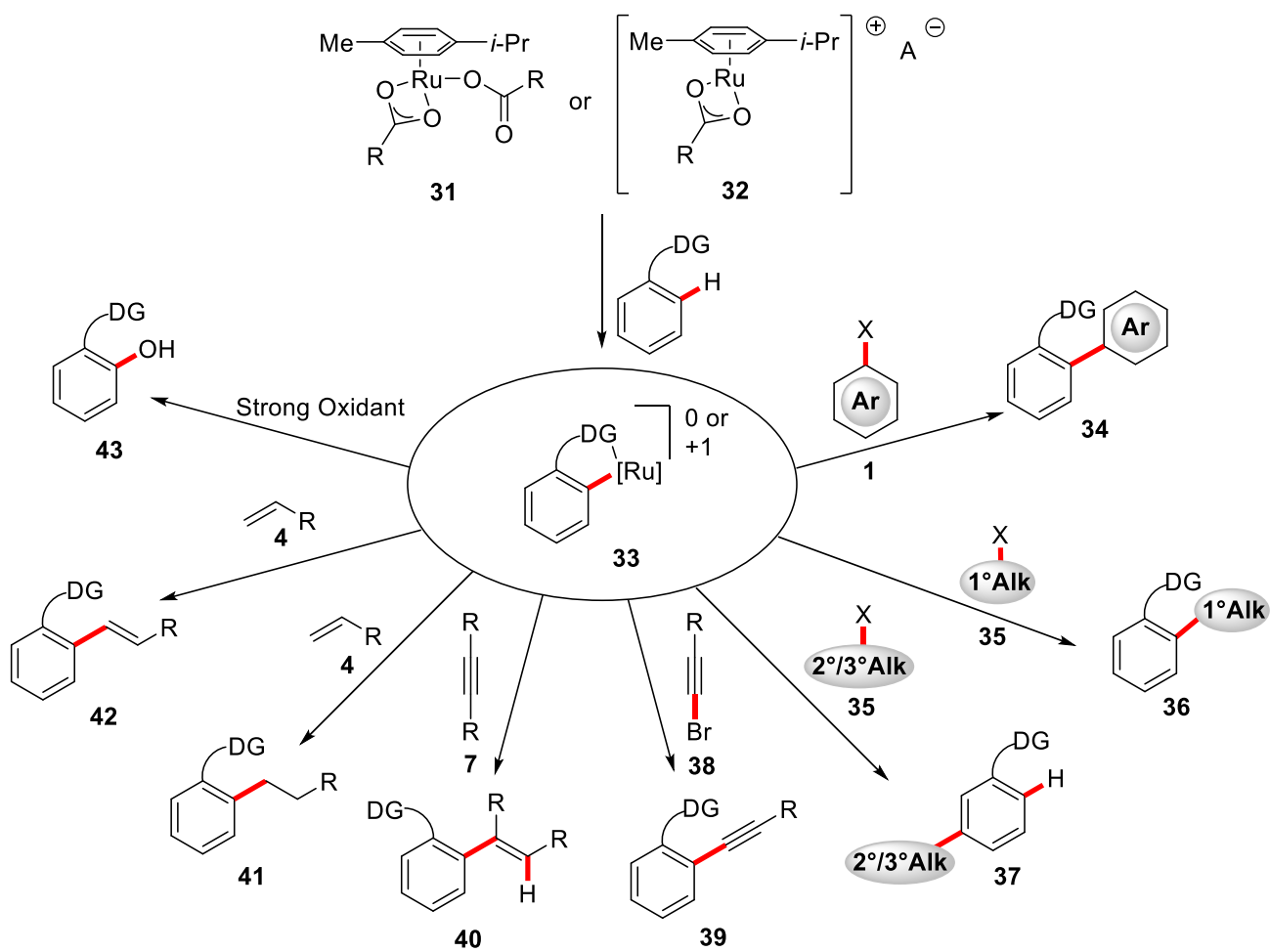
The active arene ruthenium biscarboxylate **31** or cationic arene ruthenium carboxylate catalyst **32** can be used in isolated form or generated *in-situ* from the commercial available ruthenium(II) dimer **30** and carboxylic acid salts (and non coordinating anion salts) (Scheme 9).^[34]



Scheme 9: Synthesis of the active ruthenium(II) carboxylate catalysts.

The catalytic cycle is commenced by the coordination of the active complex by the directing group, subsequently followed by the activation of the otherwise unreactive C–H bond *via* a six membered transition state that generates **33**. Ruthenacycle **33** can react with various reactants under the formation of C–C or C–heteroatom bonds (Scheme 10).^[35] The reaction with halogenated arenes,^[36] primary halogenated alkanes^[37] or alkynyl bromides^[38] resulted in the C–C bond formation in the *ortho*-position, while secondary or tertiary alkyl halides reacted *para* to the ruthenium–carbon bond.^[39] C–C multiple bonds were known to react in redox neutral hydroarylation reactions^[39b, 40] or oxidative couplings^[28, 41] in the *ortho*-position, that can be followed by annulation reactions. The reaction with strong oxidants, like PIFA^[42] or persulfates^[43] resulted in the oxygenation of the *ortho*-position.

Introduction

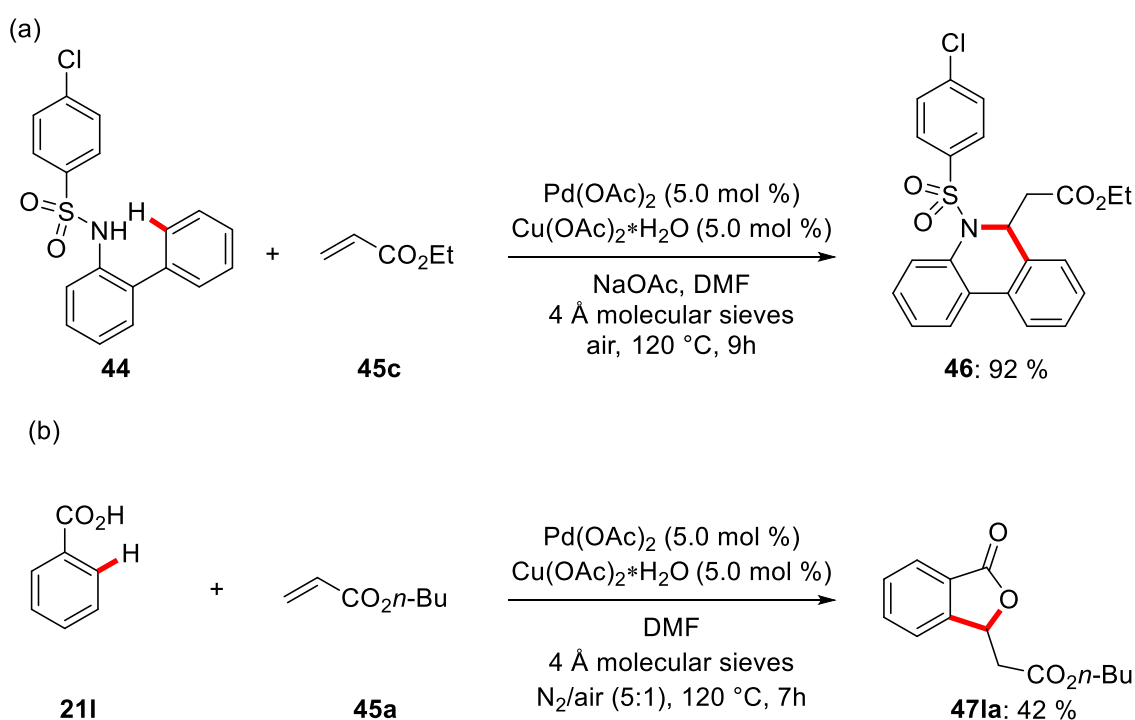


Scheme 10: Selected transformations using ruthenium catalysis.

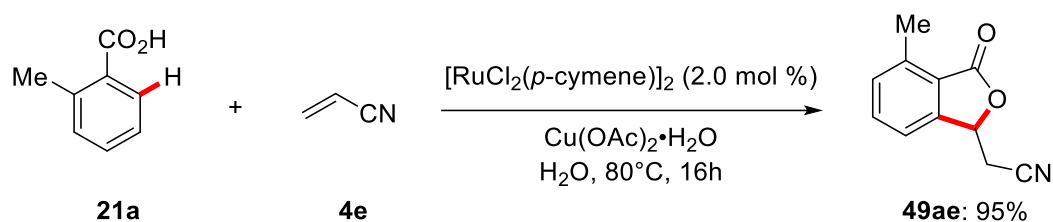
1.4 Ruthenium-Catalyzed Twofold C–H Activation Between Benzoic Acids and Acrylic Esters

Since the pioneering work of Fujiwara and Moritani in the late 1960s,^[11b-d] tremendous progress has been made in the twofold C–H activation between arenes and alkenes with various transition metals, such as palladium, rhodium and ruthenium.^[41e, 44] There are two major challenges to be addressed for this type of transformations. Achieving site-selectivity and finding a suitable reagent for the oxidation. The site-selectivity could be achieved by applying the directing group strategy that leads the catalyst directly to a certain C–H bond, thereby multiplying the effective catalyst concentration next to the target bond.^[44] Traditionally, the second challenge was addressed by the use of oxidation agents, which is accompanied by the formation of by-products.

In an early report by Miura *et al.* in 1998, this problem was solved by the use of $\text{Cu}(\text{OAc})_2 \cdot \text{H}_2\text{O}$ as oxidant in the palladium-catalyzed alkenylation of 2-phenylsulfonamides **44** with acrylates **45** (Scheme 11, a).^[45] Here, the authors showed the versatility of their C–H activation approach by demonstrating different substrates, *inter alia* benzoic acids **21** to be viable in their transformation (b).

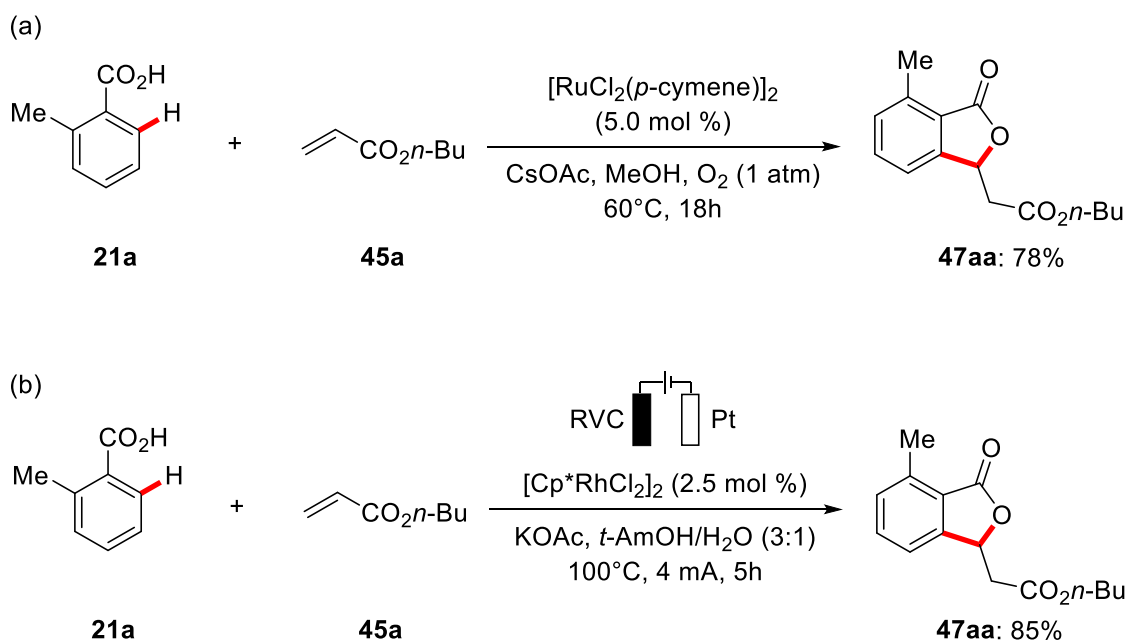


Scheme 11: Palladium-catalyzed alkenylation of 2-phenylsulfonamide (**44**) and benzoic acid (**21**).



Scheme 13: Ruthenium(II)-catalyzed alkenylation *ortho*-toluic acid (**21a**).

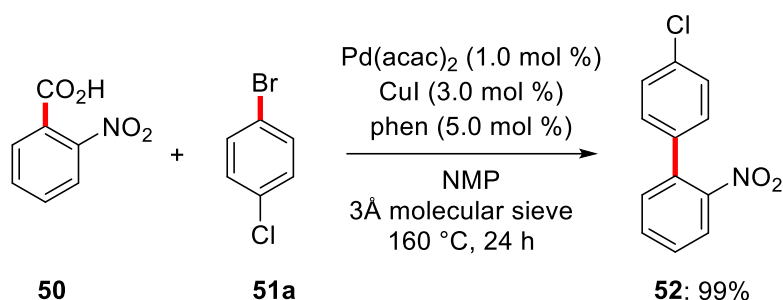
Major improvements were presented by Ackermann and co-workers, by showing ruthenium(II)-biscarboxylate catalysis could perform this reaction with oxygen as the sole oxidant (Scheme 14, a).^[41d] Later, Su and co-workers demonstrated this oxidase-type reactivity for rhodium(III)-catalysis.^[52] Recently, Ackermann and co-workers developed an electrochemical approach for the rhodium(III)-catalyzed alkenylation/annulation sequence for the synthesis of phthalides. Here, the oxidant could be replaced by applying electric current, notably in the absence of any chemical oxidant (b).^[53]



Scheme 14: Ruthenium(II)- and rhodium(III)-catalyzed synthesis of phthalides (**47**).

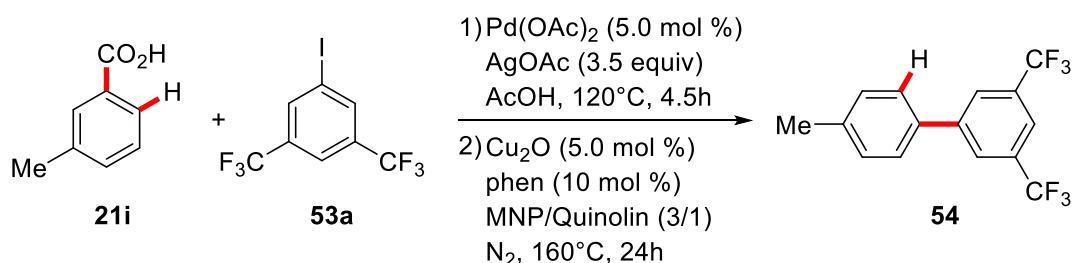
1.5 Carboxylic Acid as a Traceless Directing Group

Carboxylic acids are among the most versatile functional groups in organic chemistry. They are cheap and commercially available in a large variety and they could be functionalized by a *plethora* of well established synthetic methods.^[54] Due to their natural occurrence, they display an attractive target for modern catalytic approaches.^[54] Gooßen and co-workers elegantly merged the copper-mediated decarboxylation of benzoic acids and cross-coupling methods to a decarboxylative C–C bond formation in the *ipso*-position (Scheme 15).^[55]



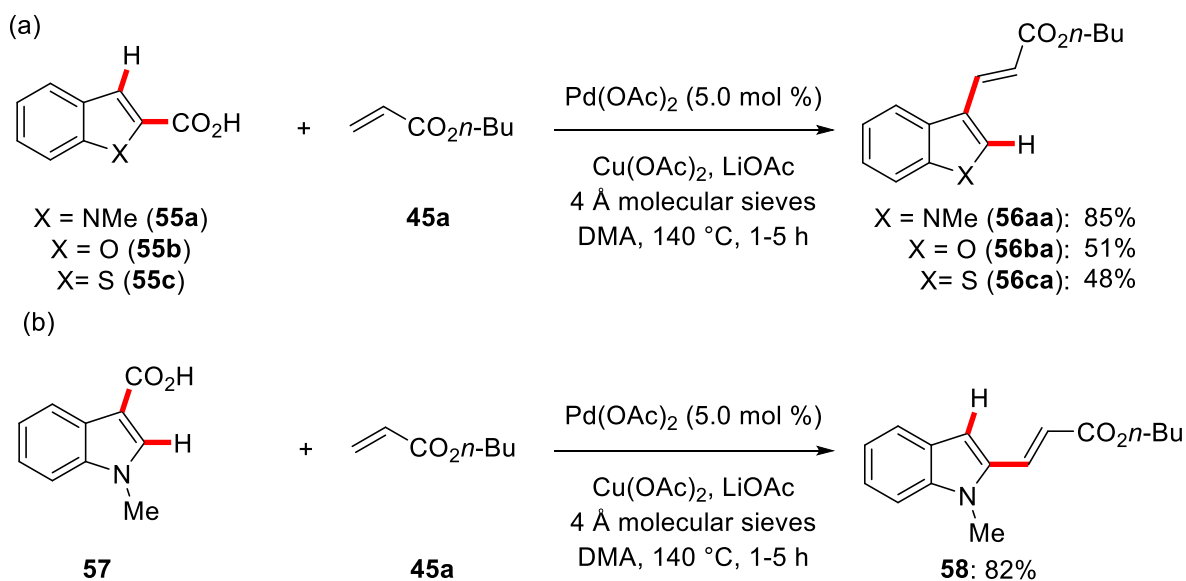
Scheme 15: Decarboxylative cross-coupling of 2-nitrobenzoic acids (**50**) with 1-bromo-4-chlorobenzene (**51a**).

In 2007, an alternative approach was presented by the Daugulis group. There, the authors combined a palladium(II)-catalyzed *ortho*-C–H arylation of benzoic acids **21** with a copper(II)-catalyzed protodecarboxylation of the directing group in a second step (Scheme 16).^[27] This two metal, two step approach gave access to a great variety of *meta*- and *para*-substituted arenes, which was largely expanded by contributions of several other groups.^[56]



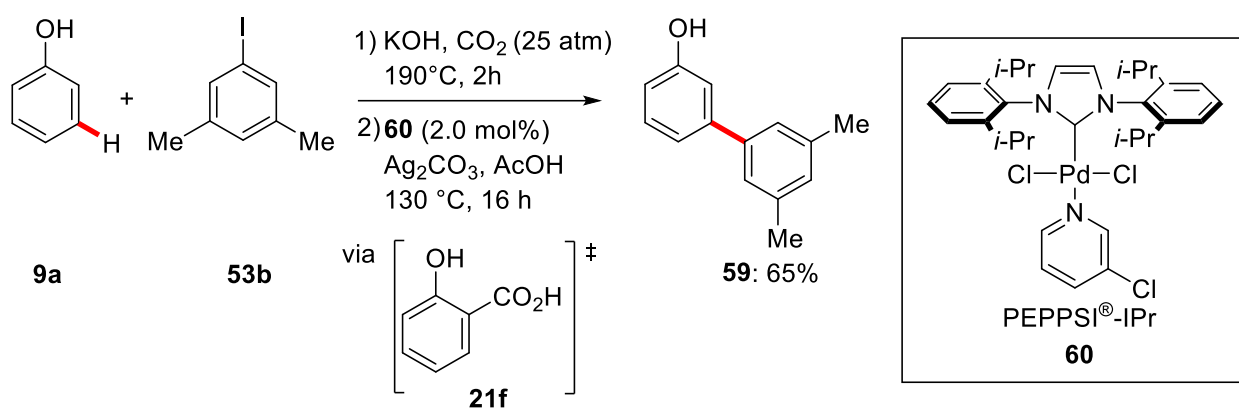
Scheme 16: Two-step protocol for decarboxylative C–H arylation by Daugulis *et al.*

In 2008, the Miura group improved this concept by the development of an *ortho*-C–H alkenylation/decarboxylation one-pot tandem process.^[57] The authors showed their system to operate with 2- and 3-carboxylic acids of pyrrole, indole, (2,3-benzo)furane, (benzo)thiophenes (**55** or **57**) with catalytic amounts of palladium(II) or rhodium(III) for the C–H activation reaction and stoichiometric amounts of copper(II) or silver(I) salts for the decarboxylation (Scheme 17).



Scheme 17: Two metal, one pot decarboxylative arylation by Miura *et al.*

Furthermore, Larrosa and co-workers expanded the scope of this transformation to *ortho*-substituted benzoic acids^[58] and salicylic acids^[59] using palladium(II) and silver(I) salts to afford *meta*-substituted arenes. It is noteworthy that the authors applied their method in a consecutive sequence of a Kolbe-Schmidt carboxylation, followed by the alkenylation/decarboxylation tandem reaction, generating *meta*-hydroxy biaryls in one-pot from simple phenols (Scheme 18).^[60]



1.6 Hydrogen Isotope Exchange Reactions (HIE) for Isotopic Labeling

Isotopologues of chemical compounds containing the heavier isotopes of hydrogen, namely deuterium (D, ^2H) and tritium (T, ^3H), have a wealth of important applications in the clarification of reaction mechanisms and biological pathways.^[64] Furthermore, deuterated compounds are commonly used as indiscernible solvents in NMR spectroscopy and as mass tagged reference materials in mass spectrometry. Thereby, these labeled analogues are tagged in specific positions, without changing the global chemical, physical and biological properties.^[65]

In comparison to C–H bonds, the C–D bond has a lower zero-point energy, which is a result of a lower vibrational frequency and a slightly shorter bond distance between carbon and deuterium. This energy gap can be observed as kinetic isotope effect (KIE) (Figure 1).^[66]

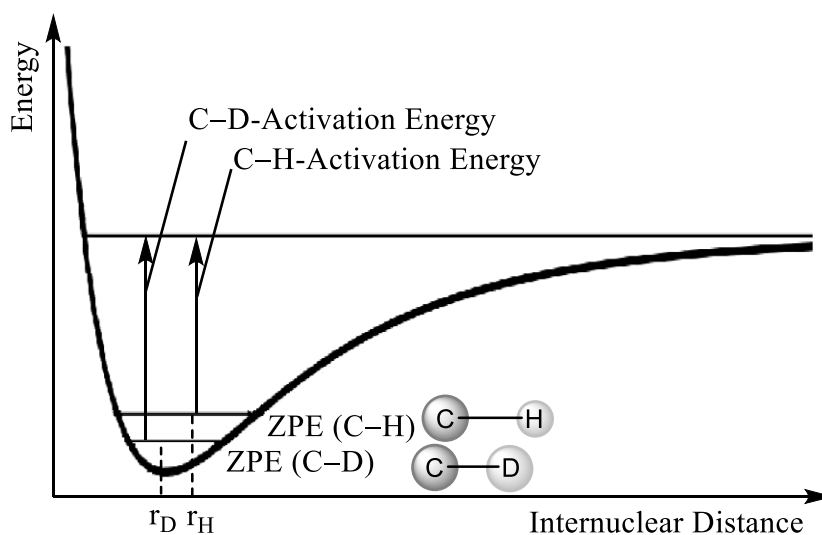
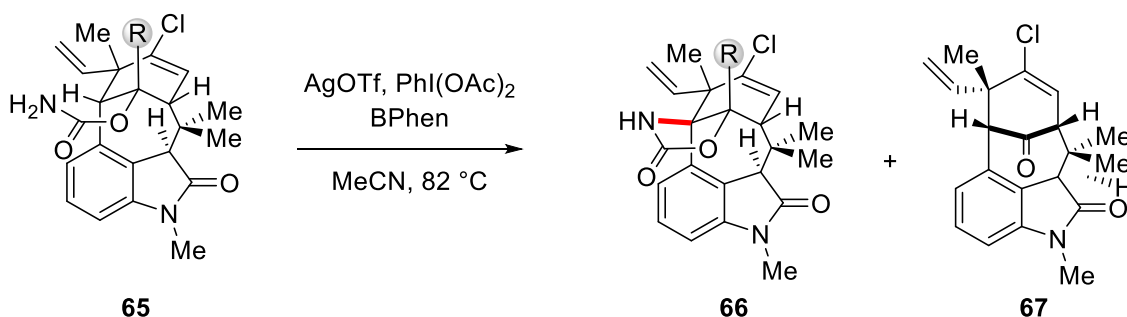


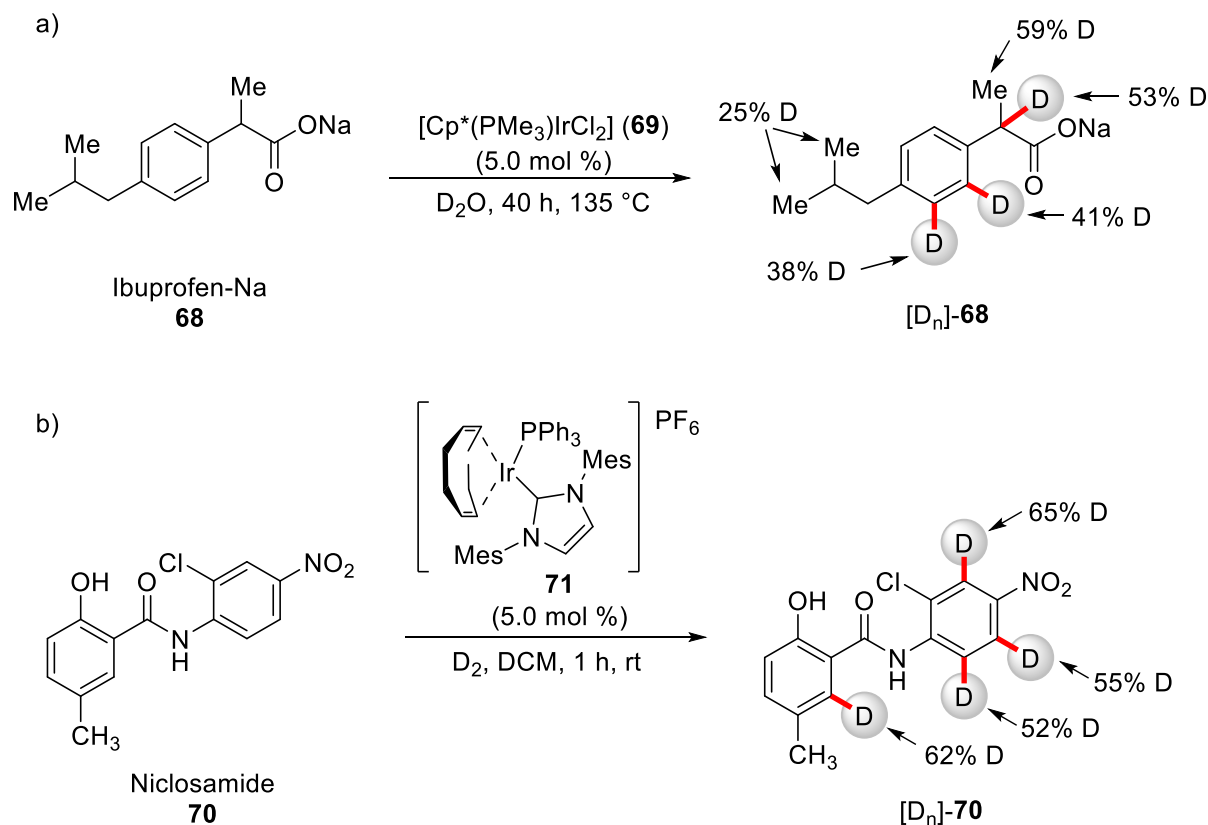
Figure 1: Graphical representation of the zero-point energy, bond-distance and the activation energies for the homolysis of a C–H and C–D bonds.^[67]

KIE's are differentiated between primary KIE's, that could be observed when the labeled bond is broken and secondary KIE's as a result of steric interactions or hybridization changes, while the bond stays intact. Garg *et al.* demonstrated the power of the KIE in their total synthesis of (–)-*N*-methylwelwitindoline C isonitrile. Specific deuterium labeling in the C¹⁰-position nearly doubled the yield of the desired nitrene insertion reaction, while the formation of by-products was suppressed (Table 3).^[68]

Table 3: Kinetic isotope effect of the nitrene insertion in the total synthesis(-)-*N*-methylwelwitindoline C isonitrile.

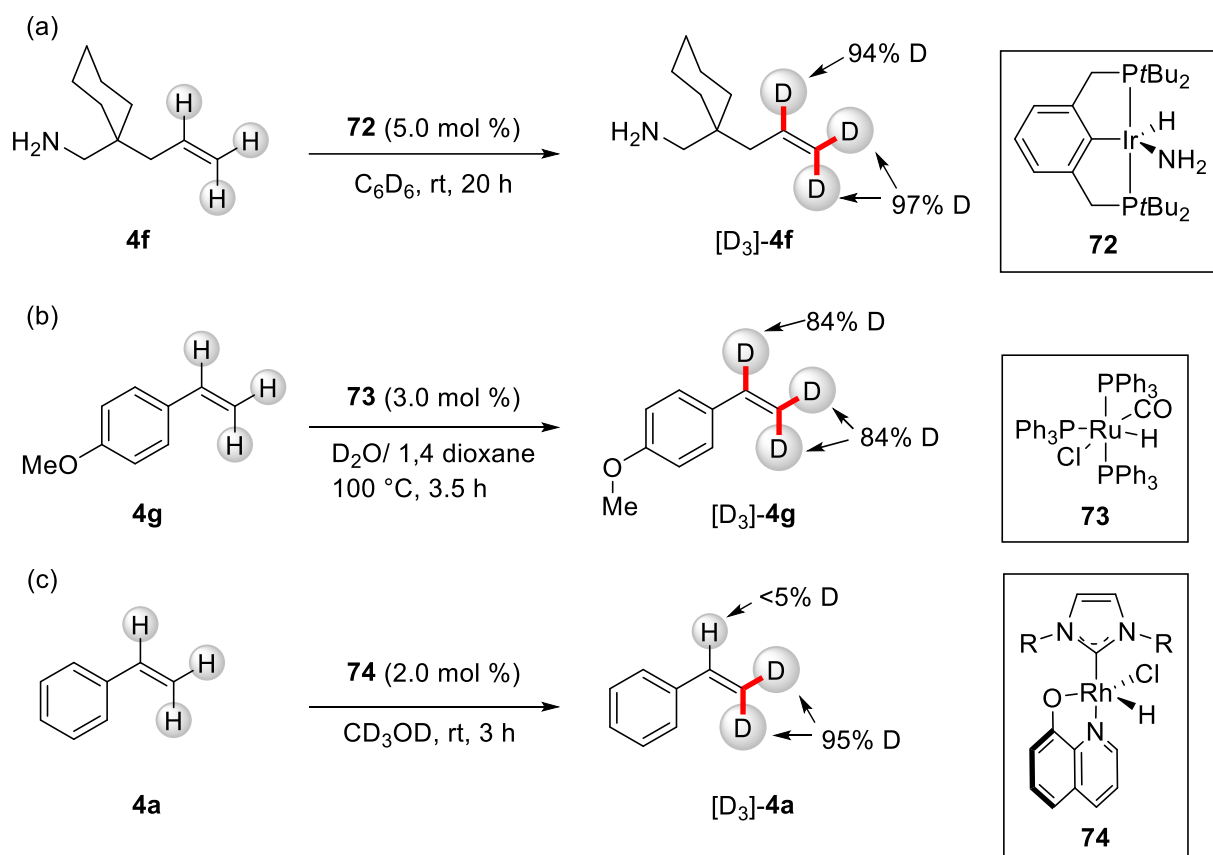
Isotope	Yield of 66 [%]	Yield of 67 [%]
R = H	33	25
R = D	60	8

In order to synthesize isotopologues there are two major approaches. The *de novo* synthesis using labeled precursors and the late-stage hydrogen isotope introduction in the desired position.^[69] Here, especially C–H functionalization methods are quite attractive, because they give easy access to otherwise unreactive positions, without the need of prefunctionalization.^[70] In 2002, Bergman and co-workers demonstrated iridium(III) complexes to be active in the exchange of C(sp³)–H and C(sp²)–H bonds of Ibuprofen (Scheme 20, a),^[71] whereas Chen et al. showed the deuteration of the anthelmintic drug Niclosamide (**68**) to be catalyzed by an iridium(I) complex based on Crabtree's catalyst^[72] (b).^[73]



Scheme 20: Iridium-catalyzed deuteration of Ibuprofen (**68**) and Niclosamide (**70**).

While the hydrogen isotope exchange of aromatic C–H bonds is well explored,^[64c, 70a] methods for the selective functionalization of alkenes are rare. In 2008, Hartwig and co-workers reported an iridium(III) pincer complex **71** that exchanges alkenyl C–H bonds with C_6D_6 as the deuterium source (Scheme 21, a).^[74] Grotjahn *et al.* used ruthenium(II) for the (per)deuteration alkenes by isomerization of the double bond with D_2O as deuterium source.^[75] Jia and Lin used commercial available $\text{RuHCl}(\text{CO})(\text{PPh}_3)_3$ (**73**, b) and Yorimitsu used catalytic amounts of $[\text{Ir}(\text{OH})(\text{cod})_2]$ and *N*-mesylbenzamides to deuterate the double bond of stilbene and methyldiene groups.^[76] Oro and co-workers showed, that NHC-supported rhodium(III) hydride catalysts (**74**) selectively deuterated the β -position of styrene (**4a**, c).^[77]

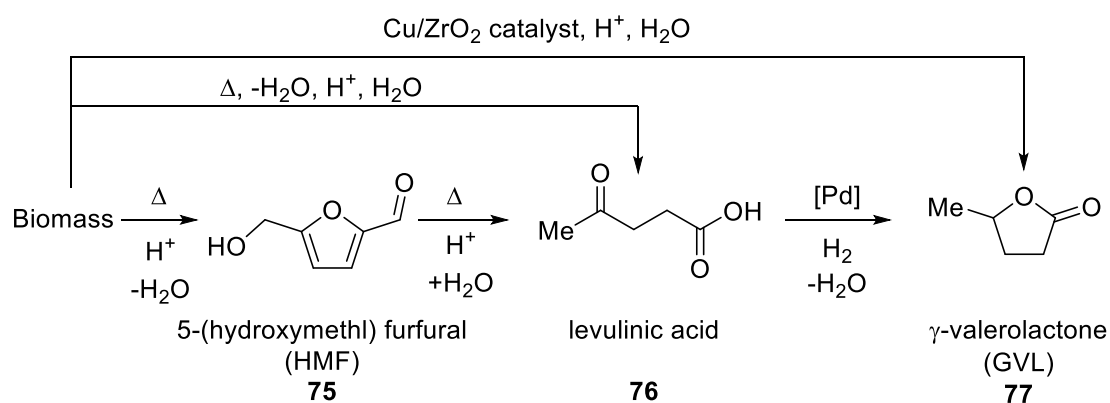


Scheme 21: Selected examples for the deuteration of alkenes via HIE.

1.7 Renewable Hydrocarbons in Organic Synthesis

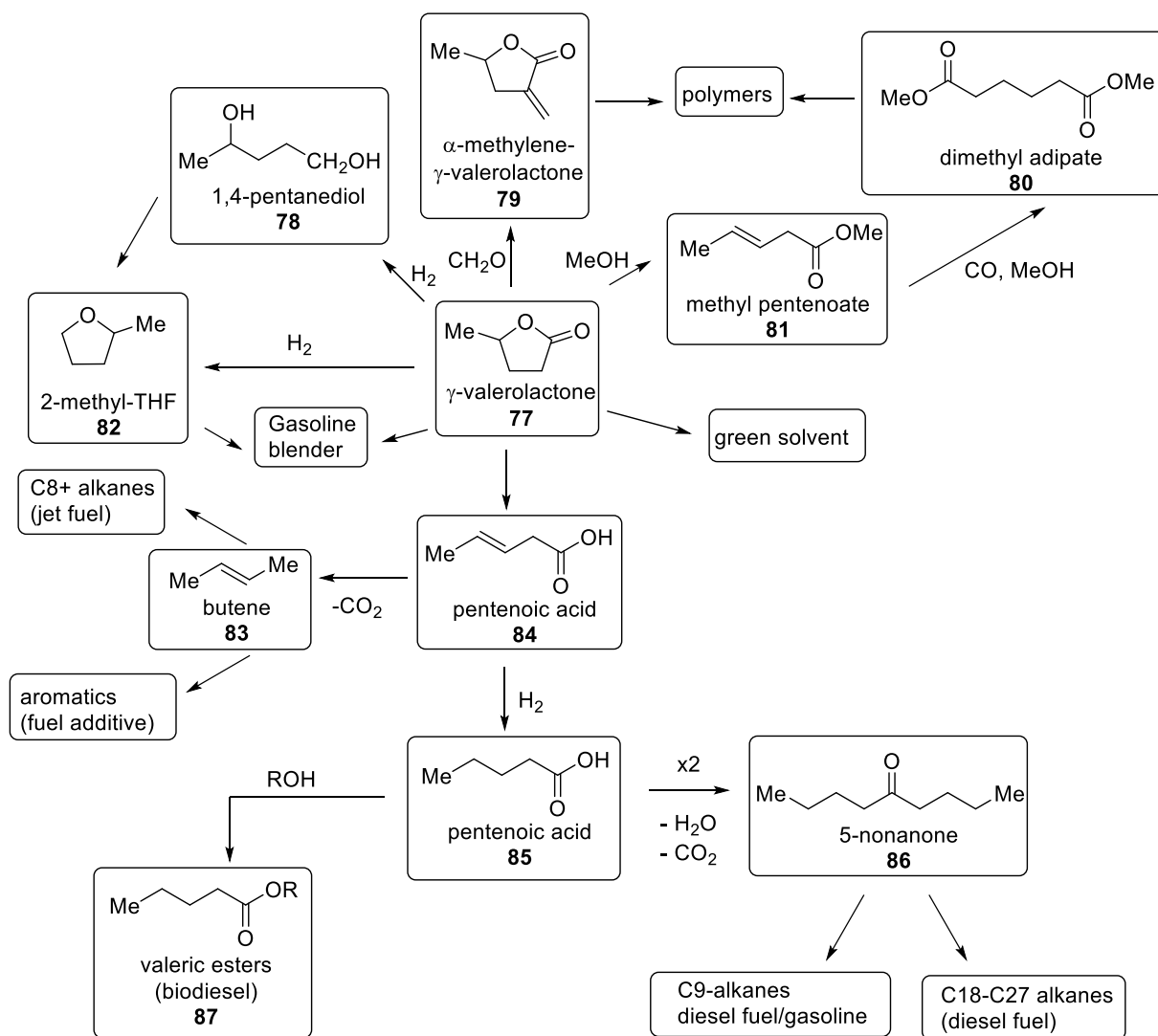
Fossil oils and gases are finite resources and going to be limited in the future.^[78] However, the majority of chemical products are based on fossil resources.^[79] In 1998, Anastas and Warner formulated the twelve principles of green chemistry, which demonstrate the major challenges on the way to a green and sustainable production of chemical products.^[80] One of these major challenges is to discover ways to acquire bulk chemicals from sustainable sources or to find sustainable alternatives for those chemicals. Especially the conversion of biomass into bulk chemicals is an attractive approach.^[81] Thereby, it is important that the substrates do not compete to food production and are, ideally, waste products from other industries.^[82] Renewable feedstocks with the biggest potential are mono-, di- and polysaccharides, lignin, proteins and extractives. Since the majority of those feedstocks are highly functionalized polymers, effective methods for hydrolysis, defunctionalization and separation have been developed to reduce their complexity and make biomass available for the chemical supply chain.^[83] Herein, several compounds have been proposed to be future platform molecules. These biomass-derived platform molecules need to be accessible in high quantities at reasonable costs and should be convertible to a plethora of chemicals by basic reactions.^[84]

γ -Valerolactone and levulinic acid are supposed to be biomass-derived future platform molecules. They could be synthesized from sugars, cellulosic and hemicellulosic biomass, that could be either directly converted to levulinic acid (**76**)^[85] and γ -valerolactone (GVL, **77**)^[86] or *via* the isolation of 5-(hydroxymethyl) furfural (HMF, **75**)^[87] as the intermediate.^[86a, 88]



Scheme 22: Examples for the production of GVL (**77**) and levulinic acid (**76**) *via* HMF (**75**) or direct.^[84]

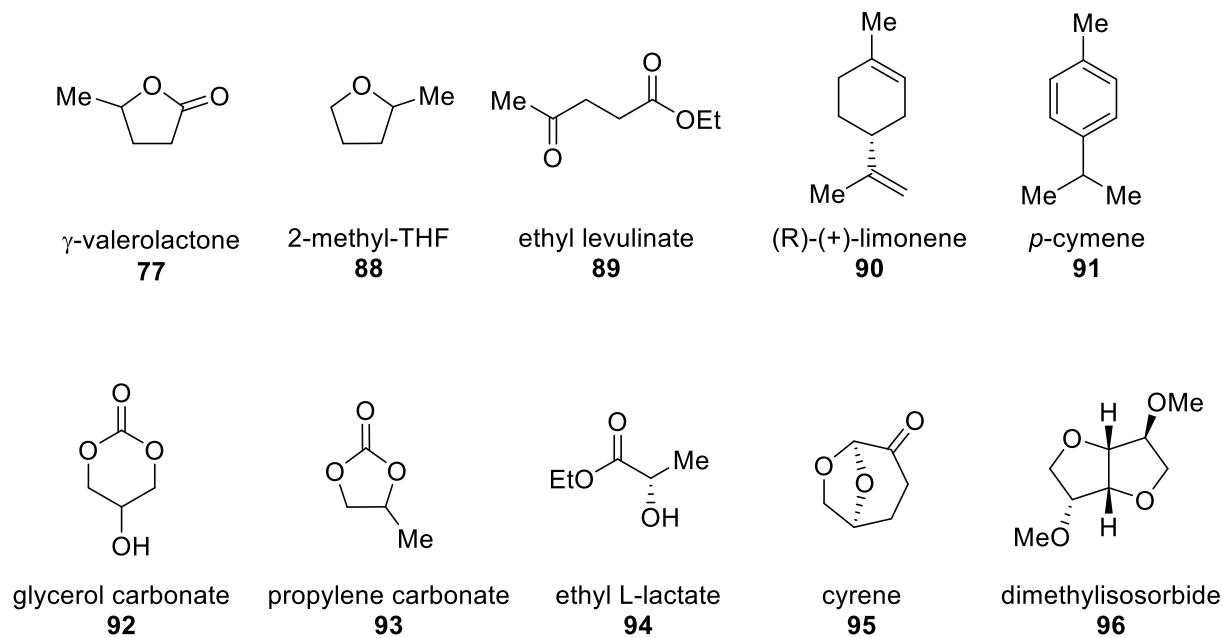
Biomass derived GVL (**77**) is a versatile precursor to various chemicals, especially for the production of fuels and polymers.^[89] Scheme 23 gives an overview of bulk chemicals and their applications, that could be synthesized from GVL (**77**) using simple and low cost standard manipulations.



Scheme 23: Synthesis of bulk chemicals from biomass-derived γ -valerolactone (**77**).^[89]

Besides the production of fuel and bulk chemicals, especially the substitution of traditional solvents has a big influence to the overall ratio between traditional and renewable reagents.^[90] Scheme 24 shows a selection of alternative solvents. In general, these solvents have higher molecular weights and higher boiling and flammability points, thereby increasing the safety compared to their traditional pendants.^[91] Since they usually bear several functional groups or stereogenic centers, these solvents have unique

properties. Therefore, it is highly important to evaluate these properties and show the applicability of these solvents in a broad set of reactions in order to install them as viable alternatives.^[92]

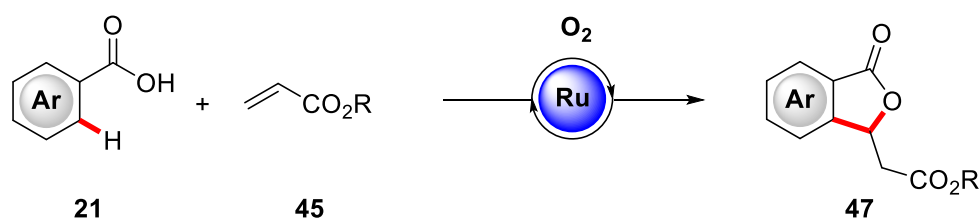


Scheme 24: Selected biomass-derived solvents.

2 Objectives

C–H Activation has emerged as a powerful and sustainable approach for the functionalization of arenes. Thereby it extended the methodological repertoire of organic chemists and changed the way organic synthesis is planned and performed.^[93] Several transition metal complexes have turned out to be broadly applicable and have been extensively developed within the last two decades. Although there is a current trend in substituting 4d and 5d metals by cheaper 3d transition metals, especially the use of weakly coordinating directing groups is unique for the heavier 4d and 5d metals.^[22] Within this context ruthenium based catalysts are particularly attractive, because of their lower price compared to the other metals in combination with a cheap and well developed synthesis of the catalytically active complexes.

Ruthenium based catalysts are applicable to a large number of oxidative and redox neutral reactions. For oxidative transformations S. Warratz and C. Kornhaas recently showed that costly stoichiometric copper(II) and silver(I) oxidants can be substituted by simple oxygen as the sole oxidant in the annulative synthesis of *iso*-coumarines.^[41d] To extend this economic and highly sustainable approach a catalytic system for the annulative synthesis of phthalides **47** from benzoic acids **21** and alkenes **45** with oxygen as sole oxidant was investigated (Scheme 25). In addition to the development of a synthetic method extensive mechanistic studies were conducted to develop a deeper understanding of the catalytic mode of action.

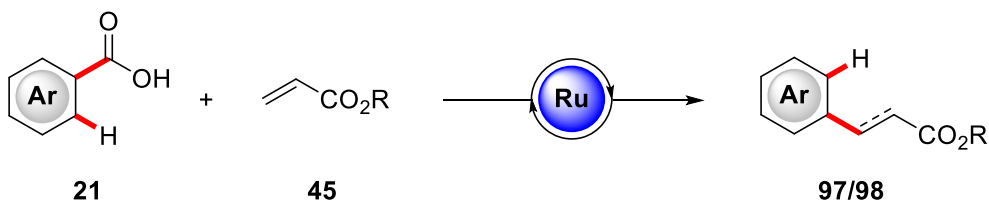


Scheme 25: Ruthenium-catalyzed oxidative alkenylation of benzoic acids **21**.

The removal or *post*-modification of the directing groups is an ongoing topic in directed C–H functionalization. In case of the phthalide synthesis the directing group is incorporated in the desired product, displaying perfect atom economy. As observed in the previous project, small amounts of a decarboxylated side product were formed during the annulation. For palladium chemistry, limited reports for C–H functionalization in combination with a decarboxylation process were available, while

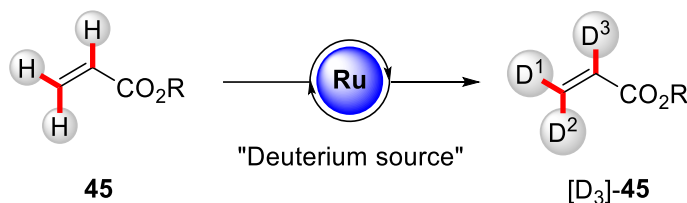
Objectives

for ruthenium catalysis only a single example was known.^[94] In order to explore this new area in ruthenium catalysis, this unprecedented reactivity was investigated, in order to develop a domino functionalization decarboxylation process (Scheme 26).



Scheme 26: Ruthenium-catalyzed decarboxylative alkylation/alkenylation.

Compounds labeled with higher isotopes of hydrogen are highly important for the study of reaction mechanisms, NMR-experiments or as specifically tagged reference materials. While arene labeling is a common and well-developed process, reports for the hydrogen isotope exchange (HIE) reaction at alkenes were limited to few examples.^[70a] Based on observations of hydrogen scrambling at the alkene during general alkenylation studies this reactivity was investigated (Scheme 27).

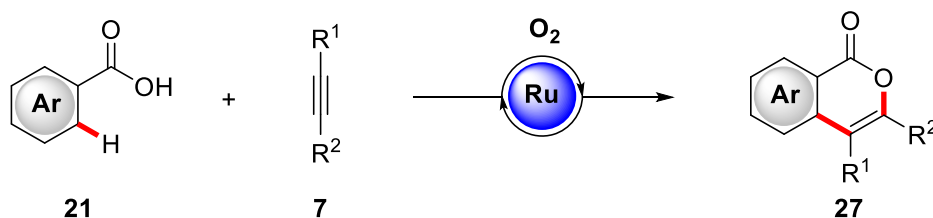


Scheme 27: Ruthenium-catalyzed deuteration of acrylic esters.

3 Results and Discussion

3.1 Ruthenium(II)-Oxidase Catalyzed Twofold C–H Alkenylation with Oxygen as the Sole Oxidant

Ruthenium(II)-biscarboxylate catalysis has emerged as a powerful tool for the introduction of alkene moieties into organic molecules. Among other catalytically active complexes based on various metals, ruthenium catalysis offers the possibility of performing the alkenylation of C–H bonds in a twofold fashion, formally abstracting two protons in an oxidative process. Copper(II) and silver(I) salts have been shown to be the oxidants of choice in these transformation, but their use is accompanied by stoichiometric metal waste formation. In 2015, Ackermann *et al.* demonstrated that ruthenium(II)-biscarboxylates are able to use molecular oxygen as a sole oxidant, forming *iso*-coumarines from benzoic acids and alkynes (Scheme 28).^[41d]



Scheme 28: Ruthenium(II)-oxidase catalyzed synthesis of *iso*-coumarines.

The following studies extended these first observations of the ruthenium(II)-oxidase reactivity by the development of a catalytic system and extensive studies on the reactions mechanism of the twofold C–H activation between benzoic acids and alkenes.

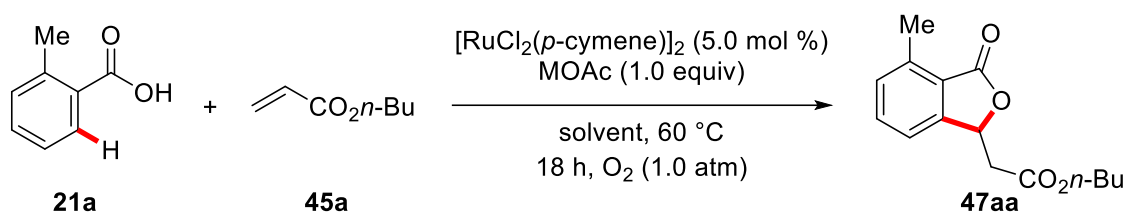
3.1.1 Optimization Studies for Ruthenium(II)-Oxidase in Traditional Solvents

The study was commenced by the optimization of the reaction of 2-methylbenzoic acid (**21a**) with *n*-butyl acrylate (**45a**) in a catalytic system consisting of an *in situ* formed ruthenium(II)-biscarboxylate catalyst, acetate base/ligand and an alcoholic solvent under an ambient atmosphere of molecular oxygen (Table 4). The acetate salt was varied in methanol as the solvent (entries 1-3), showing potassium to be the optimal counterion. The use of *n*-butanol as the solvent (entry 5) resulted in a slight improvement, while ethanol and *tert*-butanol (entries 4 and 6) showed less efficacy. The ratio between the benzoic acid and the acrylate component showed a strong dependency, which favors an excess of

Results and Discussion

the benzoic acid (entries 7, 8 and 9). The use of p.A-grade methanol and dried and purified methanol as the reaction medium gave comparable yields, highlighting the robustness of this catalytic system (entries 9 and 10). Entries 11 and 12 demonstrated the cruciality of the ruthenium(II) catalyst as well as of the acetate source. Changing the solvent to *n*-butanol improved the yield to 66%, when **21a** was used as limiting reagent (entry 13).

Table 4: Optimization of the substrate ratios, solvent and acetate source.



Entry	21a/45a [mmol]	Solvent	MOAc	Yield [%] ^[a]
1	2.0/1.0	MeOH	NaOAc	74
2	2.0/1.0	MeOH	KOAc	88
3	2.0/1.0	MeOH	CsOAc	82
4	2.0/1.0	EtOH	KOAc	78
5	2.0/1.0	<i>n</i> -BuOH	KOAc	90
6	2.0/1.0	<i>t</i> -AmylOH	KOAc	67
7	1.0/1.2	MeOH	KOAc	50
8	1.0/2.0	MeOH	KOAc	51
9	1.0/1.5	MeOH	KOAc	57
10	1.0/1.5	MeOH (p.A)	KOAc	58
11	2.0/1.0	MeOH	---	---
12 ^[b]	2.0/1.0	MeOH	KOAc	---
13	1.0/1.5	<i>n</i> -BuOH	KOAc	66

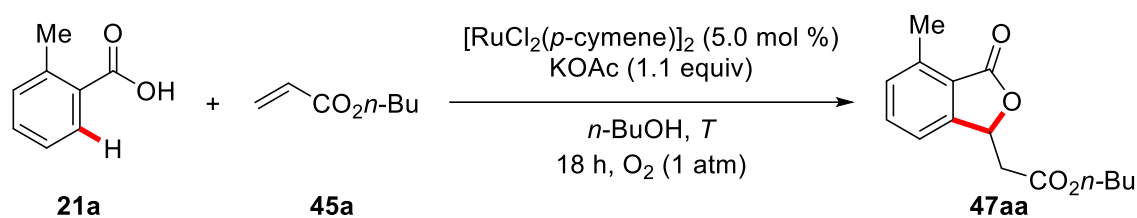
^[a] Reaction conditions: **21a**, **45b**, [RuCl₂(*p*-cymene)]₂ (**30**) (5.0 mol %), MOAc (1.0 mmol), solvent (3.0 mL), O₂ (1.0 atm), 60 °C, 18 h. Yield of isolated product. ^[b] Without [RuCl₂(*p*-cymene)]₂.

Using higher boiling *n*-butanol as the solvent the temperature was elevated to 80 °C, which improved the efficacy (Table 5). The yield of this transformation still depended on the ratio between benzoic

Results and Discussion

acid and acrylic ester (entries 1-4). Increasing the oxygen volume showed minor effects (entry 5), whereas entries six and seven demonstrated, that simple air could be used as the oxidant. Slightly better yields were observed, when the acrylate was used as reagent and solvent at 120 °C (entry 9). The ruthenium(II)-oxidase system was further found to be active even at remarkable low temperatures of 37 °C or 25 °C giving good or moderate yields at prolonged reaction times (entries 10-13).

Table 5: Optimization of the ruthenium oxidase catalysis.



Entry	21a/45a [mmol]	Solvent (3 mL)	T [°C]	Yield [%] ^[a]
1	1.0/1.5	<i>n</i>-BuOH	80	74
2 ^[b]	1.0/1.5	<i>n</i> -BuOH	80	76
3	1.5/1.0	<i>n</i>-BuOH	80	84
4	2.0/1.0	<i>n</i>-BuOH	80	90
5 ^[c]	1.5/1.0	<i>n</i> -BuOH	80	86
6 ^[d]	1.5/1.0	<i>n</i> -BuOH	80	77
7 ^[e]	1.0/1.5	<i>n</i> -BuOH	80	72
8	1.0/1.5	<i>n</i> -BuOH	120	69
9	1.0/5.0	---	120	80
10	2.0/1.0	MeOH	37	37
11 ^[f]	2.0/1.0	MeOH	37	82
12	2.0/1.0	MeOH	25	11
13 ^[f]	2.0/1.0	MeOH	25	53

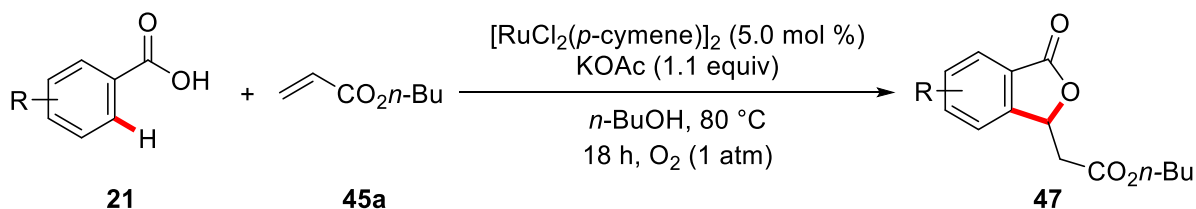
^[a] Reaction conditions: **21a**, **45b**, [RuCl₂(*p*-cymene)]₂ (**30**) (5.0 mol %), KOAc (1.1 mmol), solvent (3.0 mL), O₂ (1.0 atm), *T*, 18 h. Yield of isolated product. ^[b] CsOAc instead of KOAc. ^[c] Under 140 mL of O₂. ^[d] Under air. ^[e] Reaction performed in an autoclave under air (10 bar). ^[f] 2.5 days.

The optimized catalytic system consists of 5 mol % of $[\text{RuCl}_2(p\text{-cymene})]_2$ (**30**), 1.1 equivalents of potassium acetate and *n*-butanol as the solvent under an ambient pressure of oxygen. Depending on the price gap between the usually more valuable benzoic acid component and the acrylic reaction partner the ratio between **21** and **45** can be customized, giving higher yields for higher benzoic acid loadings (entries 1, 3 and 4).

3.1.2 Scope of Ruthenium(II)-Oxidase Catalyzed Formation of Phthalides

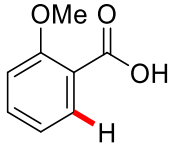
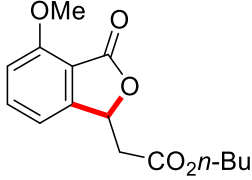
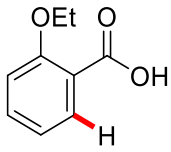
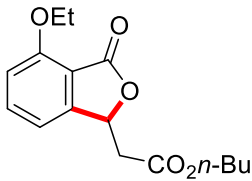
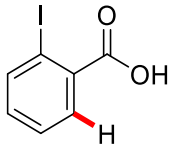
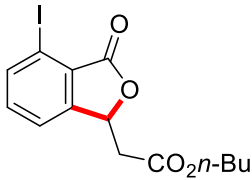
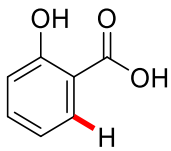
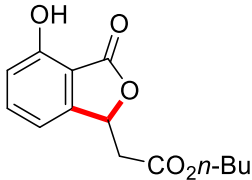
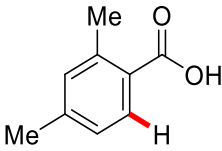
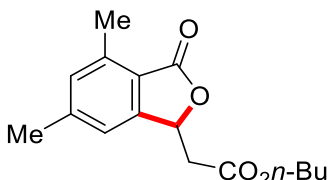
With these optimized conditions in hand, the scope for differently substituted benzoic acids was tested. The reaction smoothly proceeded with alkyl, aryl and ether substituents in the *ortho*-position (entries 1-4, 7 and 8), selectively forming the phthalides (**47**) in moderate to good yields. Reactive iodo, bromo and hydroxyl substituents (entries 5, 6 and 8) were tolerated under the reaction conditions, demonstrating the selectivity of the ruthenium catalyst for the activation of C–H bonds and giving access to *post*-synthetic modifications.

Table 6: Scope of the ruthenium(II)-oxidase alkenylation of benzoic acid (**21**) with *ortho*-substituents.

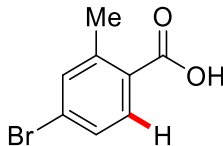
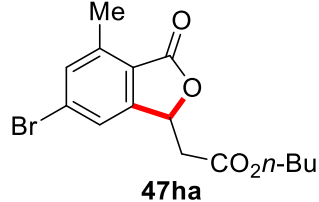


Entry	Benzoic acid	Product	Yield [%] ^[a]
1	<p>21a</p>	<p>47aa</p>	74
2	<p>21b</p>	<p>47ba</p>	60

Results and Discussion

Entry	Benzoic acid	Product	Yield [%] ^[a]
3	 21c	 47ca	51
4	 21d	 47da	49
5	 21e	 47ea	63
6	 21f	 47fa	27
7	 21g	 47ga	72

Results and Discussion

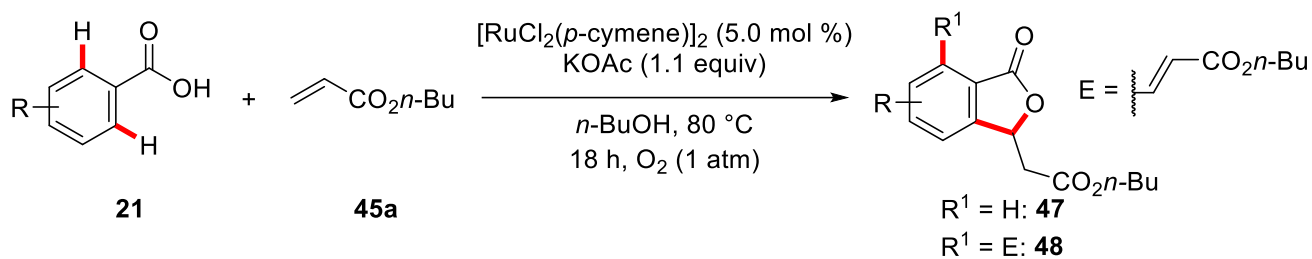
Entry	Benzoic acid	Product	Yield [%] ^[a]
8	 21h	 47ha	71

^[a] Reaction conditions: **21** (1.0 mmol), **45a** (1.5 mmol), [RuCl₂(*p*-cymene)]₂ (**30**) (5.0 mol %), KOAc (1.0 mmol), *n*-BuOH (3.0 mL), O₂ (1.0 atm), 80 °C, 18 h. Yield of isolated product.

When benzoic acids without 2-substituent were subjected to the reaction conditions, regioisomers and double alkenylations were observed. A methyl substituent in the *meta*-position of the benzoic acid selectively guides the catalyst to the sterically less crowded 6-position, without the formation of any double alkenylated species (Table 7, entry 1). When a Lewis basic methoxy group is installed in the 3-position of the benzoic acid three products were observed, with the alkenylated 5-methoxy phthalide **48jaa** being the major product (entry 2). For the *mono*-functionalized products the 2-position is preferentially alkenylated, indicating that the coordinative effect of the methoxy substituent had a stronger influence than its repulsive effects. Symmetrical 4-substituted and unsubstituted benzoic acid gave mixtures of *mono*- and *di*-functionalization with the singly functionalized phthalide as the major product (entries 3 and 4).

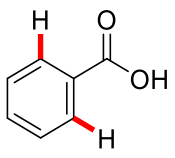
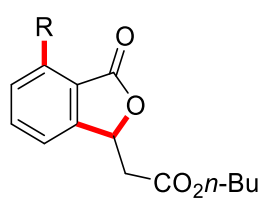
Results and Discussion

Table 7: Scope of the ruthenium(II)-catalyzed alkenylation of benzoic acids **21** without *ortho*-substituents.



Entry	Benzoic acid	Product	Yield 47 [%] ^[a]	Yield 48 [%] ^[a]
1			47ia : 47	48iaa : 0
2			47ja : 28	48jaa : 33
			47ka : 33	48kaa : 28

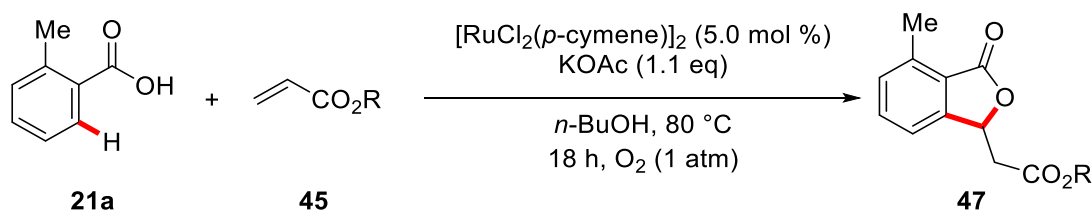
Results and Discussion

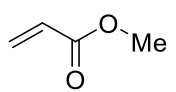
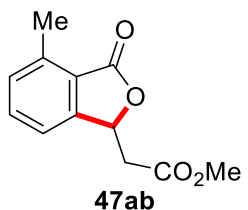
Entry	Benzoic acid	Product	Yield 47 [%] ^[a]	Yield 48 [%] ^[a]
4	 211	 47la	47la : 43	48laa : 23

^[a] Reaction conditions: **21** (1.0 mmol), **45a** (1.5 mmol), [RuCl₂(*p*-cymene)]₂ (**30**) (5.0 mol %), KOAc (1.0 mmol), *n*-BuOH (3.0 mL), O₂ (1.0 atm), 80 °C, 18 h. Yield of isolated product.

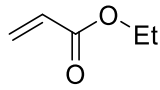
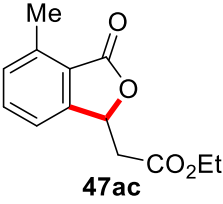
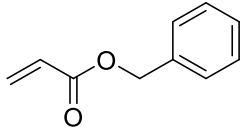
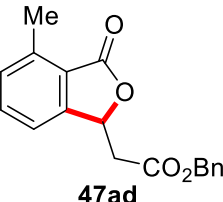
Other electron-withdrawing substituents, like chloride, fluoride, trifluoromethyl, thioether, keto, nitro or amino groups, at the benzoic acid component gave yields below two turnovers under the reaction conditions. When the acrylic ester component is varied, several alkyl substituted acrylic esters gave the desired products (entries 1 and 2). Benzyl acrylate showed good reactivity, but was accompanied by a transesterification side-reaction with the solvent (entry 3). Aromatic acrylates, acrylonitrile, methyl vinyl ketone and simple alkenes did not lead to the desired products.

Table 8: Scope of the acrylic ester component **45**.



Entry	Acrylic ester	Product	Yield [%] ^[a]
1	 45b	 47ab	72

Results and Discussion

Entry	Acrylic ester	Product	Yield [%] ^[a]
2	 45c	 47ac	62
3	 45d	 47ad	69 ^[b]

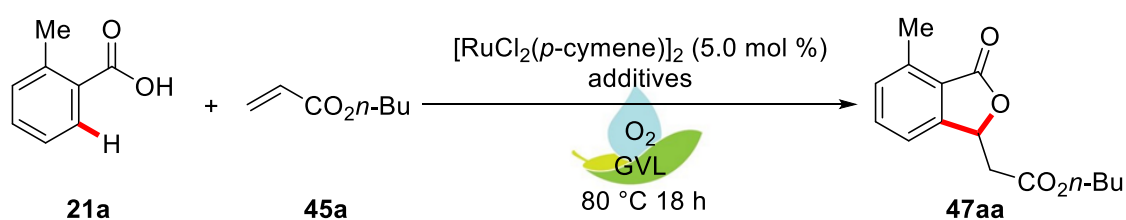
^[a] Reaction conditions: **21a** (1.0 mmol), **45** (1.5 mmol), [RuCl₂(*p*-cymene)]₂ (5.0 mol %), KOAc (1.0 mmol), *n*-BuOH (3.0 mL), O₂ (1.0 atm), 80 °C, 18 h. Yield of isolated product. ^[b] Isolated as a mixture with the transesterification product **47aa**.

In summary, a method for the alkenylation of benzoic acids with acrylates that uses oxygen as the sole oxidant was developed. The reaction conditions tolerated various substitution patterns at the arene moiety, including synthetically useful functional groups like halogens. Nevertheless, there are two major drawbacks concerning the solvent that leave room for improvement. First, the oxidation of the solvent to butanoic acid, that was observed as a side reaction. Second, *n*-butanol has a very low flash point point of 35 °C. In combination with the oxygen atmosphere and a temperature of 80 °C this is a potential safety hazard, that should be avoided, when possible.

3.1.3 Optimization Studies for Ruthenium(II)-Oxidase in Renewable Solvents

Given the findings of the previous study, we tried to overcome these drawbacks by optimizing the ruthenium(II)-oxidase system for the synthesis of phthalides in green and renewable solvents. Replacing the alcoholic solvent with environmentally benign γ -valerolactone (**77**) already improved the yields compared to the former study (Table 9, entry 1). Mesityl carboxylate as the ligand and base or reduced acetate loadings resulted in decreased product formation (entries 2-4). In analogy to the previous study, the ratio between substrates **21a** and **45a** showed a strong effect, favoring an excess of the benzoic acid (entry 5). This concentration effect was compensated by the addition of equivalent amounts of acetic acid, which led to better yields (entry 6), that were further improved by raising the concentration of the reagents to 1.0 M (entries 6, 8 and 9). Entry 7 confirmed potassium acetate to be crucial for the reactivity.

Table 9: Optimization of the additives for ruthenium(II)-oxidase in γ -valerolactone (**77**).



Entry	21a/45a [mmol]	M	Additive 1 [mmol]	Additive 2 [mmol]	Yield [%] ^[a]
1	1.0/1.5	0.3	KOAc (1.0)	---	75
2	1.0/1.5	0.3	KO ₂ CMes (1.0)	---	47
3 ^[b]	1.0/1.5	0.3	---	---	37
4	1.0/1.5	0.3	KOAc (0.5)	---	65
5	2.0/1.0	0.3	KOAc (1.0)	---	83
6	1.0/1.5	0.3	KOAc (1.0)	HOAc (1.0)	81
7	1.0/1.5	0.3	---	---	---
8	1.0/1.5	1.0	KOAc (1.0)	---	88

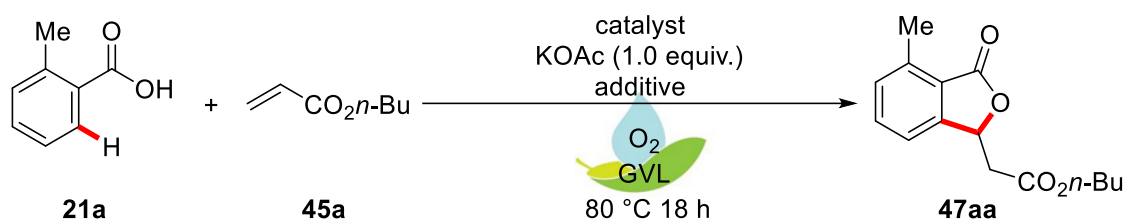
Results and Discussion

Entry	21a/45a [mmol]	M	Additive 1 [mmol]	Additive 2 [mmol]	Yield [%] ^[a]
9	1.0/1.5	1.0	KOAc (1.0)	HOAc (1.0)	90

^[a] Reaction conditions: **21a**, **45a**, [RuCl₂(*p*-cymene)]₂ (**30**) (5.0 mol %), additives, GVL (**77**) (M), O₂ (1.0 atm), 80 °C, 18 h. Yield of isolated product. ^[b][Ru(O₂CMes)₂(*p*-cymene)] (**99**) (10 mol %) as the catalyst.

Reduced loadings of the precatalyst resulted in lower yields and incomplete conversion of the starting materials (Table 10, entry 1), while no reaction was observed in its absence (entry 2). Other ruthenium(II) and ruthenium(III) sources were shown to be inactive under the reaction conditions (entries 3 and 4).

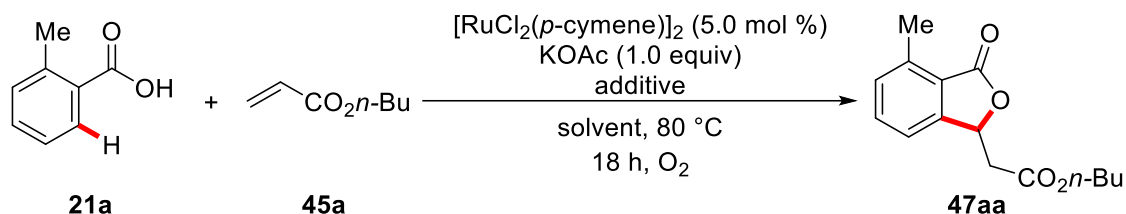
Table 10: Optimization of the catalysts the ruthenium(II)-oxidase in γ -valerolactone (**77**).



Entry	21a/45a [mmol]	M	Catalyst [mol %]	Additive [mmol]	Yield [%] ^[a]
1	1.0/1.5	1.0	[RuCl ₂ (<i>p</i> -cymene)] ₂ (30) (2.5)	HOAc (1.0)	30
2	1.0/1.5	0.3	---	---	---
3	1.0/1.5	1.0	[RuCl ₂ (cod)] _n (10)	---	---
4	1.0/1.5	1.0	RuCl ₃ ·xH ₂ O (10)	---	traces

^[a] Reaction conditions: **21a**, **45a**, catalyst (5.0 mol %), KOAc (1.0 mmol), additive, GVL (**77**) (M), O₂ (1.0 atm), 80 °C, 18 h. Yield of isolated product.

The reaction proved to be tolerant to water (Table 11, entry 1) and other green and renewable reaction media, such as L-ethyl lactate, 2-methyl THF and tetrahydrofuryl alcohol were shown to be suitable solvents for the ruthenium(II)-oxidase catalysis (entries 2-4).

Table 11: Ruthenium(II)-oxidase in green solvents.

Entry	21a/45a [mmol]	M	Solvent	Additive [mmol]	Yield [%] ^[a]
1	1.0/1.5	0.3	GVL (77)/H ₂ O (2:1)	---	49
2	1.0/1.5	1.0	L-ethyl lactate (94)	HOAc (1.0)	59
3	1.0/1.5	1.0	2-methyl THF (88)	HOAc (1.0)	81
4	1.0/1.5	1.0	tetrahydrofuryl alcohol	HOAc (1.0)	82

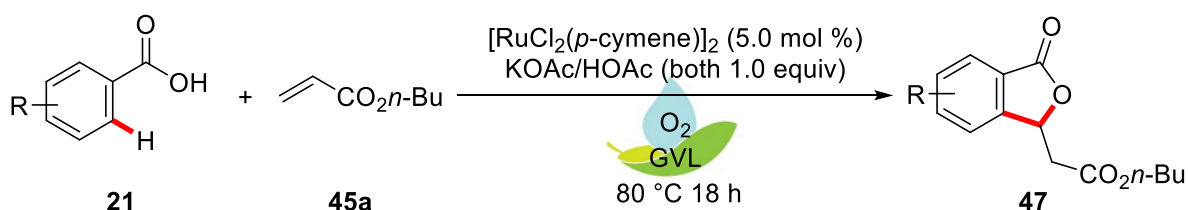
^[a] Reaction conditions: **21a**, **45a**, [RuCl₂(*p*-cymene)]₂ (**30**) (5.0 mol %), KOAc (1.0 mmol), additive, solvent (M), O₂ (1.0 atm), 80 °C, 18 h. Yield of isolated product.

The optimized reaction conditions consisted of 5.0 mol % of the [RuCl₂(*p*-cymene)]₂ (**30**) catalyst and equimolar amounts of acetic acid and potassium acetate as a 1.0 M solution in γ -valerolactone (**77**) under an ambient atmosphere of oxygen. The use of this green and environmentally benign solvent was the solution for both of the major drawbacks of the reaction in *n*-butanol. The higher flash point of 96 °C dramatically increased the safety profile of the reaction. In addition, γ -valerolactone (**77**) was stable against oxidation.

3.1.4 Scope of Ruthenium(II)-Oxidase in Biomass Derived γ -Valerolactone (77)

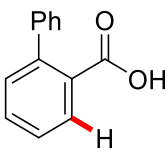
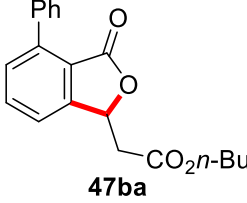
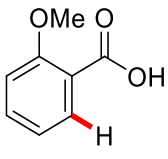
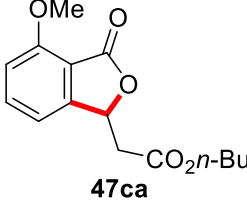
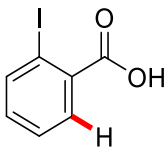
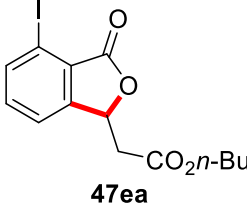
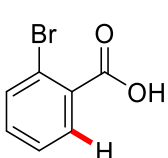
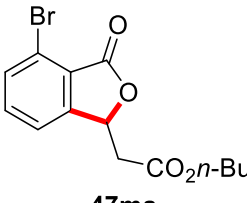
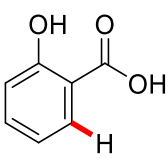
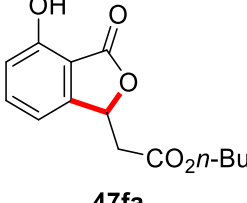
With these optimized conditions in hand, the scope for the ruthenium(II) oxidase in γ -valerolactone (77) was investigated. In general, the improved catalytic system gave higher yields with the benzoic acid **21** as the limiting component and several functional groups were tolerated under the reaction conditions. This scope was largely performed by Marcel Emir Baumert during his bachelor thesis.^[95] The benchmark system, consisting of 2-methylbenzoic acid (**21a**) and *n*-butyl acrylate (**45a**), performed effectively giving **47aa** in excellent quantities of 90% (cf. 74% in *n*-butanol) and scaling the reaction up to 5 mmol provided the product in almost quantitative 97% yield (Table 12, entry 1). As in the former study, alkyl-, aryl- and ether-groups, same as bromine and iodine (entries 2-5, 10, 11, 13, 16) were well tolerated. Hydroxyl-, mesyl- and tosyl-substituents delivered the products in moderate yields, thereby expanding the opportunities for *post*-synthetic modifications (entries 6-8). Aromatic and enolizable aliphatic ketones worked smoothly, delivering the products in very good yields (entries 9 and 15). Challenging dimethylamino groups and natural occurring vanilic acid were tolerated under the reaction conditions (entries 14 and 17). Steric effects dominated the stereoselectivity of *meta*-functionalized benzoic acids (entries 13-15). Even potentially coordinating methoxy groups or ketones showed the exclusive functionalization at the 6-position. Simple benzoic acid and symmetrical 4-dimethylaminobenzoic acid gave good yields as mixture of *mono*- and *di*-functionalized products, while the electron-rich 3,4,5-trimethoxy substituted benzoic gave the single functionalization product in almost quantitative yield (entries 16, 17 and 18).

Table 12: Ruthenium(II) oxidase scope of benzoic acids (**21**).

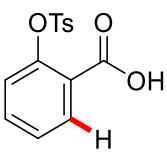
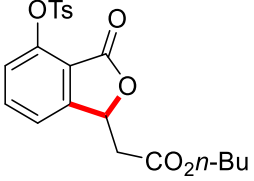
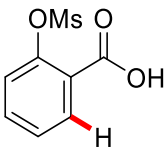
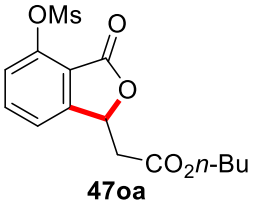
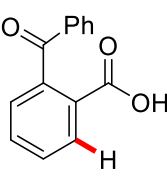
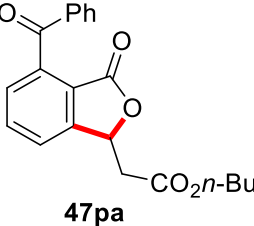
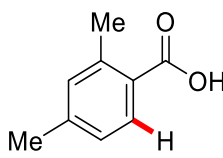
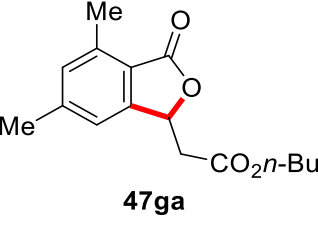
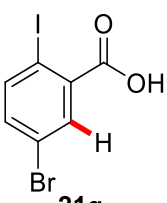
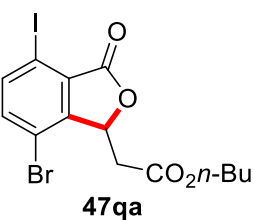


Entry	Benzoic acid	Product	Yield [%] ^[a]
1	<p style="text-align: center;">21a</p>	<p style="text-align: center;">47aa</p>	90 (5 mmol scale: 97)

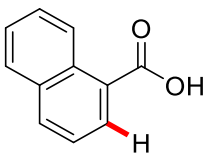
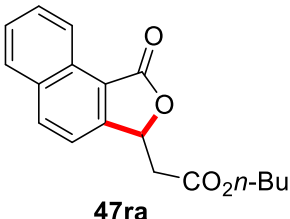
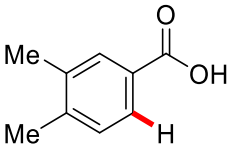
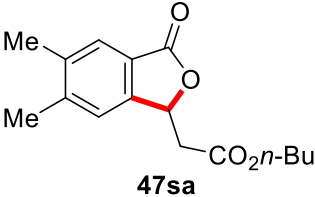
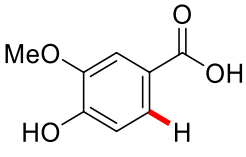
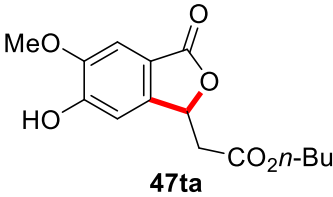
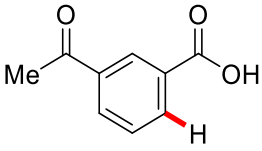
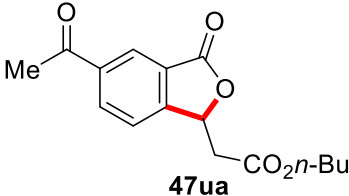
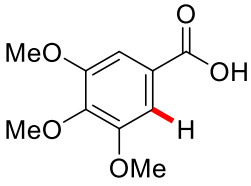
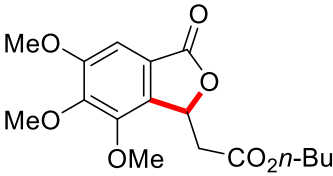
Results and Discussion

Entry	Benzoic acid	Product	Yield [%] ^[a]
2	 21b	 47ba	65
3	 21c	 47ca	60
4	 21e	 47ea	54
5	 21m	 47ma	70
6	 21f	 47fa	52

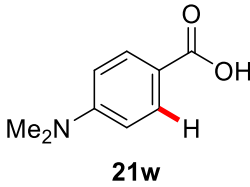
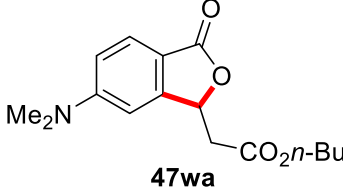
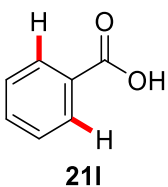
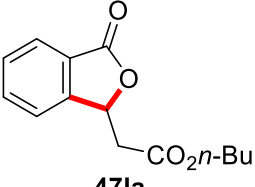
Results and Discussion

Entry	Benzoic acid	Product	Yield [%] ^[a]
7	 21n	 47na	49
8	 21o	 47oa	55
9	 21p	 47pa	82
10	 21g	 47ga	95
11	 21q	 47qa	71

Results and Discussion

Entry	Benzoic acid	Product	Yield [%] ^[a]
12	 21r	 47ra	59
13	 21s	 47sa	79
14	 21t	 47ta	56
15	 21u	 47ua	84
16	 21v	 47va	96

Results and Discussion

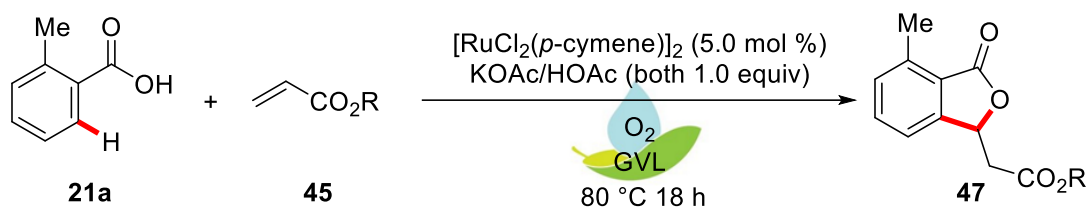
Entry	Benzoic acid	Product	Yield [%] ^[a]
17	 <p style="text-align: center;">21w</p>	 <p style="text-align: center;">47wa</p>	59 (48wa : 14)
18	 <p style="text-align: center;">21l</p>	 <p style="text-align: center;">47la</p>	40 (48la : 26)

^[a] Reaction conditions: **21** (1.0 mmol), **45a** (1.5 mmol), [RuCl₂(*p*-cymene)]₂ (**30**) (5.0 mol %), KOAc (1.0 mmol), HOAc (1.0 mmol), GVL (**77**) (1.0 mL), O₂ (1.0 atm), 80 °C, 18 h. Yield of isolated product.

The variation of the acrylic ester component **45** showed an ample and expanded scope (Table 13). Several linear and branched alkyl substituted acrylates smoothly formed the desired products in moderate to very good yields (entries 1-4), while linear and cyclic ethers gave very good yields (entries 6 and 7). In contrast to the former conditions, benzyl substituted ethers could be isolated in pure form and excellent yields. A chiral, menthol derived acrylate showed good reactivity, but here the stereoinformation showed almost no effects on the diastereomeric ratio of the product (entry 9). The outstanding selectivity of the ruthenium(II)-oxidase for acrylic alkenes is highlighted by entry 10, that offered an additional terminal aliphatic double bond, that stayed intact during the reaction.

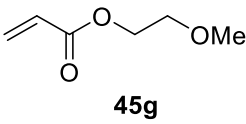
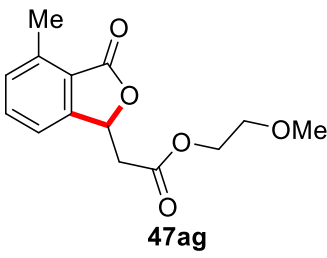
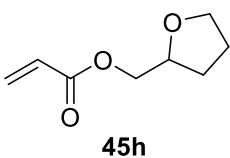
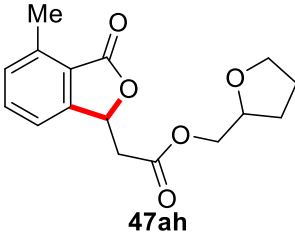
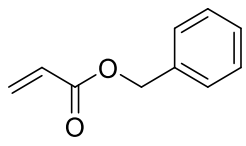
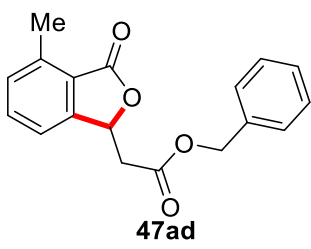
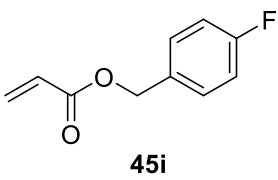
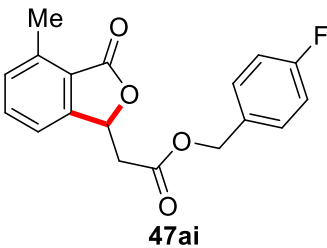
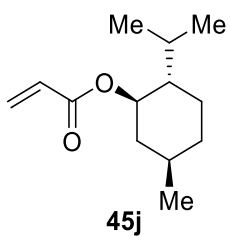
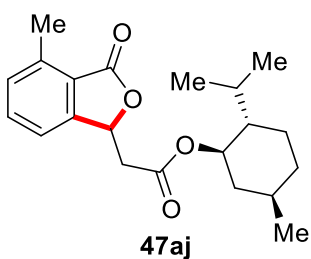
Results and Discussion

Table 13: Ruthenium(II) oxidase scope of acrylic esters (**45**).

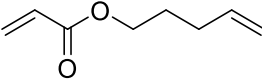
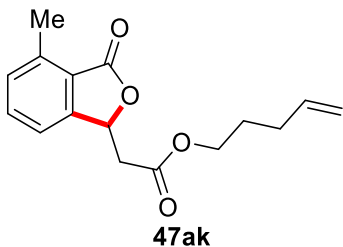


Entry	Acrylic ester	Product	Yield [%] ^[a]
1	<p style="text-align: center;">45b</p>	<p style="text-align: center;">47ab</p>	61
2	<p style="text-align: center;">45c</p>	<p style="text-align: center;">47ac</p>	83
3	<p style="text-align: center;">45e</p>	<p style="text-align: center;">47ae</p>	68
4	<p style="text-align: center;">45f</p>	<p style="text-align: center;">47af</p>	61

Results and Discussion

Entry	Acrylic ester	Product	Yield [%] ^[a]
5	 45g	 47ag	85
6	 45h	 47ah	82
7	 45d	 47ad	69 (5 mmol scale: 92)
8	 45i	 47ai	92
9	 45j	 47aj	69

Results and Discussion

Entry	Acrylic ester	Product	Yield [%] ^[a]
10	 45k	 47ak	62

^[a] Reaction conditions: **21a** (1.0 mmol), **45** (1.5 mmol), [RuCl₂(*p*-cymene)]₂ (**30**) (5.0 mol %), KOAc (1.0 mmol), HOAc (1.0 mmol), GVL (**77**) (1.0 mL), O₂ (1.0 atm), 80 °C, 18 h. Yield of isolated product.

The structure of **47ad** was unambiguously confirmed by x-ray crystallographic analysis of single crystals obtained by slow solvent evaporation of a diethylether solution. **47ad** crystallized in a monoclinic space group, with both enantiomers in the asymmetric unit.

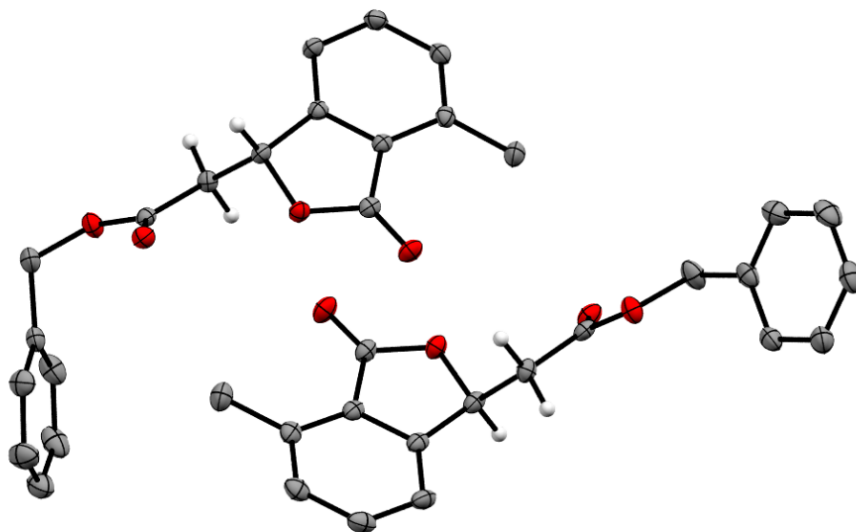


Figure 2: ORTEP plot of the crystal structure of **47rb**. Ellipsoids were drawn at a 50% probability level. Selected hydrogens were omitted for clarity.

With γ -valerolactone (**77**), a highly effective, green and renewable solvent was introduced to the field of ruthenium-catalyzed C–H activations. With the benzoic acid component **21** as the limiting reagent, the yields were generally higher compared to *n*-butanol and the scope of the ruthenium(II)-oxidase was

largely broadened, *inter alia* by valuable functional groups, such as amines and hydroxyl based mesyl- and tosyl-groups.

3.1.5 Evaluation of Ruthenium(II)-Oxidase Reactivity in Flow

Organic reactions have traditionally been performed in batch reactors. Recently, continuous flow reactions and reactors have gained a lot of attention, because they inherently increase the safety profile of a reaction.^[96] From the point of the synthetic organic chemist flow chemistry offers great possibilities for effective mixing of different phases, like the highly effective release of reaction gases at specific points and over long distances is possible, as well as the use of heterogenous catalysts that react with the reagents of the solution that flows by.^[97]

Since the ruthenium(II)-oxidase is using oxygen as the sole oxidant, the chances of applying continuous flow techniques for ruthenium-catalyzed oxidative transformations were evaluated, using the alkenylation of benzoic acids as the model system. A Vapourtec easy-MedChem flow system equipped with a tube-in-tube gas-liquid reactor, which releases the gas *via* a semi-permeable inner membrane tube was used. Following the flow setup (Figure 3) the reaction solution is pumped into the heated tube-in-tube reactor, where pure oxygen is released to the solution. Behind the reactor a back pressure regulator, which allows to adjust the reactor pressure, was installed, followed by an automated product collector.

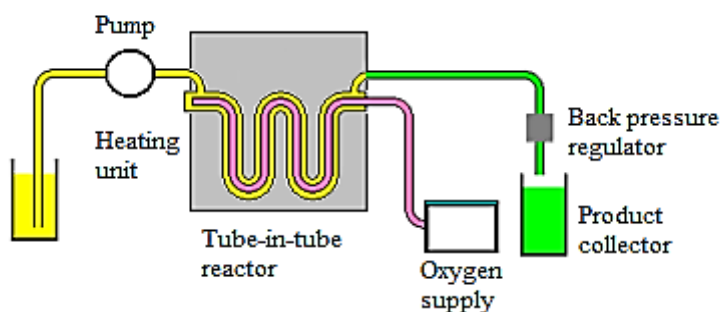


Figure 3: Tube-in-tube gas-liquid reactor flow setup.^[98]

In the second reactor setup (Figure 4), the substrate solution was pumped through the unheated gas-liquid reactor, where the reaction solution is saturated with oxygen at room temperature. Downstream a second reactor, equipped with filling material that creates a turbulent flow inside the reactor, was connected. Behind the second reactor the back pressure regulator and the automated product collector were installed.

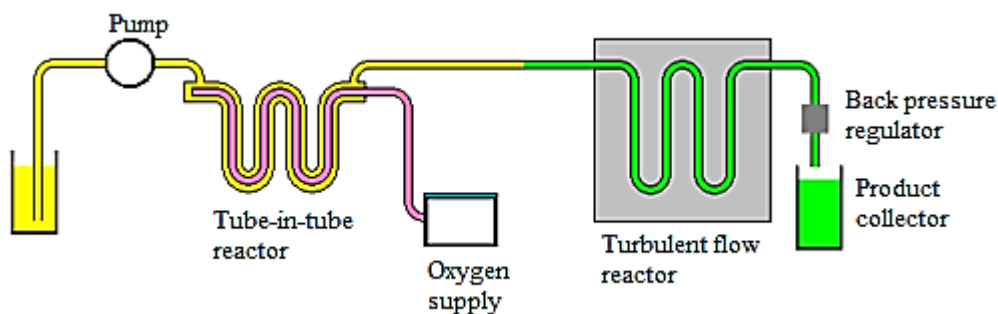
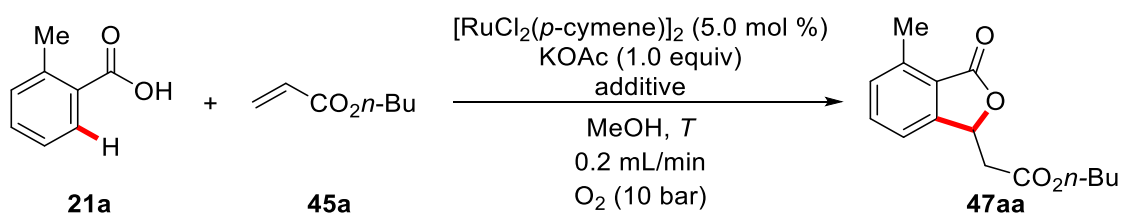


Figure 4: Turbulent flow reactor setup. ^[98]

The study was commenced by the use of an *in situ* formed catalytic system consisting of 5.0 mol % of $[\text{RuCl}_2(p\text{-cymene})]_2$ and an equivalent amount of potassium acetate in methanol as the solvent (Table **14**). A reactor pressure of ~ 1.4 bar was proven to be inefficient (entries 1 and 2). Raising the pressure to ~ 8.0 bar resulted in increased yields of around 40%, that were not affected by the addition of additional acid (entries 3 and 4). Lowering the oxygen pressure resulted in a drop in reactivity (entry 5). Higher concentrations gave a slightly better yields, but were accompanied by solubility issues (entry 6), while faster flow rates resulted in a drop in yield (entry 7). Raising the temperature to 120 °C positively affected the reactivity (entry 8). To ensure the effectivity of the gas supply of the gas-liquid reactor, the solvent was prepurged with O_2 and the reaction was carried out without additional oxygen supply, resulting in lower yields (entry 9).

Table 14: Optimization of the ruthenium(II)-oxidase catalyzed alkenylation in flow I.



Entry	Additive (equiv)	M	T [°C]	Pressure	Yield [%] ^[a]
1	---	0.3	80	~ 1.4	12
2	---	0.3	100	~ 1.4	14
3	---	0.3	100	~ 8.0	41

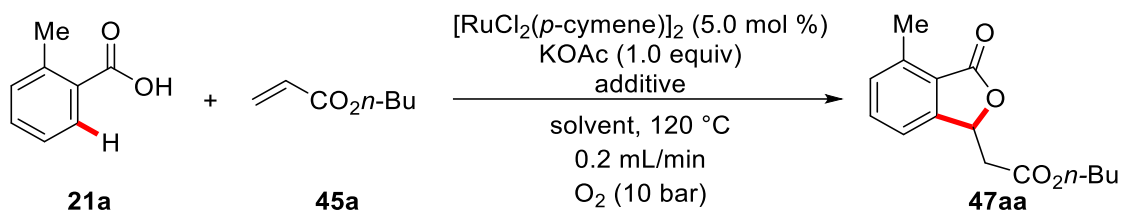
Results and Discussion

Entry	Additive (equiv)	M	T [°C]	Pressure	Yield [%] ^[a]
4	HOAc (1.0)	0.3	100	~8.0	39
5 ^[b]	---	0.3	100	~8.0	35
6	---	1.0	100	~8.0	43
7 ^[c]	---	1.0	100	~8.0	23
8	---	0.3	120	~8.0	55 (48)
9 ^[d]	---	0.3	120	~8.0	23

^[a] Reaction conditions: **21a** (1.0 mmol), **45a** (1.5 mmol), [RuCl₂(*p*-cymene)]₂ (**30**) (5.0 mol %), KOAc (1.0 mmol), additive, *n*-BuOH (M), O₂ (10 bar), T, 0.2 mL/min. Yield were determined by GC analysis vs. *n*-dodecane as internal standard. Isolated yields are given in parentheses.

^[b] O₂ (5.0 bar). ^[c] Flow rate: 0.5 mL/min. ^[d] No O₂ pressure, O₂ purged methanol used.

When *n*-butanol was applied as solvent reactivity comparable to methanol was observed (Table 15, entry 1). The use of the well-defined ruthenium mesitylate catalyst instead of the *in-situ* formed acetate complex gave lower yields, that could be raised by the addition of acetic acid (entries 2 and 3). Performing the reaction in the turbulent reactor setup gave diminished yields (entries 4 and 5). Since the use of pure *n*-butanol as solvents showed poor solubility especially for the acetate component, the solvent was changed to a *n*-butanol:methanol:water mixture, resulting in a homogenous solution of all components (entries 5-12). The use of the turbulent reaction setup showed low reactivity (entry 5), while the standard setup provided good yields, that were hardly affected by the addition of acetic acid (entries 6 and 7). Simple ruthenium(III) chloride as the catalyst did not result in the formation of product **47aa** (entry 9). Raising the temperature, lowering the flow rate to 0.1 mL/min or increasing the acrylate concentration showed somehow diminished yields (entries 8, 10 and 11). A γ -valerolactone (**77**):water mixture as solvent gave low yield, while pure GVL (**77**) could not be used due to unsatisfactory solubility properties.

Table 15: Optimization of the ruthenium(II)-oxidase catalyzed alkenylation in flow II.

entry	Additive (equiv)	Solvent	M	Yield [%] ^[a]
1	---	<i>n</i> -BuOH	0.3	54 (53)
2 ^[b]	---	<i>n</i> -BuOH	0.3	28
3 ^[b]	HOAc (1.0)	<i>n</i> -BuOH	0.3	41
4 ^[c]	---	<i>n</i> -BuOH	0.3	35
5 ^[c]	---	<i>n</i> -BuOH:MeOH:H ₂ O (5:1:1)	0.3	29
6	---	<i>n</i> -BuOH:MeOH:H ₂ O (5:1:1)	0.3	74 (71)
7	HOAc (1.0)	<i>n</i> -BuOH:MeOH:H ₂ O (5:1:1)	0.3	76 (71)
8 ^[d]	---	<i>n</i> -BuOH:MeOH:H ₂ O (5:1:1)	0.3	59
9 ^[e]	---	<i>n</i> -BuOH:MeOH:H ₂ O (5:1:1)	0.3	traces
10 ^[f]	---	<i>n</i> -BuOH:MeOH:H ₂ O (5:1:1)	0.3	32
11 ^[g]	---	<i>n</i> -BuOH:MeOH:H ₂ O (5:1:1)	0.3	62
12	---	<i>n</i> -BuOH:MeOH:H ₂ O (2:1:1)	0.5	48
13	---	GVL (77): H ₂ O (3:1)	0.5	28

^[a] Reaction conditions: **21a** (1.0 mmol), **45a** (1.5 mmol), [RuCl₂(*p*-cymene)]₂ (**30**) (5.0 mol %), KOAc (1.0 mmol), additive, *n*-BuOH (M), O₂ (10 bar), 120 °C, 0.2 mL/min. Yield were determined by GC analysis vs. *n*-dodecane as internal standard. Isolated yields are given in parentheses.

^[b] [Ru(O₂CMes)₂(*p*-cymene)] (**99**) (10 mol %), without [RuCl₂(*p*-cymene)]₂ and KOAc.

^[c] Turbulent reactor setup used. ^[d] 140 °C. ^[e] RuCl₃·*n*H₂O (10 mol %) instead of [RuCl₂(*p*-cymene)]₂. ^[f] **45a** (3.0 mmol). ^[g] Flow rate 0.1 mL/min.

This optimization showed, the ruthenium(II)-oxidase to be compatible with the flow setup, although there were several limiting factors. The short reaction time of 75 minutes, is in challenge for the kinetic profile (see 3.1.6.1) of the ruthenium(II)-oxidase, that begins fast and goes slowly to completion. Generally the small reaction scale (1.0 mmol in 3.0 mL of solvent) for the optimization were somewhat

less than perfect for the flow process. For the technical reasons, the reactor needs to be *pre-* and *post-*rinsed with pure solvent resulting in high dilution of the reactants at the beginning and the end. On a larger scale or in continuous flow this dilution effect would be minimized or vanished.

3.1.6 Kinetic and Mechanistic Studies

3.1.6.1 Oxygen Uptake Study and Investigation of the Oxidation Mode

As the next step, the kinetic profile of the reaction was investigated. Given the oxidative nature of the reaction the oxygen consumption was measured. The reaction immediately started after the acrylic ester was added and after 35 minutes a conversion of 60% was observed and of 80% after 110 minutes. Analogous studies in *n*-butanol and without solvent were performed by Dr. Svenja Warratz, showing similar reaction profiles.^[99]

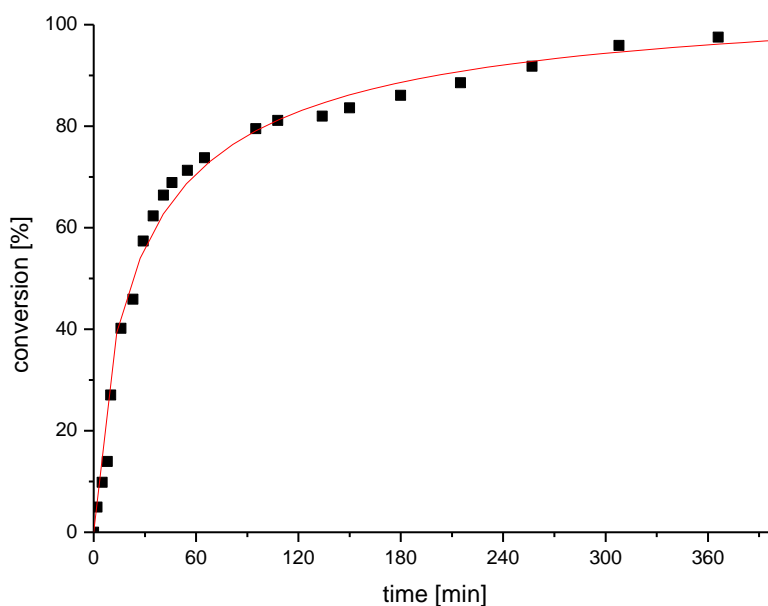
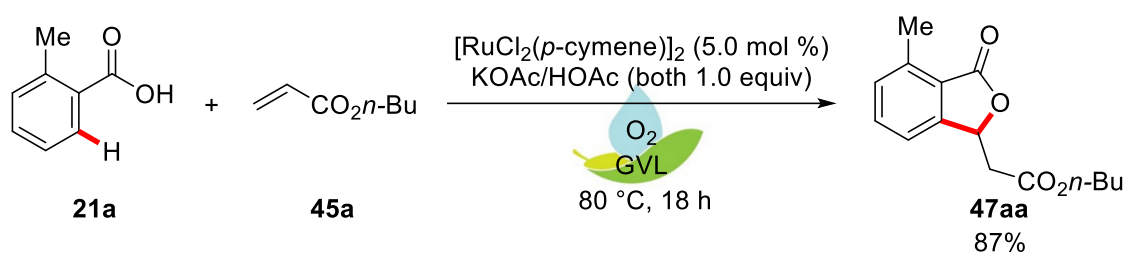
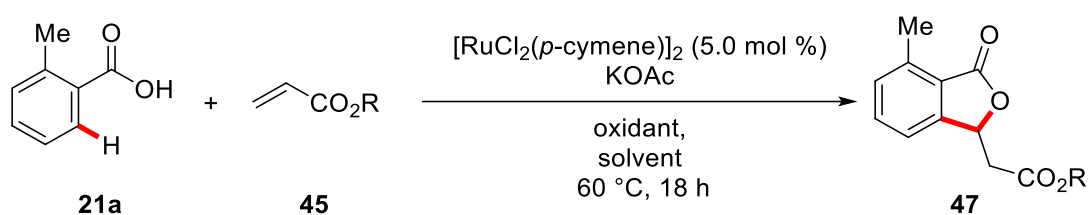


Figure 5: Oxygen uptake of the ruthenium(II)-oxidase alkenylation.

After 18 hours reaction time phthalide **47aa** was isolated in 87% (0.87 mmol), while 0.54 mmol of oxygen were consumed, indicating that oxygen is acting as a four-electron acceptor. Thereby several

scenarios of multinuclear oxygen activations or, more likely, a multistep oxygen activation with a (su)peroxo intermediate are conceivable. In order to test this hypothesis, the reaction was performed under an atmosphere of argon and several representative oxidants were added (Table 16). While *tert*-butyl hydroperoxide and di-*tert*-butyl-peroxide (entries 1 and 2) did not result in the formation of the phthalide **47**, the addition of aqueous hydrogen peroxide solution gave an exothermic reaction accompanied by product formation in moderate yields (entries 3, 4, 5 and 7). Dr. Svenja Warratz further tested potassium superoxide as an oxidant, which resulted in low product formation.^[99]

Table 16: Oxidant suitability study for ruthenium(II)-catalyzed alkenylation.



Entry	R	Solvent	Oxidant	Yield [%] ^[a]
1	Et	MeOH	<i>t</i> -BuOOH	---
2	Et	MeOH	(<i>t</i> -BuO) ₂	---
3	Et	MeOH	H ₂ O ₂ (30%, aq.)	46
4 ^[b]	<i>n</i> -Bu	<i>n</i> -BuOH	H ₂ O ₂ (30%, aq.)	47
5 ^[b,c]	<i>n</i> -Bu	<i>n</i> -BuOH	KO ₂	13
6 ^[b,d]	<i>n</i> -Bu	GVL (77)	H ₂ O ₂ (30%, aq.)	52
7 ^[b]	<i>n</i> -Bu	H ₂ O	H ₂ O ₂ (30%, aq.)	61

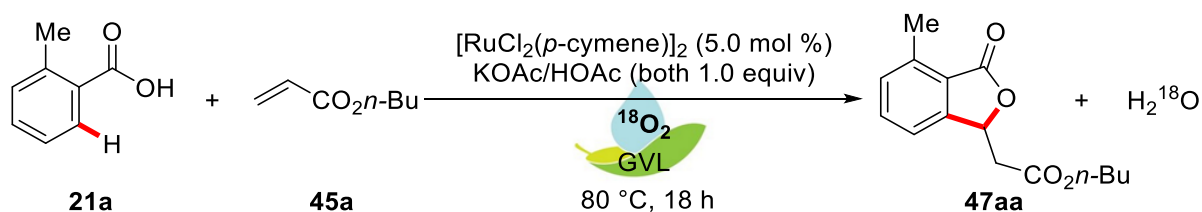
^[a] Reaction conditions: **21a** (2.0 mmol), **45** (1.0 mmol), $[\text{RuCl}_2(p\text{-cymene})]_2$ (**30**) (5.0 mol %), KOAc (1.0 mmol), solvent (M), oxidant (2.0 equiv), Ar or N₂, 60 °C, 18 h. Yield of isolated product. ^[b] 80 °C. ^[c] Reaction performed by Dr. Svenja Warratz. ^[d] HOAc (1.0 equiv) added.

In summary, the experimental data indicated that oxygen is acting as a four-electron oxidant, transferring the electrons in two consecutive two-electron steps. As an intermediate organic peroxides and hydroperoxides could be excluded, while hydrogen peroxide is a potent oxidant. The exothermic profile of the hydrogen peroxide addition makes it likely to be a quasistationary intermediate in the oxidation process that reacts faster than oxygen.

3.1.6.2 Labeled Oxygen Study

Even though the formation of water as the only byproduct is logical and likely to occur, an experimental proof was missing. Therefore, a study using $^{18}\text{O}_2$ as the oxidant was conducted in order to verify the formation H_2^{18}O . Since the direct detection of water is difficult by mass spectrometric methods, a recently developed method was applied in cooperation with Prof. Dr. Konrad Koszinowski.^[100] Here defined amounts of phosphorylchloride were added to the reaction mixture to be hydrolyzed by the formed water. Analysis of the hydrolyzation products $(\text{PO}_2\text{Cl}_2)^-$ and $[(\text{PO}_2\text{Cl}_2)_2\text{H}/\text{Na}]^-$ by ESI-MS allowed to conclude isotope ratios. The reaction was carried out using the standard condition under an ambient atmosphere of normal or labeled oxygen. After the reaction was finished phosphoryl chloride was added to the crude mixture, analyzed by ESI-MS and the products were isolated. As expected the test reaction did not show unnatural amounts of ^{18}O (entry 1). The incorporation of ^{18}O in the hydrolysis product in entry two was 28% and thus lower than expected. This low value is reproduced in entry 3 and is probably due to to exchange reactions between acetate, acetic acid and formed H_2^{18}O . The products of the entries two and three did not show any unnatural incorporation of ^{18}O .

Table 17: Labeled oxygen study.

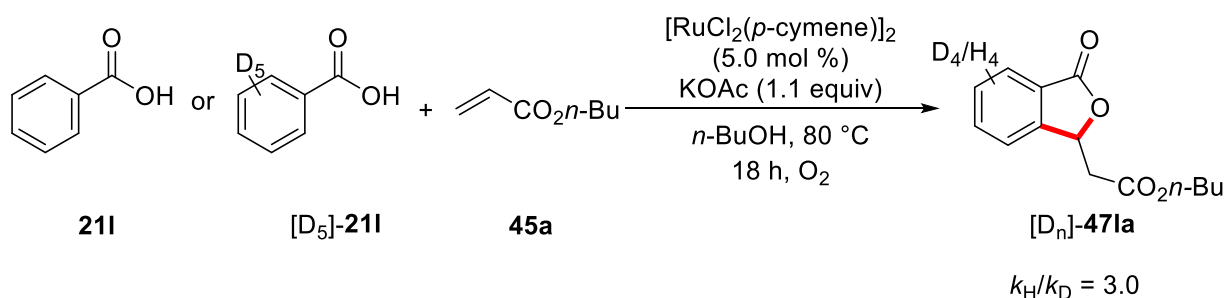


Entry	$^{16}\text{O}_2/^{18}\text{O}_2$	$[\text{P}]^-$ [%] ^[a]	^{18}O in 47aa [%]	Yield [%] ^[b]
1	$^{16}\text{O}_2$	0	0	Not isolated
2	$^{18}\text{O}_2$	28	0	81
3	$^{18}\text{O}_2$	31	0	72

^[a] Percentage of $[\text{P}^{16}\text{O}^{18}\text{OCl}_2]^-$ in $[\text{PO}_2\text{Cl}_2]^-$ ($[\text{P}]^-$). ^[b] Reaction conditions: **21a** (1.0 mmol), **45a** (1.5 mmol), $[\text{RuCl}_2(p\text{-cymene})]_2$ (**30**) (5.0 mol %), KOAc (1.0 mmol), HOAc (1.0 mmol), GVL (**77**) (1.0 mL), O_2 (1.0 atm), 80 °C, 18 h. Yield of isolated product.

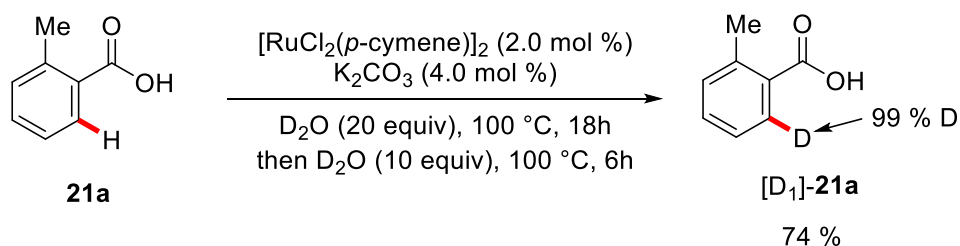
3.1.6.3 Kinetic Isotope Effect (KIE) Studies

In order to gain more information about the mode of the C–H activation, the effect of isotopically labeled substrates on the reaction kinetics were evaluated. Previous studies, performed by Dr. Svenja Warratz, showed a kinetically relevant C–H ruthenation process with a KIE of ~3.0 in *n*-butanol by comparing the reaction rates of [D₅]-benzoic acid ([D₅]-**211**) and non-deuterated benzoic acid (**211**) in independent reactions (Scheme 29).^[99]



Scheme 29: Kinetic isotope effect in *n*-butanol.

To minimize side reactions, *exempli gracia* double alkenylations, 2-methylbenzoic acid with deuterium in the 6-position ([D₁]-**21a**) was prepared by ruthenium(II)-catalyzed hydrogen isotope exchange (HIE) reaction, followed careful purification (Scheme 30).



Scheme 30: Ruthenium-catalyzed hydrogen isotope exchange (HIE) at the 6-position of 2-methylbenzoic acid.

Using GVL (**77**) as the solvent, substrates [D₁]-**21a** and **21a** were subjected to the reaction conditions and the KIE was determined by comparison of the reaction rates of independent reactions. In contrast to former observations the reaction rates were almost identical with a calculated KIE of ~1.0 (Figure 6).

Results and Discussion

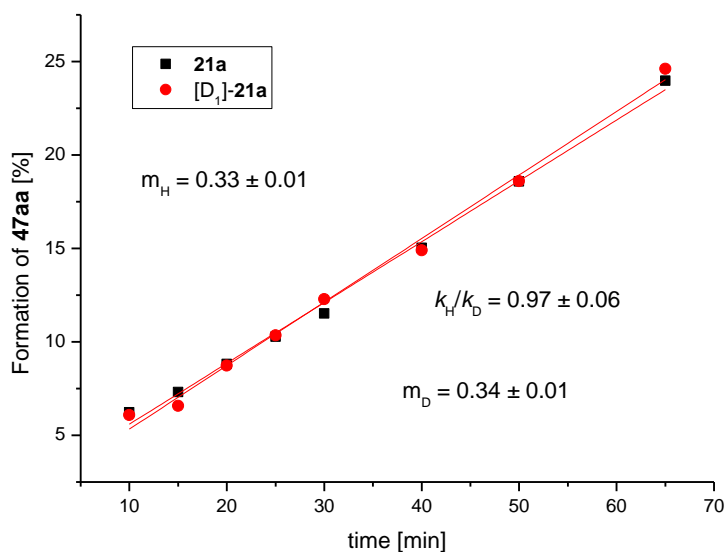
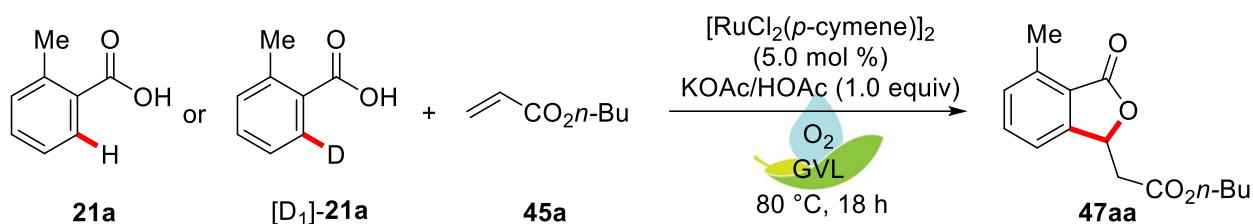


Figure 6: Conversion vs. time plot for the KIE measurement in γ -valerolactone.

To find out, if this change of the KIE results of solvent or the equimolar addition of acetic acid, the study was reperformed under identical conditions, using *n*-butanol instead of γ -valerolactone (**77**) as the solvent (Figure 7). This study showed a strong dependence of the *ortho*-position being a hydrogen or deuterium atom, with a calculated KIE of ~ 2.6 . Comparing both studies, the initial TOF of the reaction of unlabeled **21a** is higher in *n*-butanol ($3.3 \cdot \text{h}^{-1}$) compared to γ -valerolactone ($2.0 \cdot \text{h}^{-1}$), while the initial rate of the labeled **[D₁]-21a** is faster in GVL (**77**) ($2.0 \cdot \text{h}^{-1}$) as compared to the reaction in *n*-butanol ($3.3 \cdot \text{h}^{-1}$).

Results and Discussion

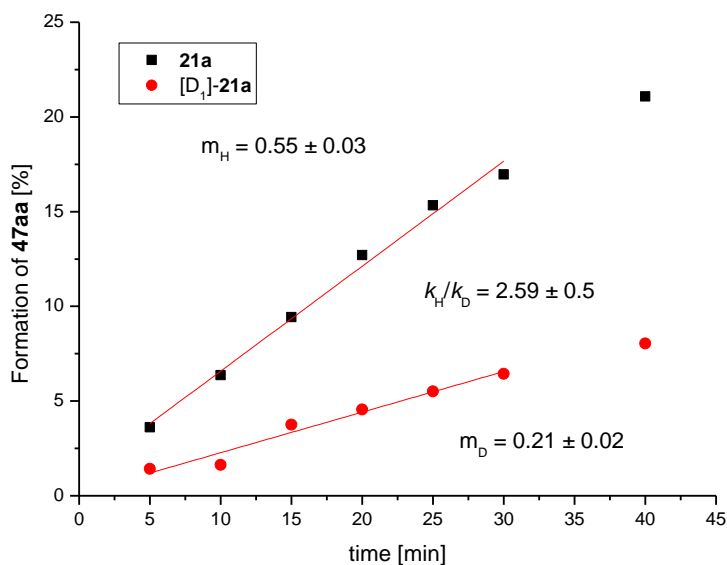
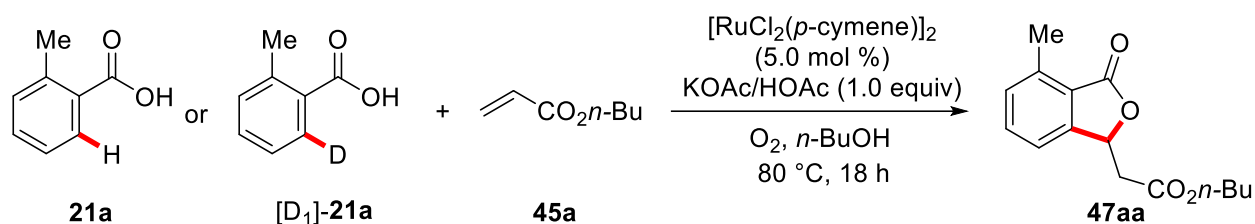
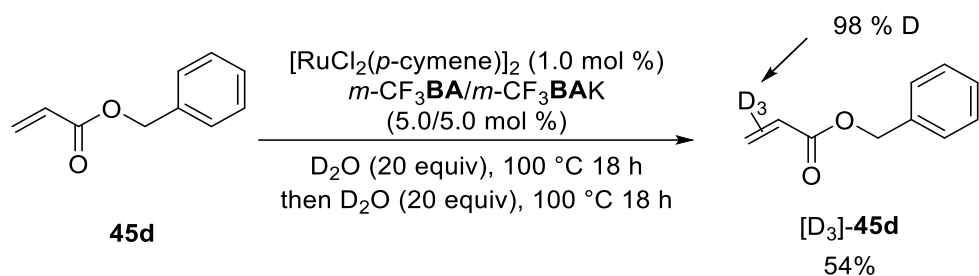


Figure 7: Conversion vs. time plot for the KIE measurement in *n*-butanol.

Within the proposed catalytic cycle (see chapter 3.1.6.5) the coordination of the acrylate is followed by the migration of one of the acrylic protons from the α - to the β -position. To test if this hydrogen migration step is a kinetically relevant event, we studied the kinetic isotope effect of the unlabeled vs. the deuterium labeled acrylic ester. Using the methodology described in chapter 3.3 α,β -labeled benzyl acrylate was synthesized by ruthenium-catalyzed hydrogen isotope exchange between acrylic esters and deuterated water (Scheme 31).

Results and Discussion



Scheme 31: Synthesis of deuterium labeled acrylic esters. **BA** = Benzoic acid.

When the labeled and unlabeled acrylates were submitted to the reaction conditions, almost similar initial rates were observed (Figure 8). With a calculated KIE of ~ 1.1 , these measurements excluded a primary KIE.

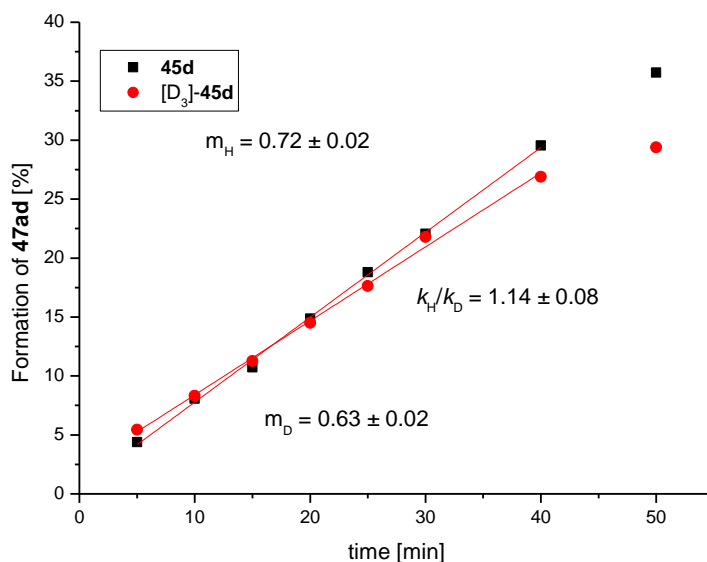
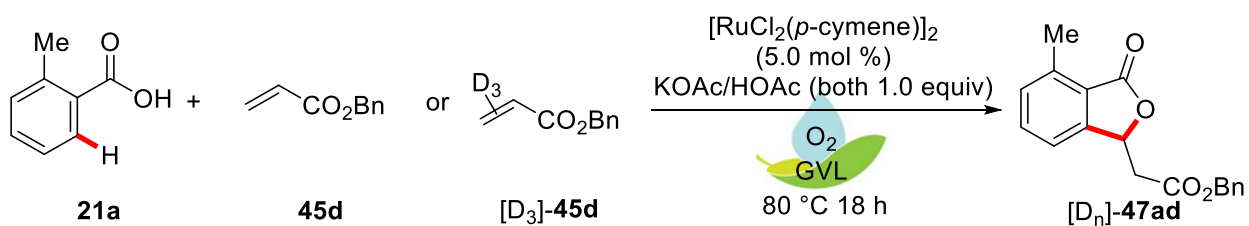


Figure 8: Conversion vs. time plot for the acrylate dependent KIE measurement.

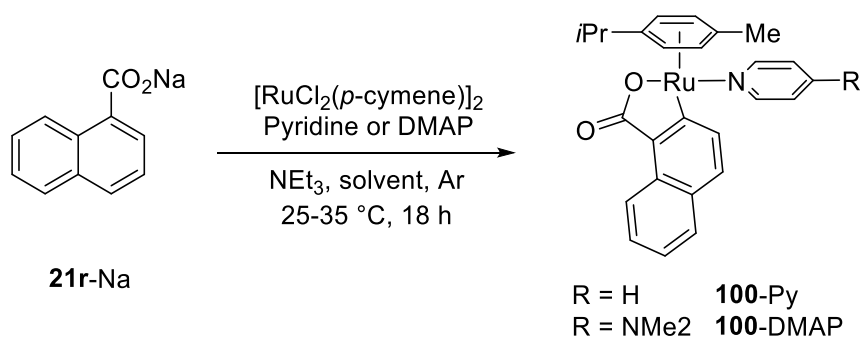
In summary, the kinetic isotope effect measurements showed a solvent dependent kinetically relevant C–H ruthenation event. In *n*-butanol as the reaction medium the C–H activation was the turnover limiting step, while in γ -valerolactone (**77**) no KIE was observed. The insertion and isomerisation step was investigated in γ -valerolactone (**77**), again the measurement did not show a kinetically relevant C–H breaking or forming event.

3.1.6.4 Synthesis of Reaction Intermediates

To gain deeper insights into the ruthenium oxidase reactivity intermediates were synthesized by selectively stopping the reaction at different stages. These intermediates were used to comprehend the elementary steps of this transformation. The general synthesis of this classes of compounds was inspired by studies performed by Dr. Svenja Warratz.^[41d, 99]

The investigations were commenced by the synthesis of the cycloruthenated complexes **100**. Since these complexes have a vacant coordination site, pyridine or DMAP were used as donor ligand in order to obtain a stable structure. While the synthesis was already described using aprotic, apolar CH₂Cl₂ as reaction medium, the isolation of **100-Py** was also possible from methanol and γ -valerolactone (**77**) as the reaction solvents, albeit in somewhat lower yields (Table 18).^[41d, 99]

Table 18: Synthesis of donor stabilized intermediates **100**.



Entry	Solvent	100-Py [%] ^[a]	100-DMAP [%] ^[a]
1	CH ₂ Cl ₂	71	72
2	MeOH	51	---
3	GVL (77)	38	---

^[a] Reaction conditions: [RuCl₂(*p*-cymene)]₂ (0.16 mmol), pyridine/DMAP (0.32 mmol), **21r-Na** (0.82 mmol), NEt₃ (0.40 mL), solvent (5.00 mL), Ar, 25-35 °C, 36 h. Yield of isolated product.

Crystallisation from CH₂Cl₂ overlaid with *n*-hexane at -30 °C delivered crystals of **100-DMAP** suitable for x-ray diffraction crystallography (Figure 9). Complex **100** crystallized with two molecules, stabilized by π -stacking of the DMAP units, in the elementary cell together with one CH₂Cl₂ molecule

and four H₂O units, stabilizing the structure by additional hydrogen bonding. The Ru1 and O1 distance is 2.078 Å and 2.058 Å between Ru1 and C12.

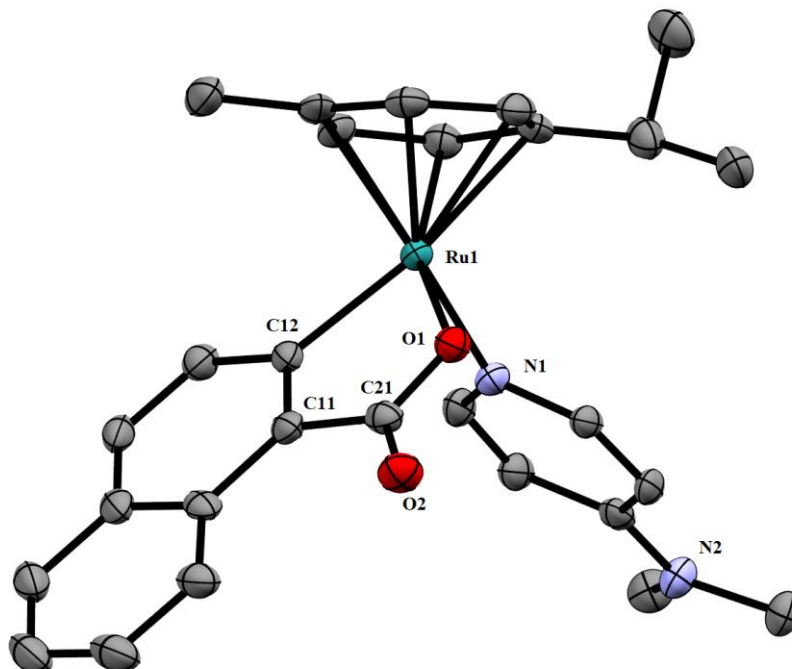
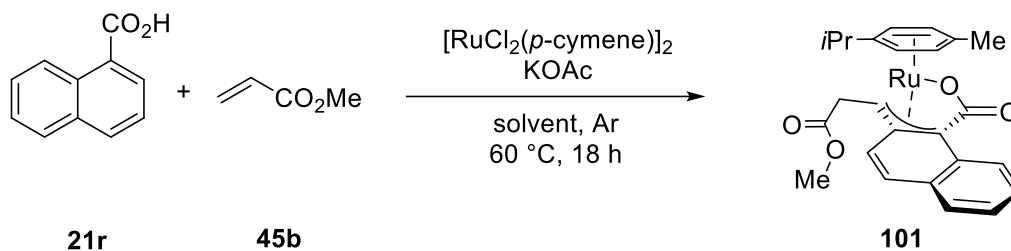


Figure 9: ORTEP plot of the crystal structure of **100-DMAP**. Ellipsoids were drawn at a 50% probability level. H₂O, CH₂Cl₂ and hydrogen atoms were omitted for clarity.

A second intermediate **101** was accessible by performing the reaction with stoichiometric amounts of [RuCl₂(*p*-cymene)]₂ (**30**) in the absence of an oxidant. The yields of this reaction were in the excellent range for different solvents, already indicating the stability of this species (Table 19). In addition, complex **101** has shown to be bench-stable for at least four months.

Table 19: Synthesis of complex **101** in different solvents.

Entry	Solvent	Isolated yield of 101 [%] ^[a]
1	MeOH	96
2	GVL (77)	85
3	PhMe	87 (>99 ^[b])

^[a] Reaction conditions: $[\text{RuCl}_2(p\text{-cymene})]_2$ (**30**) (0.1 mmol), **21r** (0.2 mmol), **45b** (0.2 mmol), potassium acetate (0.4 mmol), MeOH (5.0 mL), Ar, 60 °C, 36 h. Yield of isolated product. ^[b] 0.6 mmol scale.

Crystallization from CH_2Cl_2 overlaid with *n*-hexane at -30 °C delivered crystals of **101** suitable for x-ray crystallography (Figure 10). In contrast to the expectation the ruthenium–carbon bond was not localized at one carbon atom, but C11, C12 and C22 forming an allyl anion type interaction to the ruthenium center allowing complex **101** to reach 18 valence electrons. The bond distances are 2.232 Å for Ru1–C11, 2.189 Å for Ru1–C12 and 2.163 Å for Ru1–C22. The Ru1–O2 bond distance is 2.093 Å, and thus slightly elongated than in the previous ruthenapentacycle **100**.

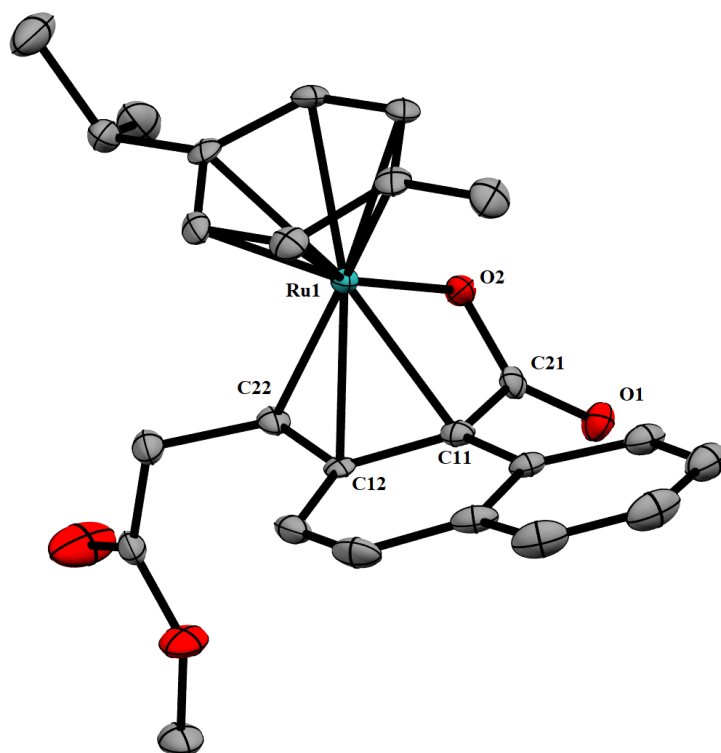
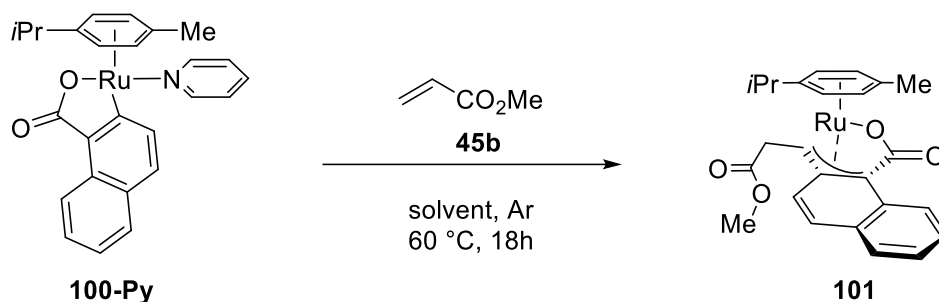


Figure 10: ORTEP plot of the crystal structure of **101**. Ellipsoids were drawn at a 50% probability level. Hydrogen atoms were omitted for clarity.

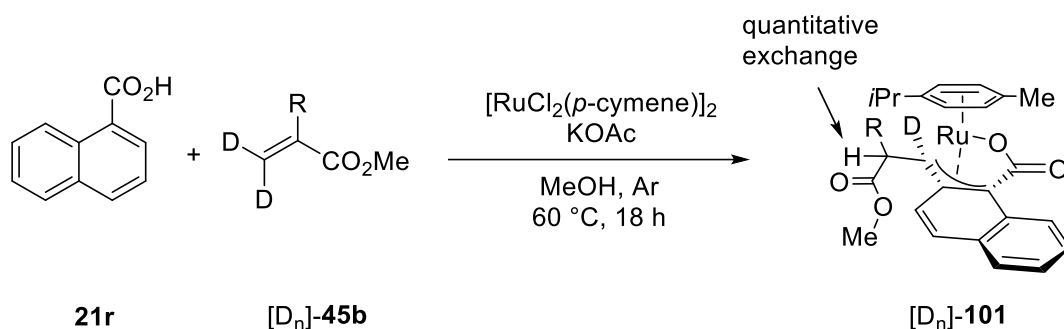
To obtain further insights to the cycloruthenation, complex **100-Py** was reacted with methylacrylate, yielding complex **101** in excellent quantities in methanol as well as in γ -valerolactone (**77**, Table 20).

Table 20: Reaction of **100-Py** with methyl acrylate (**45b**).

Entry	Solvent	Yield of 100 [%]
1	MeOH	90
2	GVL (77)	93

^[a] Reaction conditions: **100-Py** (20.6 μmol), **45b** (22.0 μmol), solvent (1.00 mL), Ar, 60 $^\circ\text{C}$, 18 h. Yield of isolated product.

In-situ nuclear magnetic resonance (NMR) studies, performed by Dr. Svenja Warratz, showed this process to proceed *via* an intermediate, that is presumably the seven-membered ruthenacycle resulting from the insertion of the double bond into the ruthenium carbon bond, before it is isomerizing to ruthenacycle **101**.^[99] In order to support this assumption, **101** was synthesized with deuterated acrylic esters [D₃]-**45b** and [D₂]-**45b**, again giving excellent yields (Table 21).

Table 21: Synthesis of **100** with deuterated acrylic esters.

Entry	Isotope	Yield of [D _n]- 101 [%]
1	R = H	85
2	R = D	93

^[a] Reaction conditions: [RuCl₂(*p*-cymene)]₂ (**30**) (0.1 mmol), **21r** (0.2 mmol), [D₂]-**45b** or [D₃]-**45b** (0.2 mmol), potassium acetate (0.4 mmol), solvent (5.0 mL), Ar, 60 °C, 36 h. Yield of isolated product.

NMR and mass spectrometry (MS) analysis of the products showed almost quantitative exchange of the migrated proton with the methanol solution, which could be a result of de- and reprotonation or an exchange by dihydrogen bonding (DHB)^[101] of a hydridic intermediate. Figure 11 zooms into the ¹H-NMR spectra of complexes **101**, [D₁]-**101** and of [D₂]-**101** showing the resonances of the methylene protons.

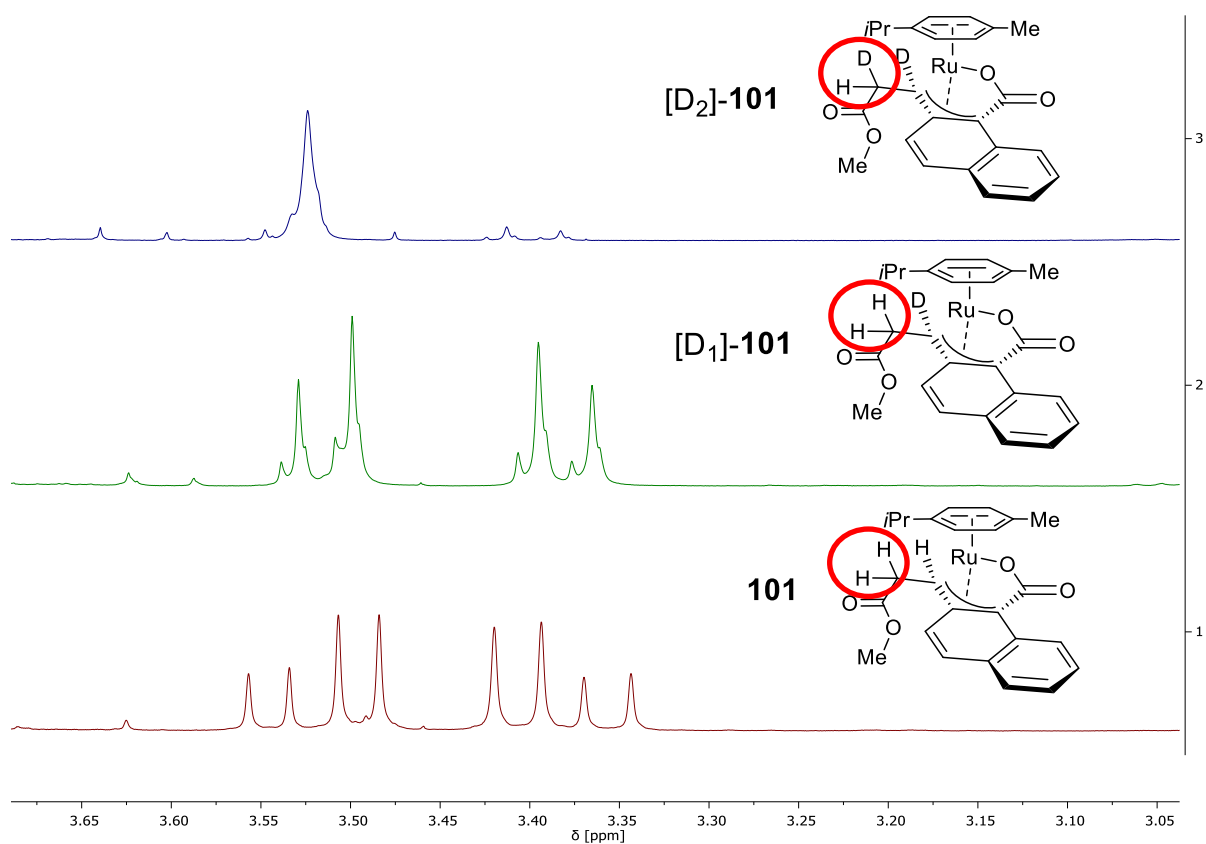
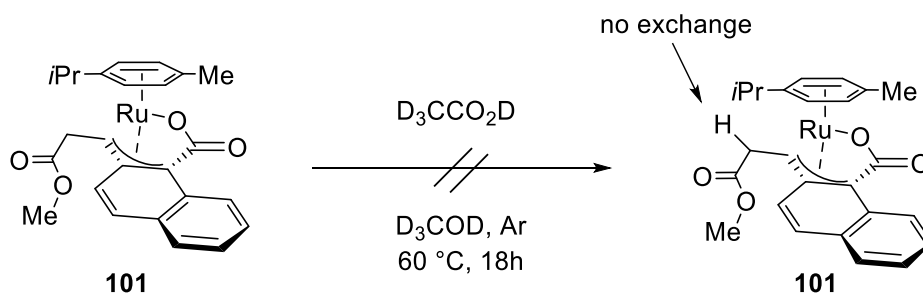


Figure 11: Expansion of the methylene region of the ^1H -NMR spectra of complexes **101**, **D₁-101** and **D₂-101**.

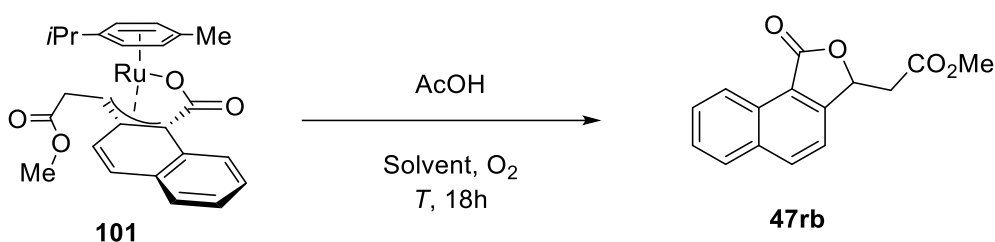
To test whether the isomerization process is reversible or not, complex **101** was subjected to the reaction conditions using perdeuterated reagents (Scheme 32). NMR-Spectroscopic and MS analysis of the reaction mixture showed no incorporation of deuterium into complex **101**, indicating the isomerization process to be irreversible.



Scheme 32: Isomerization test of complex **101**.

Finally, the product formation step was simulated by reacting a solution of complex **101** with acetic acid under an ambient oxygen atmosphere (Table 22). The reaction in methanol at 60 °C did not show any measurable conversion of **101**, while γ -valerolactone (**77**) at 80 °C gave 30% isolated yield of **47rb**. Due to several extraction steps on small scale it is assumed, that the product formation is higher than the isolated yield.

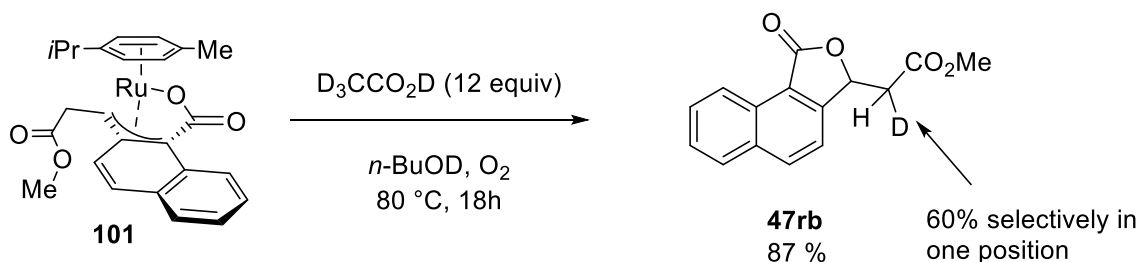
Table 22: Product release from complex **101**.



Entry	Solvent (mL)	AcOH (equiv)	T [°C]	Yield of 47rb [%]
1	MeOH (1.0)	10	60	traces
2	GVL (77) (0.5)	50	80	30

^[a] Reaction conditions: **101** (0.1 mmol), AcOH, solvent, O₂, T , 18 h. Yield of isolated product.

The release of **47rb** was repeated with [D₁]-*n*-butanol as the solvent and deuterated acetic acid giving 87% yield (Scheme 33). NMR and ESI-MS analysis showed 60% deuterium incorporation selectively at one of the methylene protons.



Scheme 33: Product release from complex **101** with deuterated solvents.

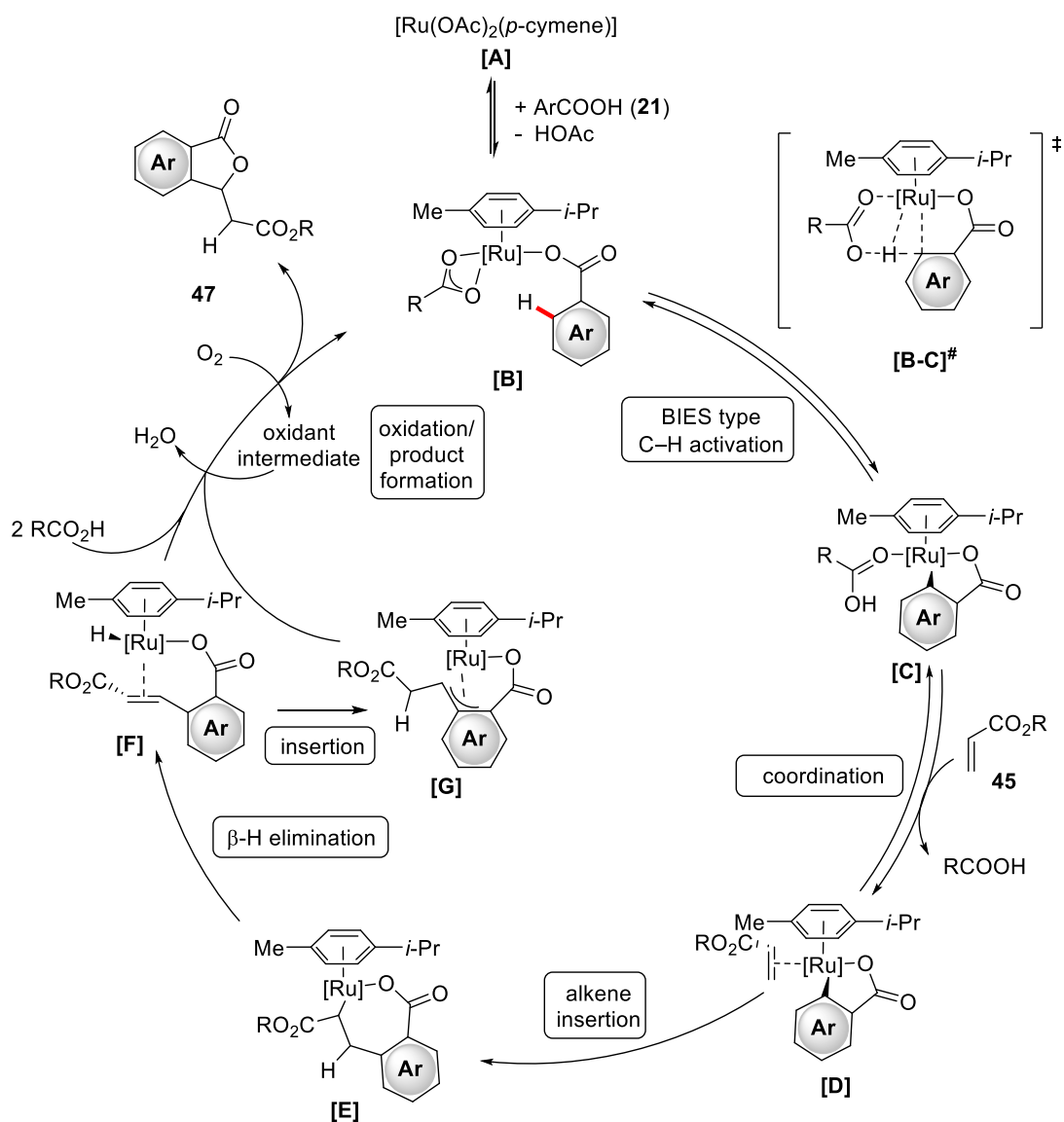
This selective partial deuterium incorporation provides further insights into the product formation step, because two possible product formation scenarios could be ruled out. A direct reductive O–C

elimination providing phthalide **47rb** would not incorporate deuterium in the methylene position. Furthermore, the release of the *ortho*-acrylated naphthoic acid followed by a ruthenium independent base catalyzed oxa-Michael reaction is implausible, because the deprotonation, addition, reprotonation sequence would lead to quantitative incorporation of deuterium from the reaction medium. The assumed formation of the product is likely to occur *via* an irreversible β -H-elimination, forming an alkenylated ruthenium-hydride intermediate, which is releasing product **47rb**. This transition state is related with the assumed transition state for the isomerisation process from **100** to **101**. Therefore it is likely, that complex **101** is an off cycle intermediate, only formed in absence of a suitable oxidant.

3.1.6.5 Proposed catalytic cycle

Computational studies, performed by Torben Rogge supported the experimental results and provided further details of a BIES-type C–H activation, which is stabilized by a weak agostic interaction between the ruthenium center and the activated hydrogen atom.^[102] Based on the experimental and computational findings, the following catalytic cycle is proposed (Scheme 34): One of the acetate ligands of the *in-situ* formed cymene ruthenium bisacetate complex **[A]** undergoes ligand exchange with benzoic acid (**21**) to form complex **[B]**. This complex reacts in an reversible BIES type C–H ruthenation process with the proposed transition state **[B-C]**[#] to form the well characterized intermediate **[C]**, resp. complex **100**. In γ -valerolactone (**77**) this process showed no kinetic isotope effect, while in *n*-butanol as the solvent the activation of the C–H bond is the turnover limiting step. The coordinated carboxylic acid is exchanged with the acrylate (**45**) to form **[D]**. The coordinated acrylic ester reacts in an 1,2-insertion into the ruthenium–carbon bond, to form ruthenaheptacycle **[E]**, which reacts in a β -H-elimination to form the ruthenium hydride species **[F]**, that exchanges the hydridic hydrogen with the solution^[101] and further reacts to the isolated off-cycle intermediate **[G]**, resp. complex **101** in the absence of a suitable oxidant. In the presence of an oxidant complexes **[F]** and **[G]** form the phthalide **47** under formation of the catalytically active species **[B]**. While the oxidation step is not fully understood as of yet, oxygen is assumed to act as a four electron oxidant in two separated two electron oxidation processes forming hydrogen peroxide as a potent oxidant intermediate.

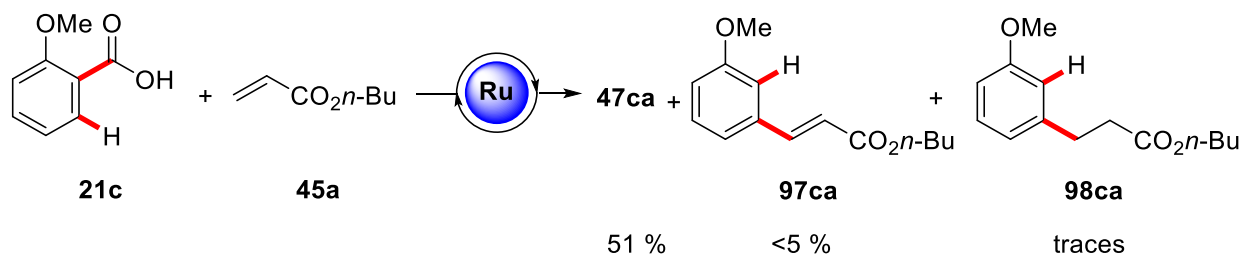
Results and Discussion



Scheme 34: Proposed catalytic cycle of the ruthenium(II)-oxidase catalyzed alkenylation of benzoic acids.

3.2 Ruthenium(II)-Catalyzed Decarboxylative Alkenylation/Alkylation of Benzoic Acids

When 2-methoxybenzoic acid (**21c**) was reacted with *n*-butyl acrylate (**45a**) under ruthenium oxidase reaction conditions in *n*-butanol, the formation of the targeted phthalide in moderate yield was accompanied by small amounts of two byproducts differing by two mass units. These byproducts were identified as *meta*-alkenylated and alkylated anisoles **97ca** and **98ca**.

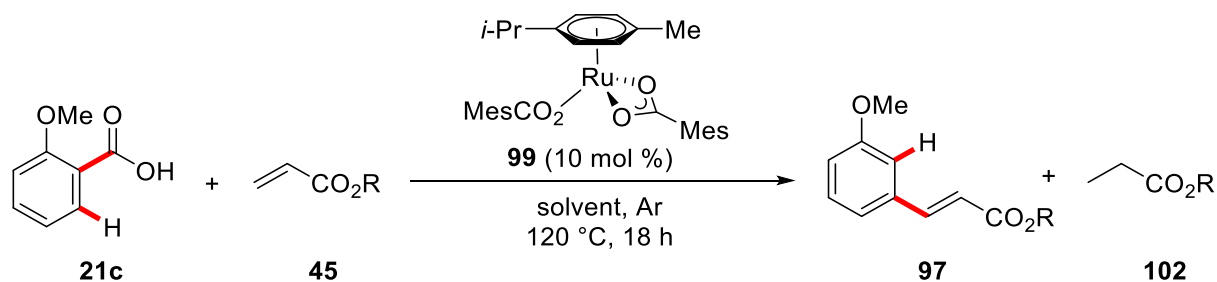


Scheme 35: Observation of decarboxylated C–H functionalization products.

Similar observations using internal alkynes as coupling partners for benzoic acids were made by Dr. N. Y. Phani Kumar.^[103] Being curious about this reactivity, the reaction was optimized in order to discover a new access to *meta*-substituted arenes by C–H functionalization.

3.2.1 Optimization Studies

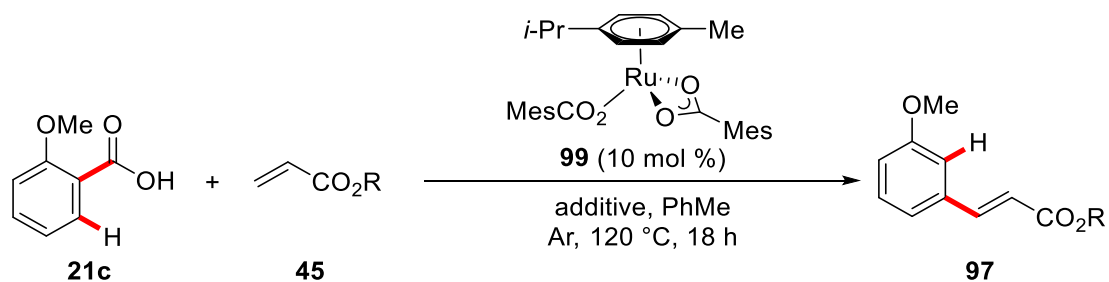
The study was commenced by reacting 2-methoxybenzoic acid (**21c**) with *n*-butyl acrylate (**45a**) or benzyl acrylate (**45d**) in a 3:1 ratio and catalytic amounts of the well-defined ruthenium mesitylate complex **99** in various solvents under inert atmosphere. PhMe as the reaction medium provided a good starting point, while 1,4-dioxane and NMP gave only small quantities of **97ca**, (Table 23, entries 1-4). Careful analysis of the reaction mixture of entries 1 and 4 showed the saturated acrylates **102** as a side product, indicating the acrylic esters to be suitable oxidants in this chemistry. Using the benzoic acid **21c** as the limiting reagent delivered less **97ca** as minor byproduct, whereas phthalide **47ca** was obtained as the major product (entry 5).

Table 23: Optimization of the ruthenium(II)-catalyzed alkenylative decarboxylation.

Entry	R	Solvent	Yield [%] ^[a]
1	<i>n</i> -Bu	PhMe	33
2	<i>n</i> -Bu	1,4-dioxane	<10 ^[b]
3	<i>n</i> -Bu	NMP	traces ^[b]
4	Bn	PhMe	28
5	<i>n</i> -Bu	PhMe	<20 ^{[b][c]}

^[a] Reaction conditions: **21c** (3.0 mmol), **45** (1.0 mmol), [Ru(O₂CMe)₂(*p*-cymene)] (**99**) (10 mol %), solvent (3.0 mL), Ar, 120 °C, 18 h. Yield of isolated product. ^[b] Determined by GC-analysis. ^[c] **21c** (1.0 mmol), **45a** (2.2 mmol).

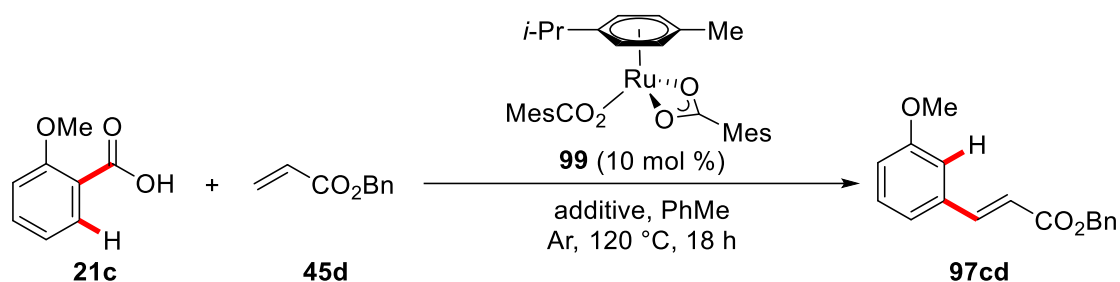
In order to prevent the reduction of the acrylic substrate, several oxidants were tested (Table 24). MnO₂ gave a slight improvement (entries 1 and 2), while silica and iron oxide were not suitable (entries 3 and 4). The best results were obtained by using vanadium(V) oxide (entries 5 and 6). Persulfate and organic oxidants did not affect the yields (entries 7-9), while the hypervalent iodine reagent PIDA shut the reaction down (entry 10).

Table 24: Optimization of additives for the ruthenium(II)-catalyzed alkenylative decarboxylation.

Entry	R	Additive (1.0 equiv)	Yield [%] ^[a]
1	<i>n</i> -Bu	MnO ₂	37
2	Bn	MnO ₂	39
3	<i>n</i> -Bu	SiO ₂	27
4	<i>n</i> -Bu	Fe ₂ O ₃	15
5	<i>n</i>-Bu	V₂O₅	55
6	Bn	V₂O₅	60
7	Bn	<i>t</i> -BuC(O)Me	31
8	Bn	Na ₂ S ₂ O ₇	32
9	Bn	Benzoquinone	35
10	Bn	PhI(OAc) ₂	---

^[a] Reaction conditions: **21c** (3.0 mmol), **45** (1.0 mmol), [Ru(O₂CMes)₂(*p*-cymene)] (**99**) (10 mol %), oxidant (1.0 equiv), PhMe (3.0 mL), Ar, 120 °C, 18 h. Yield of isolated product.

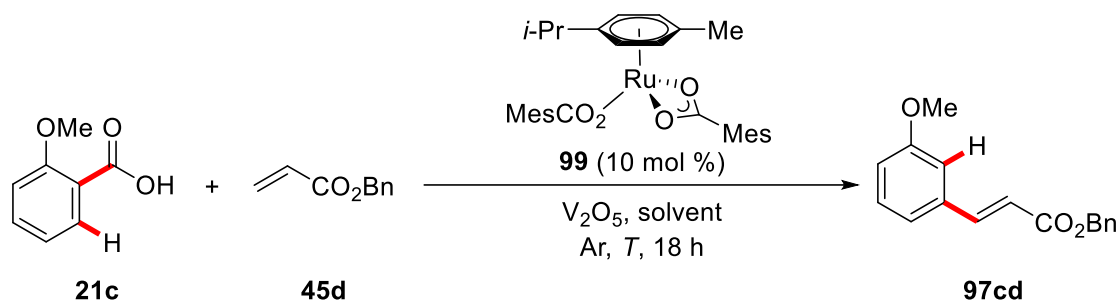
After vanadium(V) oxide had been identified as the oxidant of choice, its loading was optimized (Table 25). While overstoichiometric amounts did not induce the desired improvement, substoichiometric amounts resulted in lower yields (entries 1-4).

Table 25: Optimization of the vanadium(V) oxide concentration for the ruthenium(II)-catalyzed alkenylative decarboxylation.

entry	V ₂ O ₅ (equiv)	Yield [%]
1	1.0	60
2	2.0	62
3	0.5	46
4	0.2	28

^[a] Reaction conditions: **21c** (3.0 mmol), **45d** (1.0 mmol), [Ru(O₂CMes)₂(*p*-cymene)] (**99**) (10 mol %), V₂O₅, PhMe (3.0 mL), Ar, 120 °C, 18 h. Yield of isolated product.

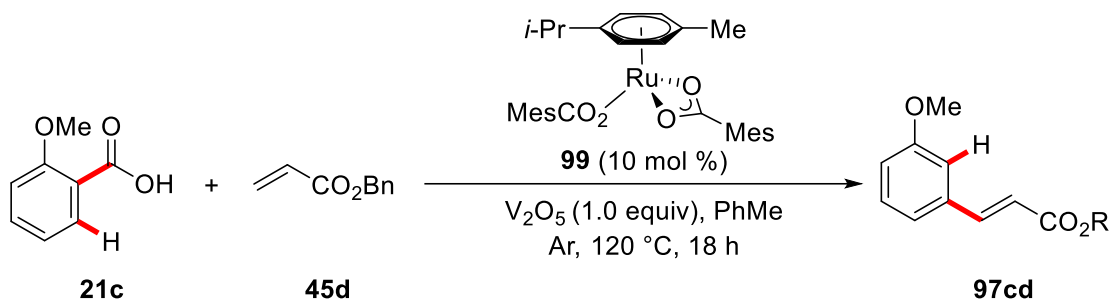
After the optimal amount of vanadium(V) oxide was identified, several solvents were tested under these optimized conditions (Table 26). Water, DCE or *n*-hexane as the solvents showed low reactivity, while acetonitrile gave 55% of the desired product (entries 1-4). The temperature was raised to 150 °C and several higher boiling solvents were evaluated. DMF delivered the product in moderate yield, while DMSO shut down the reaction (entries 5 and 6). *o*-Xylene and *m*-xylene showed comparable reactivity to PhMe at 120 °C (entries 7 and 8).

Table 26: Optimization of the solvent for the ruthenium(II)-catalyzed alkenylative decarboxylation.

Entry	Solvent	T [°C]	Yield [%]
1	H ₂ O	120	15
2	DCE	120	22
3	<i>n</i> -hexane	120	27
4	MeCN	120	55
5	DMF	150	48
6	DMSO	150	---
7	<i>o</i> -xylene	150	60
8	<i>m</i> -xylene	150	60

^[a] Reaction conditions: **21c** (3.0 mmol), **45d** (1.0 mmol), [Ru(O₂CMes)₂(*p*-cymene)] (**99**) (10 mol %), V₂O₅ (1.0 mmol), solvent (3.0 mL), Ar, T , 18 h. Yield of isolated product.

Lowering the loading of catalyst **99** to 5.0 mol % decreased the yield to 50% (Table 27, entry 1), while running the reaction without the catalyst demonstrated its crucialty for the reaction (entries 1 and 2). An independent decarboxylation event followed by a *meta*-alkenylation of anisole was also ruled out (entry 3).

Table 27: Further experiments for the optimization of the ruthenium(II)-catalyzed alkenylative decarboxylation.

Entry	Difference	Yield [%]
1	[Ru(O ₂ CMes) ₂ (p-cymene)] (5.0 mol %)	50
2	Without [Ru]	---
3	Anisole (3.0 mmol) instead of 21c	---

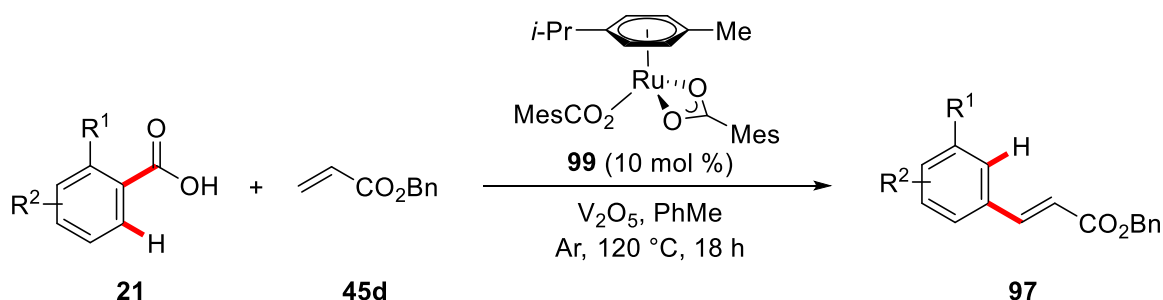
^[a] Reaction conditions: **21c** (3.0 mmol), **45d** (1.0 mmol), [Ru(O₂CMes)₂(p-cymene)] (**99**) (10 mol %), V₂O₅ (1.0 mmol), PhMe (3.0 mL), Ar, 120 °C, 18 h. Yield of isolated product.

The ruthenium(II)-catalyzed alkenylation decarboxylation tandem process was successfully optimized to give good yields of 60% in the benchmark reaction of benzoic acid **21c** with alkene **45d**. The optimized reaction conditions consisted of 10 mol % of the well-defined ruthenium(II) bismesylate catalyst **99** and vanadium(V) oxide as the oxidant as a 0.3 M solution in PhMe as the solvent.

3.2.2 Scope of the Decarboxylative Alkenylation

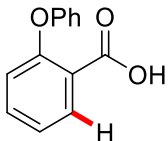
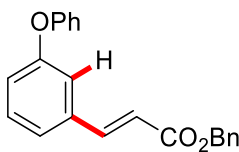
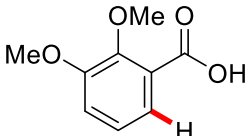
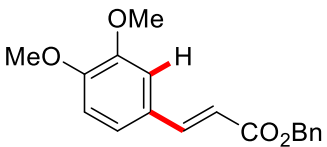
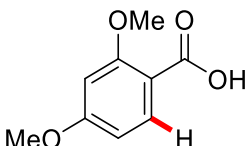
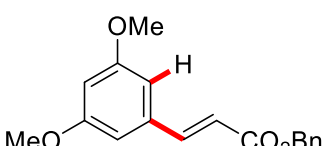
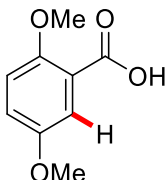
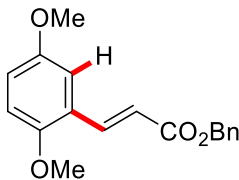
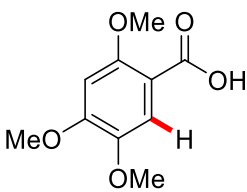
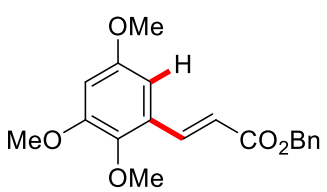
With the optimized reaction conditions in hand, the substrate scope of the decarboxylative alkenylation was tested (Table 28). The benchmark reaction between 2-methoxybenzoic acid (**21c**) and benzyl acrylate (**45d**) was performed on a 5.0 mmol scale giving an improved yield of 75% (cf. 60% on a 1.0 mmol scale), indicating that scaling up this process is possible and even beneficial (entry 1). Ethoxy- and phenoxy substituents (entries 2 and 3) in the 2-position of the benzoic acid were as well tolerated as a second or third methoxy group at different positions of the aromatic motif (entries 4-7). The installation of a methoxy group, chloride or bromide substituents in the 5-position improved the yields, which could be explained by a weak coordinative interaction synergizing with the directing group effect (entries 6-9). Naphthoic acid **21ae** was shown to be a viable substrate in this transformation (entry 10).

Table 28: Scope of benzoic acids **21** in the ruthenium(II)-catalyzed decarboxylative alkenylation.

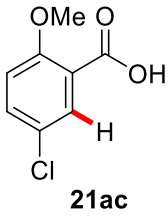
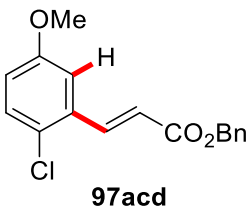
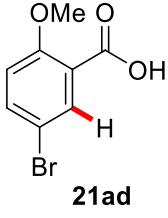
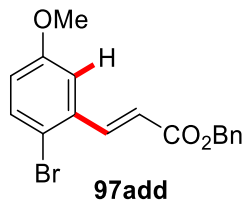
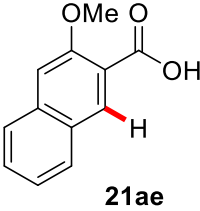
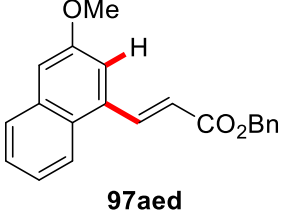


Entry	Benzoic acid	Product	Yield [%] ^[a]
1	 21c	 97cd	60 (5 mmol scale: 75)
2	 21d	 97dd	69

Results and Discussion

Entry	Benzoic acid	Product	Yield [%] ^[a]
3	 21x	 97xd	58
4	 21y	 97d	52
5	 21z	 97zd	71
6	 21aa	 97aad	81
7	 21ab	 97abd	75

Results and Discussion

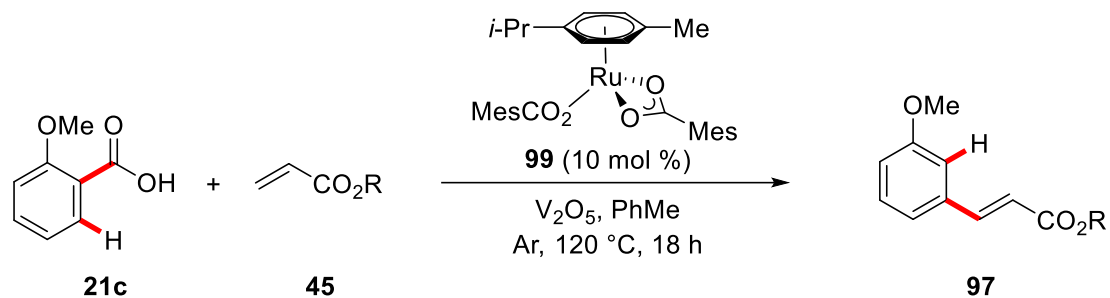
Entry	Benzoic acid	Product	Yield [%] ^[a]
8	 <p style="text-align: center;">21ac</p>	 <p style="text-align: center;">97acd</p>	81
9	 <p style="text-align: center;">21ad</p>	 <p style="text-align: center;">97add</p>	83
10	 <p style="text-align: center;">21ae</p>	 <p style="text-align: center;">97aed</p>	52

^[a] Reaction conditions: **21** (3.0 mmol), **45d** (1.0 mmol), [Ru(O₂CMes)₂(*p*-cymene)] (**109**) (10 mol %), V₂O₅ (1.0 mmol), PhMe (3.0 mL), Ar, 120 °C, 18 h. Yield of isolated product.

The scope of the decarboxylative alkenylation was further evaluated for the acrylic ester component (**45**, Table 29). Aliphatic esters gave moderate yields (entries 1 and 2), that were slightly improved by the installation of a 2-methoxyethyl group (entry 3). While tetrahydrofurfuryl acrylate gave a good yield of 70% (entry 4), the best result was obtained by the use of an acrylic ester bearing the bulky cholesteryl skeleton as the side-chain (entry 5). Since the yields in this transformation were in the moderate to good region, the optimal reagents **21ae** and cholesteryl acrylate (**45i**) were combined, showing that this catalytic system is able to provide the products in excellent quantities of 97% (entry 6).

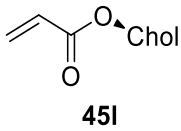
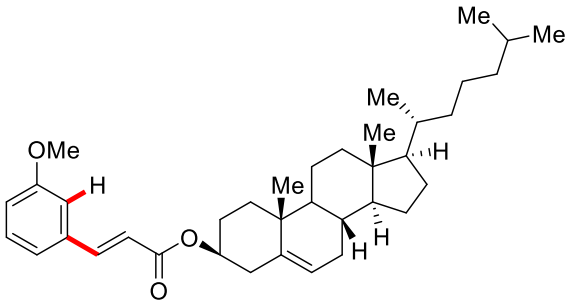
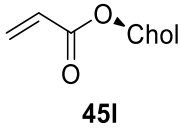
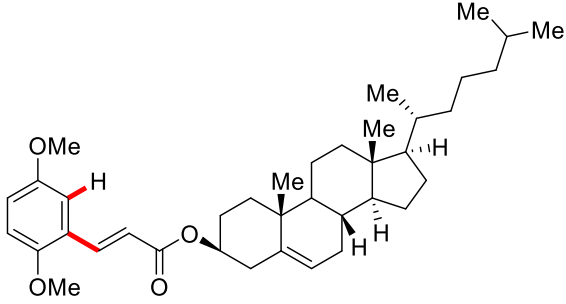
Results and Discussion

Table 29: Scope of acrylic esters **45** in the ruthenium(II)-catalyzed decarboxylative alkenylation.



Entry	Acrylic ester	Product	Yield [%] ^[a]
1			55
2			58
3			62
4			70

Results and Discussion

Entry	Acrylic ester	Product	Yield [%] ^[a]
5	 45l	 97cl	77
6 ^[b]	 45l	 97aal	97

^[a] Reaction conditions: **21c** (3.0 mmol), **45** (1.0 mmol), [Ru(O₂CMes)₂(*p*-cymene)] **99** (10 mol %), V₂O₅ (1.0 mmol), PhMe (3.0 mL), Ar, 120 °C, 18 h. Yield of isolated product.^[b] **21aa** (3.0 mmol) instead of **21c**.

The ruthenium(II)-catalyzed decarboxylative C–H alkenylation reaction showed moderate to almost quantitative isolated yields. The scope was however compromised by the requirement of an ether functionality in the *ortho*-position of the benzoic acid (**21**). Yet, several ethers, bromine, chlorine and benzannulated arenes were well tolerated at the benzoic acid (**21**). Several substituents at the acrylic moiety (**45**), bearing ether groups or a bulky cholesteryl unit were accepted in this transformation.

3.2.3 KIE and CO₂ Evolution Studies

The kinetic isotopic effect for the the reaction of benzyl acrylate **45d** with **21c** and **[D₁]-21c** was measured by comparing the initial rates in two parrallel reactions (**Figure 12**). The kinetic data clearly indicated a turnover limiting C–H ruthenation event, with a kinetic isotope effect of 2.5. The results were supported by independent DFT calculations, subsequently performed by Hong and co-workers.^[104]

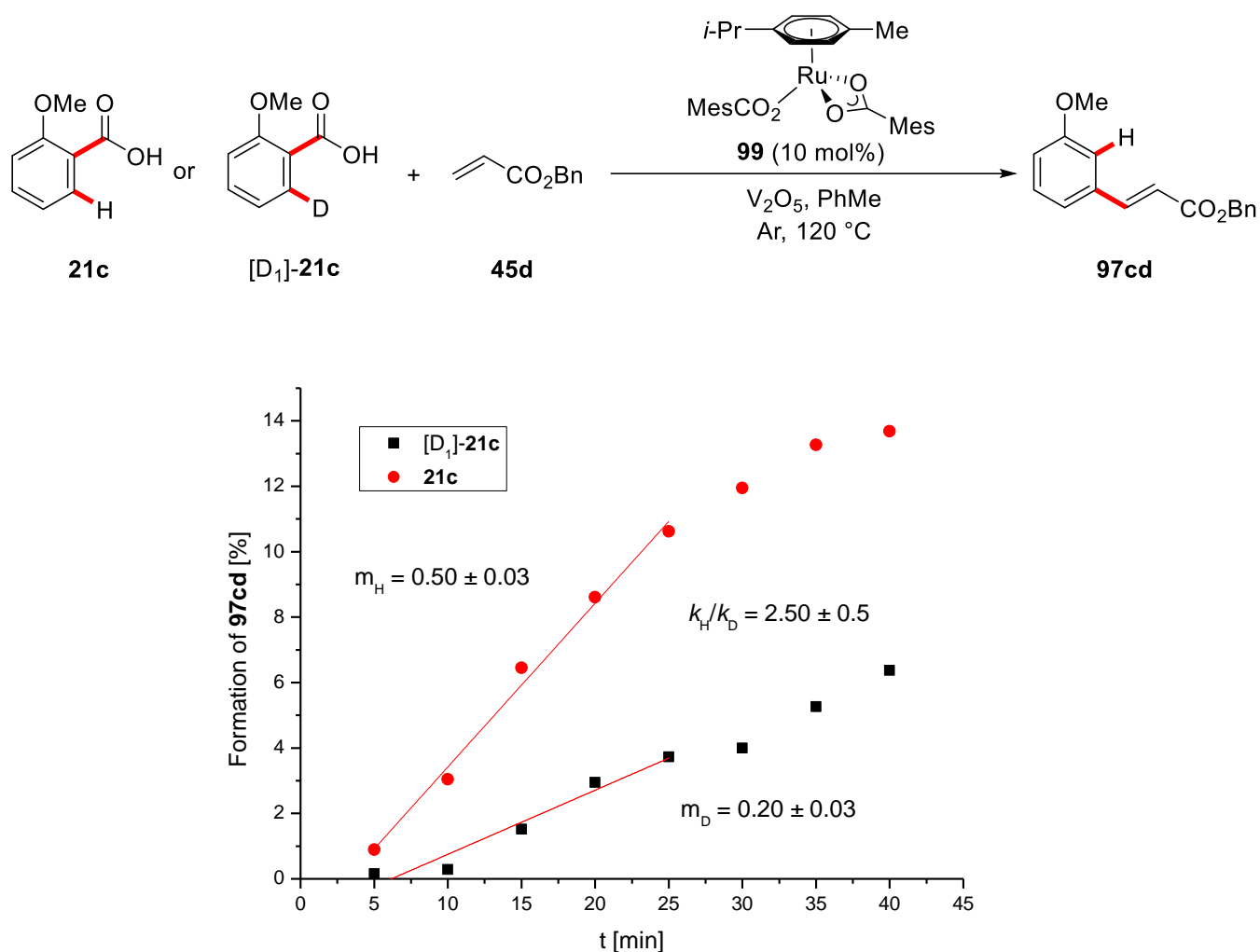
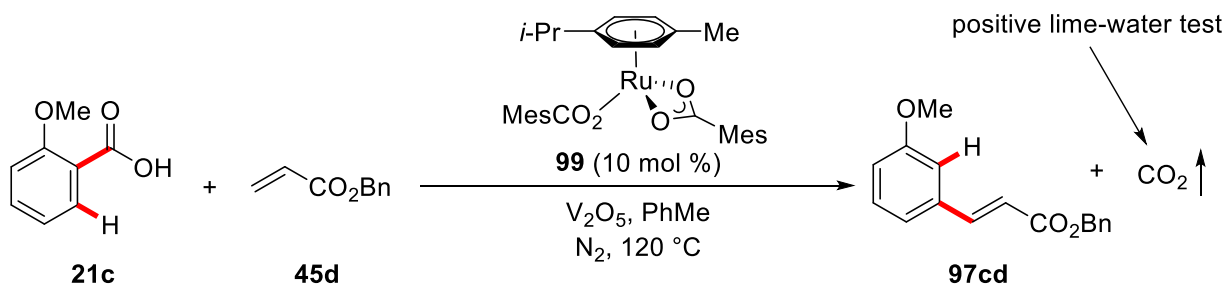


Figure 12: Conversion vs. time plot of the kinetic isotope effect measurement of the decarboxylative alkenylation.

Optical observation of a significant amount of gas bubbles that were formed during the course of the reaction gave a first hint of the expected CO₂ evolution. To prove this, a fermentation tube filled with limewater was connected to the atmosphere of the reaction. Clouding, especially in the region next to the reaction atmosphere confirmed the formation CO₂ (Scheme 36).



Scheme 36: Lime-water test for the decarboxylative alkenylation.

The kinetics of the decarboxylative C–H alkenylation were studied by performing the reaction with the atmosphere connected to a gas measurement construction and (Figure 13). In order to avoid inaccuracies by boiling solvent, the reaction temperature was lowered to 100 °C, with the catalytic system performing at the same efficacy level.

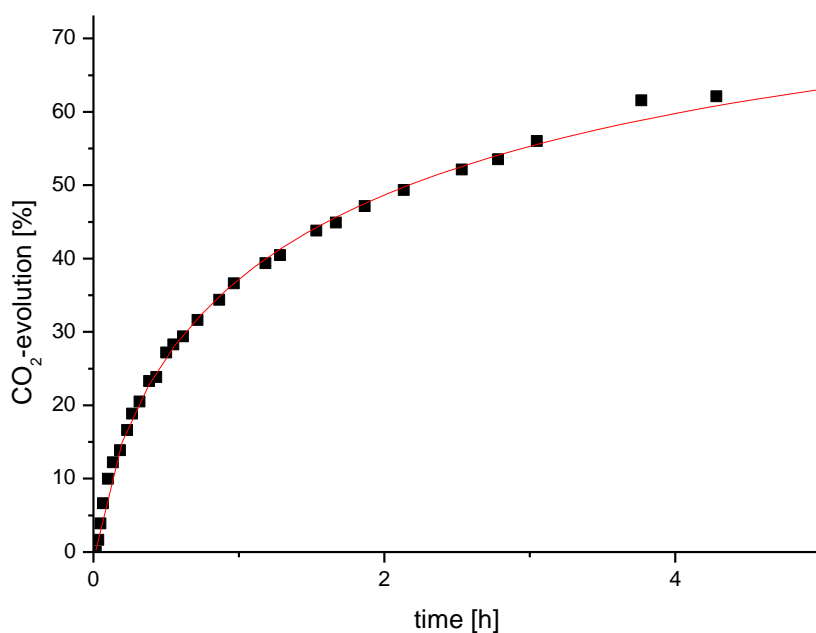
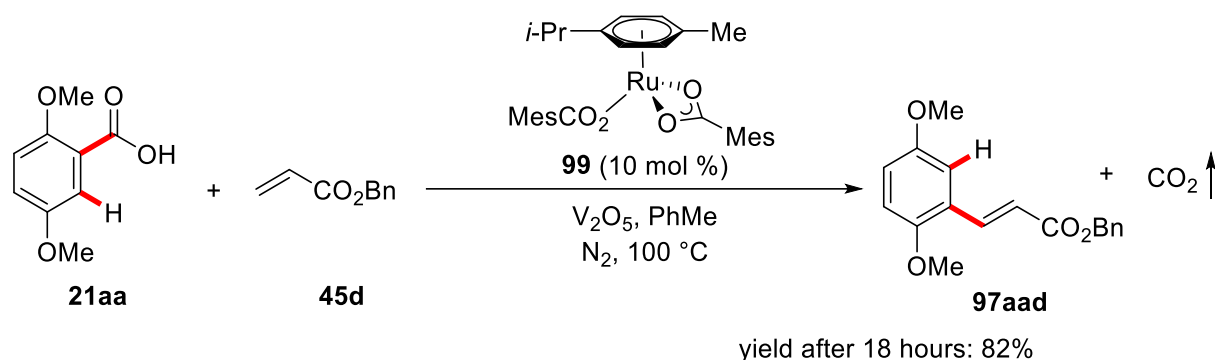
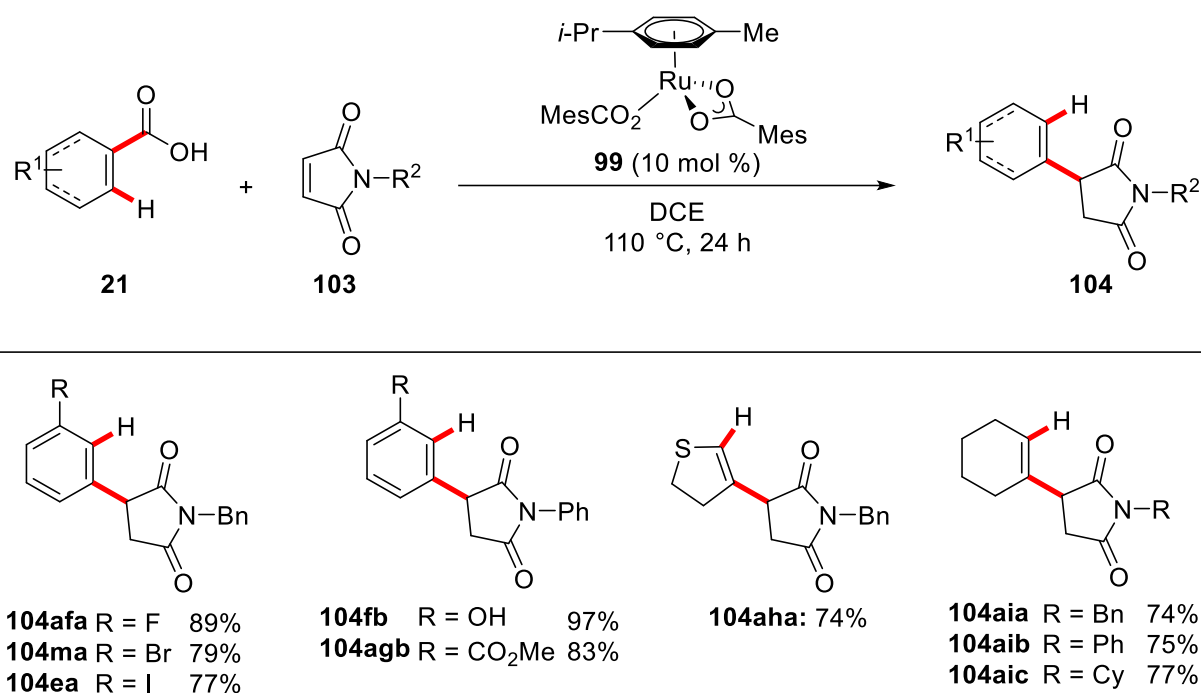


Figure 13: CO_2 release study for the ruthenium(II)-catalyzed decarboxylative alkenylation.

The reaction immediately started after adding the acrylate, reaching two turnovers already after 19 minutes. In the following the curve flattened, showing 60% conversion in four hours, before the reaction slowly went to completion. After 18 hours the gas volume indicated roughly 77% of product to be formed, correlating with 82% of **97aad** that were isolated after workup and purification.

3.2.4 Mechanistic and Kinetic Studies of Ruthenium(II)-Catalyzed Decarboxylative Alkylation

In addition to the decarboxylative alkenylation of benzoic acids, Dr. N. Y. Phani Kumar developed a protocol for the decarboxylative hydroarylation of maleimides.^[105] The reaction showed a broad substrate scope and worked even at a remarkable low temperature of 50 °C, when necessary. Scheme 37 shows the general reaction equation of this transformation together with selected examples representing the broad substrate scope.^[105]



Scheme 37: Ruthenium(II)-catalyzed decarboxylative alkylation.^[105]

Based on the experience gained in the ruthenium(II)-catalyzed decarboxylative alkenylation, mechanistic studies of this system were conducted to compare these two transformations. The KIE was determined to be 1.14 by ¹⁹F-NMR (Figure 14), 1.16 by GC measurement and 1.05 by *in operando* infrared measurement, that closely correlates with a value of 1.08 estimated by DFT calculations.^[106] In contrast to the decarboxylative alkenylation reaction, the C–H activation process is not the turnover-limiting step. This result could be explained by additional steric bulk of the maleimide, which increases the energetic barrier of the coordination step and makes it turnover-limiting.^[105]

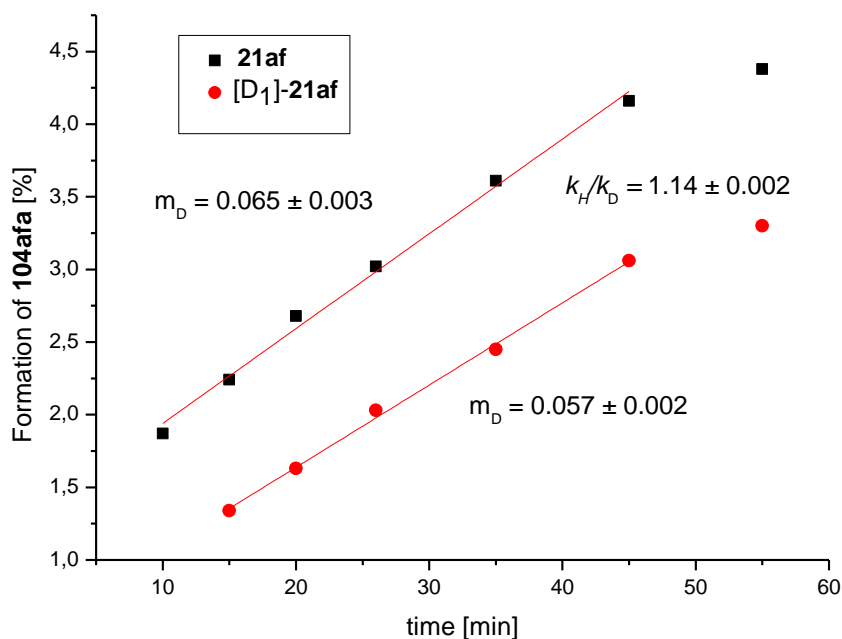
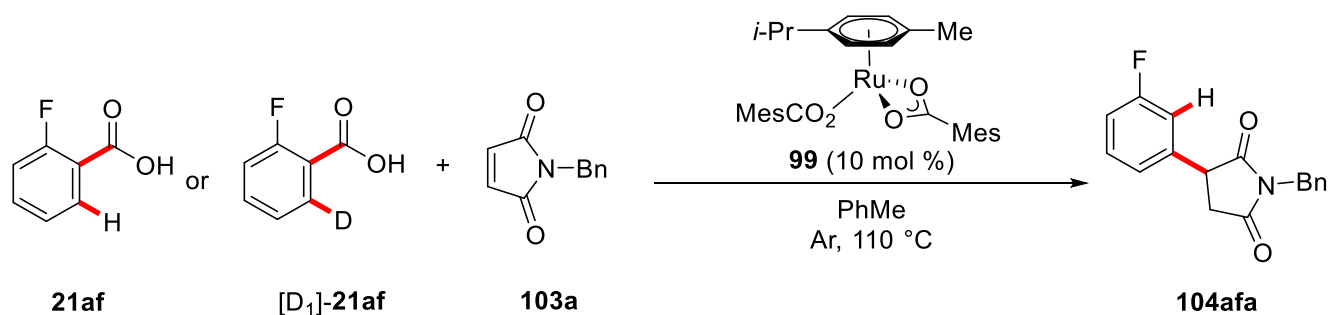
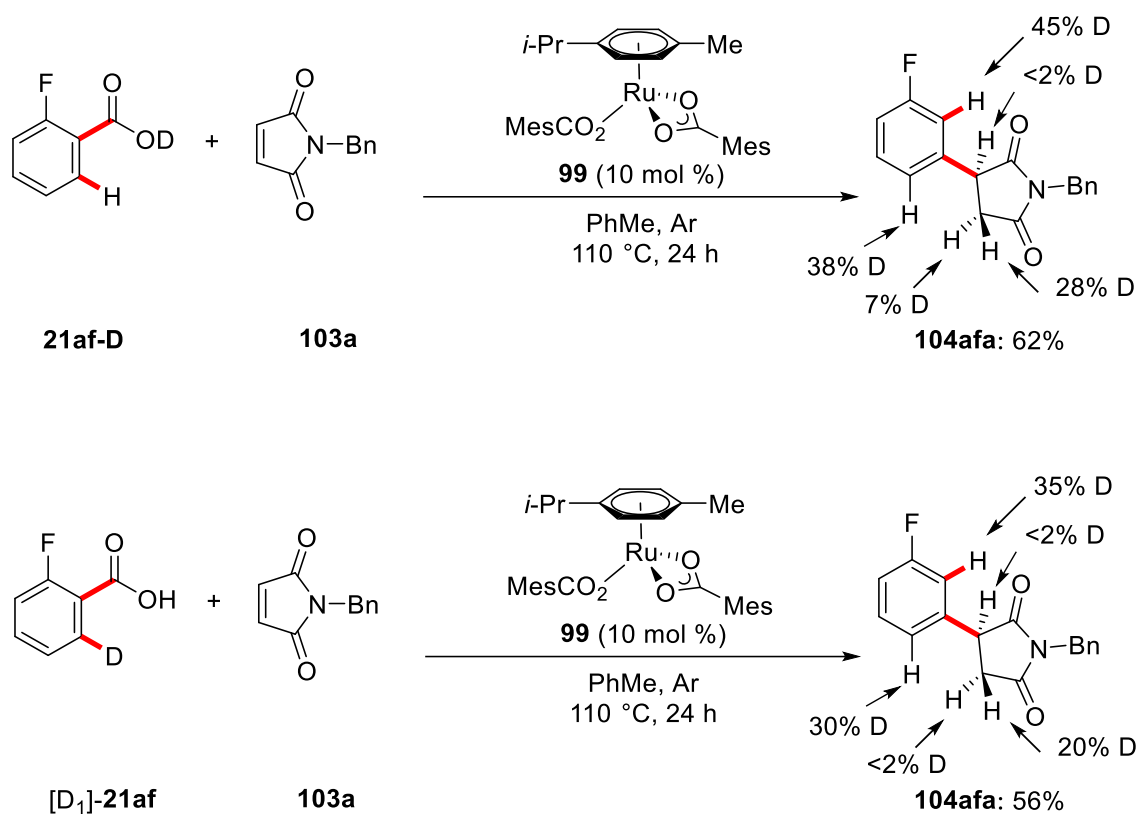


Figure 14: Kinetic isotope effect measurement of the decarboxylative alkylation.

Differently deuterium labelled benzoic acids **21** were subjected to the reaction conditions in order to retrace the labels in the products (Scheme 38). Deuteration at the acid moiety led to unspecific incorporation of deuterium in the product, with three major incorporation sites at the *ipso*-position, the 5-position and the *syn*-position of the succinimide. An equal incorporation motif with a slightly lower deuterium incorporation was observed when the 6-position of the benzoic acid was isotopically labeled. The results indicated that both, the acidic proton as well as the proton in the 6-position were cleaved and both positions were reprotated by the solvent. The position of the deuterium at the succinimide revealed the *syn*-insertion of the maleimide to be favored, while the deuteration in the original 5-position of substrate **21af** indicated the succinimide moiety to act as a directing group.



Scheme 38: Isotope labeling study for the ruthenium(II)-catalyzed decarboxylative alkylation.

The kinetics of the reaction were followed by measuring the carbon dioxide formation (**Figure 15**). The speed and the kinetic of this transformation are comparable to the related decarboxylative C–H alkylation. Again, the isolated yield of 79% is in good accordance with the 81%, estimated by the CO₂ quantity.

Results and Discussion

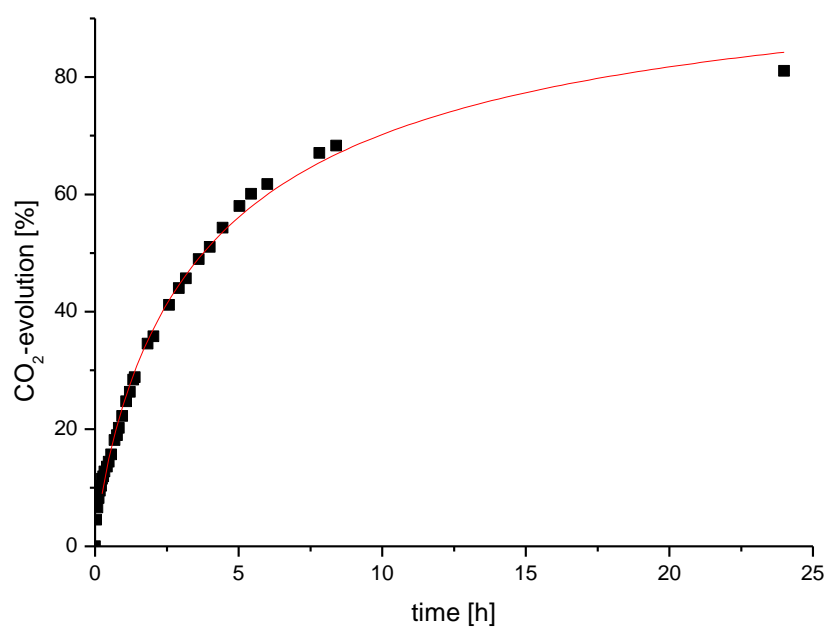
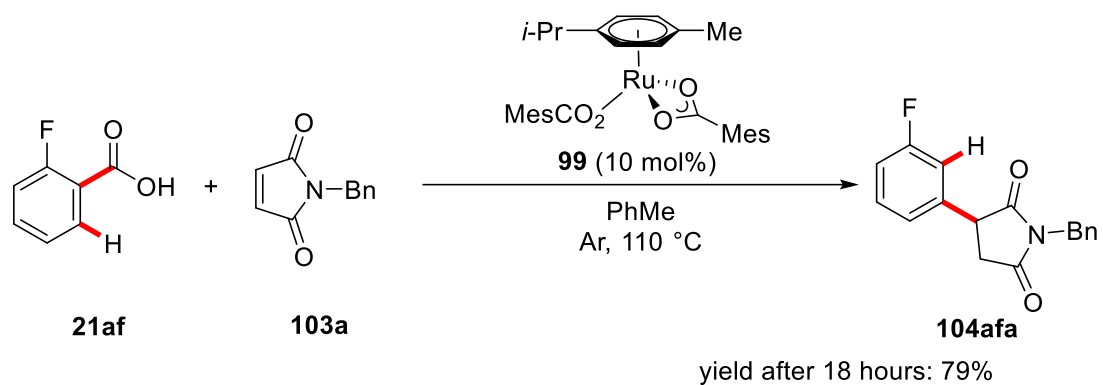
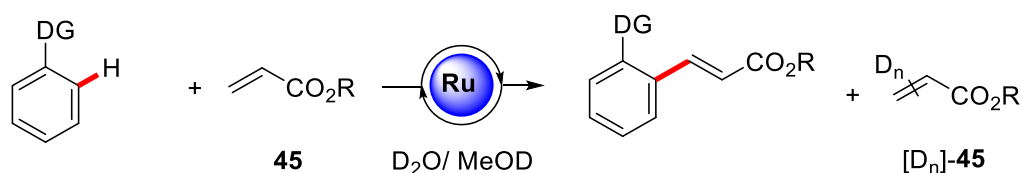


Figure 15: CO₂ release study for the ruthenium(II)-catalyzed decarboxylative alkylation.

3.3 Ruthenium(II)-Catalyzed Hydrogen Isotope Exchange on Acrylic Esters

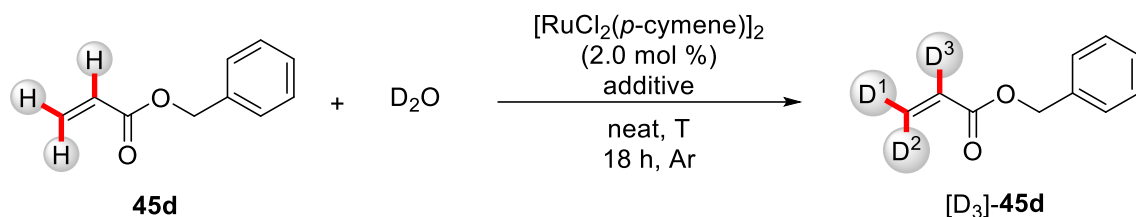
Deuterated compounds are commonly used in NMR spectroscopy, as tagged references in mass spectrometry and for the clarification of reaction mechanisms and biological processes.^[64a, 64c] While the exchange of arene C(sp²)-H bonds is a well known process, examples for the direct labeling of olefinic C(sp²)-H bonds continue to be limited.^[70a] Within general studies on the ruthenium(II)-catalyzed C-H alkenylation of various substrates, the incorporation of deuterium to acrylic C-H bonds was observed (Scheme 39). Further investigation of this reactivity led to a powerful method for the selective preparation of deuterated acrylic esters (**45**).



Scheme 39: Observation of deuterium incorporation at acrylic C-H bonds during mechanistic studies.

3.3.1 Optimization of the Hydrogen Isotope Exchange on Acrylic Esters

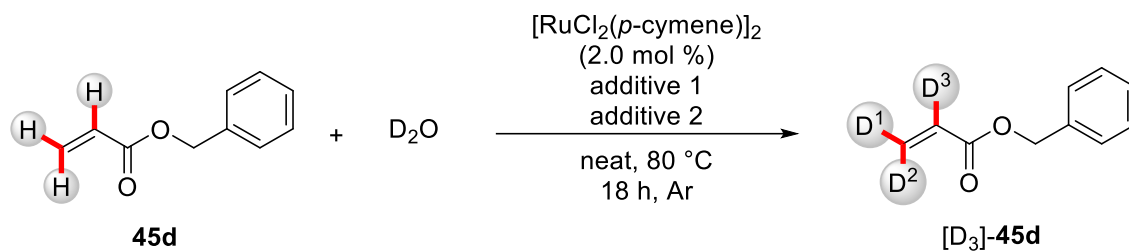
The optimization of the reaction conditions was commenced by changing various reaction parameters for the deuteration of benzyl acrylate (**45d**) in a biphasic reaction system with D₂O as the isotope source. The experiments showed similar deuteration values of the β-hydrogens, while the α-position seemed to be slightly less reactive. Potassium acetate as additive at 80 °C led to minor deuteration at the acrylic positions, which was increased at elevated temperatures (entries 1 and 2). Cationic ruthenium(II) species or potassium methoxide as ligand showed no exchange of the hydrogen atoms (entries 3 and 4). Potassium *tert*-butanoxide gave very good incorporation in the β- and moderate incorporation in the α-position, indicating that steric effects might play a role (entry 5). The well defined ruthenium(II) mesitylate complex **99** showed moderate activity, which was slightly increased using the related bulkier adamantyl complex **105** (entries 6 and 7). Additional co-catalytic amounts of the corresponding adamantyl carboxylic acid to the well defined complex **105** led to major improvements (entry 8, cf. entry 7).

Table 30: Optimization of the ruthenium(II)-catalyzed deuteration of acrylic ester **45d**.

Entry	Additive (mol %)	T [°C]	Recovered [%] ^[a]	D ¹ [%]	D ² [%]	D ³ [%]
1	KOAc (10)	80	82	<10	<10	<10
2	KOAc (10)	100	64	63	63	16
3 ^[b]	KOAc (10)	80	56	0	0	0
4	KOMe (10)	80	55	0	0	0
5	KO <i>t</i> -Bu (10)	80	52	90	90	68
6 ^[c]	---	80	80	44	44	27
7 ^[d]	---	80	70	53	53	30
8 ^[d]	AdCO ₂ H (10)	80	68	90	90	74

- ^[a] Reaction conditions: **45d** (1.0 mmol), [RuCl₂(*p*-cymene)] (**30**) (2.0 mol %), additive, D₂O (1.0 mL), Ar, 80 °C, 18 h. Yield of isolated product, deuterium incorporation was determined by ¹H-NMR. ^[b] [Ru₂Cl₃(*p*-cymene)₂][PF₆] (2.0 mol %) instead of [RuCl₂(*p*-cymene)]₂. ^[c] [Ru(O₂CMes)₂(*p*-cymene)₂] (**99**) (4.0 mol %) instead of [RuCl₂(*p*-cymene)]₂. ^[d] [Ru(O₂CAd)₂(*p*-cymene)₂] (**105**) (4.0 mol %) instead of [RuCl₂(*p*-cymene)]₂.

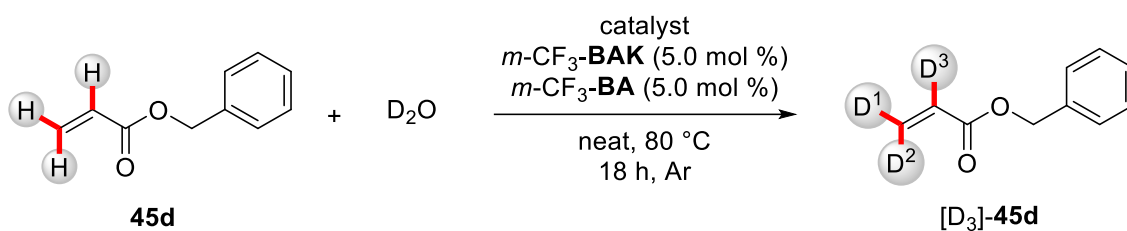
The *in-situ* generated adamantyl carboxylate and 2,4,6-tri-*iso*-propylbenzoate based catalyst systems showed less efficacy than the mixtures of well defined adamantylate complex and acid (Table 31, entries 1 and 2). A trifluoromethyl group attached to any position of the ligand gave complete incorporation of deuterium in the range of the stochastic D to H ratio of the reaction solution, with the *meta*-trifluoromethylbenzoic acid (*m*-CF₃-**BA**, **106**) being optimal (entries 3-6). The power of this ligand system was further highlighted by perfect incorporation, even at a reduced catalyst loading of only 1.0 mol %. Double trifluoromethylated benzoic acid ligands showed a lower deuterium incorporation accompanied by a switch in selectivity between the α- and the β-positions (entries 7 and 8).

Table 31: Optimization of the ruthenium(II)-catalyzed deuteration of acrylic ester **45d**.

Entry	Additive 1 (mol %)	Additive 2 (mol %)	Recovered [%] ^[a]	D ¹ [%]	D ² [%]	D ³ [%]
1	AdCO ₂ K (10)	AdCO ₂ H (10)	82	79	79	53
2	2,4,6- <i>i</i> -Pr ₃ - BAK (10)	2,4,6- <i>i</i> -Pr ₃ - BA (10)	83	76	76	71
3	<i>m</i> -CF ₃ - BAK (10)	<i>m</i> -CF ₃ - BA (10)	74	>95	>95	>95
4 ^[b]	<i>m</i> -CF ₃ - BAK (5.0)	<i>m</i> -CF ₃ - BA (5.0)	68	>95	>95	>95
5 ^[b]	<i>o</i> -CF ₃ - BAK (5.0)	<i>o</i> -CF ₃ - BA (5.0)	46	>95	>95	>95
6 ^[b]	<i>p</i> -CF ₃ - BAK (5.0)	<i>p</i> -CF ₃ - BA (5.0)	37	>95	>95	>95
7 ^[b]	2,6-CF ₃ - BAK (5.0)	2,6-CF ₃ - BA (5.0)	82	27	27	30
8 ^[b]	3,5-CF ₃ - BAK (5.0)	3,5-CF ₃ - BA (5.0)	83	38	38	55

^[a] Reaction conditions: **45d** (1.0 mmol), [RuCl₂(*p*-cymene)] (**30**) (2.0 mol %), additive 1, additive 2, D₂O (1.0 mL), Ar, 80 °C, 18 h. Yield of isolated product, deuterium incorporation was determined by ¹H-NMR spectroscopy. ^[b] [RuCl₂(*p*-cymene)]₂ (1.0 mol %).

The ruthenium(II) catalyst was proven to be crucial for the reactivity (Table 32, entry 1) and further shown to be active in polar aprotic γ -valerolactone (**77**) as the solvent (entry 2). In addition, benzene and PhMe proved to be suitable solvents for the hydrogen isotope exchange reaction. RuCl₃·(H₂O)_{*n*} and [Cp*CoI₂]₂ did not show any reactivity (entries 3 and 4), while [Cp*RhCl₂]₂ and [Mn(CO)₅Br] led to the decomposition of **45d** (entries 5 and 6).

Table 32: Catalyst test for the deuterium labeling of acrylic ester **45d**.

Entry	Catalyst (mol %)	Recovered [%] ^[a]	D ¹ [%]	D ² [%]	D ³ [%]
1 ^[b]	---	>95	0	0	0
2 ^[c]	[RuCl ₂ (<i>p</i> -cymene)] ₂ (30) (1.0)	55	>95	>95	>95
3 ^[b,d]	RuCl ₃ ·xH ₂ O (1.0)	>95	0	0	0
4 ^[b]	[Cp* <i>Rh</i> Cl ₂] ₂ (1.0)	8	<10	<10	<10
5 ^[b]	[Cp* <i>Co</i> I ₂] ₂ (1.0)	>96	0	0	0
6 ^[b]	[Mn(CO) ₅ Br] (2.0)	<5	<10	<10	<10

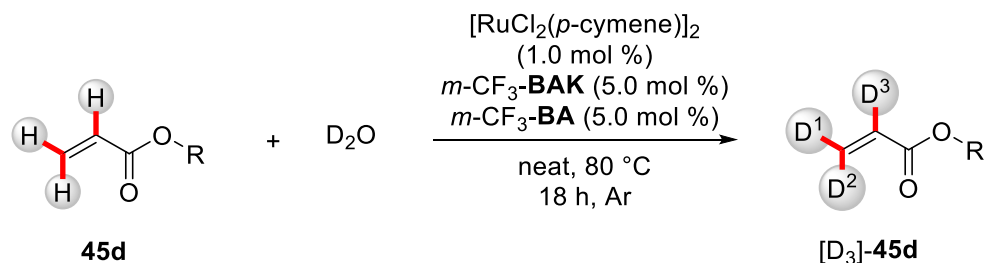
^[a] Reaction conditions: **45d** (1.0 mmol), catalyst, *m*-CF₃-**BA** (**106**) (5.0 mol %), *m*-CF₃-**BAK** (**106-K**) (5.0 mol %), D₂O (1.0 mL), Ar, 80 °C, 18 h. Yield of isolated product, deuterium incorporation was determined by ¹H-NMR. ^[b] NMR conversion vs. internal standard. ^[c] GVL (**77**) (1.0 mL) added. ^[d] *m*-CF₃-**BAK** (**106**) (15 mol %), *m*-CF₃-**BAK** (**106-K**) (15 mol %).

The optimized catalytic system consisted of 1.0 mol % of [RuCl₂(*p*-cymene)]₂ and 5.0 mol % of *meta*-trifluoromethylbenzoic acid (**106**) and the corresponding benzoate ligand (**106-K**) without further solvent other than on D₂O as a simple and user-friendly isotope source.

3.3.2 Scope for Hydrogen Isotope Exchange Labeling on Acrylic Esters

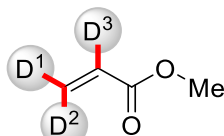
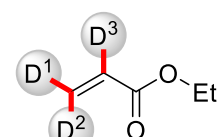
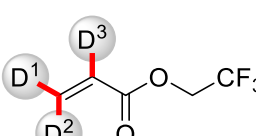
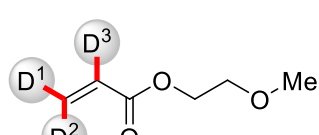
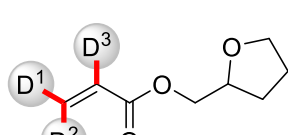
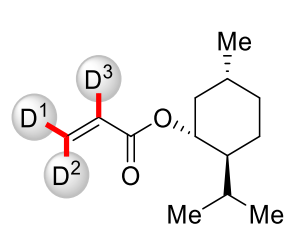
Next, the scope of this hydrogen isotope exchange reaction was tested. Due to the volatility of this class of reagents, yields and deuterium incorporations were determined by ^1H - and ^2H -NMR of reaction solution extracts, referenced by internal standards and confirmed by mass spectrometry. Among the tested substrates, benzyl or primary and secondary alkyl substituted acrylic esters **45** generally showed excellent deuterium incorporations in the range of the stochastic D to H ratio of the reaction mixture (Table 33). Highly volatile methyl and ethyl acrylate (**45b** and **45c**) needed the addition of C_6D_6 (or usual benzene or PhMe) as a solvent in order to prevent evaporation or condensation, when the reaction was performed on a 1.0 mmol scale (entries 2 and 3). Higher boiling liquid acrylic esters with a trifluorethyl substituent, linear and cyclic ethers or natural occurring chiral alcohols smoothly reacted on the water surface (entries 3-8). Acrylates with high melting point, as cholesteryl acrylate needed the addition of C_6D_6 as the co-solvent (entry 9). The outstanding selectivity of this labeling reaction is highlighted by excellent deuteration rates in the acrylic positions, while the distal terminal alkene remained almost untouched ($\ll 5\%$) (entry 10).

Table 33: Scope of aliphatic acrylic esters for the ruthenium(II)-catalyzed deuteration.

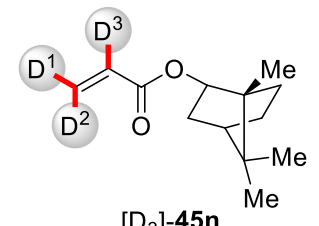
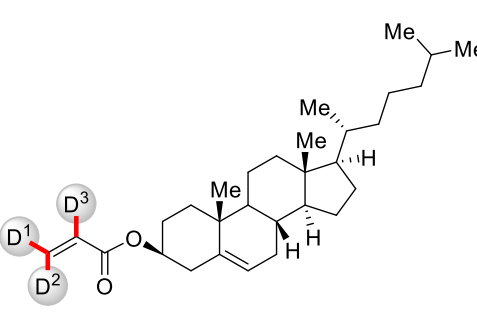
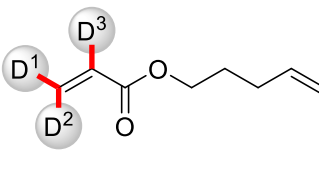


Entry	Product	Yield [%] ^[a]	D ¹ [%]	D ² [%]	D ³ [%]
1	 [D ₃]- 45d	90	96	96	96

Results and Discussion

Entry	Product	Yield [%] ^[a]	D ¹ [%]	D ² [%]	D ³ [%]
2 ^[b]	 [D ₃]-45b	>95	95	95	95
3 ^[b]	 [D ₃]-45c	>95	96	96	96
4	 [D ₃]-45m	>95	95	95	94
5	 [D ₃]-45g	75	95	95	95
6	 [D ₃]-45h	91	95	95	94
7	 [D ₃]-45j	>95	98	98	98

Results and Discussion

Entry	Product	Yield [%] ^[a]	D ¹ [%]	D ² [%]	D ³ [%]
8	 [D ₃]-45n	>95	97	97	97
9 ^[b]	 [D ₃]-45l	>95	99	99	98
10 ^[b]	 [D ₃]-45k	>95	96	96	96

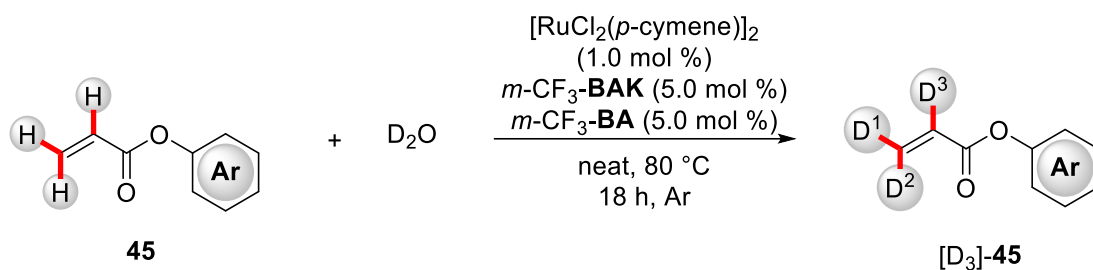
^[a] Reaction conditions: **45** (1.0 mmol), [RuCl₂(*p*-cymene)]₂ (**30**) (1.0 mol %), *m*-CF₃-**BA** (**106**) (5.0 mol %), *m*-CF₃-**BAK** (**106-K**) (5.0 mol %), D₂O (1.0 mL), Ar, 80 °C, 18 h. Conversion and deuterium incorporation was determined by ¹H-NMR vs. internal standards. ^[b] C₆D₆ (1.0 mL) added.

The labeling reaction was not limited to aliphatic and benzylic acrylates, also aromatic acrylic esters **45** smoothly reacted under the optimized reaction conditions, showing an unexpected broad functional group tolerance. Trifluoromethyl groups were accepted as well as chlorine, bromine, iodine and ethers on the arene (entries 1-6). An acetyl group *para* to the acrylic ester showed minor incorporation at the enolizable methyl group as a side reaction (entry 7). Even coordinating or oxidizing substituents, such

Results and Discussion

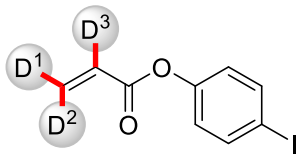
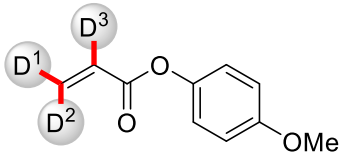
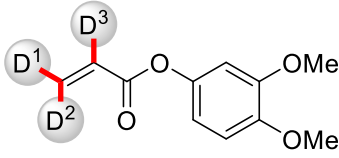
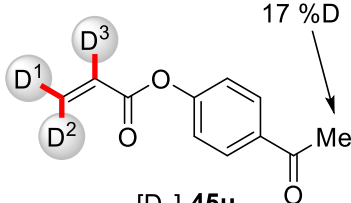
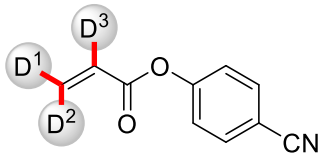
as cyano- und nitro-groups smoothly reacted, with slightly diminished incorporation in the α -position (entries 8 and 9).

Table 34: Scope of aromatic acrylic esters for the ruthenium(II)-catalyzed deuteration.

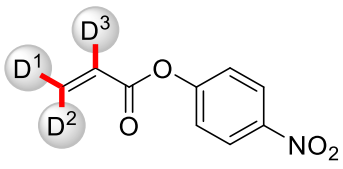


Entry	Product	Yield [%]	D ¹ [%]	D ² [%]	D ³ [%]
1	 [D ₃]-45o	>95	96	96	84
2	 [D ₃]-45p	80	96	96	96
3	 [D ₃]-45q	>95	95	95	95

Results and Discussion

Entry	Product	Yield [%]	D ¹ [%]	D ² [%]	D ³ [%]
4	 [D ₃]-45r	84	92	92	92
5	 [D ₃]-45s	>95	97	97	97
6	 [D ₃]-45t	>95	94	94	94
7 ^[b]	 [D ₃]-45u	>95	96	96	70
8 ^[b]	 [D ₃]-45v	89	85	85	52

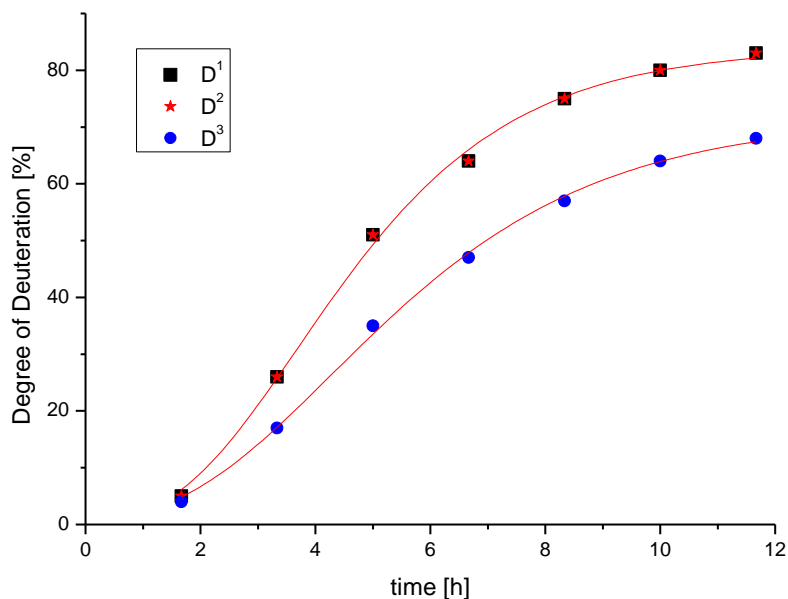
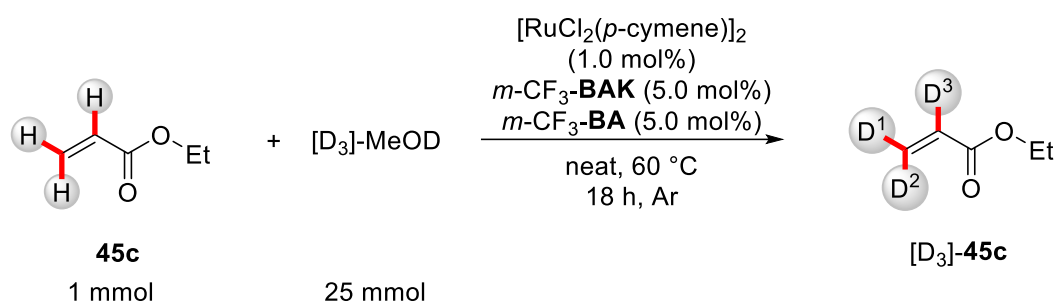
Results and Discussion

Entry	Product	Yield [%]	D ¹ [%]	D ² [%]	D ³ [%]
9 ^[b]	 [D ₃]- 45w	>95	95	95	36

^[a] Reaction conditions: **45d** (1.0 mmol), [RuCl₂(*p*-cymene)]₂ (**30**) (1.0 mol %), *m*-CF₃-**BA** (**106**) (5.0 mol %), *m*-CF₃-**BAK** (**106-K**) (5.0 mol %), D₂O (1.0 mL), Ar, 80 °C, 18 h. Conversion and deuterium incorporation was determined by ¹H-NMR vs. internal standards. ^[b] C₆D₆ (1.0 mL) added.

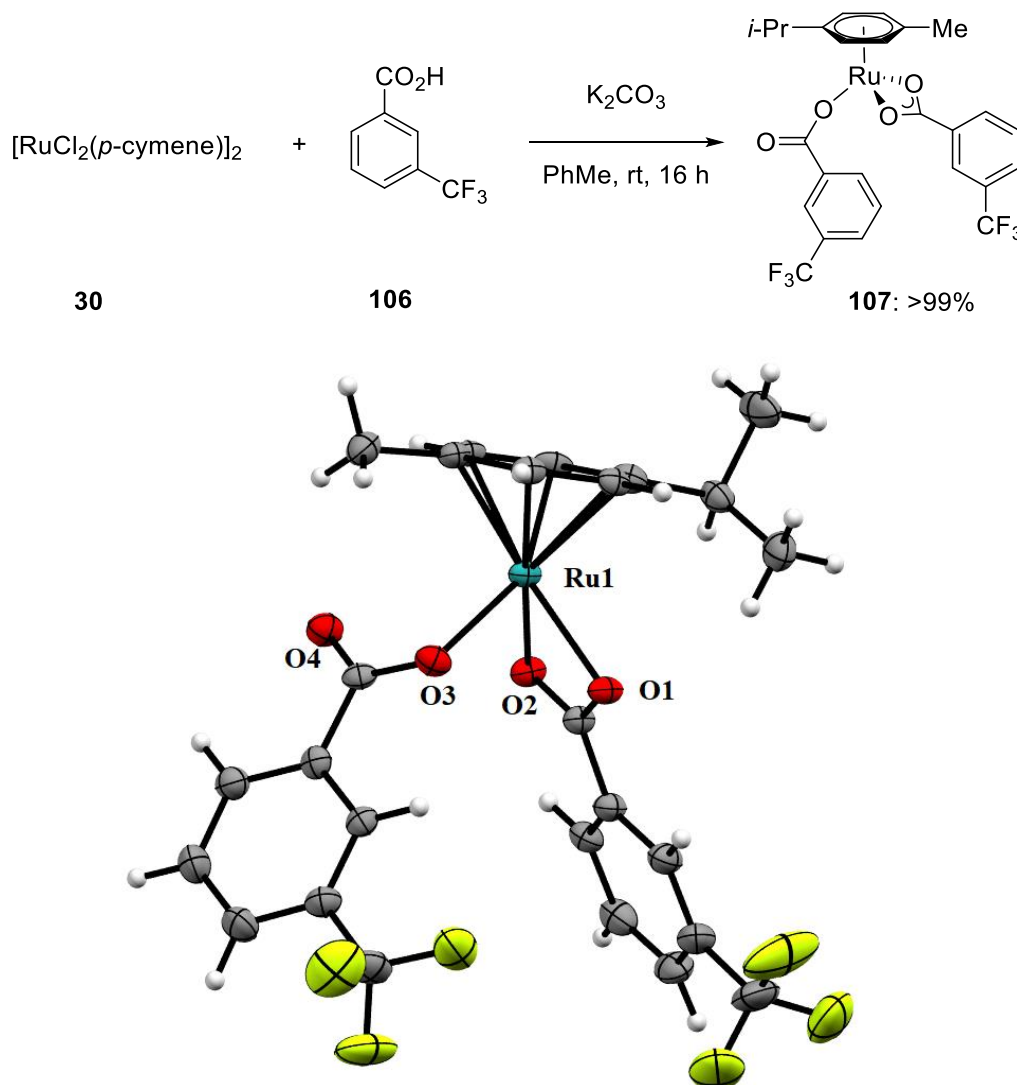
3.3.3 Kinetic Studies and Catalyst Investigations

Next to deuterium oxide, deuterated methanol was identified as a second possible deuterium atom source, which offered the possibility of performing the reaction in a homogenous fashion and studying the kinetics of the hydrogen isotope exchange reaction by *in operando* NMR studies. The deuterium incorporation in both β -positions showed identical values, while the exchange in the α -position was slightly slower.



Scheme 40: *In operando* NMR study of the ruthenium(II)-catalyzed hydrogen isotope exchange reaction.

In order to explain the highly beneficial effect of trifluoromethylated benzoic acids as ligands, the *in situ* formed catalyst was synthesized and crystallized it from $\text{CH}_2\text{Cl}_2/n$ -hexane at -30°C . Complex **107** crystallized with two diametrically opposed molecules in the asymmetric unit. The ruthenium–oxygen distances are with 2.068 Å, 2.150 Å and 2.147 Å inconspicuous and comparable with those reported by Milstein and co-workers for the related acetate complex.^[107]

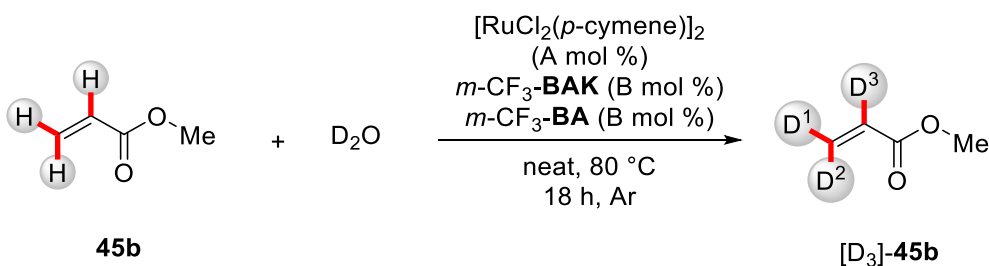


Scheme 41: Synthesis and crystal structure of the catalyst **107**.

3.3.4 Scale-Up and Synthetic Applications of Deuterated Acrylates

In order to synthesize synthetically useful amounts of the deuterated acrylates, the reaction was scaled up. Volatile methyl acrylate (**45b**) was chosen to be the ideal substrate, since it could be directly condensed from the reaction solution. Successively the catalyst loading was lowered to 0.5 mol %, 0.2 mol % and even down to 0.1 mol %, still giving excellent deuteration rates in the range of the D to H ratio of the reaction solution and remarkable turnover numbers (TON) up to 1070 per ruthenium center (entries 1-3). Further reduction of the catalyst loading to 0.1 mol % showed the limits of effectivity (entry 6). Since the deuteration rate of the products represented the stochastic ratio of D to H of the reaction solution, high deuterium incorporation needed a huge excess of the deuterium source. In order to reduce this excess, the labeling reaction was performed in two consecutive steps. First predeuteration to 75% with a low D to H ratio of 3.0 was performed. In a second step, the deuteration was increased to 93% with a D to H ratio of 10, yielding $[D_3]$ -**45b** in 68% over both steps using an overall D to H excess of ~5 (entries 4 and 5).

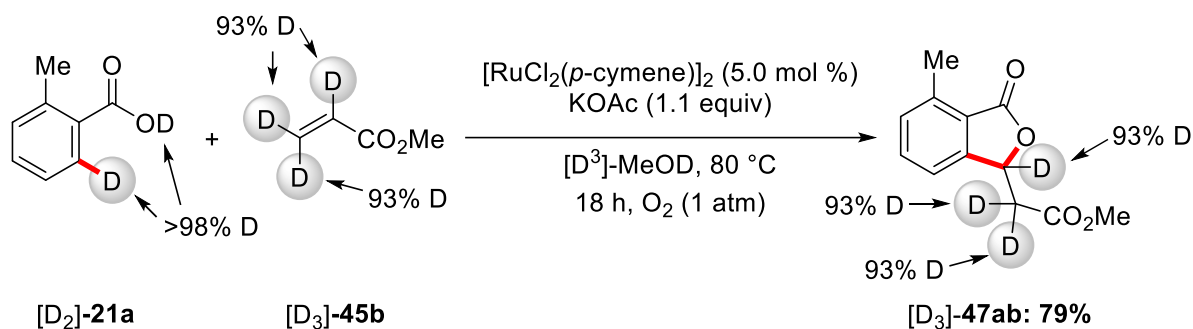
Table 35: Scale up of the ruthenium(II)-catalyzed deuteration of acrylic esters.



Entry	45b [mmol]	A/B	D/H	Yield [%] ^[a]	% D	TON ^[b]
1	22	0.5/2.5	9.7	74	90	200
2	55	0.2/1.0	3.0	88	75	495
3	22	0.1/0.5	9.9	82	87	1070
4	55	0.1/0.5	3.0	82	72	890
5 ^[c]	40	0.1/0.5	10	83	93	---
6	55	0.01/0.05	3.0	not isolated	12	---

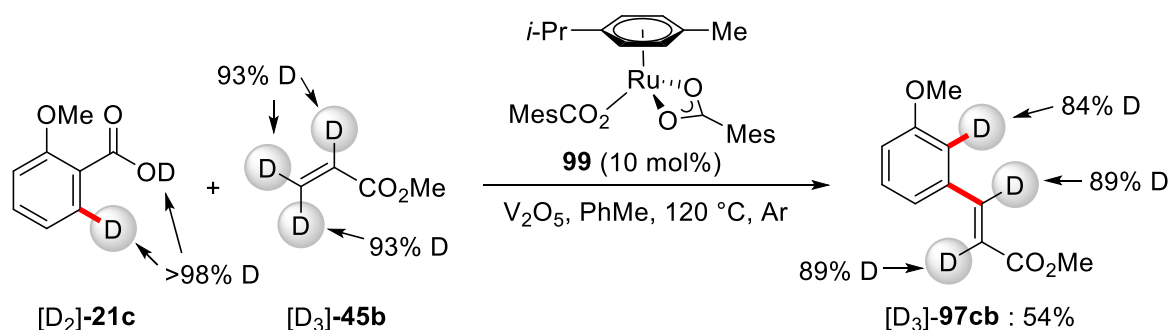
^[a] Yield of isolated product. deuterium incorporation was determined by ¹H-NMR. ^[b] Based on isolated product and turnovers per ruthenium center. ^[c] Product of entry 4 as the substrate.

With multigram amounts of the deuterated methyl acrylate ([D₃]-**45b**) in hand, the labeled alkene was applied in ruthenium(II)-catalyzed annulative alkenylation and decarboxylative alkenylation reactions. D₂-**21a** smoothly reacted with [D₃]-**45b** under ruthenium(II)-oxidase conditions, forming the phthalide [D₃]-**47ab** in 79% yield and 93% deuteration in the labeled positions (Scheme 42).



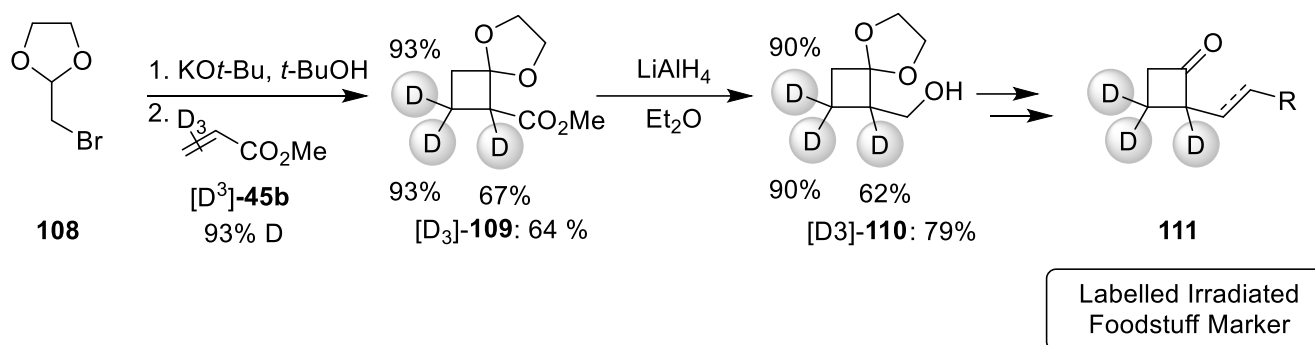
Scheme 42: Selective synthesis of deuterium labeled phthalides.

Under decarboxylative reaction conditions [D₃]-**45b** reacted with [D₂]-**21c** to the alkenylated arene in 54% yield and 84% deuteration the *ipso*-position, while the olefinic hydrogen atoms were deuterated in 89% (Scheme 43).



Scheme 43: Selective synthesis of deuterium labeled meta-alkenylated arenes.

In addition the deuterium labeled methyl acrylate was successfully applied in the synthesis of a labeled cyclobutene alcohol **110** (Scheme 44). Cyclobutene **110** is a common precursor to various 2-alkylcyclobutenones and 2-alkenylcyclobutanones **111** which are important markers for the analysis of irradiated foodstuffs.^[108] The synthesis started by *in situ* formation of methylene dioxolan, from **108**. A 2+2 cycloaddition with the deuterated methyl acrylate formed methyl ester [D₃]-**109** in 64% yield. Subsequent reduction delivered alcohol [D₃]-**110** in 79% and 90% deuterium at both C³ positions and 62% in the C² position. Various labeled cyclobutanone foodstuff markers **110** could be accessed from this key intermediate by an oxidation, Wittig reaction, deprotection sequence.



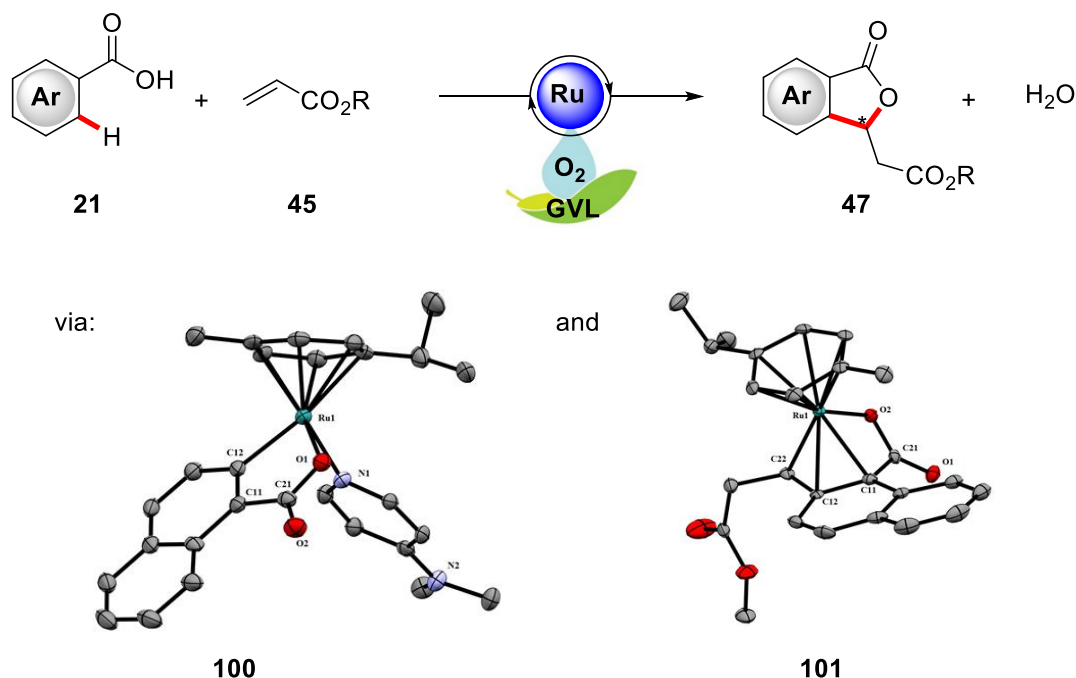
Scheme 44: Synthesis of the labeled key intermediate [D₃]-**121** of alkyl- and alkenylcuclobutenones **122**.

In conclusion, the synthesis of isotopically labeled methyl acrylate was successfully scaled up to multigram scale. The catalytic system proved to be highly efficient, working at remarkably low loadings of 1.0 mol% and TON's up to 1070. The labeled acrylic esters were applied in the synthesis of labeled phthalide [D₃]-**47ab**, *meta*- substituted alkenylarene [D₃]-**97cd** and [D₃]-**110**, which could be used as a key intermediate for the synthesis of labeled irradiated foodstuffs markers.

4 Summary and Outlook

Within the last two decades C–H activation processes have evolved from a promising concept to a powerful class of reactions for the construction of organic molecules, especially pharmaceutically active compounds.^[22a, 30a, 31a, 32b, 32c, 41e, 109] Compared to commonly employed cross-coupling reactions, the need for prefunctionalization of the reactants is reduced to a minimum. Thereby the production process of the target molecule is optimized from the economic point of view by reducing the number of steps, as well as from the ecologic point of view by preventing undesired waste formation.

Ruthenium(II) complexes have been shown to act as potent catalysts in a variety of C–H functionalizations, *inter alia* enabling the twofold oxidative C–H alkenylation between arenes and alkenes.^[41e, 44] Thus far, these oxidative transformations were restricted to the use of stoichiometric amounts of costly and ecologically problematic copper(II) and silver(I) salts as oxidant. In 2015, Ackermann *et al.* showed, that these salts could be substituted by simple and environmentally benign oxygen as the oxidant.^[41d] Based on these findings, the synthesis of phthalides (**47**) from benzoic acids (**21**) and acrylic esters (**45**) was proven viable (Scheme 45).

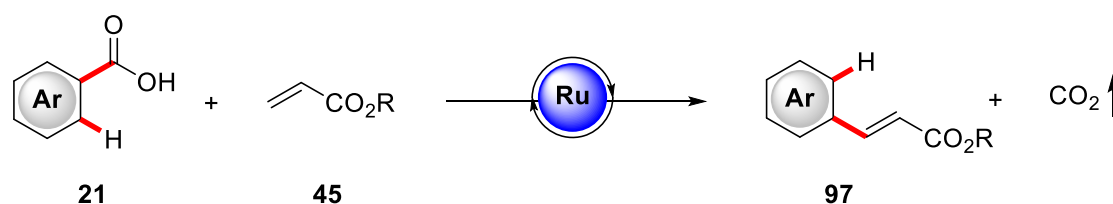


Scheme 45: Ruthenium(II) oxidase catalyzed twofold C–H alkenylation for the synthesis of phthalides (**47**).

Thereby, a robust catalytic system based on *n*-butanol as the solvent was developed.^[110] Subsequently, the sustainability and applicability of this system was largely increased by the use of the environmentally benign, renewable γ -valerolactone (**77**) as the solvent.^[111] This method for the synthesis of phthalides (**47**) was characterized by a broad substrate scope, yields of up to 98% and environmentally benign water as the only byproduct. The isolation and characterization of two reaction intermediates in combination with extensive mechanistic studies gave major insights into the catalytic mode of action. The ruthenium(II)-oxidase system has been shown to perform in batch, as well as in flow and for large scale applications the security profile of the reaction could be further improved by the substitution of oxygen by less hazardous hydrogen peroxide.

Throughout the reaction a racemic mixture of isomers is formed, which is just minorly affected by the use of chiral acrylic esters. The mechanistic studies indicated, that the stereoinformation of the product is set by the benzoic acid orientation in the cycloruthenation step. Therefore the development of ruthenium(II)-biscarboxylate catalysts, bearing chiral information would be highly interesting, in order to form the products in an enantioselective fashion.

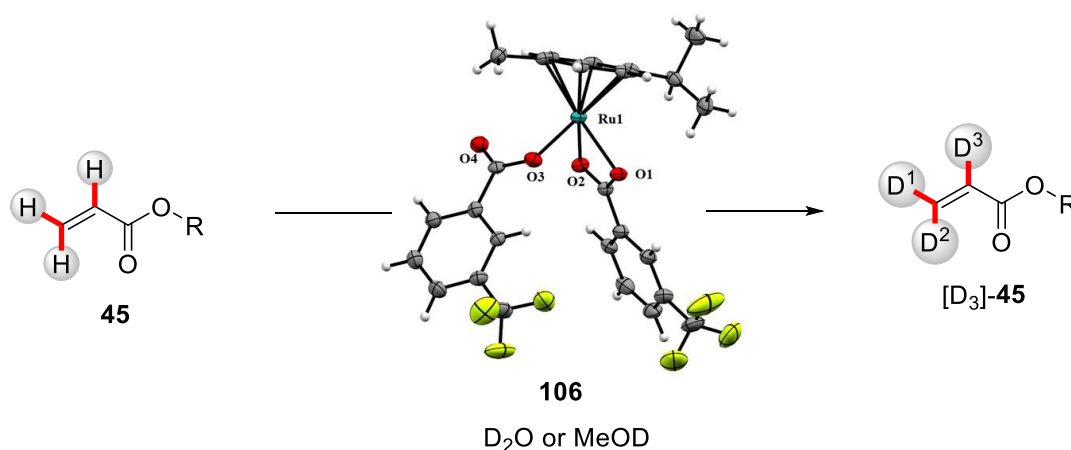
A different reactivity was observed, when the reaction was performed with salicylic ethers under inert conditions. Instead of the formal oxa-Michael addition, these conditions led to the extrusion of carbon dioxide providing a new route to *meta*-substituted arenes (Scheme 46).^[112] Optimization of the reaction conditions led to a stable catalytic system for the decarboxylative C–H alkenylation, which provided the targeted *meta*-alkenylated arenes in up to 97% yield. Our studies demonstrated this unique reaction is occurring *via* a domino process, with the C–H alkenylation occurring prior to the decarboxylation event. It is noteworthy, that transformations of this type were formerly unknown for ruthenium catalysis.



Scheme 46: Ruthenium(II)-biscarboxylate-catalyzed decarboxylative C–H alkenylation of benzoic acids.

In contrast to the related redox neutral decarboxylative alkenylation with alkynes, this unique transformation is restricted to salicylic ethers as the substrates, while other substituents provide mixtures of products. Therefore, efforts to broaden the substrate scope of this transformation would be highly interesting. In addition, the substitution of vanadium(V) oxide by less harmful and greener oxidants or electric current and the reduction of the benzoic acid excess would improve the economical applicability of this reaction.

Methods for hydrogen isotope exchange (HIE) of arene C–H bonds are well established,^[64c, 70a] while studies on the isotopic labeling of olefinic C–H bonds are limited to few reports. During general labeling studies, ruthenium(II)-biscarboxylates were found to exchange hydrogen atoms at the acrylic moiety with the solvent. Optimization led to a highly effective method for deuterium labeling, which selectively takes place at the alkene positions (Scheme 47). The labeling reaction effectively worked with D₂O or in deuterated methanol as deuterium source with an ample substrate scope and very low catalyst loadings down to 1%.



Scheme 47: Ruthenium(II)-catalyzed hydrogen isotope exchange of olefinic C–H bonds.

Since the tritiation of bioactive compounds is an important diagnostic tool for pharmaceutical research,^[70a] it would be highly interesting to expand this reactivity to the radioactive isotope tritium.

5 Experimental Section

5.1 General Remarks

Unless otherwise noted, all reactions were performed under an Ar or N₂ atmosphere using pre-dried glassware and standard Schlenk-techniques.

Solvents

All solvents for reactions involving moisture-sensitive reagents were dried, distilled and stored under an inert atmosphere (Ar or N₂) according to the following standard procedures.

Water (H₂O) was degassed before its use, applying repeated freeze-pump-thaw degassing procedure.

Methanol (MeOH) was distilled from magnesium methanolate.

***n*-Butanol** (*n*-BuOH) was distilled and stored over 4Å molecular sieve.

***tert*-Amyl alcohol** (*t*-AmOH) was stirred over Na chips for 5 h at 120 °C and then distilled at ambient pressure.

Dichloromethane (CH₂Cl₂) and **tetrahydrofuran** (THF) were purified using a solvent purification system (SPS) from MBraun.

1,2-Dichloroethane (DCE) was dried over CaH₂ for 8 h, degassed and distilled.

***N*-Methyl-2-pyrrolidone** (NMP) was dried over NaH and subsequently distilled under reduced pressure.

***N,N*-Dimethylformamide** (DMF) and **dimethylsulfoxide** (DMSO) were dried over CaH₂ for 4 h at 150 °C and subsequently distilled under reduced pressure.

Benzene, **toluene**, ***m*-xylene**, ***p*-xylene**, ***n*-hexane** and **1,4-dioxane** were dried by distillation from Na using benzophenone as indicator.

γ -Valerolactone (**77**), ***L*-ethyl lactate**, **2-methyl THF** and **tetrahydrofuryl alcohol** were distilled and stored over 4 Å molecular sieves.

Deuterium oxide was purchased from Deutero and used as received.

Benzene-*d*₆ was purchased from Deutero and stored over 4 Å molecular sieves.

Flow Reactions

Flow reactions were performed on a Vapourtech® easy-MedChem E-Series flow reactor equipped with V-3 pumps, collection valve and back pressure regulator, gas-liquid reactor and CFC-tube tubular mixing reactor.

Vacuum

A Vacuubrand[®] RD4 rotary vane vacuum pump was used. Measured vacuum: 0.1 mbar (uncorrected value).

Melting Points (M. p.)

Melting points were measured, using a Stuart[®] Melting Point Apparatus SMP3 from Barloworld scientific. Reported values are uncorrected.

Chromatography

Analytical thin layer chromatography (TLC) was performed on 0.25 mm silica gel 60F-plates with 254 nm fluorescent indicator from Merck[®]. Plates were visualized under UV-light or developed by treatment with a potassium permanganate solution followed by carefully heating. Chromatographic purification of products was accomplished by flash column chromatography on MERCK Geduran[®] silica gel, grade 60 (40–63 μm , 70–230 mesh ASTM).

Gas Chromatography (GC)

The conversion of the reactions was monitored *via* gas chromatography or coupled gas chromatography-mass spectrometry using a 7890 GC-system with/without mass detector 5975 (Triple-Axis-Detector) or a 7890B GC-system coupled with a 5977A mass detector, both from Agilent Technologies[®].

Single crystal X-ray diffraction analysis

Data collection was done on a Bruker[®] D8 Venture four-circle-diffractometer or Bruker[®] D8 three-circle-diffractometer from Bruker AXS GmbH; used detector: Photon II from Bruker AXS GmbH; used X-ray sources: microfocus $\text{I}\mu\text{S}$ Cu/Mo or Mo Microsource from Incoatec GmbH with mirror optics HELIOS and single-hole collimator from Bruker AXS GmbH.

Used programs: APEX3 Suite (v2017.3-0) and therein integrated programs SAINT (Integration) und SADABS (Absorption correction) from Bruker AXS GmbH;^[113] structure solution was done with SHELXT, refinement with SHELXS^[114] or SHELXL^[115] in the graphical user interface SHELXLE;^[116] OLEX² was used for data finalization.^[117]

Special Utilities: SMZ1270 stereomicroscope from Nikon Metrology GmbH was used for sample preparation; crystals were mounted on MicroMounts or MicroLoops from MiTeGen; for sensitive samples the X-TEMP 2 System was used for picking of crystals;^[118] crystals were cooled to given temperature with Cryostream 800 from Oxford Cryosystems.

Recycling Preparative HPLC

Recycling preparative HPLC (GPC) was performed on a system from JAI® (LC-92XX II Series, injection-and control-valve, UV and RI detector) connected to JAIGEL HH series columns. Chloroform of HPLC grade was employed.

Nuclear Magnetic Resonance Spectroscopy (NMR)

Nuclear magnetic resonance (NMR) spectroscopy was performed at 300, 400, 500 or 600 MHz (¹H-NMR), 61 or 77 MHz (²H-NMR), 75, 100 or 126 MHz (¹³C-NMR, APT) and 283 MHz or 471 MHz (¹⁹F-NMR) at BRUKER (*Avance III 300, Avance III HD 300, Avance III 400, Avance III HD 400, Avance III HD 500*) and VARIAN (*Mercury VX300, Mercury Plus 300, VNMRS 300, Inova 500 and Inova 600*) instruments. Chemical shifts were reported as δ -values in ppm relative to the residual proton peak or carbon peak of the deuterated.

Solvent	¹ H-NMR	¹³ C-NMR
CDCl ₃	7.26	77.16
C ₆ D ₆	7.16	128.06
Methanol-d ₄	4.87, 3.31	49.00
Toluene-d ₈	2.09	137.86
DMSO-d ₆	2.50, 3.30	39.52

For characterization of the observed resonance multiplicities the following abbreviations were applied: *s* (singlet), *d* (doublet), *t* (triplet), *q* (quartet), *p* (pentet), *hept* (heptet), *m* (multiplet), *dd* (doublet of doublet), *dt* (doublet of triplet), or analogue representations. The coupling constants *J* are reported in Hertz (Hz).

Infrared Spectroscopy (IR)

Infrared spectra were recorded on a Bruker *Alpha-P* ATR-spectrometer. Analysis of the spectral data has been done by using the *OPUS 3.1* software from Bruker, respectively *OPUS 6*. Absorption ($\tilde{\nu}$) was given in wave numbers (cm^{-1}). Spectra were recorded in the range of 4000 to 400 cm^{-1} .

Mass Spectrometry (MS)

Electron ionization (EI) and EI high resolution mass spectra (HR-MS) were measured on a time-of-flight (TOF) mass spectrometer AccuTOF from JOEL. Electrospray ionization (ESI) mass spectra were recorded on an Ion-Trap mass spectrometer LCQ from Finnigan[®], a quadrupole time-of-flight maXis from Bruker Daltonic[®] or on a time-of-flight mass spectrometer *microTOF* from Bruker Daltonic[®]. ESI-HR-MS spectra were recorded on a Bruker[®] Apex IV or a Bruker Daltonic[®] 7T, fourier transform ion cyclotron resonance (FTICR) mass spectrometer. The ratios of mass to charge (m/z) were indicated, intensities relative to the base peak ($I = 100$) were written in parentheses.

Reagents

Chemicals obtained from commercial sources with purity above 95% were used without further purification. The following compounds were synthesized according to previously described methods: 2-tosylbenzoic acid (**21n**),^[119] 2-mesylbenzoic acid (**21o**),^[119] 5-chloro-2-methoxybenzoic acid (**21γ**),^[120] 5-bromo-2-methoxybenzoic acid (**21δ**),^[121] 2-methoxy-2-naphthoic acid (**21ε**),^[120] [D₂] methyl acrylate ([D₂]-**45b**),^[122] benzyl acrylate (**45d**),^[123] 4-fluorobenzyl acrylate (**45i**),^[123] menthyl acrylate (**45j**),^[123] pent-4-enyl acrylate (**45k**),^[123] cholesteryl acrylate (**45l**),^[123] 2-trifluoromethylphenyl acrylate (**45o**),^[123] 4-chlorophenylacrylate (**45p**),^[123] 4-bromophenyl acrylate (**45q**),^[123] 4-iodophenyl acrylate (**45r**),^[123] 4-acetylphenyl acrylate (**45u**),^[123] 4-cyanophenylacrylate (**45v**),^[123] 4-nitrophenylacrylate (**45w**)^[123].

The following compounds were obtained by the generous courtesy of the persons named below:

Karsten Rauch: [Ru(O₂CMe)₂(*p*-cymene)] (**99**), [RuCl₂(*p*-cymene)]₂ (**30**), [Cp*RhCl₂]₂.

Dr. Svenja Warratz: [Ru(O₂CAd)₂(*p*-cymene)] (**105**), [Ru₂Cl₃(*p*-cymene)₂][PF₆].

Dr. Ruhuai Mei: [Cp*CoI₂]₂.

M. Sc. Torben Rogge: [Ru(O₂CAd)₂(*p*-cymene)] (**105**).

M. Sc. Korkit Korvorapun: Bornyl acrylate (**45n**).

5.2 Representative Procedures

5.2.1 Representative Procedure A: Ruthenium(II)-Catalyzed Oxidative Alkenylation of Benzoic Acids in *n*-Butanol

Benzoic acid **21** (1.00 mmol, 1.0 equiv), [RuCl₂(*p*-cymene)]₂ (**30**) (30.6 mg, 0.05 mmol, 5.0 mol %) and KOAc (108 mg, 1.10 mmol, 1.1 equiv) were placed in a pre-dried 25 mL Schlenk-tube. The flask was evacuated and refilled with O₂ three times. *n*-BuOH (3.0 mL) and acrylate **45** (1.50 mmol, 1.5 equiv) were added and the reaction mixture was stirred at 80 °C for 18 h. At ambient temperature, all volatiles were removed *in vacuo*. The residue was purified by column chromatography on silica gel (*n*-hexane/EtOAc).

5.2.2 Representative Procedure B: Ruthenium(II)-Catalyzed Oxidative Alkenylation of Benzoic Acids in γ -Valerolactone (**77**)

Benzoic acid **21** (1.00 mmol, 1.0 equiv), [RuCl₂(*p*-cymene)]₂ (**30**) (30.6 mg, 0.05 mmol, 5.0 mol %) and KOAc (98.0 mg, 1.00 mmol, 1.0 equiv) were placed in a pre-dried 25 mL Schlenk-tube. The flask was evacuated and refilled with O₂ three times. γ -Valerolactone (**77**) (1.0 mL), HOAc (60 mg, 1.00 mmol, 1.0 equiv) and acrylate **45** (1.50 mmol, 1.5 equiv) were added and the reaction mixture was stirred at 80 °C for 18 h. At ambient temperature, the mixture was diluted with H₂O (10 mL), extracted with *n*-hexane/MTBE (1/1, 3×10 mL) and washed with H₂O (5·10 mL). All volatiles were removed *in vacuo* and the residue was purified by column chromatography on silica gel (*n*-hexane/EtOAc).

5.2.3 Representative Procedure C: Ruthenium(II)-Catalyzed Decarboxylative Alkenylation of Benzoic Acids

Benzoic acid (**21**) (3.00 mmol, 3.0 equiv), [Ru(O₂CMes)₂(*p*-cymene)] (**99**) (56.2 mg, 0.10 mmol, 10.0 mol %) and V₂O₅ (182 mg, 1.00 mmol) were placed in a pre-dried pressure tube equipped with a rubber septum. The tube was evacuated and refilled with N₂ or Ar three times. Dry PhMe (3.0 mL) and acrylate **45** (1.00 mmol, 1.0 equiv) were added. The tube was closed and the reaction mixture was stirred at 120 °C for 18 h. At ambient temperature, all volatiles were removed *in vacuo* and the residue was purified by column chromatography on silica gel (*n*-hexane/EtOAc).

5.2.4 Representative Procedure D: Ruthenium(II)-Catalyzed Deuteration of Acrylic Esters

[RuCl₂(*p*-cymene)]₂ (**30**) (6.1 mg, 0.01 mmol, 1.0 mol %), *m*-CF₃-benzoic acid (**106**) (9.5 mg, 0.05 mmol, 5.0 mol %) and potassium *m*-CF₃-benzoate (**106-K**) (12 mg, 0.05 mmol, 5.0 mol %) were placed in a pre-dried 25 mL Schlenk-tube equipped with a rubber septum. The tube was evacuated and refilled with Ar three times. Acrylic ester (**45**) (1.00 mmol, 1.0 equiv) and D₂O (1.0 mL, 55 mmol, 55.0 equiv) were added and the mixture was heated to 80 °C for 18 h. At ambient temperature, the internal standard was added and the mixture was extracted with CDCl₃ (1.0 mL). An aliquote (0.1 mL) of the organic phase was removed, filtered and rinsed with CDCl₃ through a small plug of silica and analyzed by NMR spectroscopy.

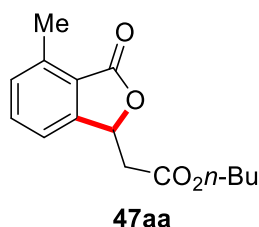
5.2.5 Representative Procedure E: Ruthenium(II)-Catalyzed Deuteration of Acrylic Esters in C₆D₆

[RuCl₂(*p*-cymene)]₂ (**30**) (6.1 mg, 0.01 mmol, 1.0 mol %), *m*-CF₃-benzoic acid (**106**) (9.5 mg, 0.05 mmol, 5.0 mol %) and potassium *m*-CF₃-benzoate (**106-K**) (11.5 mg, 0.05 mmol, 5.0 mol %) were placed in a pre-dried 25 mL Schlenk-tube equipped with a rubber septum. The tube was evacuated and refilled with Ar three times. Acrylic ester (**45**) (1.00 mmol, 1.0 equiv), C₆D₆ (1.0 mL) and D₂O (1.0 mL, 55 mmol, 55.0 equiv) were added and the mixture was heated to 80 °C for 18 h. At ambient temperature, the internal standard was added. An aliquote (0.1 mL) of the organic phase was removed, filtered and rinsed with C₆D₆ through a small plug of silica and analyzed by NMR spectroscopy.

5.3 Experimental Procedures and Analytical Data

5.3.1 Ruthenium(II)-Oxidase C–H Alkenylation of Benzoic Acids

5.3.1.1 Experimental Data for the Synthesis of Phthalides



n-Butyl 2-(4-methyl-3-oxo-1,3-dihydroisobenzofuran-1-yl)acetate (**47aa**):

a) The representative procedure **A** was followed using 2-methylbenzoic acid (**21a**) (136 mg, 1.00 mmol, 1.0 equiv) and *n*-butyl acrylate (**45a**) (192 mg, 1.50 mmol). Purification by column chromatography (*n*-hexane/EtOAc: 4/1 + 5% NEt₃) yielded **47aa** (180 mg, 0.74 mmol, 74%) as a colorless oil.

b) The representative procedure **B** was followed using 2-methylbenzoic acid (**21a**) (136 mg, 1.00 mmol, 1.0 equiv) and *n*-butyl acrylate (**45a**) (192 mg, 1.50 mmol, 1.5 equiv). Purification by column chromatography (*n*-hexane/EtOAc: 4/1 + 5% NEt₃) yielded **47aa** (237 mg, 0.90 mmol 90%) as a colorless oil.

c) The representative procedure **B** was followed using 2-methylbenzoic acid (**21a**) (680 mg, 5.00 mmol, 1.0 equiv) and *n*-butyl acrylate (**45a**) (960 mg, 7.50 mmol, 1.5 equiv). Purification by column chromatography (*n*-hexane/EtOAc: 4/1 + 5% NEt₃) yielded **47aa** (1265 mg, 4.85 mmol 97%) as a colorless oil.

¹H-NMR (400 MHz, CDCl₃): δ = 7.53 (dd, *J* = 7.6, 7.6 Hz, 1H), 7.31–7.27 (m, 2H), 5.81 (t, *J* = 6.8 Hz, 1H), 4.16 (t, *J* = 6.7 Hz, 2H), 2.87 (dd, *J* = 6.5, 2.2 Hz, 2H), 2.69 (s, 3H), 1.67–1.56 (m, 2H), 1.43–1.32 (m, 2H), 0.93 (t, *J* = 7.4 Hz, 3H).

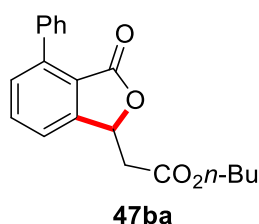
¹³C-NMR (101 MHz, CDCl₃): δ = 170.2 (C_q), 169.6 (C_q), 149.4 (C_q), 140.1 (C_q), 134.1 (CH), 131.3 (CH), 123.6 (C_q), 119.4 (CH), 76.2 (CH), 65.3 (CH₂), 39.9 (CH₂), 30.7 (CH₂), 19.2 (CH₂), 17.5 (CH₃), 13.8 (CH₃).

IR (ATR): 2960, 2933, 2874, 1755, 1731, 1602, 1167, 1088, 1046, 787 cm⁻¹.

MS (EI) m/z (relative intensity): 262 (14) $[M]^+$, 206 (74), 160 (82), 147 (100), 132 (25), 119 (33), 91 (35), 46 (13).

HR-MS (ESI) m/z calcd for $C_{15}H_{19}O_4$, $[M+H]^+$ 263.1287, found 263.1276.

The spectral data are in accordance with those reported in the literature.^[41g]



***n*-Butyl 2-(4-phenyl-3-oxo-1,3-dihydroisobenzofuran-1-yl)acetate (47ba):**

a) The representative procedure **A** was followed using 2-phenylbenzoic acid (**21b**) (198 mg, 1.00 mmol, 1.0 equiv) and *n*-butyl acrylate (**45a**) (192 mg, 1.50 mmol, 1.5 equiv). Purification by column chromatography (*n*-hexane/EtOAc: 4/1 + 5% NEt_3) yielded **47ba** (195 mg, 0.60 mmol, 60%) as a colorless oil.

b) The representative procedure **B** was followed using 2-phenylbenzoic acid (**21b**) (198 mg, 1.00 mmol, 1.0 equiv) and *n*-butyl acrylate (**45a**) (192 mg, 1.50 mmol, 1.5 equiv). Purification by column chromatography (*n*-hexane/EtOAc: 4/1 + 5% NEt_3) yielded **47ba** (211 mg, 0.65 mmol, 65%) as a colorless oil.

1H -NMR (300 MHz, $CDCl_3$): δ = 7.61 (dd, J = 7.6, 7.6 Hz, 1H), 7.49–7.42 (m, 2H), 7.42–7.30 (m, 5H), 5.78 (t, J = 6.5 Hz, 1H), 4.09 (t, J = 6.7 Hz, 2H), 2.85 (d, J = 6.7 Hz, 2H), 1.62–1.45 (m, 2H), 1.40–1.19 (m, 2H), 0.85 (t, J = 7.3 Hz, 3H).

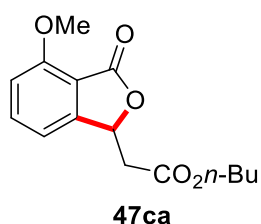
^{13}C -NMR (75 MHz, $CDCl_3$): δ = 169.5 (C_q), 168.7 (C_q), 150.2 (C_q), 143.0 (C_q), 136.4 (C_q), 134.1 (CH), 131.4 (CH), 129.6 (CH), 128.5 (CH), 128.1 (CH), 122.1 (C_q), 120.8 (CH), 75.7 (CH), 65.3 (CH_2), 39.9 (CH_2), 30.6 (CH_2), 19.2 (CH_2), 13.8 (CH_3).

IR (ATR): 2958, 1759, 1729, 1595, 1345, 1286, 1169, 1079, 1039, 817 cm^{-1} .

MS (EI) m/z (relative intensity): 324 (28) $[M]^+$, 268 (39), 250 (75), 223 (100), 209 (82), 181 (55), 152 (84), 76 (8).

HR-MS (ESI) m/z calcd for $C_{20}H_{21}O_4$, $[M+H]^+$ 325.1434, found 325.1438.

The spectral data are in accordance with those reported in the literature.^[51]



***n*-Butyl 2-(4-methoxy-3-oxo-1,3-dihydroisobenzofuran-1-yl)acetate (47ca):**

a) The representative procedure **A** was followed using 2-methoxybenzoic acid (**21c**) (152 mg, 1.00 mmol, 1.0 equiv) and *n*-butyl acrylate (**45a**) (192 mg, 1.50 mmol, 1.5 equiv). Purification by column chromatography (*n*-hexane/EtOAc: 4/1 + 5% NEt_3) yielded **47ca** (141 mg, 0.51 mmol, 51%) as a colorless oil.

b) The representative procedure **B** was followed using 2-methoxybenzoic acid (**21c**) (152 mg, 1.00 mmol, 1.0 equiv) and *n*-butyl acrylate (**45a**) (192 mg, 1.50 mmol, 1.5 equiv). Purification by column chromatography (*n*-hexane/EtOAc: 4/1 + 5% NEt_3) yielded **47ca** (167 mg, 0.60 mmol, 60%) as a colorless oil.

1H -NMR (300 MHz, $CDCl_3$): δ = 7.61 (dd, J = 8.3, 7.6 Hz, 1H), 7.00 (d, J = 7.6 Hz, 1H), 6.95 (d, J = 8.3 Hz, 1H), 7.07–6.93 (m, 2H), 5.79 (dd, J = 7.0, 6.2 Hz, 1H), 4.15 (t, J = 6.7 Hz, 2H), 3.99 (s, 3H), 2.96–2.76 (m, 2H), 1.70–1.50 (m, 2H), 1.44–1.25 (m, 2H), 0.93 (t, J = 7.3 Hz, 3H).

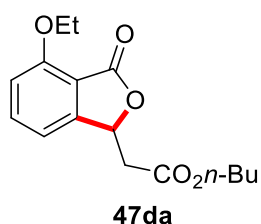
^{13}C -NMR (75 MHz, $CDCl_3$): δ = 169.5 (C_q), 168.0 (C_q), 158.9 (C_q), 151.8 (C_q), 136.6 (CH), 113.7 (CH), 113.6 (C_q), 111.3 (CH), 76.1 (CH), 65.3 (CH_2), 56.2 (CH_3), 39.9 (CH_2), 30.7 (CH_2), 19.2 (CH_2), 13.8 (CH_3).

IR (ATR): 2959, 1758, 1730, 1601, 1396, 1276, 1239, 1169, 777, 690 cm^{-1} .

MS (EI) m/z (relative intensity): 278 (25) $[M]^+$, 222 (62), 163 (100), 135 (33), 120 (11), 105 (25), 77 (26), 41 (18).

HR-MS (ESI) m/z calcd for $C_{15}H_{19}O_5$, $[M+H]^+$ 279.1228, found 279.1227.

The spectral data are in accordance with those reported in the literature.^[41g]



***n*-Butyl 2-(4-ethoxy-3-oxo-1,3-dihydroisobenzofuran-1-yl)acetate (47da):**

The representative procedure **A** was followed using 2-ethoxybenzoic acid (**21d**) (166 mg, 1.00 mmol, 1.0 equiv) and *n*-butyl acrylate (**45a**) (192 mg, 1.50 mmol, 1.5 equiv). Purification by column chromatography (*n*-hexane/EtOAc: 4/1 + 5% NEt_3) yielded **47ca** (144 mg, 0.49 mmol, 49%) as a colorless oil.

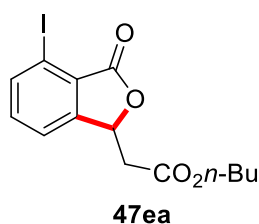
1H -NMR (500 MHz, $CDCl_3$): δ = 7.57 (dd, J = 8.2, 7.7 Hz, 1H), 6.97 (d, J = 7.7 Hz, 1H), 6.92 (d, J = 8.2 Hz, 1H), 5.77 (t, J = 6.6 Hz, 1H), 4.24 (q, J = 7.0 Hz, 2H), 4.15 (t, J = 6.7 Hz, 2H), 2.90–2.79 (m, 2H), 1.66–1.58 (m, 2H), 1.51 (t, J = 7.0 Hz, 3H), 1.40–1.32 (m, 2H), 0.93 (t, J = 7.4 Hz, 3H).

^{13}C -NMR (126 MHz, $CDCl_3$): δ = 169.6 (C_q), 167.8 (C_q), 158.3 (C_q), 151.7 (C_q), 136.4 (CH), 113.6 (C_q), 113.4 (CH) 112.2 (CH), 75.9 (CH), 65.3 (CH_2), 64.8 (CH_2), 39.9 (CH_2), 30.7 (CH_2), 19.2 (CH_2), 14.6 (CH_3), 13.8 (CH_3).

IR (ATR): 2960, 2934, 2874, 1761, 1731, 1602, 1471, 1197, 1036, 1008, 691 cm^{-1} .

MS (EI) m/z (relative intensity): 292 (28) $[M]^+$, 277 (56), 236 (48), 221 (51), 190 (53), 177 (72), 163 (64), 149 (100), 121 (32), 65 (28).

HR-MS (ESI) m/z calcd for $C_{16}H_{21}O_5$, $[M+H]^+$ 293.1384, found 293.1384.



***n*-Butyl 2-(4-iodo-3-oxo-1,3-dihydroisobenzofuran-1-yl)acetate (47ea):**

a) The representative procedure **A** was followed using 2-iodobenzoic acid (**21e**) (201 mg, 1.00 mmol, 1.0 equiv) and *n*-butyl acrylate (**45a**) (192 mg, 1.50 mmol, 1.5 equiv). Purification by column chromatography (*n*-hexane/EtOAc: 1/1 + 1% NEt₃) yielded **47ea** (231 mg, 0.63 mmol, 63%) as a colorless oil.

b) The representative procedure **B** was followed using 2-iodobenzoic acid (**21e**) (201 mg, 1.00 mmol, 1.0 equiv) and *n*-butyl acrylate (**2a**) (192 mg, 1.50 mmol, 1.5 equiv). Purification by column chromatography (*n*-hexane/EtOAc: 1/1 + 1% NEt₃) yielded **47ea** (201 mg, 0.54 mmol, 54%) as a colorless oil.

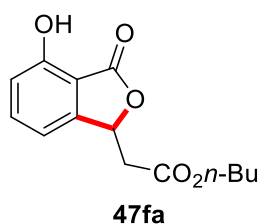
¹H-NMR (500 MHz, CDCl₃): δ = 8.00 (d, *J* = 7.7 Hz, 1H), 7.48 (d, *J* = 7.7 Hz, 1H), 7.34 (dd, *J* = 7.7, 7.7 Hz, 1H), 5.76 (t, *J* = 6.9 Hz, 1H), 4.14 (t, *J* = 6.7 Hz, 2H), 3.08–2.75 (m, 2H), 1.69–1.52 (m, 2H), 1.44–1.20 (m, 2H), 0.92 (t, *J* = 7.4 Hz, 3H).

¹³C-NMR (126 MHz, CDCl₃): δ = 169.3 (C_q), 168.0 (C_q), 151.1 (C_q), 141.1 (CH), 135.1 (CH), 127.2 (C_q), 122.0 (CH), 92.5 (C_q), 74.9 (CH), 65.4 (CH₂), 39.4 (CH₂), 30.6 (CH₂), 19.2 (CH₂), 13.8 (CH₃).

IR (ATR): 2959, 1763, 1727, 1457, 1304, 1173, 1076, 968, 781, 678 cm⁻¹.

MS (EI) *m/z* (relative intensity): 374 (22) [M]⁺, 318 (100), 273 (75), 259 (81), 231 (29), 203 (9), 104 (10), 76 (19).

HR-MS (EI) *m/z* calcd for C₁₄H₁₅IO₄, [M]⁺ 374.0015, found 374.0026.



***n*-Butyl 2-(4-hydroxy-3-oxo-1,3-dihydroisobenzofuran-1-yl)acetate (**47fa**):**

a) The representative procedure **A** was followed using salicylic acid (**21f**) (138 mg, 1.00 mmol, 1.0 equiv) and *n*-butyl acrylate (**45a**) (192 mg, 1.50 mmol, 1.5 equiv). Purification by column chromatography (*n*-hexane/EtOAc: 1/1 + 1% MeOH) yielded **47fa** (72 mg, 0.27 mmol, 27%) as a colorless oil.

b) The representative procedure **B** was followed using salicylic acid (**21f**) (138 mg, 1.00 mmol, 1.0 equiv) and *n*-butyl acrylate (**2a**) (192 mg, 1.50 mmol, 1.5 equiv). Purification by column chromatography (*n*-hexane/EtOAc: 1/1 + 1% MeOH) yielded **47fa** (138 mg, 0.52 mmol, 52%) as a colorless oil.

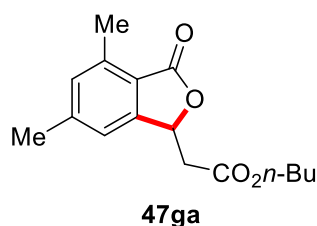
¹H-NMR (300 MHz, CDCl₃): δ = 7.76 (s, 1H), 7.52 (dd, J = 8.3, 7.5 Hz, 1H), 6.98–6.87 (m, 2H), 5.86 (t, J = 6.6 Hz, 1H), 4.13 (t, J = 6.7 Hz, 2H), 2.88 (d, J = 6.6 Hz, 2H), 1.68–1.51 (m, 2H), 1.45–1.22 (m, 2H), 0.90 (t, J = 7.4 Hz, 3H).

¹³C-NMR (75 MHz, CDCl₃): δ = 171.4 (C_q), 169.2 (C_q), 156.6 (C_q), 149.1 (C_q), 137.2 (CH), 116.0 (CH), 113.4 (CH), 111.0 (C_q), 78.3 (CH), 65.2 (CH₂), 39.3 (CH₂), 30.5 (CH₂), 19.1 (CH₂), 13.7 (CH₃).

IR (ATR): 2960, 1727, 1615, 1464, 1280, 1158, 997, 801, 689, 436 cm⁻¹.

MS (EI) m/z (relative intensity): 264 (15) [M]⁺, 208 (95), 165 (35), 162 (100), 149 (95), 134 (15), 121 (30), 65 (20).

HR-MS (EI) m/z calcd for C₁₄H₁₆O₅, [M]⁺ 264.0998, found 264.1000.



***n*-Butyl 2-(4,6-dimethyl-3-oxo-1,3-dihydroisobenzofuran-1-yl)acetate (**47ga**):**

a) The representative procedure **A** was followed using 2,4-dimethylbenzoic acid (**21g**) (150 mg, 1.00 mmol, 1.0 equiv) and *n*-butyl acrylate (**45a**) (192 mg, 1.50 mmol, 1.5 equiv). Purification by column chromatography (*n*-hexane/EtOAc: 4/1 + 5% NEt₃) yielded **47ga** (200 mg, 0.72 mmol, 72%) as a colorless oil.

b) The representative procedure **B** was followed using 2,4-dimethylbenzoic acid (**21g**) (150 mg, 1.00 mmol, 1.0 equiv) and *n*-butyl acrylate (**45a**) (192 mg, 1.50 mmol, 1.5 equiv). Purification by column chromatography (*n*-hexane/EtOAc: 4/1 + 5% NEt₃) yielded **47ga** (261 mg, 0.95 mmol, 95%) as a colorless oil.

¹H-NMR (300 MHz, CDCl₃): δ = 7.10 (s, 1H), 7.05 (s, 1H), 5.76 (t, *J* = 6.5 Hz, 1H), 4.16 (t, *J* = 6.7 Hz, 2H), 2.85 (d, *J* = 6.5 Hz, 2H), 2.64 (s, 3H), 2.42 (s, 3H), 1.68–1.54 (m, 2H), 1.45–1.30 (m, 2H), 0.93 (t, *J* = 7.3 Hz, 3H).

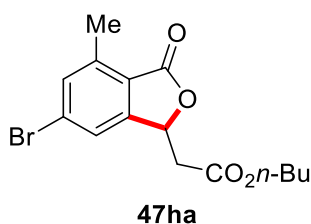
¹³C-NMR (75 MHz, CDCl₃): δ = 170.2 (C_q), 169.7 (C_q), 150.0 (C_q), 145.3 (C_q), 139.7 (C_q), 132.4 (CH), 121.1 (C_q), 119.8 (CH), 76.0 (CH), 65.3 (CH₂), 40.0 (CH₂), 30.7 (CH₂), 22.1 (CH₃), 19.2 (CH₂), 17.4 (CH₃), 13.8 (CH₃).

IR (ATR): 2960, 1754, 1731, 1613, 1310, 1270, 1203, 1170, 1013, 686 cm⁻¹.

MS (EI) *m/z* (relative intensity): 276 (20) [M]⁺, 220 (60), 174 (95), 161 (100), 146 (35), 133 (40), 105 (25), 77 (15).

HR-MS (EI) *m/z* calcd for C₁₆H₂₀O₄, [M]⁺ 276.1362, found 276.1359.

The spectral data are in accordance with those reported in the literature.^[51]



***n*-Butyl 2-(6-bromo-4-methyl-3-oxo-1,3-dihydroisobenzofuran-1-yl)acetate (47ha):**

The representative procedure **A** was followed using 2-methyl-4-bromobenzoic acid (**21h**) (150 mg, 1.00 mmol, 1.0 equiv) and *n*-butyl acrylate (**45a**) (192 mg, 1.50 mmol, 1.5 equiv). Purification by column chromatography (*n*-hexane/EtOAc: 4/1 + 5% NEt₃) yielded **47ha** (243 mg, 0.71 mmol, 71%) as a colorless oil.

¹H-NMR (500 MHz, CDCl₃): δ = 7.47–7.45 (m, 2H), 5.76 (t, *J* = 6.5 Hz, 1H), 4.20–4.13 (m, 2H), 2.95–2.80 (m, 2H), 2.66 (s, 3H), 1.65–1.58 (m, 2H), 1.41–1.33 (m, 2H), 0.93 (t, *J* = 6.5 Hz, 3H).

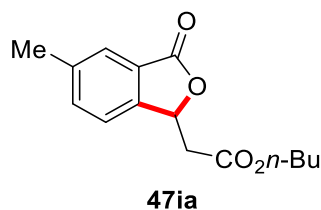
¹³C-NMR (126 MHz, CDCl₃): δ = 169.3 (C_q), 169.2 (C_q), 151.2 (C_q), 141.7 (C_q), 134.5 (C_q), 129.1 (CH), 121.1 (C_q), 123.0 (CH), 122.7 (C_q), 75.6 (CH), 65.4 (CH₂), 39.6 (CH₂), 30.7 (CH₂), 19.2 (CH₂), 17.3 (CH₃), 13.8 (CH₃).

IR (ATR): 2960, 2873, 1757, 1589, 1337, 1197, 1172, 1011, 865, 678 cm⁻¹.

MS (EI) *m/z* (relative intensity): 340 (8) [M]⁺, 286 (86), 284 (84), 240 (92), 225 (100), 210 (20), 197 (24), 118 (32), 89 (34), 69 (22).

HR-MS (EI): *m/z* calcd for C₁₅H₁₇⁷⁹BrO₄, [M]⁺ 340.0310, found: 340.0316.

The spectral data are in accordance with those reported in the literature.^[51]

***n*-Butyl 2-(5-methyl-3-oxo-1,3-dihydroisobenzofuran-1-yl)acetate (47ia):**

The representative procedure **A** was followed using 3-methylbenzoic acid (**21i**) (136 mg, 1.00 mmol, 1.0 equiv) and *n*-butyl acrylate (**45a**) (192 mg, 1.50 mmol, 1.5 equiv). Purification by column chromatography (*n*-hexane/EtOAc: 4/1 + 5% NEt₃) yielded **47ha** (124 mg, 0.72 mmol, 47%) as a colorless oil.

¹H-NMR (500 MHz, CDCl₃): δ = 7.70 (s, 1H), 7.48 (d, *J* = 7.8 Hz, 1H), 7.37 (d, *J* = 7.8 Hz, 2H), 5.84 (t, *J* = 6.6 Hz, 1H), 4.16 (t, *J* = 6.7 Hz, 2H), 2.94–2.80 (m, 2H), 2.46 (s, 3H), 1.64–1.58 (m, 2H), 1.40–1.32 (m, 2H), 0.93 (t, *J* = 6.5 Hz, 3H).

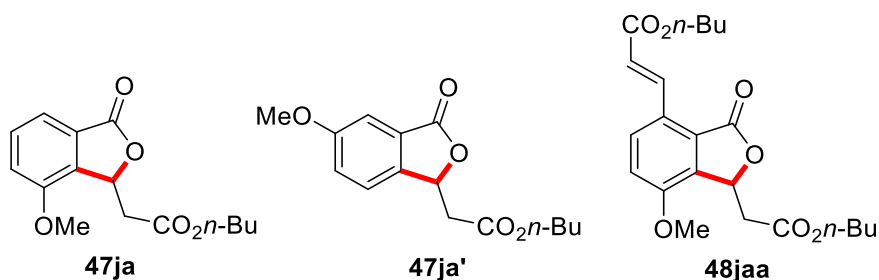
¹³C-NMR (126 MHz, CDCl₃): δ = 170.2 (C_q), 169.5 (C_q), 146.3 (C_q), 140.0 (C_q), 135.5 (CH), 126.3 (C_q), 126.0 (CH), 121.9 (CH), 77.1 (CH), 65.3 (CH₂), 39.8 (CH₂), 30.7 (CH₂), 21.4 (CH₃), 19.2 (CH₂), 13.8 (CH₃).

IR (ATR): 2960, 2873, 1763, 1730, 1287, 1153, 1057, 1006, 779, 555 cm⁻¹.

MS (EI) *m/z* (relative intensity): 262 (8) [M]⁺, 206 (75), 163 (38), 160 (96), 147 (100), 119 (44), 91 (28), 65 (15), 41 (12).

HR-MS (EI) *m/z* calcd for C₁₅H₁₈O₄, [M]⁺ 262.1205, found: 262.1207.

The spectral data are in accordance with those reported in the literature.^[124]



The representative procedure **A** was followed using 3-methoxybenzoic acid (**21j**) (152 mg, 1.00 mmol, 1.0 equiv) and *n*-butyl acrylate (**45a**) (192 mg, 1.50 mmol, 1.5 equiv). Purification by column chromatography (*n*-hexane/EtOAc: 4/1 + 5% NEt₃) yielded **47ja** (77 mg, 0.28 mmol, 28%) as a white solid, **3ja'** (77 mg, 0.13 mmol, 13%) as a colorless oil and **48jaa** (133 mg, 0.33 mmol, 33%) as a yellow solid.

***n*-Butyl 2-(7-methoxy-3-oxo-1,3-dihydroisobenzofuran-1-yl)acetate (47ja):**

M. p. = 78–80 °C.

¹H-NMR (500 MHz, CDCl₃): δ = 7.53–7.47 (m, 2H), 7.11 (dd, *J* = 7.8, 2.0 Hz, 1H), 5.88 (m, 1H), 4.12 (t, *J* = 6.7 Hz, 2H), 3.91 (s, 3H), 3.23–3.27 (m, 1H), 2.97–2.84 (m, 1H), 1.62–1.56 (m, 2H), 1.40–1.31 (m, 2H), 0.92 (t, *J* = 7.4 Hz, 3H).

¹³C-NMR (126 MHz, CDCl₃): δ = 170.0 (C_q), 169.7 (C_q), 154.3 (C_q), 136.4 (C_q), 131.5 (CH), 128.2 (C_q), 117.5 (CH), 115.2 (CH), 76.4 (CH), 65.2 (CH₂), 55.8 (CH₃), 39.0 (CH₂), 30.7 (CH₂), 19.2 (CH₂), 13.8 (CH₃).

IR (ATR): 2946, 1762, 1732, 1610, 1491, 1313, 1173, 1033, 745, 506 cm⁻¹.

MS (EI) *m/z* (relative intensity): 278 (8) [M]⁺, 222 (52), 176 (84), 163 (100), 135 (22), 105 (26), 77 (22), 43 (28).

HR-MS (EI) *m/z* calcd for C₁₅H₁₈O₅, [M]⁺ 278.1154, found 278.1163.

***n*-Butyl 2-(5-methoxy-3-oxo-1,3-dihydroisobenzofuran-1-yl)acetate (47ja'):**

¹H-NMR (500 MHz, CDCl₃): δ = 7.38 (d, *J* = 8.4 Hz, 1H), 7.33 (d, *J* = 2.2 Hz, 1H), 7.23 (dd, *J* = 8.4, 2.4 Hz, 1H), 5.82 (t, *J* = 6.8 Hz, 1H), 4.16 (t, *J* = 6.7 Hz, 2H), 3.87 (s, 3H), 2.96–2.76 (m, 2H), 1.67–1.55 (m, 2H), 1.45–1.30 (m, 2H), 0.93 (t, *J* = 7.4 Hz, 3H).

Experimental Section

^{13}C -NMR (500 MHz, CDCl_3): δ = 170.0 (C_q), 169.6 (C_q), 161.1 (C_q), 141.4 (C_q), 127.6 (C_q), 123.3 (CH), 123.2 (CH), 107.8 (C_q), 77.0 (CH), 65.3 (CH_2), 56.0 (CH_3), 39.9 (CH_2), 30.7 (CH_2), 19.2 (CH_2), 13.8 (CH_3).

IR (ATR): 2960, 2935, 2873, 1760, 1495, 1322, 1242, 1052, 838, 779 cm^{-1} .

MS (EI) m/z (relative intensity): 278 (25) $[\text{M}]^+$, 222 (51), 176 (100), 163 (186), 135 (52), 77 (17), 43 (36).

HR-MS (EI) m/z calcd for $\text{C}_{15}\text{H}_{18}\text{O}_5$, $[\text{M}]^+$ 278.1154, found 278.1156.

***n*-Butyl 3-[1-(2-*n*-butoxy-2-oxoethyl)-5-methoxy-3-oxo-1,3-dihydroisobenzofuran-4-yl]acrylate (48jaa):**

M. p. = 78–80 °C.

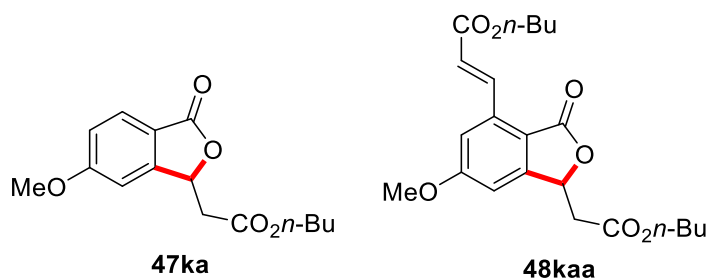
^1H -NMR (500 MHz, CDCl_3): δ = 8.63 (d, J = 16.2 Hz, 1H), 7.76 (d, J = 8.5 Hz, 1H), 7.11 (d, J = 8.6 Hz, 1H), 6.49 (d, J = 16.2 Hz, 1H), 5.84–5.81 (m, 1H), 4.22 (t, J = 6.7 Hz, 2H), 4.11 (t, J = 6.7 Hz, 2H), 3.94 (s, 3H), 3.31–3.25 (m, 1H), 2.69–2.63 (m, 1H), 1.73–1.66 (m, 2H), 1.61–1.54 (m, 2H), 1.48–1.40 (m, 2H), 1.38–1.31 (m, 2H), 0.96 (t, J = 7.4 Hz, 3H), 0.91 (t, J = 7.4 Hz, 3H).

^{13}C -NMR (126 MHz, CDCl_3): δ = 169.5 (C_q), 169.0 (C_q), 166.7 (C_q), 155.2 (C_q), 137.3 (CH), 137.0 (C_q), 129.1 (CH), 127.0 (C_q), 125.4 (C_q), 120.6 (CH), 115.4 (CH), 75.4 (CH), 65.2 (CH_2), 64.7 (CH_2), 56.1 (CH), 37.8 (CH_2), 30.9 (CH_2), 30.7 (CH_2), 19.3 (CH_2), 19.2 (CH_2), 13.9 (CH_3), 13.8 (CH_3).

IR (ATR): 2957, 2873, 1764, 1722, 1612, 1505, 1280, 1159, 1013, 830, 545, 492 cm^{-1} .

MS (EI) m/z (relative intensity): 404 (16) $[\text{M}]^+$, 330 (100), 302 (67), 274 (44), 246 (70), 229 (82), 187 (92), 131 (22), 57 (33), 41 (84).

HR-MS (EI) m/z calcd for $\text{C}_{22}\text{H}_{28}\text{O}_7$, $[\text{M}]^+$ 404.1835, found 404.1838.



The representative procedure **A** was followed using 4-methoxybenzoic acid (**21k**) (152 mg, 1.00 mmol, 1.0 equiv) and *n*-butyl acrylate (**45a**) (192 mg, 1.50 mmol, 1.5 equiv). Purification by column chromatography (*n*-hexane/EtOAc: 4/1 + 5% NEt₃) yielded **47ka** (92 mg, 0.33 mmol, 33%) as a colorless oil and **48kaa** (77 mg, 0.19 mmol, 19%) as a white solid.

***n*-Butyl 2-(6-methoxy-3-oxo-1,3-dihydroisobenzofuran-1-yl)acetate (47ka):**

¹H-NMR (500 MHz, CDCl₃): δ = 7.81 (d, *J* = 8.5 Hz, 1H), 6.93 (dd, *J* = 8.5, 2.2 Hz, 1H), 6.93 (d, *J* = 2.2 Hz, 2H), 5.88 (t, *J* = 8.5 Hz, 1H), 4.17 (t, *J* = 6.7 Hz, 2H), 3.89 (s, 3H), 2.97–2.80 (m, 2H), 1.66–1.59 (m, 2H), 1.42–1.33 (m, 2H), 0.93 (t, *J* = 7.4 Hz, 3H).

¹³C-NMR (126 MHz, CDCl₃): δ = 169.7 (C_q), 169.6 (C_q), 165.0 (C_q), 151.2 (C_q), 127.5 (CH), 118.4 (C_q), 116.9 (CH), 106.4 (CH), 76.4 (CH), 65.3 (CH₂), 56.0 (CH₃), 39.8 (CH₂), 30.7 (CH₂), 19.2 (CH₂), 13.8 (CH₃).

IR (ATR): 2960, 2874, 1754, 1731, 1606, 1490, 1173, 1153, 1006, 689 cm⁻¹.

MS (EI) *m/z* (relative intensity): 278 (14) [M]⁺, 222 (53), 176 (91), 163 (100), 135 (37), 77 (15), 43 (15).

HR-MS (EI) *m/z* calcd for C₁₅H₁₈O₅, [M]⁺ 278.1154, found 278.1147.

***n*-Butyl 3-[1-(2-*n*-butoxy-2-oxoethyl)-5-methoxy-3-oxo-1,3-dihydroisobenzofuran-4-yl]acrylate (48kaa):**

M. p. = 89–91 °C.

¹H-NMR (500 MHz, CDCl₃): δ = 8.61 (d, *J* = 16.2 Hz, 1H), 7.23 (d, *J* = 2.2 Hz, 1H), 6.94 (t, *J* = 2.1 Hz, 1H), 6.57 (d, *J* = 16.2 Hz, 1H), 5.76 (t, *J* = 6.8 Hz, 1H), 4.23 (t, *J* = 6.7 Hz, 2H), 4.16 (t, *J* = 6.7 Hz, 2H), 3.91 (s, 3H), 2.96–2.81 (m, 2H), 1.74–1.67 (m, 2H), 1.65–1.58 (m, 2H), 1.49–1.42 (m, 2H), 1.39–1.32 (m, 2H), 0.96 (t, *J* = 7.4 Hz, 3H), 0.93 (t, *J* = 7.4 Hz, 3H).

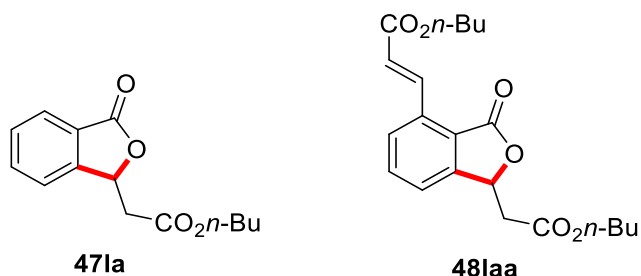
Experimental Section

^{13}C -NMR (126 MHz, CDCl_3): δ = 169.5 (C_q), 168.8 (C_q), 166.3 (C_q), 164.6 (C_q), 152.6 (C_q), 137.5 (CH), 136.6 (C_q), 123.3 (CH), 116.0 (C_q), 113.3 (CH), 107.9 (CH), 75.7 (CH), 65.4 (CH_2), 65.0 (CH_2), 56.2 (CH), 39.7 (CH_2), 30.9 (CH_2), 30.7 (CH_2), 19.3 (CH_2), 19.2 (CH_2), 13.9 (CH_3), 13.8 (CH_3).

IR (ATR): 2959, 2874, 1735, 1603, 1338, 1260, 1173, 1064, 1011, 682 cm^{-1} .

MS (EI) m/z (relative intensity): 404 (16) $[\text{M}]^+$, 331 (22), 303 (83), 229 (100), 201 (36), 187 (25), 163 (24), 57 (16), 41 (34).

HR-MS (EI) m/z calcd for $\text{C}_{22}\text{H}_{28}\text{O}_7$, $[\text{M}]^+$ 404.1835, found 404.1835.



a) The representative procedure **A** was followed using benzoic acid (**21I**) (122 mg, 1.00 mmol, 1.0 equiv) and *n*-butyl acrylate (**45a**) (192 mg, 1.50 mmol, 1.5 equiv). Purification by column chromatography (*n*-hexane/EtOAc: 4/1 + 5% NEt_3) yielded **471a** (106 mg, 0.43 mmol, 43%) and **481aa** (85 mg, 0.23 mmol, 23%) as colorless oils.

b) The representative procedure **B** was followed using benzoic acid (**21I**) (122 mg, 1.00 mmol, 1.0 equiv) and *n*-butyl acrylate (**45a**) (192 mg, 1.50 mmol, 1.5 equiv). Purification by column chromatography (*n*-hexane/EtOAc: 4/1 + 5% NEt_3) yielded **471a** (100 mg, 0.40 mmol, 40%) and **481aa** (96 mg, 0.26 mmol, 26%) as colorless oils.

***n*-Butyl 2-(3-oxo-1,3-dihydroisobenzofuran-1-yl)acetate (471a):**

^1H -NMR (500 MHz, CDCl_3): δ = 7.91 (d, J = 7.7 Hz, 1H), 7.68 (ddd, J = 7.5, 7.5, 1.1 Hz, 1H), 7.58–7.48 (m, 2H), 5.88 (t, J = 6.6 Hz, 1H), 4.16 (t, J = 6.7 Hz, 2H), 2.97–2.84 (m, 2H), 1.65–1.57 (m, 2H), 1.42–1.32 (m, 2H), 0.93 (t, J = 7.4 Hz, 3H).

^{13}C -NMR (126 MHz, CDCl_3): δ = 170.0 (C_q), 169.5 (C_q), 149.0 (C_q), 134.4 (CH), 129.7 (CH), 126.1 (C_q), 126.0 (CH), 122.2 (CH), 77.1 (CH), 65.3 (CH_2), 39.7 (CH_2), 30.7 (CH_2), 19.2 (CH_2), 13.8 (CH_3).

Experimental Section

IR (ATR): 2960, 2934, 2873, 1761, 1466, 1287, 1171, 1059, 1002, 747 cm^{-1} .

MS (EI) m/z (relative intensity): 248 (8) $[\text{M}]^+$, 192 (60), 175 (10), 146 (54), 133 (100), 105 (35), 77 (29), 41 (18).

HR-MS (ESI) m/z calcd for $\text{C}_{14}\text{H}_{16}\text{O}_4$, $[\text{M}+\text{H}]^+$ 248.1055, found 248.1055.

The spectral data are in accordance with those reported in the literature.^[125]

***n*-Butyl 3-[1-(2-*n*-butoxy-2-oxoethyl)-3-oxo-1,3-dihydroisobenzofuran-4-yl]acrylate (48laa):**

^1H -NMR (500 MHz, CDCl_3): δ = 8.71 (d, J = 16.2 Hz, 1H), 7.77 (d, J = 7.8 Hz, 1H), 7.66 (t, J = 7.9 Hz, 1H), 7.48 (d, J = 7.6 Hz, 1H), 6.60 (d, J = 16.2 Hz, 1H), 5.85 (t, J = 6.5 Hz, 1H), 4.24 (t, J = 6.7 Hz, 2H), 4.15 (t, J = 6.7 Hz, 2H), 2.90–2.79 (m, 2H), 1.72–1.67 (m, 2H), 1.64–1.57 (m, 2H), 1.47–1.32 (m, 4H), 0.94 (t, J = 7.4 Hz, 3H), 0.92 (t, J = 7.4 Hz, 3H).

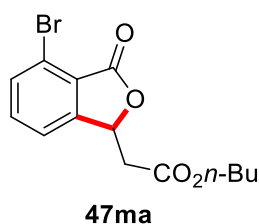
^{13}C -NMR (126 MHz, CDCl_3): δ = 169.3 (C_q), 169.0 (C_q), 166.3 (C_q), 149.9 (C_q), 137.4 (CH), 135.2 (C_q), 134.4 (CH), 126.8 (CH), 123.4 (C_q), 123.3 (CH), 123.1 (CH), 76.2 (CH), 65.4 (CH_2), 64.9 (CH_2), 39.6 (CH_2), 30.8 (CH_2), 30.6 (CH_2), 19.3 (CH_2), 19.2 (CH_2), 13.9 (CH_3), 13.8 (CH_3).

IR (ATR): 2959, 2874, 1711, 1640, 1287, 1165, 1078, 1047, 804, 791 cm^{-1} .

MS (EI) m/z (relative intensity): 374 (14) $[\text{M}]^+$, 301 (65), 273 (63), 244 (33), 199 (100), 171 (31), 157 (30), 57 (21), 41 (32).

HR-MS (ESI) m/z calcd for $\text{C}_{14}\text{H}_{16}\text{O}_4$, $[\text{M}+\text{H}]^+$ 374.1729, found 374.1735.

The spectral data are in accordance with those reported in the literature.^[126]

***n*-Butyl 2-(4-bromo-3-oxo-1,3-dihydroisobenzofuran-1-yl)acetate (47ma):**

The representative procedure **B** was followed using 2-bromobenzoic acid (**21m**) (201 mg, 1.00 mmol, 1.0 equiv) and *n*-butyl acrylate (**45a**) (192 mg, 1.50 mmol, 1.5 equiv). Purification by column chromatography (*n*-hexane/EtOAc: 1/1 + 1% MeOH) yielded **47ma** (227 mg, 0.70 mmol, 70%) as a colorless oil.

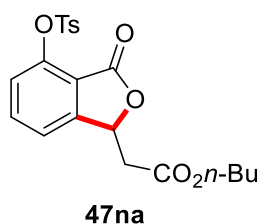
¹H-NMR (300 MHz, CDCl₃): δ = 7.64 (d, *J* = 7.6 Hz, 1H), 7.44 (dd, *J* = 7.6, 7.6 Hz, 1H), 7.38 (d, *J* = 7.6 Hz, 1H), 5.74 (t, *J* = 6.5 Hz, 1H), 4.09 (t, *J* = 6.7 Hz, 2H), 2.99–2.69 (m, 2H), 1.61–1.43 (m, 2H), 1.37–1.23 (m, 2H), 0.86 (t, *J* = 7.3 Hz, 3H).

¹³C-NMR (75 MHz, CDCl₃): δ = 169.3 (C_q), 167.3 (C_q), 151.4 (C_q), 135.3 (CH), 134.4 (CH), 124.5 (C_q), 121.4 (C_q), 121.2 (CH), 75.4 (CH), 65.5 (CH₂), 39.6 (CH₂), 30.7 (CH₂), 19.2 (CH₂), 13.8 (CH₃).

IR (ATR): 2957, 1735, 1599, 1456, 1340, 1204, 1079, 1043, 797, 677 cm⁻¹.

MS (EI) *m/z* (relative intensity): 326 (5) [⁷⁹Br-M⁺], 272 (91), 227 (88), 211 (100), 183 (30), 155 (18), 104 (10), 75 (30).

HR-MS (ESI) *m/z* calcd for C₁₄H₁₆⁷⁹BrO₄, [M+H]⁺ 327.0226, found 327.0228.

***n*-Butyl 2-(4-tosyloxy-3-oxo-1,3-dihydroisobenzofuran-1-yl)acetate (47na):**

The representative procedure **B** was followed using 2-tosyloxybenzoic acid (**21n**) (292 mg, 1.00 mmol, 1.0 equiv) and *n*-butyl acrylate (**45a**) (192 mg, 1.50 mmol, 1.5 equiv). Purification by column

Experimental Section

chromatography (*n*-hexane/EtOAc: 1/1 + 1% MeOH) yielded **47na** (206 mg, 0.49 mmol, 49%) as a colorless oil.

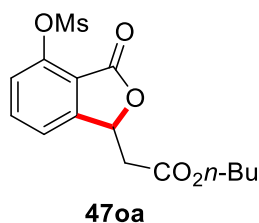
¹H-NMR (300 MHz, CDCl₃): δ = 7.84 (d, *J* = 8.2 Hz, 1H), 7.84 (d, *J* = 8.5 Hz, 1H), 7.66 (m, 1H), 7.40 (d, *J* = 8.0 Hz, 2H), 7.30 (d, *J* = 8.0 Hz, 2H), 5.75 (t, *J* = 6.5 Hz, 1H), 4.10 (t, *J* = 6.7 Hz, 2H), 2.83 (d, *J* = 6.5 Hz, 2H), 2.41 (s, 3H), 1.65–1.46 (m, 2H), 1.40–1.18 (m, 2H), 0.89 (t, *J* = 7.5 Hz, 1H).

¹³C-NMR (75 MHz, CDCl₃): δ = 169.1 (C_q), 165.4 (C_q), 151.2 (C_q), 146.5 (C_q), 145.9 (C_q), 136.0 (CH), 132.0 (C_q), 129.8 (CH), 128.9 (CH), 123.7 (CH), 120.9 (CH), 118.7 (C_q), 76.0 (CH), 65.2 (CH₂), 39.3 (CH₂), 30.5 (CH₂), 21.8 (CH₃), 19.1 (CH₂), 13.7 (CH₃).

IR (ATR): 2960, 1769, 1732, 1475, 1172, 997, 812, 748, 668, 548 cm⁻¹.

MS (EI) *m/z* (relative intensity): 418 (5) [M]⁺, 354 (7), 303 (14), 263 (45), 207 (44), 163 (22), 155 (87), 91 (100).

HR-MS (EI) *m/z* calcd for C₂₁H₂₂O₇S, [M]⁺ 418.1086, found 418.1071.



***n*-Butyl 2-(4-methylsulfonyloxy-3-oxo-1,3-dihydroisobenzofuran-1-yl)acetate (47oa):**

The representative procedure **B** was followed using 2-methylsulfonyloxybenzoic acid (**21o**) (192 mg, 1.00 mmol, 1.0 equiv) and *n*-butyl acrylate (**45a**) (192 mg, 1.50 mmol, 1.5 equiv). Purification by column chromatography (*n*-hexane/EtOAc: 1/1 + 1% MeOH) yielded **47oa** (188 mg, 0.55 mmol, 55%) as a colorless oil.

¹H-NMR (300 MHz, CDCl₃): δ = 7.74 (dd, *J* = 7.5, 7.5 Hz, 1H), 7.48–7.47 (m, 1H), 7.45–7.44 (m, 1H), 5.87 (t, *J* = 6.4 Hz, 1H), 4.15 (t, *J* = 6.7 Hz, 2H), 3.41 (s, 3H), 3.03–2.86 (m, 2H), 1.67–1.56 (m, 2H), 1.44–1.29 (m, 2H), 0.94 (t, *J* = 7.3 Hz, 3H).

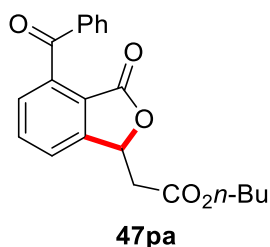
Experimental Section

^{13}C -NMR (75 MHz, CDCl_3): δ = 169.1 (C_q), 166.4 (C_q), 151.4 (C_q), 146.3 (C_q), 136.4 (CH), 124.9 (CH), 121.2 (CH), 118.8 (C_q), 76.6 (CH), 65.5 (CH_2), 39.3 (CH_2), 39.2 (CH_3), 30.6 (CH_2), 19.2 (CH_2), 13.8 (CH_3).

IR (ATR): 2961, 2874, 1764, 1729, 1618, 1476, 1365, 1117, 1003, 787 cm^{-1} .

MS (EI) m/z (relative intensity): 342 (22) $[\text{M}]^+$, 286 (100), 240 (52), 227 (75), 207 (100), 162 (82), 149 (81), 120 (32).

HR-MS (ESI) m/z calcd for $\text{C}_{15}\text{H}_{19}\text{O}_7\text{S}$, $[\text{M}+\text{H}]^+$ 343.0846, found 343.0859.



***n*-Butyl 2-(4-benzoyl-3-oxo-1,3-dihydroisobenzofuran-1-yl)acetate (47pa):**

The representative procedure **B** was followed using 2-benzoylbenzoic acid (**21p**) (226 mg, 1.00 mmol, 1.0 equiv) and *n*-butyl acrylate (**45a**) (192 mg, 1.50 mmol, 1.5 equiv). Purification by column chromatography (*n*-hexane/EtOAc: 1/1 + 1% MeOH) yielded **47pa** (287 mg, 0.82 mmol, 82%) as a colorless oil.

^1H -NMR (300 MHz, CDCl_3): δ = 7.82–7.74 (m, 3H), 7.68–7.52 (m, 3H), 7.49–7.41 (m, 2H), 5.93 (t, J = 6.6 Hz, 1H), 4.17 (t, J = 6.7 Hz, 2H), 3.09–2.83 (m, 2H), 1.69–1.55 (m, 2H), 1.47–1.29 (m, 2H), 0.94 (t, J = 7.4 Hz, 3H).

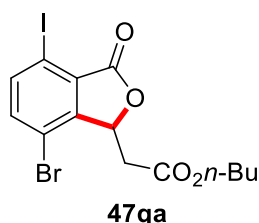
^{13}C -NMR (75 MHz, CDCl_3): δ = 194.6 (C_q), 169.4 (C_q), 167.6 (C_q), 149.6 (C_q), 139.4 (C_q), 136.6 (C_q), 134.3 (CH), 134.0 (CH), 130.0 (CH), 128.7 (CH), 128.6 (CH), 123.9 (C_q), 123.7 (CH), 77.0 (CH), 65.4 (CH_2), 39.6 (CH_2), 30.7 (CH_2), 19.2 (CH_2), 13.8 (CH_3).

IR (ATR): 2959, 1763, 1730, 1669, 1282, 1174, 1077, 1005, 711, 696 cm^{-1} .

MS (EI) m/z (relative intensity): 352 (20) $[\text{M}]^+$, 278 (75), 252 (30), 236 (75), 208 (45), 152 (30), 105 (100), 77 (65).

Experimental Section

HR-MS (EI) m/z calcd for $C_{21}H_{20}O_5$, $[M]^+$ 352.1311, found 352.1302.



***n*-Butyl 2-(7-bromo-4-iodo-3-oxo-1,3-dihydroisobenzofuran-1-yl)acetate (47qa):**

The representative procedure **B** was followed using 2-iodo-5-bromobenzoic acid (**21q**) (327 mg, 1.00 mmol, 1.0 equiv) and *n*-butyl acrylate (**45a**) (192 mg, 1.50 mmol, 1.5 equiv). Purification by column chromatography (*n*-hexane/EtOAc: 4/1 + 5% NEt_3) yielded **47qa** (320 mg, 0.71 mmol, 71%) as a colorless oil.

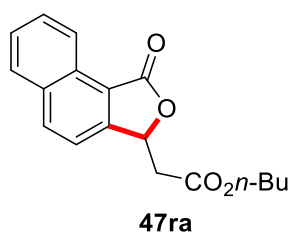
1H -NMR (300 MHz, $CDCl_3$): δ = 7.88 (dd, J = 8.2, 0.6 Hz, 1H), 7.47 (d, J = 8.2 Hz, 1H), 5.70 (ddd, J = 8.0, 3.0, 0.6 Hz, 1H), 4.10 (t, J = 6.7 Hz, 2H), 3.46 (dd, J = 16.7, 3.0 Hz, 1H), 2.81 (dd, J = 16.8, 8.0 Hz, 1H), 1.63–1.52 (m, 2H), 1.41–1.26 (m, 2H), 0.92 (t, J = 7.3 Hz, 3H).

^{13}C -NMR (126 MHz, $CDCl_3$): δ = 168.5 (C_q), 166.6 (C_q), 149.2 (C_q), 142.3 (CH), 138.0 (CH), 129.5 (C_q), 116.5 (C_q), 91.0 (C_q), 75.5 (CH), 65.3 (CH_2), 36.7 (CH_2), 30.5 (CH_2), 19.1 (CH_2), 13.8 (CH_3).

IR (ATR): 2958, 2932, 2872, 1769, 1730, 1449, 1338, 1172, 1060, 831 cm^{-1} .

MS (EI) m/z (relative intensity): 452 (15) [^{79}Br - M^+], 396 (100), 350 (85), 337 (75), 309 (15), 154 (10), 75 (165, 41 (20)).

HR-MS (EI) m/z calcd for $C_{14}H_{14}^{79}BrIO_4$, $[M]^+$ 451.9120, found 451.9136.

***n*-Butyl 2-(1-oxo-1,3-dihydronaphtho[1,2-*c*]furan-3-yl)acetate (**47ra**):**

The representative procedure **B** was followed using 1-naphthoic-acid (**21r**) (172 mg, 1.00 mmol, 1.0 equiv) and *n*-butyl acrylate (**45a**) (192 mg, 1.50 mmol, 1.5 equiv). Purification by column chromatography (*n*-hexane/EtOAc: 4/1 + 5% NEt₃) yielded **47ra** (177 mg, 0.59 mmol, 59%) as a colorless solid.

M. p. = 78–80 °C.

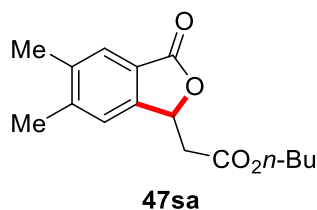
¹H-NMR (300 MHz, CDCl₃): δ = 9.01 (dd, *J* = 8.2, 1.2 Hz, 1H), 8.15 (d, *J* = 8.4 Hz, 1H), 7.98 (d, *J* = 8.3 Hz, 1H), 7.75 (ddd, *J* = 8.2, 6.9, 1.4 Hz, 1H), 7.65 (ddd, *J* = 8.2, 6.9, 1.4 Hz, 1H), 7.53 (d, *J* = 8.4 Hz, 1H), 5.96 (t, *J* = 6.6 Hz, 1H), 4.18 (t, *J* = 6.7 Hz, 2H), 2.96 (d, *J* = 6.6 Hz, 2H), 1.68–1.56 (m, 2H), 1.44–1.29 (m, 2H), 0.92 (t, *J* = 7.4 Hz, 3H).

¹³C-NMR (75 MHz, CDCl₃): δ = 170.3 (C_q), 169.6 (C_q), 150.6 (C_q), 135.9 (CH), 133.7 (C_q), 129.4 (CH), 128.6 (CH), 127.7 (CH), 123.7 (CH), 120.4 (C_q), 120.1 (C_q), 118.6 (CH), 76.5 (CH), 65.4 (CH₂), 39.6 (CH₂), 30.7 (CH₂), 19.2 (CH₂), 13.8 (CH₃).

IR (ATR): 3073, 2956, 2932, 2871, 1739, 1400, 1290, 1175, 695, 502 cm⁻¹.

MS (EI) *m/z* (relative intensity): 298 (26) [M]⁺, 242 (75), 199 (26), 196 (100), 183 (62), 155 (42), 127 (56), 115 (8).

HR-MS (ESI) *m/z* calcd for C₁₈H₁₉O₄, [M+H]⁺ 299.1278, found 299.1279.

***n*-Butyl 2-(5,6-dimethyl-3-oxo-1,3-dihydroisobenzofuran-1-yl)acetate (47sa):**

The representative procedure **B** was followed using 3,4-dimethylbenzoic-acid (**21s**) (150 mg, 1.00 mmol, 1.0 equiv) and *n*-butyl acrylate (**45a**) (192 mg, 1.50 mmol, 1.5 equiv). Purification by column chromatography (*n*-hexane/EtOAc: 4/1 + 5% NEt₃) yielded **47sa** (219 mg, 0.79 mmol, 79%) as a colorless oil.

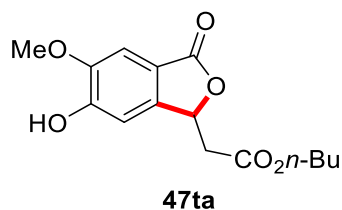
¹H-NMR (300 MHz, CDCl₃): δ = 7.65 (s, 1H), 7.23 (s, 1H), 5.80 (t, J = 6.6 Hz, 1H), 4.16 (t, J = 6.7 Hz, 2H), 2.97–2.75 (m, 2H), 2.38 (s, 3H), 2.35 (s, 3H), 1.67–1.57 (m, 2H), 1.45–1.30 (m, 2H), 0.93 (t, J = 7.3 Hz, 3H).

¹³C-NMR (75 MHz, CDCl₃): δ = 170.3 (C_q), 169.7 (C_q), 147.1 (C_q), 144.6 (C_q), 138.9 (C_q), 126.2 (CH), 123.9 (C_q), 122.9 (CH), 76.8 (CH), 65.3 (CH₂), 39.9 (CH₂), 30.7 (CH₂), 21.0 (CH₃), 20.1 (CH₃), 19.2 (CH₂), 13.8 (CH₃).

IR (ATR): 2960, 2873, 1759, 1731, 1460, 1390, 1340, 1170, 1015, 990 cm⁻¹.

MS (EI) m/z (relative intensity): 276 (13) [M]⁺, 220 (51), 177 (44), 174 (100), 161 (84), 133 (34), 105 (16), 77 (12).

HR-MS (ESI) m/z calcd for C₁₆H₂₁O₄, [M+H]⁺ 277.1434, found 277.1436.



***n*-Butyl 2-(5-methoxy-6-hydroxy-3-oxo-1,3-dihydroisobenzofuran-1-yl)acetate (47ta):**

The representative procedure **B** was followed using vanillic acid (**21t**) (168 mg, 1.00 mmol, 1.0 equiv) and *n*-butyl acrylate (**45a**) (192 mg, 1.50 mmol, 1.5 equiv). Purification by column chromatography (*n*-hexane/EtOAc: 1/1 + 1% MeOH) yielded **47ta** (164 mg, 0.56 mmol, 56%) as colorless solid.

M. p. = 118–120 °C.

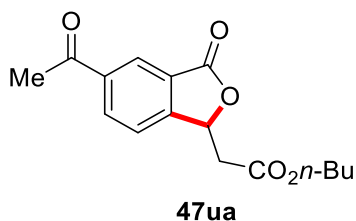
¹H-NMR (300 MHz, CDCl₃): δ = 7.30 (s, 1H), 6.97 (d, J = 0.8 Hz, 1H), 6.27 (s, 1H), 5.76 (ddd, J = 7.0, 6.2, 0.8 Hz, 1H), 4.16 (t, J = 6.7 Hz, 2H), 3.98 (s, 3H), 2.94–2.75 (m, 2H), 1.70–1.54 (m, 2H), 1.45–1.30 (m, 2H), 0.94 (t, J = 7.3 Hz, 3H).

¹³C-NMR (75 MHz, CDCl₃): δ = 170.3 (C_q), 169.6 (C_q), 152.0 (C_q), 148.2 (C_q), 144.0 (C_q), 117.7 (C_q), 107.4 (CH), 106.3 (CH), 76.6 (CH), 65.3 (CH₂), 56.6 (CH₃), 39.8 (CH₂), 30.7 (CH₂), 19.2 (CH₂), 13.8 (CH₃).

IR (ATR): 3300, 2961, 2927, 2874, 1737, 1707, 1600, 1498, 1062, 1043 cm⁻¹.

MS (EI) m/z (relative intensity): 294 (16) [M]⁺, 238 (36), 195 (42), 193 (61), 192 (100), 179 (70), 164 (10), 151 (27).

HR-MS (ESI) m/z calcd for C₁₅H₁₉O₆, [M+H]⁺ 295.1176, found 295.1176.

***n*-Butyl 2-(5-acetyl-3-oxo-1,3-dihydroisobenzofuran-1-yl)acetate (47ua):**

The representative procedure **B** was followed using 3-acetylbenzoic acid (**21u**) (180 mg, 1.00 mmol, 1.0 equiv) and *n*-butyl acrylate (**45a**) (192 mg, 1.50 mmol, 1.5 equiv). Purification by column chromatography (*n*-hexane/EtOAc: 1/1 + 1% MeOH) yielded **47ua** (244 mg, 0.84 mmol, 84%) as a colorless oil.

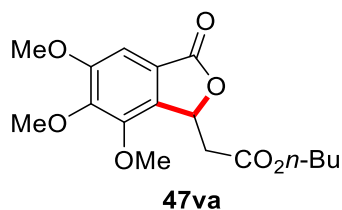
¹H-NMR (300 MHz, CDCl₃): δ = 8.37 (s, 1H), 8.26 (d, *J* = 8.1 Hz, 1H), 7.60 (d, *J* = 8.1 Hz, 1H), 5.88 (t, *J* = 6.4 Hz, 1H), 4.09 (t, *J* = 6.7 Hz, 2H), 2.92 (dd, *J* = 6.4, 1.9 Hz, 2H), 2.62 (s, 3H), 1.63–1.45 (m, 2H), 1.39–1.19 (m, 2H), 0.86 (t, *J* = 7.3 Hz, 3H).

¹³C-NMR (75 MHz, CDCl₃): δ = 196.3 (C_q), 169.0 (C_q), 169.0 (C_q), 152.9 (C_q), 138.6 (C_q), 133.9 (CH), 126.8 (C_q), 126.0 (CH), 122.8 (CH), 77.1 (CH), 65.3 (CH₂), 39.0 (CH₂), 30.5 (CH₂), 26.8 (CH₃), 19.0 (CH₂), 13.6 (CH₃).

IR (ATR): 2961, 1772, 1734, 1690, 1345, 1397, 1288, 1181, 1075, 605 cm⁻¹.

MS (EI) *m/z* (relative intensity): 290 (10) [M]⁺, 275 (15), 234 (100), 189 (70), 175 (95), 147 (20), 119 (10), 43 (35).

HR-MS (EI) *m/z* calcd for C₁₆H₁₈O₅, [M]⁺ 290.1154, found 290.1159.

***n*-Butyl-2-(5,6,7-trimethoxy-3-oxo-1,3-dihydroisobenzofuran-1-yl)acetate (47va):**

The representative procedure **B** was followed using 3,4,5-trimethoxybenzoic-acid (**21v**) (212 mg, 1.00 mmol, 1.0 equiv) and *n*-butyl acrylate (**45a**) (192 mg, 1.50 mmol, 1.5 equiv). Purification by column chromatography (*n*-hexane/EtOAc: 4/1 + 5% NEt₃) yielded **47va** (326 mg, 0.96 mmol, 96%) as a colorless oil.

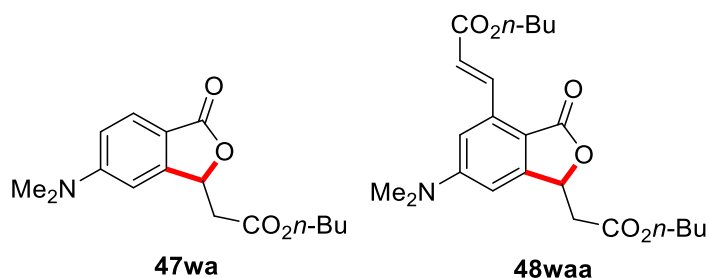
¹H-NMR (300 MHz, CDCl₃): δ = 7.12 (s, 1H), 5.82 (dd, *J* = 8.6, 3.4 Hz, 1H), 4.12 (t, *J* = 6.7 Hz, 2H), 3.99 (s, 3H), 3.93 (s, 3H), 3.91 (s, 3H), 3.20 (dd, *J* = 16.3, 3.4 Hz, 1H), 2.64 (dd, *J* = 16.3, 8.6 Hz, 1H), 1.65–1.54 (m, 2H), 1.45–1.26 (m, 2H), 0.92 (t, *J* = 7.5 Hz, 3H).

¹³C-NMR (75 MHz, CDCl₃): δ = 169.9 (C_q), 169.5 (C_q), 156.2 (C_q), 147.6 (C_q), 146.8 (C_q), 133.9 (C_q), 121.5 (C_q), 102.7 (CH), 75.9 (CH), 65.2 (CH₂), 61.3 (CH₃), 61.1 (CH₃), 56.6 (CH₃), 38.6 (CH₂), 30.7 (CH₂), 19.2 (CH₂), 13.8 (CH₃).

IR (ATR): 2958, 2874, 1765, 1733, 1477, 1420, 1339, 1170, 1104, 765 cm⁻¹.

MS (EI) *m/z* (relative intensity): 338 (42) [M]⁺, 282 (24), 237 (78), 236 (100), 223 (100), 195 (24), 180 (16), 165 (16).

HR-MS (ESI) *m/z* calcd for C₁₇H₂₃O₇, [M+H]⁺ 339.1438, found 339.1448.



The representative procedure **B** was followed using 4-dimethylaminobenzoic acid (**21w**) (165 mg, 1.00 mmol, 1.0 equiv) and *n*-butyl acrylate (**45a**) (192 mg, 1.50 mmol, 1.5 equiv). Purification by column chromatography (*n*-hexane/EtOAc: 1/1 + 1% MeOH) yielded **47wa** (169 mg, 0.59 mmol, 59%) as a colorless oil and **48waa** (60 mg, 0.14 mmol, 14%) as a yellow oil.

***n*-Butyl-2-(6-dimethylamino-3-oxo-1,3-dihydroisobenzofuran-1-yl)acetate (**47wa**):**

¹H-NMR (300 MHz, CDCl₃): δ = 7.69 (d, *J* = 8.7 Hz, 1H), 6.76 (dd, *J* = 8.7, 2.3 Hz, 1H), 6.54 (d, *J* = 2.3 Hz, 1H), 5.73 (t, *J* = 6.2 Hz, 1H), 4.16 (t, *J* = 6.7 Hz, 2H), 3.08 (s, 6H), 2.94–2.75 (m, 2H), 1.67–1.52 (m, 2H), 1.41–1.25 (m, 2H), 0.93 (t, *J* = 7.4 Hz, 3H).

¹³C-NMR (75 MHz, CDCl₃): δ = 170.5 (C_q), 169.9 (C_q), 154.6 (C_q), 151.9 (C_q), 127.0 (CH), 113.2 (CH), 112.5 (C_q), 102.6 (CH), 76.3 (CH), 65.2 (CH₂), 40.5 (CH₃), 40.2 (CH₂), 30.7 (CH₂), 19.2 (CH₂), 13.8 (CH₃).

IR (ATR): 2958, 1730, 1606, 1517, 1368, 1321, 1167, 1003, 691, 608 cm⁻¹.

MS (EI) *m/z* (relative intensity): 291 (100) [M]⁺, 235 (25), 180 (70), 176 (100), 162 (10), 148 (40), 119 (15), 77 (10).

HR-MS (EI) *m/z* calcd for C₁₆H₂₁NO₄, [M]⁺ 291.1471, found 291.1479.

***n*-Butyl-3-(1-(2-*n*-butoxy-2-oxoethyl)-6-(dimethylamino)-3-oxo-1,3-dihydroisobenzofuran-4-yl)acrylate (**48waa**):**

¹H-NMR (300 MHz, CDCl₃): δ = 8.54 (d, *J* = 16.4 Hz, 1H), 6.89 (d, *J* = 2.2 Hz, 1H), 6.59 (d, *J* = 16.6 Hz, 1H), 6.59–6.51 (m, 1H), 5.68 (dd, *J* = 6.8, 6.8 Hz, 1H), 4.20 (t, *J* = 6.7 Hz, 2H), 4.13 (t, *J* = 6.7 Hz, 2H), 3.09 (s, 6H), 2.84 (dd, *J* = 6.6, 2.6 Hz, 2H), 1.76–1.55 (m, 4H), 1.50–1.25 (m, 4H), 0.94 (t, *J* = 7.4 Hz, 3H), 0.90 (d, *J* = 7.4 Hz, 3H).

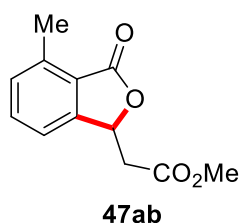
Experimental Section

^{13}C -NMR (75 MHz, CDCl_3): δ = 169.8 (C_q), 169.5 (C_q), 166.6 (C_q), 154.2 (C_q), 152.5 (C_q), 139.0 (CH), 135.6 (C_q), 122.3 (CH), 110.4 (C_q), 110.0 (CH), 104.1 (CH), 75.6 (CH), 65.2 (CH_2), 64.7 (CH_2), 40.5 (CH_3), 40.1 (CH_2), 30.8 (CH_2), 30.7 (CH_2), 19.3 (CH_2), 19.2 (CH_2), 13.8 (CH_3), 13.8 (CH_3).

IR (ATR): 2957, 1731, 1604, 1518, 1368, 1230, 1168, 1003, 819, 691 cm^{-1} .

MS (EI) m/z (relative intensity): 417 (100) $[\text{M}]^+$, 344 (15), 316 (35), 242 (85), 214 (30), 200 (20), 174 (10), 115 (5).

HR-MS (EI) m/z calcd for $\text{C}_{23}\text{H}_{31}\text{NO}_6$, $[\text{M}]^+$ 417.2151, found 417.2150.



Methyl-2-(4-methyl-3-oxo-1,3-dihydroisobenzofuran-1-yl)acetate (**47ab**):

a) The representative procedure **A** was followed using 2-methylbenzoic acid (**21a**) (136 mg, 1.00 mmol, 1.0 equiv) and methyl acrylate (**45b**) (129 mg, 1.50 mmol, 1.5 equiv). Purification by column chromatography (*n*-hexane/EtOAc: 4/1 + 5% NEt_3) yielded **47ab** (159 mg, 0.72 mmol, 72%) as colorless solid.

b) The representative procedure **B** was followed using 2-methylbenzoic acid (**21a**) (136 mg, 1.00 mmol, 1.0 equiv) and methyl acrylate (**45b**) (129 mg, 1.50 mmol, 1.5 equiv). Purification by column chromatography (*n*-hexane/EtOAc: 4/1 + 5% NEt_3) yielded **47ab** (135 mg, 0.61 mmol, 61%) as colorless solid.

M. p. = 89–90 $^{\circ}\text{C}$.

^1H -NMR (300 MHz, CDCl_3): δ = 7.53 (dd, J = 7.6, 7.6 Hz, 1H), 7.32–7.25 (m, 2H), 5.82 (t, J = 6.6 Hz, 1H), 3.77 (s, 3H), 2.87 (d, J = 6.6 Hz, 2H), 2.69 (s, 3H).

^{13}C -NMR (75 MHz, CDCl_3): δ = 170.1 (C_q), 170.0 (C_q), 149.3 (C_q), 140.1 (C_q), 134.1 (CH), 131.3 (CH), 123.5 (C_q), 119.4 (CH), 76.1 (CH), 52.3 (CH_3), 39.8 (CH_2), 17.5 (CH_3).

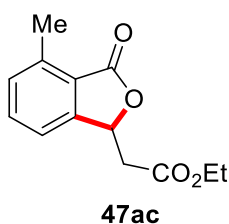
Experimental Section

IR (ATR): 2952, 1757, 1732, 1600, 1441, 1400, 1199, 1086, 1007, 687 cm^{-1} .

MS (EI) m/z (relative intensity): 220 (20) $[\text{M}]^+$, 160 (100), 147 (90), 132 (37), 119 (38), 91 (39), 65 (16), 58 (38).

HR-MS (ESI) m/z calcd for $\text{C}_{12}\text{H}_{13}\text{O}_4$, $[\text{M}+\text{H}]^+$ 221.0808, found 221.0810.

The spectral data are in accordance with those reported in the literature.^[127]



Ethyl-2-(4-methyl-3-oxo-1,3-dihydroisobenzofuran-1-yl)acetate (**47ac**):

a) The representative procedure **A** was followed using 2-methylbenzoic acid (**21a**) (136 mg, 1.00 mmol, 1.0 equiv) and ethyl acrylate (**45c**) (150 mg, 1.50 mmol, 1.5 equiv). Purification by column chromatography (*n*-hexane/EtOAc: 4/1 + 5% NEt_3) yielded **47ac** (145 mg, 0.62 mmol, 62%) as colorless solid.

b) The representative procedure **B** was followed using 2-methylbenzoic acid (**21a**) (136 mg, 1.00 mmol, 1.0 equiv) and ethyl acrylate (**45c**) (150 mg, 1.50 mmol, 1.5 equiv). Purification by column chromatography (*n*-hexane/EtOAc: 4/1 + 5% NEt_3) yielded **47ac** (195 mg, 0.83 mmol, 83%) as colorless solid.

M. p. = 50–52 $^{\circ}\text{C}$.

^1H -NMR (300 MHz, CDCl_3): δ = 7.53 (dd, J = 7.6, 7.6 Hz, 1H), 7.31–7.25 (m, 2H), 5.81 (t, J = 6.6 Hz, 1H), 4.22 (q, J = 7.1 Hz, 2H), 2.86 (d, J = 6.6 Hz, 2H), 2.69 (s, 3H), 1.27 (t, J = 7.1 Hz, 3H).

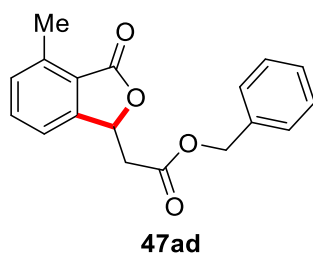
^{13}C -NMR (75 MHz, CDCl_3): δ = 170.2 (C_q), 169.5 (C_q), 149.4 (C_q), 140.1 (C_q), 134.1 (CH), 131.3 (CH), 123.6 (C_q), 119.4 (CH), 76.2 (CH), 61.4 (CH_2), 40.0 (CH_2), 17.5 (CH_3), 14.3 (CH_3).

IR (ATR): 2988, 2926, 1744, 1725, 1602, 1475, 1171, 1097, 1007, 689 cm^{-1} .

MS (EI) m/z (relative intensity): 234 (18) $[M]^+$, 160 (100), 147 (87), 132 (32), 119 (31), 91 (31), 65 (13), 43 (25).

HR-MS (ESI) m/z calcd for $C_{13}H_{15}O_4$, $[M+H]^+$ 235.0965, found 235.0967.

The spectral data are in accordance with those reported in the literature.^[41g]



Benzyl-2-(4-methyl-3-oxo-1,3-dihydroisobenzofuran-1-yl)acetate (47ad):

a) The representative procedure **A** was followed using 2-methylbenzoic acid (**21a**) (136 mg, 1.00 mmol, 1.0 equiv) and benzyl acrylate (**45d**) (243 mg, 1.50 mmol, 1.5 equiv). Purification by column chromatography (*n*-hexane/EtOAc: 4/1 + 5% NEt_3) yielded **47ad** (205 mg, 0.69 mmol, 69%) as a 7:1 mixture with **47aa**.

b) The representative procedure **B** was followed using 2-methylbenzoic acid (**21a**) (136 mg, 1.00 mmol, 1.0 equiv) and benzyl acrylate (**45d**) (243 mg, 1.50 mmol, 1.5 equiv). Purification by column chromatography (*n*-hexane/EtOAc: 4/1 + 5% NEt_3) yielded **47ad** (204 mg, 0.69 mmol, 69%) as colorless solid.

c) The representative procedure **B** was followed using 2-methylbenzoic acid (**21a**) (0.63 g, 5.00 mmol, 1.0 equiv) and benzyl acrylate (**45d**) (1.22 g, 7.50 mmol, 1.5 equiv). Purification by column chromatography (*n*-hexane/EtOAc: 4/1 + 5% NEt_3) yielded **47ad** (1.37 g, 4.60 mmol, 92%) as colorless solid.

M. p. = 58–61 °C.

1H -NMR (300 MHz, $CDCl_3$): δ = 7.49 (dd, J = 7.6, 7.6 Hz, 1H), 7.36 (m, 5H), 7.29–7.25 (m, 1H), 7.20 (d, J = 7.6 Hz, 1H), 5.82 (t, J = 6.6 Hz, 1H), 5.20 (m, 2H), 2.92 (dd, J = 6.6, 2.9 Hz, 2H), 2.67 (s, 3H).

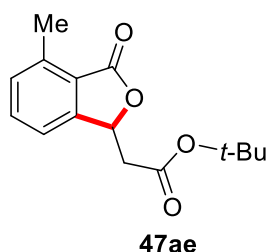
Experimental Section

^{13}C -NMR (75 MHz, CDCl_3): δ = 170.1 (C_q), 169.3 (C_q), 149.3 (C_q), 140.1 (C_q), 135.4 (C_q), 134.1 (CH), 131.3 (CH), 128.8 (CH), 128.6 (CH), 128.6 (CH), 123.5 (C_q), 119.4 (CH), 76.1 (CH), 67.2 (CH_2), 39.9 (CH_2), 17.5 (CH_3).

IR (ATR): 3037, 2944, 1745, 1599, 1478, 1386, 1311, 1291, 1203, 1002 cm^{-1} .

MS (EI) m/z (relative intensity): 296 (15) $[\text{M}]^+$, 205 (54), 162 (71), 147 (55), 119 (40), 91 (100), 77 (11), 65 (23).

HR-MS (EI) m/z calcd for $\text{C}_{18}\text{H}_{16}\text{O}_4$, $[\text{M}]^+$ 296.1049, found 296.1054.



***t*-Butyl-2-(4-methyl-3-oxo-1,3-dihydroisobenzofuran-1-yl)acetate (**47ae**):**

The representative procedure **B** was followed using 2-methylbenzoic acid (**21a**) (136 mg, 1.00 mmol, 1.0 equiv) and *tert*-butyl acrylate (**45e**) (192 mg, 1.50 mmol, 1.5 equiv). Purification by column chromatography (*n*-hexane/EtOAc: 4/1 + 5% NEt_3) yielded **47ae** (178 mg, 0.68 mmol, 68%) as colorless solid.

M. p. = 74–75 $^{\circ}\text{C}$.

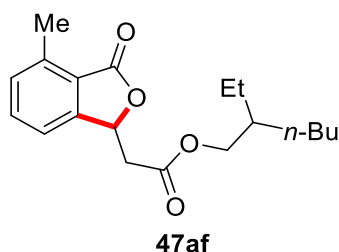
^1H -NMR (300 MHz, CDCl_3): δ = 7.52 (dd, J = 7.6, 7.6 Hz, 1H), 7.30–7.26 (m, 2H), 5.76 (t, J = 6.4 Hz, 1H), 2.81 (d, J = 6.4 Hz, 2H), 2.69 (s, 3H), 1.44 (s, 9H).

^{13}C -NMR (75 MHz, CDCl_3): δ = 170.3 (C_q), 168.7 (C_q), 149.7 (C_q), 140.0 (C_q), 134.0 (CH), 131.1 (CH), 123.7 (C_q), 119.4 (CH), 82.0 (C_q), 76.5 (CH), 41.0 (CH_2), 28.2 (CH_3), 17.5 (CH_3).

IR (ATR): 2980, 2929, 1740, 1598, 1478, 1049, 1003, 908, 828, 794 cm^{-1} .

MS (EI) m/z (relative intensity): 206 (85), 189 (23), 161 (50), 147 (100), 119 (26), 91 (24), 57 (64), 43 (85).

HR-MS (ESI) m/z calcd for $C_{15}H_{19}O_4$, $[M+H]^+$ 263.1278, found 263.1279.



2-Ethylhexyl-2-(4-methyl-3-oxo-1,3-dihydroisobenzofuran-1-yl)acetate (47af):

The representative procedure **B** was followed using 2-methylbenzoic acid (**21a**) (136 mg, 1.00 mmol, 1.0 equiv) and 2-ethylhexyl acrylate (**45f**) (276 mg, 1.50 mmol, 1.5 equiv). Purification by column chromatography (*n*-hexane/EtOAc: 4/1 + 5% NEt_3) yielded **47af** (196 mg, 0.61 mmol, 61%) as colorless solid.

M. p. = 42–44 °C.

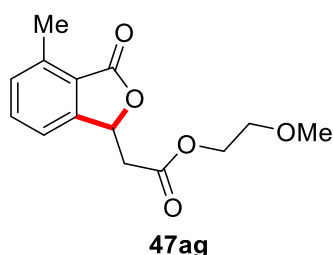
1H -NMR (300 MHz, $CDCl_3$): δ = 7.52 (dd, J = 7.6, 7.6 Hz, 1H), 7.33–7.22 (m, 2H), 5.81 (t, J = 6.6 Hz, 1H), 4.08 (m, 2H), 2.88 (m, 2H), 2.69 (s, 3H), 1.63–1.51 (m, 1H), 1.43–1.22 (m, 8H), 0.93–0.85 (m, 6H).

^{13}C -NMR (75 MHz, $CDCl_3$): δ = 170.2 (C_q), 169.7 (C_q), 149.5 (C_q), 140.1 (C_q), 134.1 (CH), 131.3 (CH), 123.6 (C_q), 119.4 (CH), 76.2 (CH), 67.8 (CH_2), 39.9 (CH_2), 38.8 (CH), 30.5 (CH_2), 29.0 (CH_2), 23.8 (CH_2), 23.1 (CH_2), 17.5 (CH_3), 14.2 (CH_3), 11.1 (CH_3).

IR (ATR): 2957, 2928, 2860, 1743, 1601, 1461, 1399, 1202, 1049, 1001 cm^{-1} .

MS (EI) m/z (relative intensity): 318 (1) $[M]^+$, 206 (100), 161 (52), 147 (90), 119 (18), 91 (20), 71 (12), 57 (19).

HR-MS (ESI) m/z calcd for $C_{19}H_{27}O_4$, $[M+H]^+$ 319.1904, found 319.1910.

**2-Methoxyethyl-2-(4-methyl-3-oxo-1,3-dihydroisobenzofuran-1-yl)acetate (47ag):**

The representative procedure **B** was followed using 2-methylbenzoic acid (**21a**) (136 mg, 1.00 mmol, 1.0 equiv) and 2-methoxyethyl acrylate (**45g**) (195 mg, 1.50 mmol, 1.5 equiv). Purification by column chromatography (*n*-hexane/EtOAc: 4/1 + 5% NEt₃) yielded **47ag** (224 mg, 0.85 mmol, 85%) as a colorless oil.

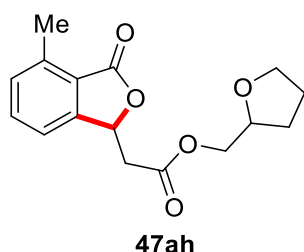
¹H-NMR (300 MHz, CDCl₃): δ = 7.53 (dd, *J* = 7.6, 7.6 Hz, 1H), 7.29 (m, 2H), 5.82 (t, *J* = 6.6 Hz, 1H), 4.37–4.27 (m, 2H), 3.66–3.56 (m, 2H), 3.39 (s, 3H), 2.92 (dd, *J* = 6.6, 1.6 Hz, 2H), 2.69 (s, 3H).

¹³C-NMR (126 MHz, CDCl₃): δ = 170.2 (C_q), 169.5 (C_q), 149.4 (C_q), 140.1 (C_q), 134.1 (CH), 131.3 (CH), 123.6 (C_q), 119.5 (CH), 76.1 (CH), 70.4 (CH₂), 64.3 (CH₂), 59.2 (CH₃), 39.9 (CH₂), 17.5 (CH₃).

IR (ATR): 2927, 1753, 1733, 1382, 1238, 1127, 1045, 1005, 787, 687 cm⁻¹.

MS (EI) *m/z* (relative intensity): 264 (16) [M]⁺, 160 (76), 147 (100), 132 (21), 119 (23), 91 (27), 58 (19), 45 (17).

HR-MS (ESI) *m/z* calcd for C₁₄H₁₇O₅, [M+H]⁺ 265.1071, found 265.1071.

**(Tetrahydrofuran-2-yl)methyl-2-(4-methyl-3-oxo-1,3-dihydroisobenzofuran-1-yl)acetate (47ah):**

The representative procedure **B** was followed using 2-methylbenzoic acid (**21a**) (136 mg, 1.00 mmol, 1.0 equiv) and tetrahydrofurfuryl acrylate (**45h**) (234 mg, 1.50 mmol, 1.5 equiv). Purification by

column chromatography (*n*-hexane/EtOAc: 4/1 + 5% NEt₃) yielded **47ah** (237 mg, 0.82 mmol, 82%) as a colorless oil.

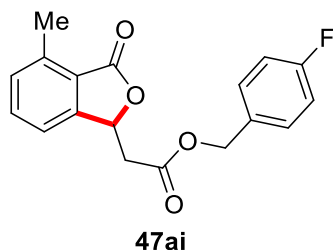
¹H-NMR (300 MHz, CDCl₃): δ = 7.53 (dd, *J* = 7.6, 7.6 Hz, 1H), 7.29 (m, 2H), 5.83 (t, *J* = 6.7 Hz, 1H), 4.29–4.21 (m, 1H), 4.18–4.06 (m, 2H), 3.93–3.75 (m, 2H), 2.92 (d, *J* = 6.7 Hz, 2H), 2.69 (s, 3H), 2.10–1.85 (m, 3H), 1.68–1.55 (m, 1H).

¹³C-NMR (126 MHz, CDCl₃): δ = 170.0 (C_q), 169.3 (C_q), 149.2 (C_q), 140.0 (C_q), 134.0 (CH), 131.2 (CH), 123.5 (C_q), 119.4 (CH), 76.5 (CH), 76.1 (CH), 68.6 (CH₂), 67.3 (CH₂), 40.0 (CH₂), 28.2 (CH₂), 25.9 (CH₂), 17.6 (CH₃).

IR (ATR): 2953, 2872, 1753, 1734, 1380, 1167, 1005, 787, 687, 472 cm⁻¹.

MS (EI) *m/z* (relative intensity): 290 (4) [M]⁺, 247 (13), 220 (20), 207 (18), 162 (15), 147 (46), 84 (26), 71 (100).

HR-MS (ESI) *m/z* calcd for C₁₆H₁₉O₅, [M+H]⁺ 291.1227, found 291.1228.



4-(Fluorobenzyl)-2-(4-methyl-3-oxo-1,3-dihydroisobenzofuran-1-yl)acetate (**47ai**):

The representative procedure **B** was followed using 2-methylbenzoic acid (**21a**) (136 mg, 1.00 mmol, 1.0 equiv) and 4-fluorobenzyl acrylate (**45i**) (249 mg, 1.50 mmol, 1.5 equiv). Purification by column chromatography (*n*-hexane/EtOAc: 1/1 + 5% NEt₃) yielded **47ai** (277 mg, 0.92 mmol, 92%) as a colorless oil.

¹H-NMR (300 MHz, CDCl₃): δ = 7.49 (dd, *J* = 7.6, 7.6 Hz, 1H), 7.38–7.25 (m, 3H), 7.20 (d, *J* = 7.6 Hz, 1H), 7.05 (dd, *J* = 8.8, 8.8 Hz, 2H), 5.81 (t, *J* = 6.5 Hz, 1H), 5.15 (m, 2H), 2.91 (d, *J* = 6.5 Hz, 2H), 2.67 (s, 3H).

Experimental Section

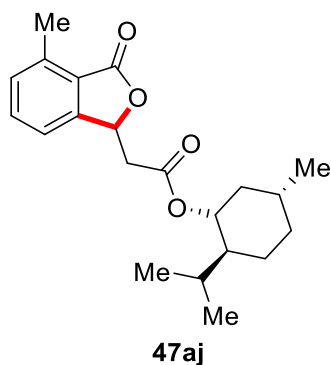
^{13}C -NMR (75 MHz, CDCl_3): δ = 170.1 (C_q), 169.2 (C_q), 162.9 (d, $^1J_{\text{C-F}} = 247.4$ Hz, C_q), 149.2 (C_q), 140.2 (C_q), 134.1 (CH), 131.3 (CH), 131.3 (C_q), 130.6 (d, $^3J_{\text{C-F}} = 8.3$ Hz, CH), 123.5 (C_q), 119.3 (CH), 115.7 (d, $^2J_{\text{C-F}} = 21.5$ Hz, CH), 76.0 (CH), 66.4 (CH_2), 39.9 (CH_2), 17.5 (CH_3).

^{19}F -NMR (282 MHz, CDCl_3): δ = -113.18.

IR (ATR): 2959, 2924, 1602, 1482, 1385, 1289, 1090, 1046, 787, 687 cm^{-1} .

MS (EI) m/z (relative intensity): 314 (26) $[\text{M}]^+$, 205 (52), 162 (68), 147 (53), 119 (42), 109 (100), 91 (28), 83 (16).

HR-MS (EI) m/z calcd for $\text{C}_{18}\text{H}_{15}\text{FO}_4$, $[\text{M}]^+$ 314.0954, found 314.0963.



(1R,2S,5R)-2-iso-Propyl-5-methylcyclohexyl-2-(4-methyl-3-oxo-1,3-dihydroisobenzofuran-1-yl)acetate (47aj):

The representative procedure **B** was followed using 2-methylbenzoic acid (**21a**) (136 mg, 1.00 mmol, 1.0 equiv) and *R*-(-)-menthyl acrylate (**45j**) (316 mg, 1.50 mmol, 1.5 equiv). Purification by column chromatography (*n*-hexane/EtOAc: 4/1 + 5% NEt_3) yielded **47aj** (238 mg, 0.69 mmol, 69%) as colorless solid. The product was observed as a 57:43 mixture of two diastereomers.^[128]

M. p. = 81–84 °C.

^1H -NMR (300 MHz, CDCl_3): δ = 7.52 (dd, $J = 7.6, 7.6$ Hz, 1H), 7.31–7.27 (m, 2H), 5.80 (m, 1H), 4.76 (m, 1H), 2.97–2.78 (m, 2H), 2.69 (s, 3H), 2.06–1.62 (m, 4H), 1.58–1.25 (m, 2H), 1.11–0.83 (m, 9H), 0.76 (m, 3H).

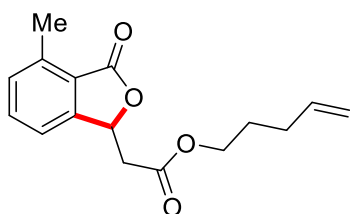
Experimental Section

^{13}C -NMR (75 MHz, CDCl_3): δ = 170.2 (C_q), 169.1 (C_q), 149.4 (C_q), 140.0 (C_q), 134.0 (CH), 131.2 (CH), 119.4 (CH), 100.2 (C_q), 76.3 (CH), 75.5 (CH), 47.1 (CH), 40.9 (CH_2), 40.1 (CH_2), 34.3 (CH_2), 31.6 (CH), 26.4 (CH), 23.5 (CH_2), 22.1 (CH_3), 20.9 (CH_3), 17.5 (CH_3), 16.4 (CH_3).

IR (ATR): 2938, 2864, 1751, 1725, 1601, 1481, 1288, 1199, 1175, 688 cm^{-1} .

MS (EI) m/z (relative intensity): 344 (1) $[\text{M}]^+$, 206 (70), 189 (16), 161 (18), 147 (100), 138 (21), 123 (14), 95 (33).

HR-MS (ESI) m/z calcd for $\text{C}_{21}\text{H}_{29}\text{O}_4$, $[\text{M}+\text{H}]^+$ 345.2060, found 345.2057.



47ak

Pent-4-en-1-yl-2-(4-methyl-3-oxo-1,3-dihydroisobenzofuran-1-yl)acetate (47ak):

The representative procedure **B** was followed using 2-methylbenzoic acid (**21a**) (136 mg, 1.00 mmol, 1.0 equiv) and pent-4-en-1-yl acrylate (**45k**) (210 mg, 1.50 mmol, 1.5 equiv). Purification by column chromatography (*n*-hexane/EtOAc: 4/1 + 5% NEt_3) yielded **47ak** (169 mg, 0.62 mmol, 62%) as a colorless oil.

^1H -NMR (300 MHz, CDCl_3): δ = 7.53 (dd, J = 7.6, 7.6 Hz, 1H), 7.34–7.22 (m, 2H), 5.87–5.70 (m, 2H), 5.08–4.96 (m, 2H), 4.17 (t, J = 6.5 Hz, 2H), 2.87 (d, J = 6.5 Hz, 2H), 2.69 (s, 3H), 2.11 (m, 2H), 1.74 (m, 2H).

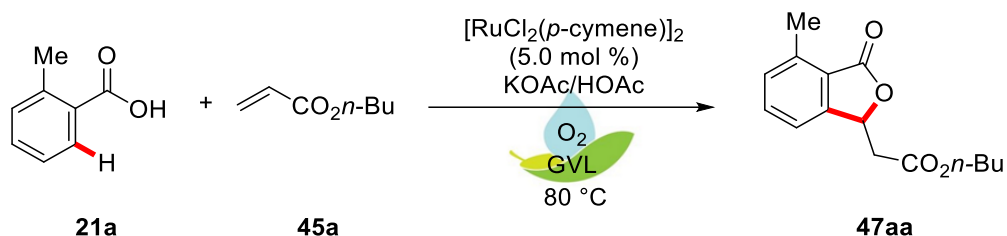
^{13}C -NMR (75 MHz, CDCl_3): δ = 170.2 (C_q), 169.5 (C_q), 149.4 (C_q), 140.1 (C_q), 137.4 (CH), 134.1 (CH), 131.3 (CH), 123.6 (C_q), 119.4 (CH), 115.6 (CH_2), 76.2 (CH), 64.8 (CH_2), 39.9 (CH_2), 30.1 (CH_2), 27.8 (CH_2), 17.5 (CH_3).

IR (ATR): 3078, 2927, 1755, 1731, 1601, 1237, 1046, 912, 687, 630 cm^{-1} .

MS (EI) m/z (relative intensity): 274 (3) $[\text{M}]^+$, 207 (40), 189 (11), 160 (24), 147 (100), 119 (19), 91 (26), 68 (46).

HR-MS (ESI) m/z calcd for $\text{C}_{16}\text{H}_{19}\text{O}_4$, $[\text{M}+\text{H}]^+$ 275.1278, found 275.1281.

5.3.1.2 Kinetic and Mechanistic Studies

O₂-Uptake study for the synthesis of phthalide 3aa

2-Methylbenzoic acid (**21a**) (136 mg, 1.00 mmol, 1.0 equiv), $[\text{RuCl}_2(p\text{-cymene})]_2$ (**30**) (30.6 mg, 0.05 mmol, 5.0 mol %) and KOAc (108 mg, 1.10 mmol, 1.1 equiv) were placed in a pre-dried 25 mL Schlenk-flask. The flask was evacuated and refilled with ambient oxygen 3 times. *n*-Butyl acrylate (**45a**) (192 mg, 1.50 mmol, 1.5 equiv) and HOAc (60.0 mg, 1.00 mmol, 1.0 equiv) in O₂ saturated GVL (**77**) (1.0 mL) were added. The Schlenk-tube was connected to a burette with a reservoir filled with O₂ saturated water. The mixture was stirred at 80 °C and the changes in volume were determined as shown in (Figure 16, Table 36). Purification by column chromatography (*n*-hexane/EtOAc: 4/1 + 5% NEt₃) yielded **47aa** (229 mg, 0.87 mmol, 87%) as a colorless oil.

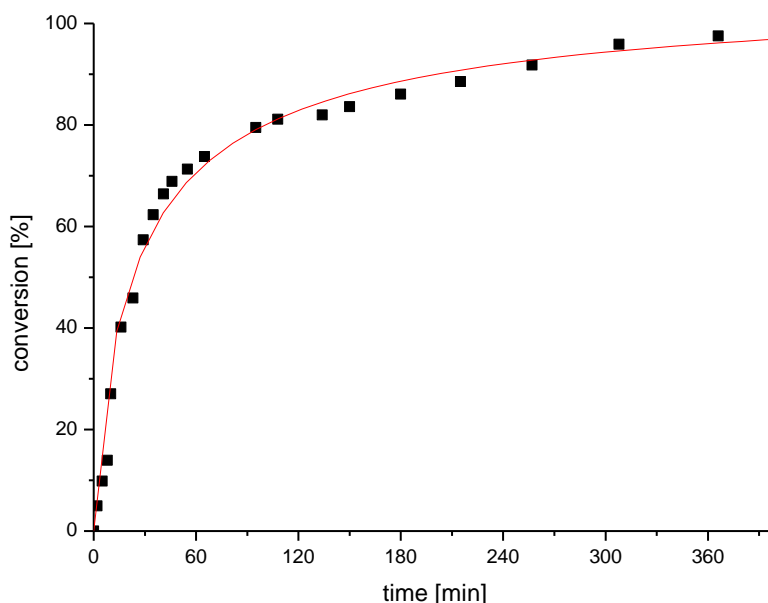


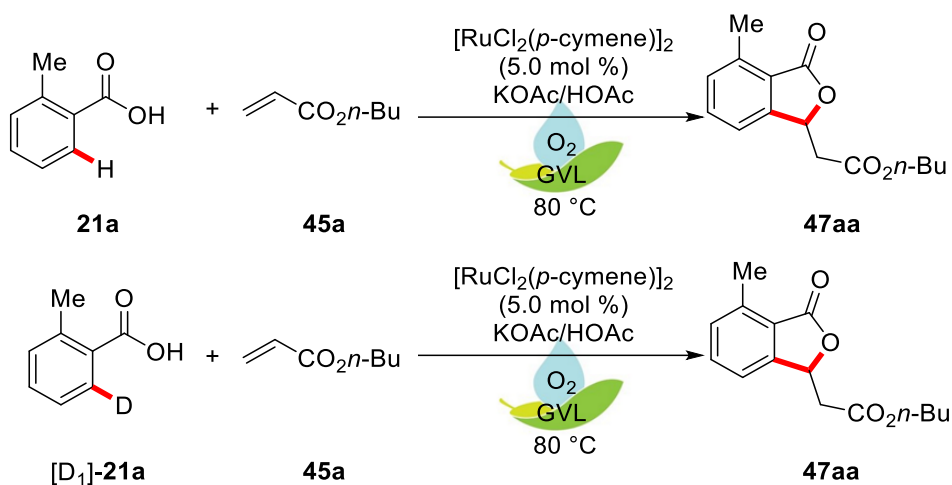
Figure 16: Graphical representation of the oxygen uptake measurement.

Experimental Section

Table 36: Data of the oxygen uptake study.

t [min]	V [mL]	ΔV [mL]	n [mmol]	t [min]	V [mL]	ΔV [mL]	n [mmol]
0	23.2	0.00	0.00	65	14.2	9.0	0.36885
2	22.6	0.6	0.02459	95	13.5	9.7	0.39754
5	22.0	1.2	0.04918	108	13.3	9.9	0.40574
8	21.5	1.7	0.06967	134	13.2	10.0	0.40984
10	19.9	3.3	0.13525	150	13.0	10.2	0.41803
16	18.3	4.9	0.20082	180	12.7	10.5	0.43033
23	17.6	5.6	0.22951	215	12.4	10.8	0.44262
29	16.2	7.0	0.28689	257	12.0	11.2	0.45902
35	15.6	7.6	0.31148	308	11.5	11.7	0.47951
41	15.1	8.1	0.33197	366	11.3	11.9	0.4877
46	14.8	8.4	0.34426	1344	10.0	13.2	0.54098
55	14.5	8.7	0.35656				

Benzoic acid depending kinetic isotope effect measurement in γ -valerolactone (77)



Two independent reactions of *n*-butyl acrylate (45a) with 2-methylbenzoic acids 21a and $[\text{D}_1]$ -21a respectively were performed to determine the KIE value by comparison of the initial rates.

The representative procedure **B** was followed using 21a (136 mg, 1.00 mmol) or $[\text{D}_1]$ -21a (137 mg, 1.00 mmol), acrylate 45a (192 mg, 1.00 mmol), $[\text{RuCl}_2(p\text{-cymene})]_2$ (30) (30.6 mg, 0.05mmol), *n*-dodecane (100 mg), HOAc (60.0 mg, 1.00 mmol) and KOAc (98.0 mg, 1.00 mmol) in GVL (77) (2.0 mL) under an ambient atmosphere of O_2 . The mixture was stirred at 80 °C, an aliquot (10 μL) was periodically removed by a syringe and analyzed by GC (Figure 17, Table 37).

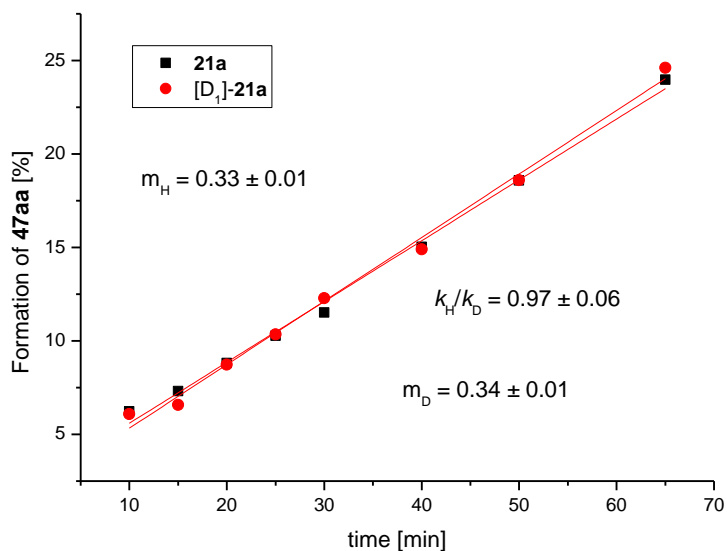
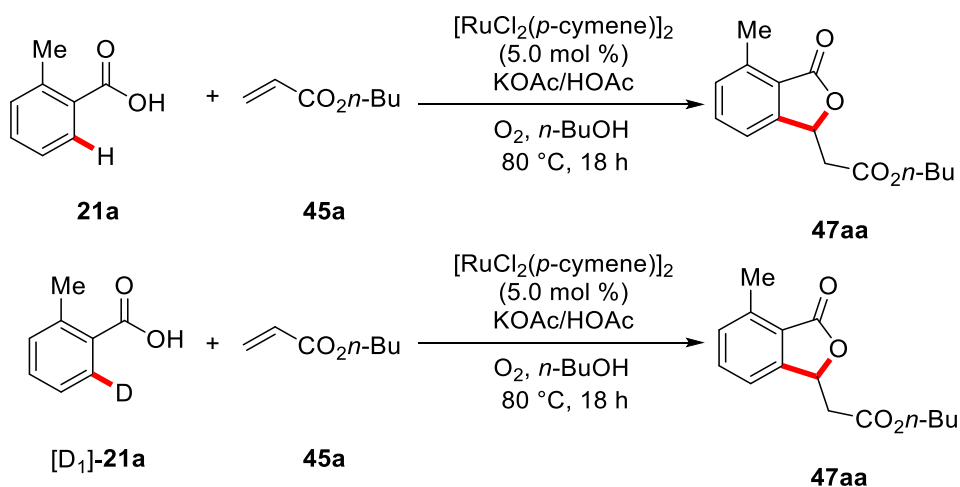


Figure 17: Graphical representation of the benzoic acid depending kinetic isotope effect measurement in γ -valerolactone (**77**).

Table 37: Data of the benzoic acid depending kinetic isotope effect measurement in γ -valerolactone (**77**).

time	Product formation with 21a [%]	Product formation with [D ₃]- 21a [%]
10	6.22905	6.08418
15	7.31185	6.57329
20	8.81117	8.73404
25	10.27729	10.34562
30	11.52389	12.28783
40	15.02926	14.90412
50	18.57822	18.60369
65	23.96968	24.61338

Benzoic acid depending kinetic isotope effect measurement with addition of HOAc in *n*-butanol



Two independent reactions of *n*-butyl acrylate (**45a**) with 2-methylbenzoic acids **21a** and $[\text{D}_1]\text{-21a}$ respectively were performed to determine the KIE value by comparison of the initial rates.

The representative procedure **A** was followed using **21a** (136 mg, 1.00 mmol) or $[\text{D}_1]\text{-21a}$ (137 mg, 1.00 mmol), acrylate **45a** (192 mg, 1.00 mmol), $[\text{RuCl}_2(p\text{-cymene})]_2$ (**30**) (30.6 mg, 0.05 mmol), *n*-dodecane (100 mg), HOAc (60.0 mg, 1.00 mmol) and KOAc (98.0 mg, 1.00 mmol) in *n*-butanol (2.0 mL) under an ambient atmosphere of O_2 . The mixture was stirred at 80 °C, an aliquot (10 μL) was periodically removed by a syringe and analyzed by GC (Figure 18, Table 38).

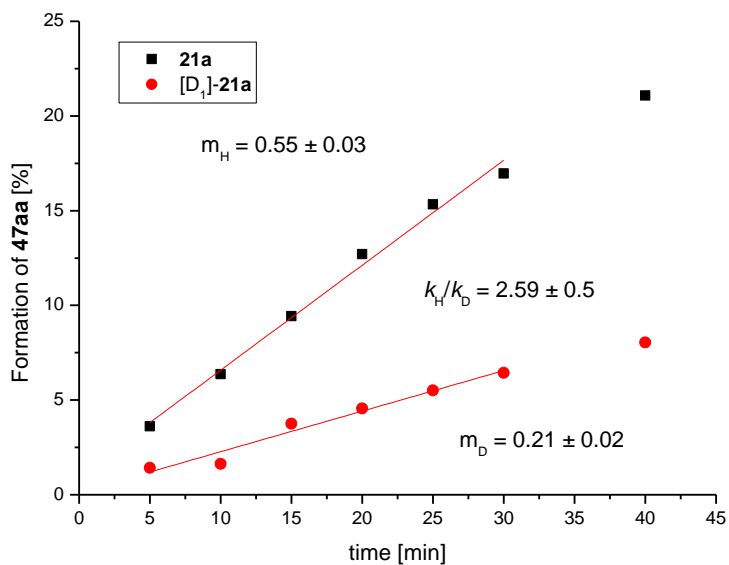
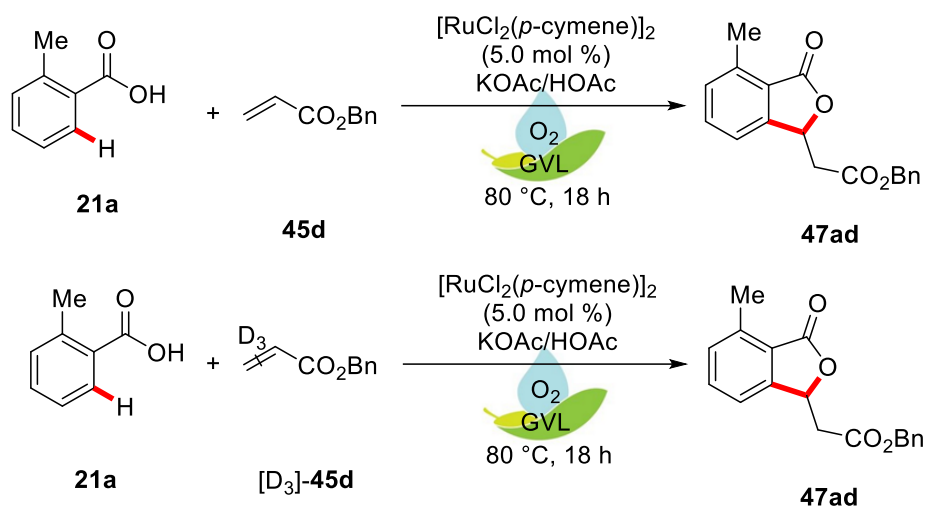


Figure 18: Graphical representation of the benzoic acid depending kinetic isotope effect measurement in *n*-butanol.

Table 38: Data of the benzoic acid depending kinetic isotope effect measurement in *n*-butanol.

time	Product formation with 21a [%]	Product formation with [D ₃]- 21a [%]
5	3.60468	1.42328
10	6.36762	1.62497
15	9.43342	3.74658
20	12.70033	4.54636
25	15.33569	5.50538
30	16.96373	6.43273
40	21.07747	8.04151
50	23.46574	9.08231

Acrylate depending kinetic isotope effect measurement in γ -valerolactone (77)


Two independent reactions of 2-methylbenzoic acid (**21a**) with benzyl acrylate (**45d**) and $[D_3]$ -benzyl acrylate ($[D_3]$ -**45d**) respectively were performed to determine the KIE value by comparison of the initial rates.

The representative procedure **B** was followed using **21a** (136 mg, 1.00 mmol) and benzyl acrylate **45d** (192 mg, 1.00 mmol) or $[D_3]$ -**45d** (195 mg, 1.00 mmol), $[RuCl_2(p\text{-cymene})]_2$ (30.6 mg, 0.05 mmol), *n*-dodecane (100 mg), HOAc (60.0 mg, 1.00 mmol) and KOAc (98.0 mg, 1.00 mmol) in GVL (**77**) (2.0 mL) under an ambient atmosphere of O_2 . The mixture was stirred at 80 °C, an aliquot (10 μ L) was periodically removed by a syringe and analyzed by GC (Figure 19, Table 39).

Experimental Section

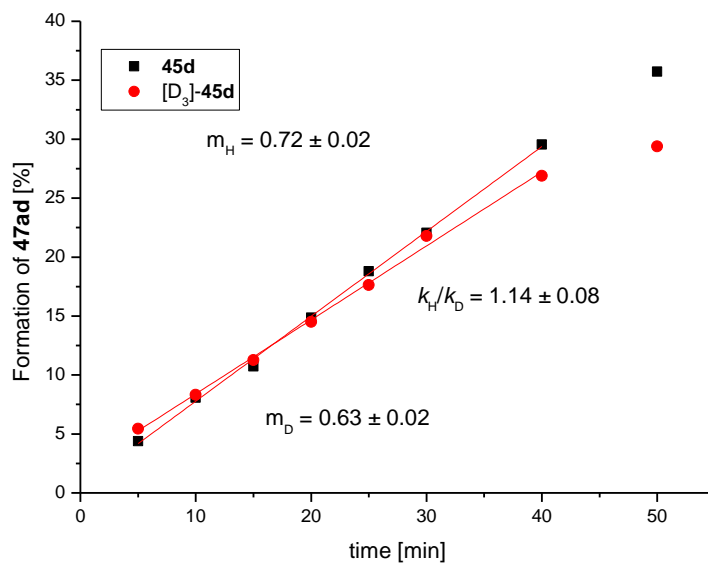
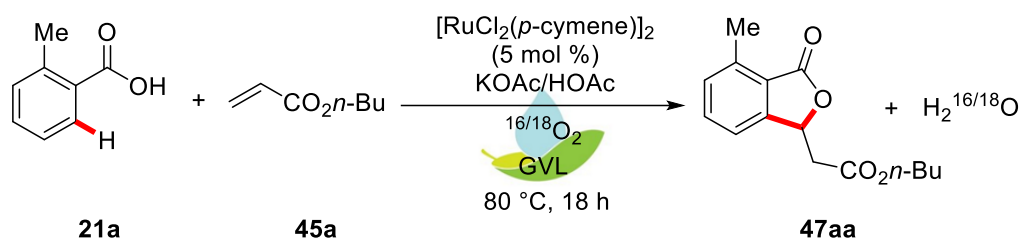


Figure 19: Graphical representation of the acrylate depending kinetic isotope effect measurement.

Table 39: Data of the acrylate depending kinetic isotope effect measurement in γ -valerolactone (**77**).

time	Product formation with 45a [%]	Product formation with [D ₃]- 45a [%]
5	4.39572	5.45038
10	8.07793	8.32636
15	10.71772	11.25543
20	14.87325	14.51241
25	18.79746	17.62722
30	22.04618	21.79044
40	29.53813	26.88421
50	35.72619	29.37908

Labelled Oxygen Study



The representative procedure **B** was followed using **21a** (136 mg, 1.00 mmol) and benzyl acrylate **45d** (192 mg, 1.00 mmol), $[\text{RuCl}_2(p\text{-cymene})]_2$ (**30**) (30.6 mg, 0.05 mmol), HOAc (60.0 mg, 1.00 mmol) and KOAc (98.0 mg, 1.00 mmol) in GVL (**77**) (1.0 mL) under an ambient atmosphere of $^{16}\text{O}_2$ or $^{18}\text{O}_2$. Prior to the work-up POCl_3 (153 mg, 1.00 mmol) was added and the mixture was stirred for 15 minutes. An aliquot ($\sim 10 \mu\text{L}$) was removed, diluted by a factor of 10^3 in MeCN and analyzed *via* ESI-MS. K_2CO_3 (138 mg, 1.00 mmol) and 1-iodobutane (184 mg, 1.00 mmol) were added and the reaction solution was stirred at $60 \text{ } ^\circ\text{C}$ for 18 h, before the regular work-up procedure was continued. Purification by column chromatography (*n*-hexane/EtOAc: 4/1 + 5% NEt_3) yielded **47aa** as a colorless oil (Table 40).

For analysis, the sample solutions were injected into the ESI source of a micrOTOF-Q II mass spectrometer (Bruker Daltonik) via a gastight syringe at a flow rate of $5 \mu\text{L min}^{-1}$. The ESI source was operated with a stainless-steel capillary and with nitrogen as nebulizer gas (typical backing pressure of 0.7 bar) and drying gas (typical flow rate of 5 L min^{-1}). Negative-ion mode ESI mass spectra over an m/z range of 50-1000 were recorded with an ESI voltage of +3.5 kV and a drying-gas temperature of $200 \text{ } ^\circ\text{C}$ (Figure 20). The mass spectrometer was externally calibrated with a mixture of $\text{CF}_3\text{CO}_2\text{H}$ and phosphazenes in $\text{H}_2\text{O}/\text{MeCN}$. The detected ions were identified on the basis of their exact m/z ratios and their isotope patterns. For the calculation of theoretical m/z ratios and the simulation of isotope patterns, the Bruker DataAnalysis software package was used.

Experimental Section

Table 40: Labelled oxygen studies

Entry	$^{16}\text{O}_2/^{18}\text{O}_2$	$[\mathbf{P}^*]^-$ [%] ^[a]	H/Na $[\mathbf{P}^*\mathbf{P}]^-$ [%] ^[c]	H/Na $[\mathbf{P}^*_2]^-$ [%] ^[c]	Yield [%] ^[c]
1	$^{16}\text{O}_2$	0	0		Not isolated.
2	$^{18}\text{O}_2$	28	38	10	81
3	$^{18}\text{O}_2$	31	39	12	72

^[a] Percentage of $[\text{P}^{16}\text{O}^{18}\text{OCl}_2]^-$ in $[\text{PO}_2\text{Cl}_2]^-$. ^[b] Percentage of $[\text{P}^{16}\text{O}_3^{18}\text{OCl}_2]^-$ in $[\text{HPO}_4\text{Cl}_4]^-$ or $[\text{NaPO}_4\text{Cl}_4]^-$. ^[c] Percentage of H/Na $[\text{P}^{16}\text{O}_3^{18}\text{O}_2\text{Cl}_2]^-$ in H/Na $[\text{PO}_4\text{Cl}_4]^-$. $\mathbf{P}^* = [\text{P}^{16}\text{O}^{18}\text{OCl}_2]$, $\mathbf{P} = [\text{P}^{16}\text{O}_2\text{Cl}_2]$.

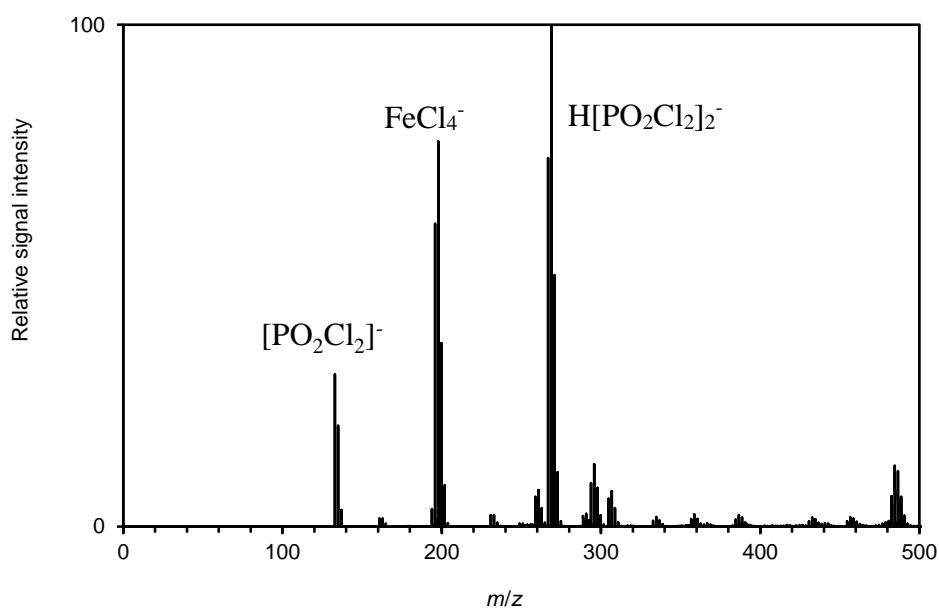


Figure 20: ESI-MS overview spectrum of entry 1.

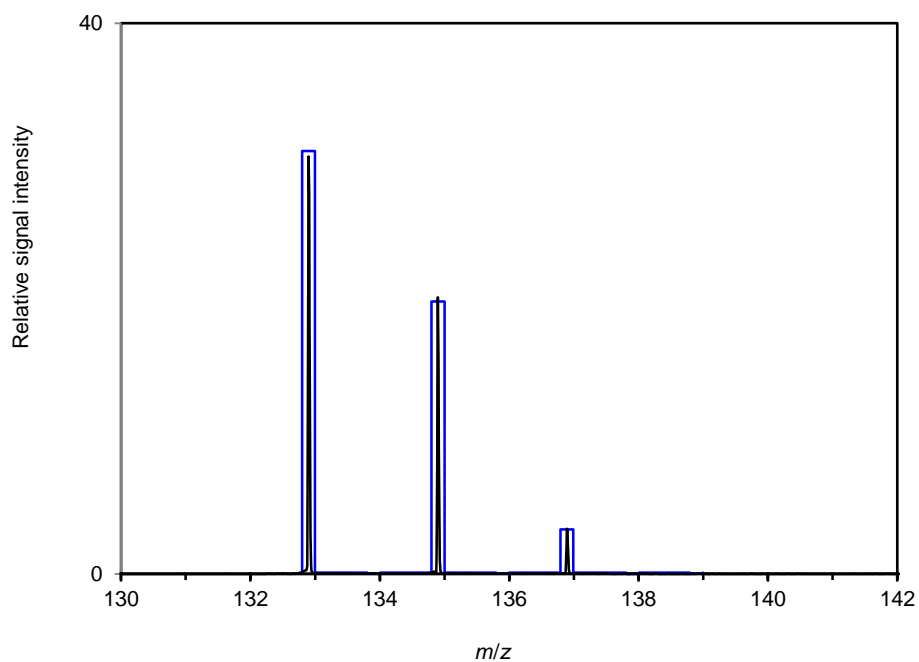


Figure 21: Expansion of the $[\text{PO}_2\text{Cl}_2]^-$ region of the measured ESI-MS spectrum (black) and the simulation (blue) of entry 1. Simulated for 100% $[\text{PO}_2\text{Cl}_2]^-$ and 0% $[\text{P}^{16}\text{O}^{18}\text{OCl}_2]^-$.

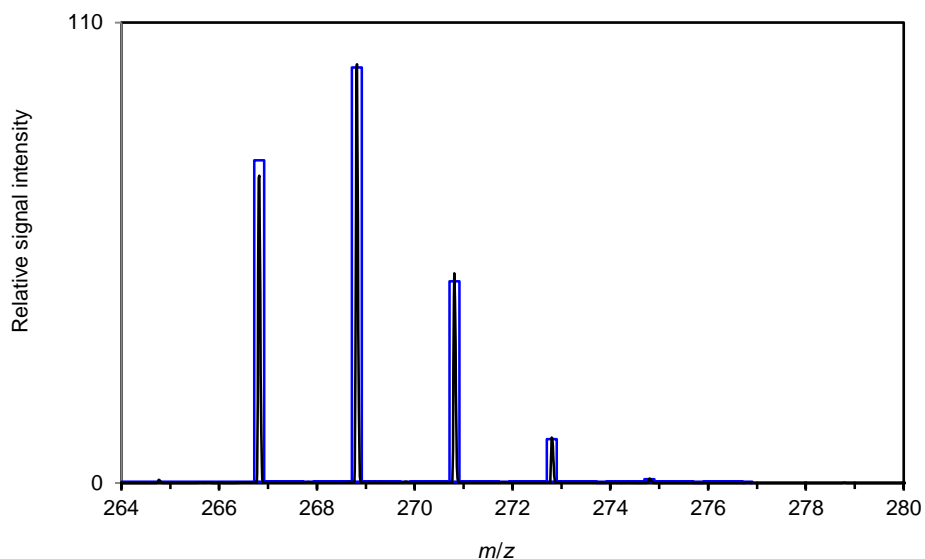


Figure 22: Expansion of the $\text{H}[\text{PO}_2\text{Cl}_2]_2^-$ region of the measured ESI-MS spectrum (black) and the simulation (blue) of entry 1. Simulated for 100% $\text{H}[\text{P}^{16}\text{O}_2\text{Cl}_2]_2^-$, 0% $\text{H}[\text{P}^{16}\text{O}_2\text{Cl}_2][\text{P}^{16}\text{O}^{18}\text{OCl}_2]^-$ and 0% $\text{H}[\text{P}^{16}\text{O}^{18}\text{OCl}_2]_2^-$.

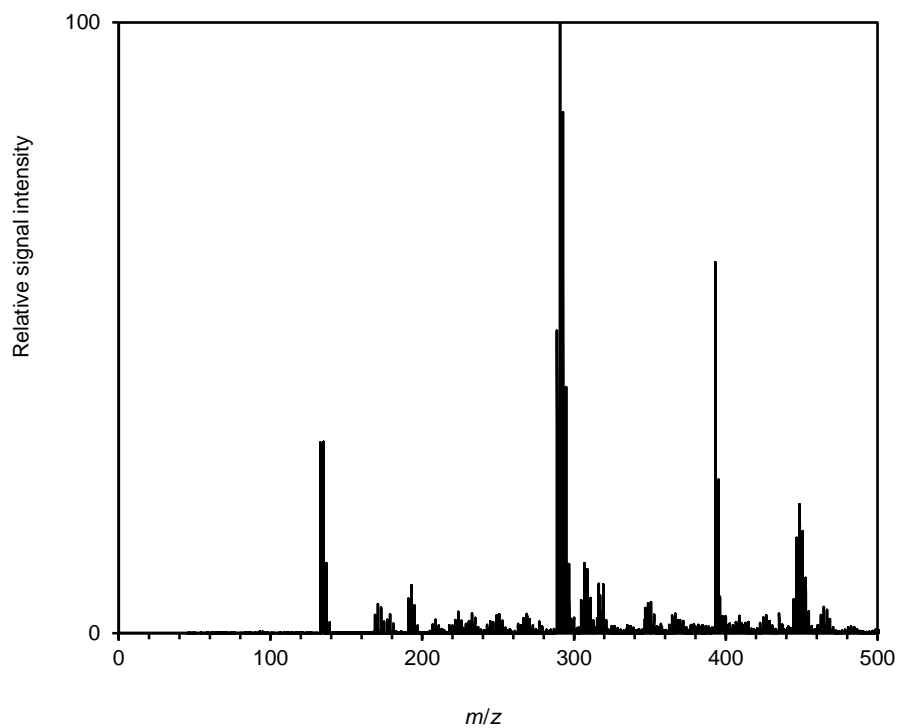


Figure 23:ESI-MS overview spectrum of entry 2.

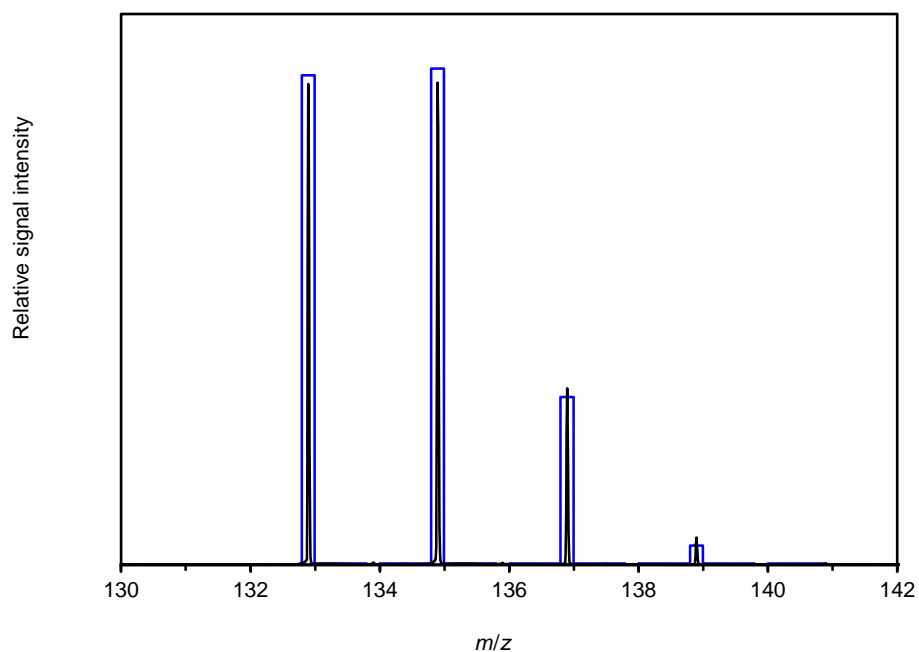


Figure 24: Expansion of the $[\text{PO}_2\text{Cl}_2]^-$ region of the measured ESI-MS spectrum (black) and the simulation (blue) of entry 2. Simulated for 72% $[\text{PO}_2\text{Cl}_2]^-$ and 18% $[\text{P}^{16}\text{O}^{18}\text{OCl}_2]^-$.

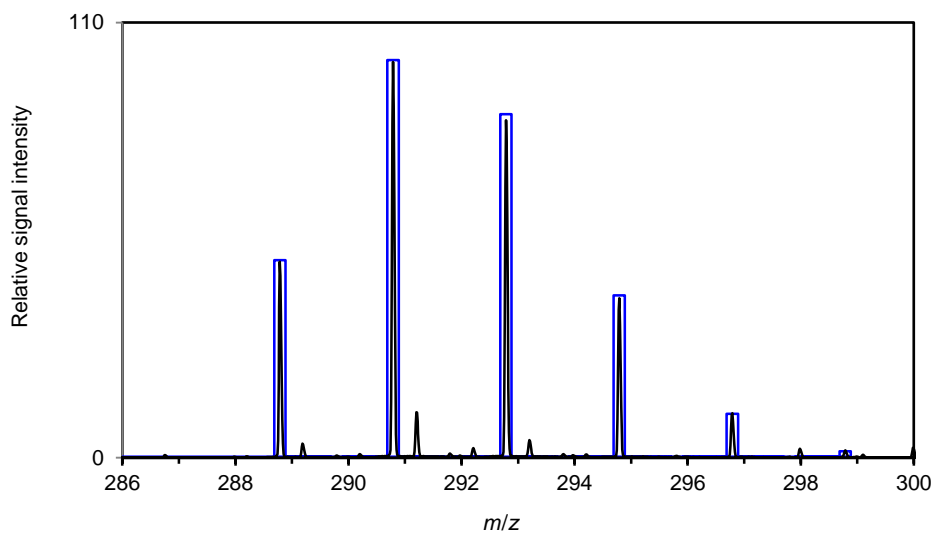


Figure 25: Expansion of the $\text{H}[\text{PO}_2\text{Cl}_2]_2^-$ region of the measured ESI-MS spectrum (black) and the simulation (blue) of entry 2. Simulated for 52.5% $\text{H}[\text{P}^{16}\text{O}_2\text{Cl}_2]_2^-$, 38% $\text{H}[\text{P}^{16}\text{O}_2\text{Cl}_2][\text{P}^{16}\text{O}^{18}\text{OCl}_2]^-$ and 9.5% $\text{H}[\text{P}^{16}\text{O}^{18}\text{OCl}_2]_2^-$.

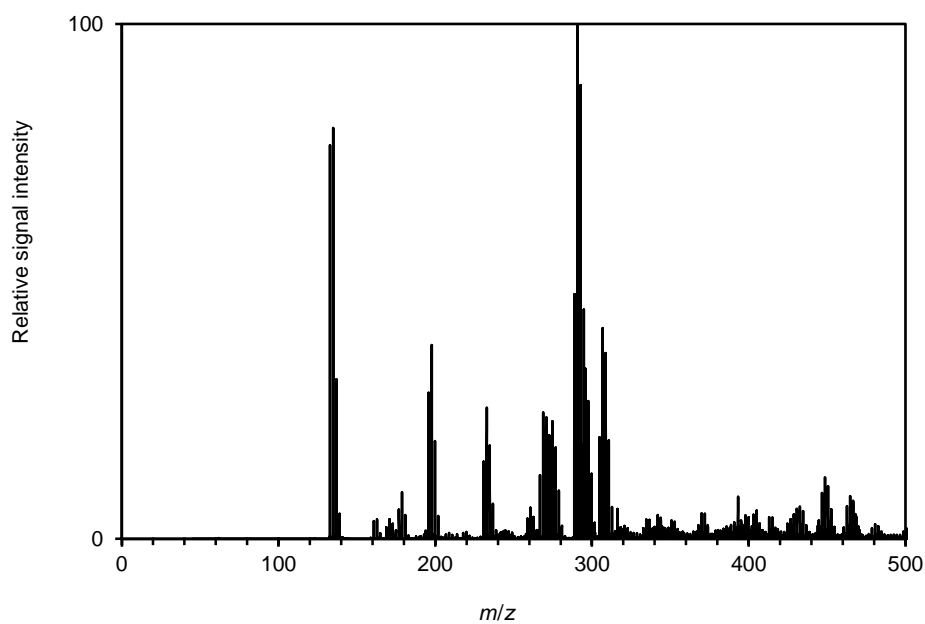


Figure 26: ESI-MS overview spectrum of entry 3.

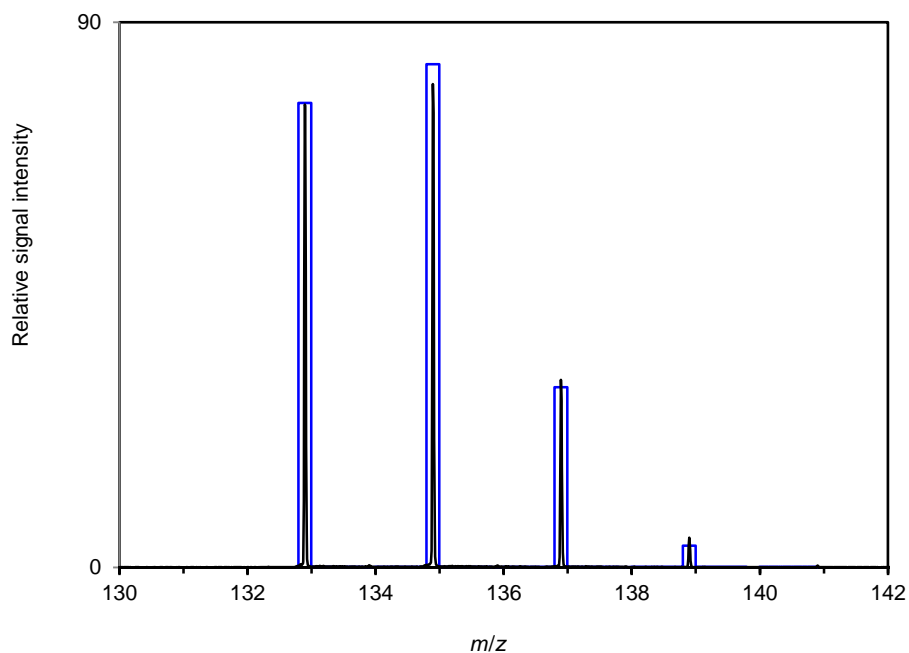


Figure 27: Expansion of the $[\text{PO}_2\text{Cl}_2]^-$ region of the measured ESI-MS spectrum (black) and the simulation (blue) of entry 3. Simulated for 69.5% $[\text{PO}_2\text{Cl}_2]^-$ and 30.5% $[\text{P}^{16}\text{O}^{18}\text{OCl}_2]^-$.

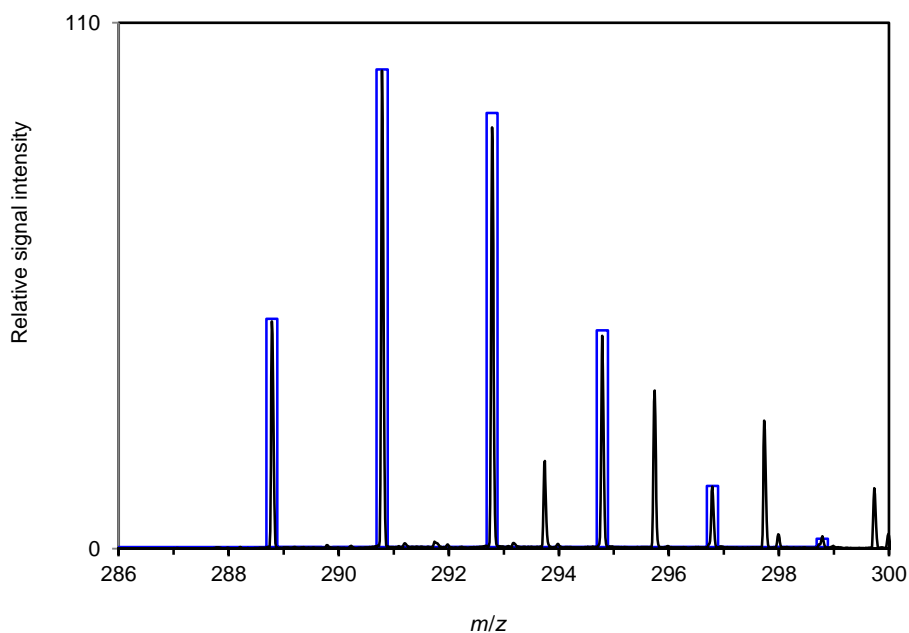
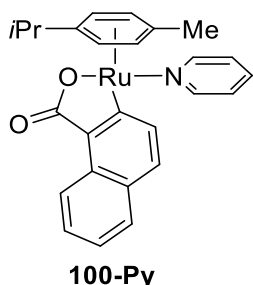


Figure 28: Expansion of the $\text{H}[\text{PO}_2\text{Cl}_2]_2^-$ region of the measured ESI-MS spectrum (black) and the simulation (blue) of entry 3. Simulated for 49% $\text{H}[\text{P}^{16}\text{O}_2\text{Cl}_2]_2^-$, 39% $\text{H}[\text{P}^{16}\text{O}_2\text{Cl}_2][\text{P}^{16}\text{O}^{18}\text{OCl}_2]^-$ and 12% $\text{H}[\text{P}^{16}\text{O}^{18}\text{OCl}_2]_2^-$.

5.3.1.3 Synthesis of Reaction Intermediates

Synthesis of donor stabilized intermediates **100**:

[RuCl₂(*p*-cymene)]₂ (**30**) (100 mg, 0.16 mmol, 1.0 equiv) was placed in a pre-dried 25 mL Schlenk-tube equipped with a rubber septum. The tube was evacuated and refilled with Ar three times. Solvent (either CH₂Cl₂, MeOH or γ -Valerolactone (**77**), 5.0 mL) was added together with pyridine (26.0 mg, 0.32 mmol, 2.0 equiv) and stirred for 2 h. 1-Naphthoic acid sodium salt (**21r-K**) (155 mg, 0.82 mmol, 5.0 equiv) and triethylamine (0.4 mL) were added and the mixture was stirred for 36 h at 35 °C. All volatiles were removed *in vacuo* and column chromatography (using a solvent gradient from CH₂Cl₂/MeOH: 40/1 to CH₂Cl₂/MeOH: 20/1) of the crude reaction mixture yielded **100-Py** (68.0 mg, 0.23 mmol, 71% from CH₂Cl₂, 49.0 mg, 0.16 mmol, 51% from MeOH, 36.0 mg, 12 mmol, 38% from γ -valerolactone (**77**)).

M. p. (decomp.) = 147 °C.

¹H-NMR (400 MHz, CDCl₃): δ = 9.46 (d, *J* = 8.7 Hz, 1H), 8.50 (d, *J* = 5.4 Hz, 2H), 8.19 (d, *J* = 8.2 Hz, 1H), 7.67 (d, *J* = 8.1 Hz, 2H), 7.40–7.27 (m, 2H), 7.23 (ddd, *J* = 8.3, 6.9, 1.3 Hz, 1H), 6.92–6.86 (m, 2H), 5.58 (d, *J* = 5.1 Hz, 1H), 5.49 (d, *J* = 5.7 Hz, 1H), 5.27 (d, *J* = 6.0 Hz, 1H), 4.82 (d, *J* = 5.7 Hz, 1H), 2.46–2.28 (m, 1H), 1.67 (s, 3H), 0.94 (d, *J* = 6.9 Hz, 3H), 0.94 (d, *J* = 6.9 Hz, 3H).

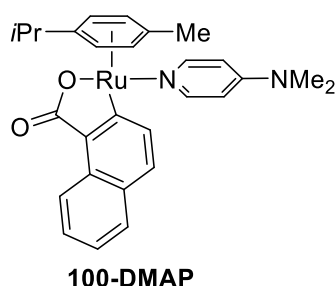
¹³C-NMR (100 MHz, CDCl₃): δ = 181.5 (C_q), 180.0 (C_q), 153.6 (CH), 136.7 (CH), 135.8 (CH), 132.7 (C_q), 131.5 (C_q), 130.4 (C_q), 130.0 (CH), 127.6 (CH), 126.2 (CH), 124.3 (CH), 123.7 (CH), 123.3 (CH), 102.2 (C_q), 98.4 (C_q), 88.1 (CH), 87.3 (CH), 85.1 (CH), 80.1 (CH), 30.8 (CH), 22.5 (CH₃), 22.3 (CH₃), 18.0 (CH₃).

IR (ATR): 3045, 2963, 2211, 1601, 1267, 819, 728 cm⁻¹;

HR-MS (ESI) *m/z* calcd for C₂₆H₂₇NO₂Ru, [M+H]⁺ 486.1009, found 486.1001.

Experimental Section

The spectral data are in accordance with those reported in the literature.^[41d]



[RuCl₂(*p*-cymene)]₂ (**30**) (100 mg, 0.16 mmol, 1.0 equiv) and *N,N*-dimethylaminopyridine (DMAP) (39.0 mg, 0.32 mmol, 2.0 equiv) were placed in a pre-dried 25 mL Schlenk-tube equipped with a rubber septum. The tube was evacuated and refilled with Ar three times. CH₂Cl₂ (5 mL) was added and stirred for 2 h. 1-Naphthoic acid sodium salt (**21r-K**) (155 mg, 0.82 mmol, 5.0 equiv) and triethylamine (0.4 mL) were added and the mixture was stirred for 36 h at 35 °C. All volatiles were removed *in vacuo* and column chromatography (using a solvent gradient from CH₂Cl₂/MeOH: 40/1 to CH₂Cl₂/MeOH: 20/1) of the crude reaction mixture yielded **100-DMAP** (122 mg, 0.23 mmol, 72%) as a yellow solid.

M. p. (decomp.) = 154 °C.

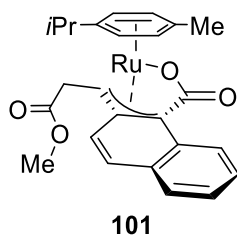
¹H-NMR (500 MHz, CDCl₃): δ = 9.52 (d, *J* = 8.6 Hz, 1H), 8.20 (d, *J* = 8.1 Hz, 1H), 7.87 (d, *J* = 6.2 Hz, 2H), 7.68 (t, *J* = 7.3 Hz, 2H), 7.35 (ddd, *J* = 8.5, 6.7, 1.5 Hz, 1H), 7.21 (ddd, *J* = 7.9, 6.7, 1.1 Hz, 1H), 5.91 (d, *J* = 5.6 Hz, 2H), 5.56 (d, *J* = 5.5 Hz, 1H), 5.46 (d, *J* = 5.8 Hz, 1H), 5.22 (d, *J* = 5.8 Hz, 1H), 4.77 (d, *J* = 5.3 Hz, 1H), 2.70 (s, 6H), 2.36 (hept, *J* = 6.1 Hz, 1H), 1.72 (s, 3H), 1.00–0.94 (m, 6H).

¹³C-NMR (125 MHz, CDCl₃): δ = 181.5 (C_q), 181.0 (C_q), 153.4 (C_q), 152.1 (CH), 136.1 (CH), 132.7 (C_q), 131.4 (C_q), 130.5 (C_q), 129.4 (CH), 127.4 (CH), 125.9 (CH), 123.9 (CH), 123.0 (CH), 106.9 (CH), 101.5 (C_q), 98.1 (C_q), 87.6 (CH), 87.2 (CH), 84.6 (CH), 79.7 (CH), 38.9 (CH₃), 30.9 (CH), 22.7 (CH₃), 22.5 (CH₃), 18.3 (CH₃).

IR (ATR): 2959, 1613, 1529, 1421, 1382, 1224, 1190, 1136, 811 cm⁻¹.

HR-MS (ESI) *m/z* calcd for C₂₈H₃₁N₂O₂Ru, [M+H]⁺ 529.1431, found 529.1428.

The spectral data are in accordance with those reported in the literature.^[41d]

Synthesis of intermediate **101**:

[RuCl₂(*p*-cymene)]₂ (**30**) (61.0 mg, 0.10 mmol, 1.0 equiv), 1-naphtioic acid (**21r**) (34.0 mg, 0.20 mmol, 2.0 equiv) and potassium acetate (39.0 mg, 0.40 mmol, 4.0 equiv) were placed in a pre-dried 25 mL Schlenk-tube equipped with a rubber septum. The tube was evacuated and refilled with Ar three times. Solvent (methanol, γ -valerolactone (**77**) or PhMe, 5.0 mL) was added together with methyl acrylate (**45b**) (17.0 mg, 0.20 mmol, 2.0 equiv) and the mixture was stirred at 60 °C for 36 h. All volatiles were removed *in vacuo* and column chromatography (using a solvent gradient from CH₂Cl₂/MeOH: 1/0 to CH₂Cl₂/MeOH: 10/1) of the crude reaction mixture yielded **101** (84.0 mg, 0.17 mmol, 85% in methanol, 94.0 mg, 0.19 mmol, 96% in γ -valerolactone (**77**) and 86.0 mg, 0.18 mmol, 87% in PhMe) as a yellow solid.

The reaction was scaled to 0.3 mmol of [RuCl₂(*p*-cymene)]₂ (**30**) in PhMe yielding **101** (299 mg, 0.60 mmol, >99%).

M. p. (decomp.) = 160–164 °C.

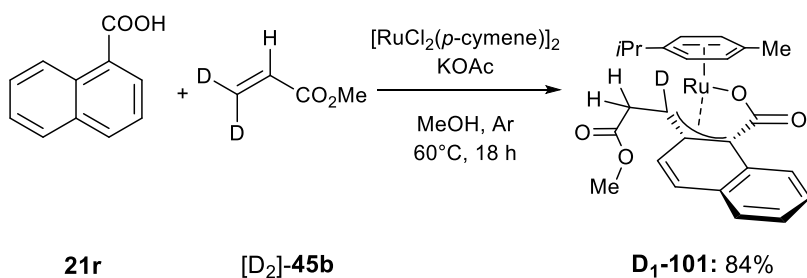
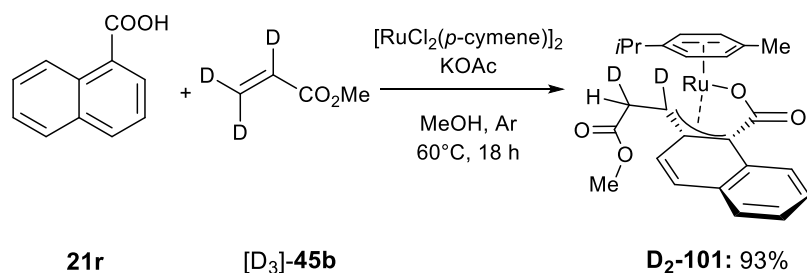
¹H-NMR (300 MHz, CDCl₃): δ = 8.53 (d, *J* = 7.9 Hz, 1H), 7.70–7.47 (m, 3H), 7.47 (d, *J* = 8.9 Hz, 1H), 7.01 (d, *J* = 9.7 Hz, 1H), 5.26 (dd, *J* = 5.8, 1.3 Hz, 1H), 4.81 (dd, *J* = 6.0, 1.3 Hz, 1H), 4.68 (dd, *J* = 6.0, 1.3 Hz, 1H), 4.06 (dd, *J* = 5.8, 1.3 Hz, 1H), 3.76 (s, 3H), 3.54 (dd, *J* = 15.0, 6.9 Hz, 1H), 3.40 (dd, *J* = 15.0, 7.8 Hz, 1H), 2.39 (dd, *J* = 7.8, 6.9 Hz, 1H), 2.30 (hept, *J* = 6.9 Hz, 1H), 1.24 (s, 3H), 1.20 (d, *J* = 6.9 Hz, 3H), 1.18 (d, *J* = 6.9 Hz, 3H).

¹³C-NMR (126 MHz, CDCl₃): δ = 172.2 (C_q), 169.3 (C_q), 135.1 (C_q), 132.4 (CH), 131.3 (C_q), 128.5 (CH), 128.3 (CH), 127.7 (CH), 126.9 (CH), 123.6 (CH), 110.0 (C_q), 99.3 (C_q), 96.8 (C_q), 85.8 (CH), 85.2 (CH), 83.9 (CH), 83.8 (C_q), 80.6 (CH), 57.3 (CH), 52.3 (CH), 38.8 (CH₂), 30.9 (CH₃), 23.1 (CH₃), 23.1 (CH₃), 16.6 (CH₃).

IR (ATR): 3058, 2962, 1724, 1650, 1430, 1252, 1172, 1011, 874 cm⁻¹.

HR-MS (ESI) m/z calcd for $C_{25}H_{27}O_4Ru$, $[M+H]^+$ 493.0954, found: 493.0958.

Synthesis of 101 using isotopically labeled acrylates:



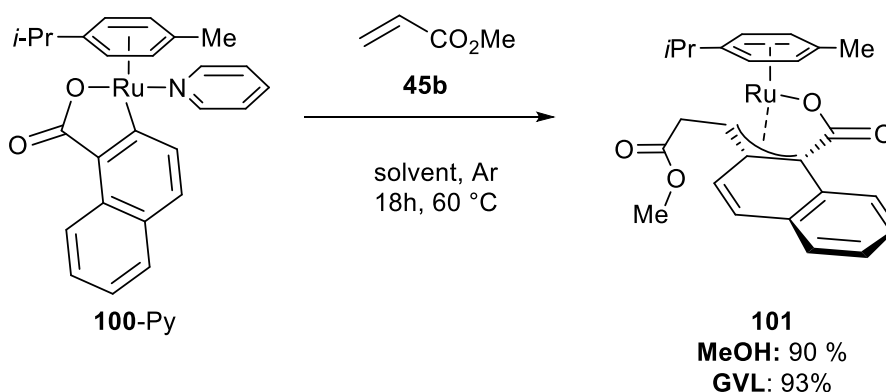
[D₂]-101 (92.0 mg, 19.0 mmol, 93%) was synthesized according to the previous procedure using **[D₃]-45b**.

HR-MS (ESI) m/z calcd for $C_{25}H_{25}O_4RuD_2$, $[M+H]^+$ 495.1080, found 495.1082.

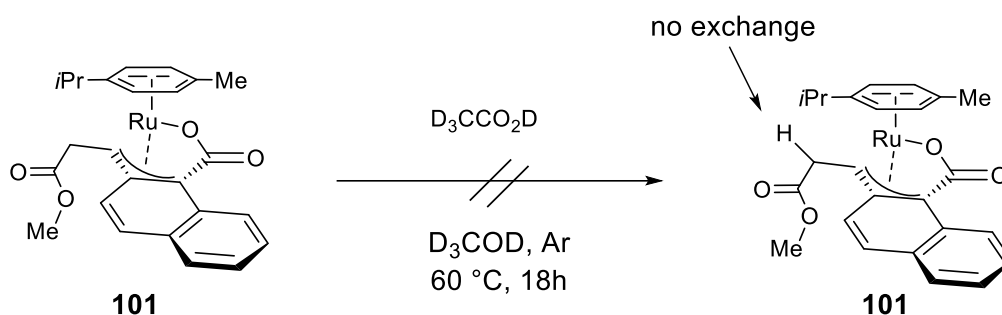
[D₁]-101 (84.0 mg, 17.0 mmol, 84%) was synthesized according to the previous procedure using **[D₂]-45b**.

HR-MS (ESI) m/z calcd for $C_{25}H_{26}O_4RuD_1$, $[M+H]^+$ 494.1017, found 494.1021.

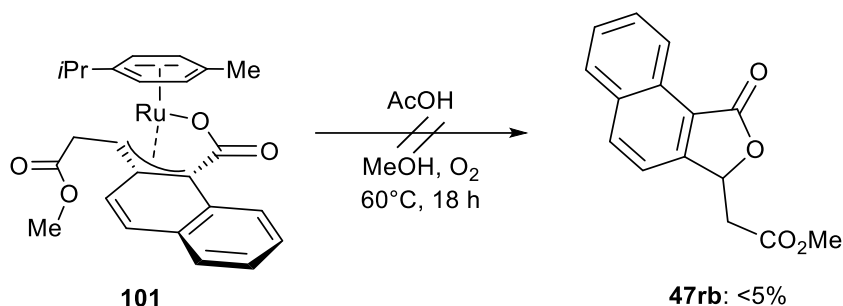
¹H-NMR analysis of **[D₂]-101** and **[D₁]-101** indicate a hydrogen exchange with the reaction medium (see Figure 11, page 67).

Synthesis of intermediate 101 from donor stabilized intermediate 100-Py


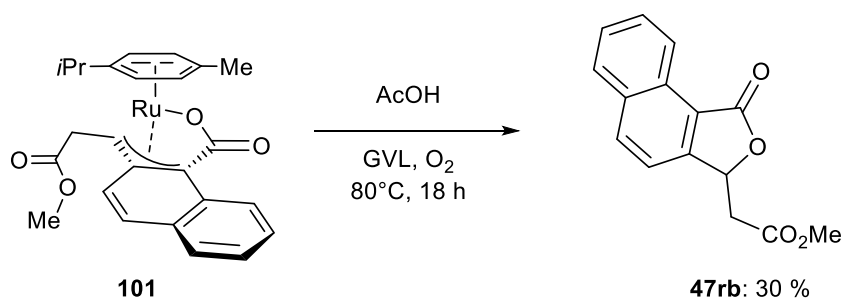
100-Py (10.0 mg, 20.6 μmol , 1.0 equiv) was placed in a pre-dried 25 mL Schlenk-tube equipped with a rubber septum. The tube was evacuated and refilled with Ar three times and solvent (methanol or γ -valerolactone (**77**), 1.0 mL) and methyl acrylate (**45b**) (2.00 mg, 22.0 μmol , 1.0 equiv) were added. The mixture was stirred at 60 °C for 18 h. Column chromatography (using a solvent gradient from $\text{CH}_2\text{Cl}_2/\text{MeOH}$: 1/0 to $\text{CH}_2\text{Cl}_2/\text{MeOH}$: 10/1) of the crude reaction mixture yielded **101** (8.90 mg, 18.5 μmol , 90% in methanol, 9.20 mg, 19.2 μmol , 93% in γ -valerolactone (**77**)).

Attempted hydrogen exchange at 101


101 (44.0 mg, 0.10 mmol, 1.0 equiv) was placed in a pre-dried 25 mL Schlenk-tube equipped with a rubber septum. The tube was evacuated and refilled with Ar three times and d^3 -MeOD (1.0 mL) and d^4 -acetic acid (2.00 mg, 22.0 μmol , 1.0 equiv) were added. The mixture was stirred at 60 °C for 18 h. An aliquot (0.1 mL) was removed and analysis by high resolution ESI-MS did not show incorporation of deuterium at **101**. The solution was heated to 80 °C for 18 h and analyzed by high resolution ESI-MS. Again, complex **101** did not show any deuterium incorporation.

Product release from 101:


101 (50.0 mg, 0.10 mmol, 1.0 equiv) was placed in a pre-dried 25 mL Schlenk-tube equipped with a rubber septum. The tube was evacuated and refilled with O₂ three times and MeOH (1.0 mL) and acetic acid (60.0 mg, 1.00 μmol, 10.0 equiv) were added. The reaction mixture was stirred at 60 °C for 18 h. GC and TLC analysis of the reaction mixture just showed traces of product.



101 (50.0 mg, 0.10 mmol, 1.0 equiv) was placed in a pre-dried 25 mL Schlenk-tube equipped with a rubber septum. The tube was evacuated and refilled with O₂ three times and γ -valerolactone (**77**) (0.5 mL) and acetic acid (30.0 mg, 0.50 μmol, 50.0 equiv) were added. The reaction mixture was stirred at 80 °C for 18 h. The mixture was diluted with water (10 mL) and extracted with MTBE/*n*-hexane (1/1 mixture, 10 mL). The organic phase was washed with water (4·10 mL) and dried over anhydrous sodium sulfate. The solvent was removed and purification by column chromatography (*n*-hexane/EtOAc: 4/1 + 5% NEt₃) yielded **47rb** (9.30 mg, 0.03 mmol, 30 %) as colorless solid.

M. p. = 64–66 °C.

Experimental Section

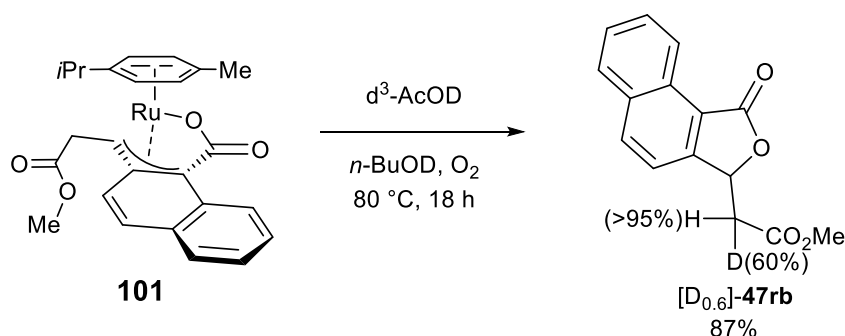
$^1\text{H-NMR}$ (300 MHz, CDCl_3): $\delta = 9.02\text{--}8.97$ (m, 1H), 8.15 (dd, $J = 8.4, 0.7, 0.7$ Hz, 1H), 7.97 (ddd, $J = 8.1, 1.3, 0.6, 0.6$ Hz, 1H), 7.74 (ddd, $J = 8.4, 7.0, 1.4$ Hz, 1H), 7.64 (ddd, $J = 8.2, 6.9, 1.4$ Hz, 1H), 7.52 (dd, $J = 8.4, 0.6$ Hz, 1H), 5.96 (ddd, $J = 6.9, 6.2, 0.5$ Hz, 1H), 3.79 (s, 3H), 2.96 (dd, $J = 6.7, 0.9$ Hz, 2H).

$^{13}\text{C-NMR}$ (126 MHz, CDCl_3): $\delta = 169.9$ (C_q), 169.7 (C_q), 150.2 (C_q), 135.7 (CH), 133.4 (C_q), 129.1 (CH), 129.1 (C_q), 128.4 (CH), 127.5 (CH), 123.5 (CH), 120.1 (C_q), 118.3 (CH), 76.3 (CH), 52.3 (CH_2), 39.3 (CH_3).

IR (ATR): 2944, 1730, 1578, 1517, 1435, 1328, 1106, 963, 891, 694 cm^{-1} .

MS (EI) m/z (relative Intensity): 256 (25) $[\text{M}]^+$, 242 (5), 196 (100), 183 (35), 168 (10), 155 (30), 127 (35), 115 (5).

HR-MS (ESI) m/z calcd for $\text{C}_{15}\text{H}_{13}\text{O}_4$, $[\text{M}+\text{H}]^+$ 257.0808, found 257.0803.

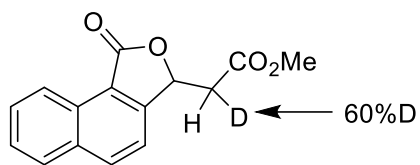


101 (19.0 mg, 0.04 mmol, 1.0 equiv) was placed in a pre-dried 25 mL Schlenk-tube equipped with a rubber septum. The tube was evacuated and refilled with O_2 three times and $n\text{-BuOD}$ (0.5 mL) and d^4 -acetic acid (30.0 mg, 0.50 mmol, 12.0 equiv) were added. The reaction mixture was stirred at 80 $^\circ\text{C}$ for 18 h. The solvent was removed and purification by column chromatography ($n\text{-hexane/EtOAc}$: 4/1 + 5% NEt_3) yielded **[D_{0.6}]-47rb** (8.6 mg, 0.29 mmol, 87%).

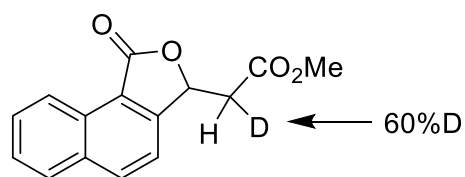
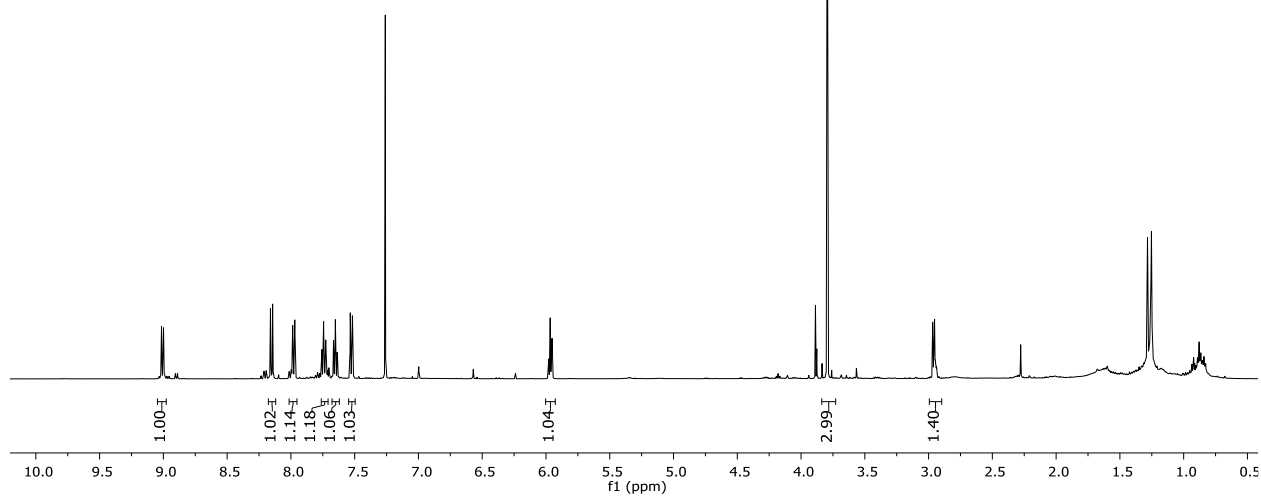
HR-MS (ESI) m/z calcd for $\text{C}_{15}\text{H}_{11}\text{O}_4\text{DNa}$, $[\text{M}+\text{Na}]^+$ 280.0691, found 280.0692; Intensity: 100%.

HR-MS (ESI) m/z calcd for $\text{C}_{15}\text{H}_{12}\text{O}_4\text{Na}$, $[\text{M}+\text{Na}]^+$ 279.0628, found 279.0629; Intensity: 60%.^[129]

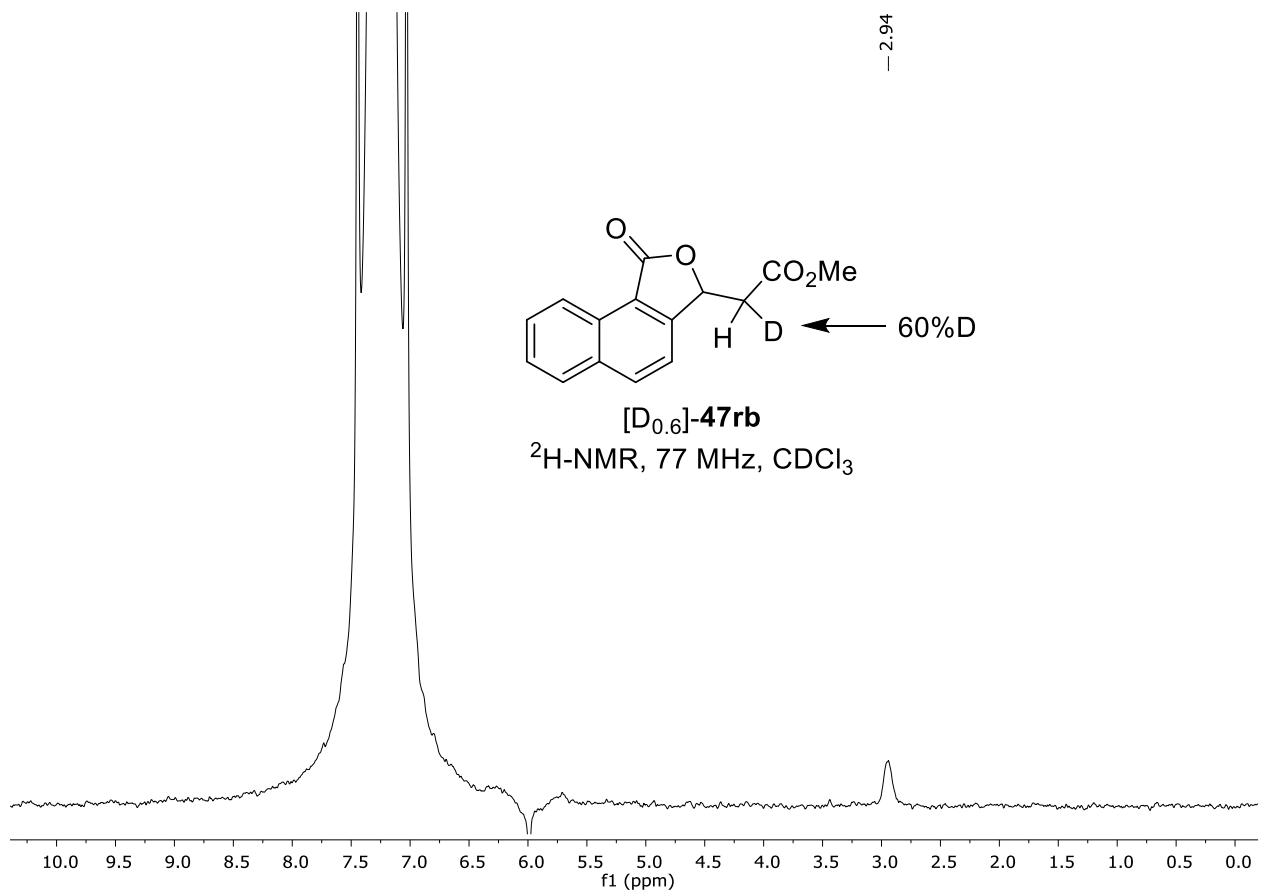
Experimental Section



[D_{0.6}]-47rb
¹H-NMR, 500 MHz, CDCl₃

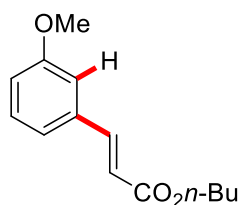


[D_{0.6}]-47rb
²H-NMR, 77 MHz, CDCl₃



5.3.2 Data for the Ruthenium(II) Decarboxylative Alkenylation of Benzoic Acids

5.3.2.1 Data of Alkenylated Arenes



97ca

n-Butyl-(*E*)-3-(3-methoxyphenyl)acrylate (**97ca**):

The general procedure **C** was followed using 2-methoxybenzoic acid (**21c**) (456 mg, 3.00 mmol) and *n*-butyl acrylate (**45a**) (128 mg, 1.00 mmol). Purification by column chromatography (*n*-hexane/EtOAc: 15/1) yielded **97ca** (129 mg, 55%) as a colorless oil.

¹H-NMR (500 MHz, CDCl₃): δ = 7.71 (d, *J* = 15.9 Hz, 1H), 7.36 (dd, *J* = 8.3 Hz, 7.6 Hz, 1H), 7.18 (d, *J* = 7.6 Hz, 1H), 7.11 (dd, *J* = 1.7 Hz, 1.6 Hz, 1H), 7.00 (ddd, *J* = 8.3, 1.7, 1.6 Hz, 1H), 6.49 (d, *J* = 15.9 Hz, 1H), 4.28 (t, *J* = 6.7 Hz, 2H), 3.90 (s, 3H), 1.80–1.72 (m, 2H), 1.56–1.46 (m, 2H), 1.03 (t, *J* = 7.4 Hz, 3H).

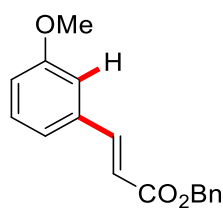
¹³C-NMR (126 MHz, CDCl₃): δ = 167.2 (C_q), 160.1 (C_q), 144.6 (CH), 136.0 (C_q), 130.0 (CH), 120.9 (CH), 118.8 (CH), 116.3 (CH), 113.0 (CH), 64.6 (CH₂), 55.5 (CH₃), 30.9 (CH₂), 19.4 (CH₂), 13.9 (CH₃).

IR (ATR): 2959, 2873, 1707, 1637, 1580, 1292, 1164, 1040, 781, 679 cm⁻¹.

MS (EI) *m/z* (relative intensity): 234 (40) [M]⁺, 178 (100), 161 (90), 133 (25), 118 (20), 103 (10), 90 (15), 77 (15), 63 (10).

HR-MS (ESI) *m/z* calcd for C₁₄H₁₉O₃, [M+H]⁺ 235.1322, found 235.1329.

The analytical data are in accordance with those reported in the literature. ^[130]



97cd

Benzyl-(*E*)-3-(3-methoxyphenyl)acrylate (97cd):

a) The general procedure **C** was followed using 2-methoxybenzoic acid (**21c**) (456 mg, 3.00 mmol) and benzyl acrylate (**45d**) (162 mg, 1.00 mmol). Purification by column chromatography (*n*-hexane/EtOAc: 15/1) yielded **97cd** (161 mg, 0.60 mmol, 60%) as a colorless oil.

b) The general procedure **C** scaled up by a factor of 5 was followed using 2-methoxybenzoic acid (**21c**) (2.28 g, 15.0 mmol) and benzyl acrylate (**45d**) (0.81 g, 5.00 mmol). Purification by column chromatography (*n*-hexane/EtOAc: 15/1) yielded **97cd** (1.01 g, 3.75 mmol, 75%) as a colorless oil.

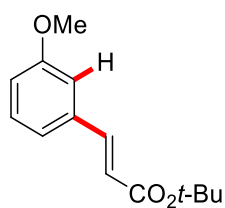
¹H-NMR (300 MHz, CDCl₃): δ = 7.70 (d, *J* = 16.0 Hz, 1H), 7.46–7.27 (m, 6H), 7.12 (ddd, *J* = 7.6, 1.1, 0.5 Hz, 1H), 7.04 (dd, *J* = 2.6, 1.6 Hz, 1H), 6.94 (ddd, *J* = 8.3, 2.6, 1.1 Hz, 1H), 6.48 (d, *J* = 16.0 Hz, 1H), 5.26 (s, 2H), 3.83 (s, 3H).

¹³C-NMR (126 MHz, CDCl₃): δ = 166.8 (C_q), 160.0 (C_q), 145.2 (CH), 136.2 (C_q), 135.9 (C_q), 130.0 (CH), 128.7 (CH), 128.4 (CH), 128.4 (CH), 121.0 (CH), 118.3 (CH), 116.4 (CH), 113.0 (CH), 66.5 (CH₂), 55.4 (CH₃).

IR (ATR): 3032, 2956, 2835, 1707, 1636, 1228, 1153, 979, 696, 678 cm⁻¹.

MS (EI) *m/z* (relative intensity): 268 (35) [M]⁺, 221 (45), 177 (30), 161 (60), 134 (20), 91 (100), 77 (20), 65 (20).

HR-MS (EI) *m/z* calcd for C₁₇H₁₆O₃, [M]⁺ 268.1099, found 268.1089.

**97ce*****t*-Butyl-(*E*)-3-(3-methoxyphenyl)acrylate (**97ce**):**

The general procedure **C** was followed using 2-methoxybenzoic acid (**21c**) (456 mg, 3.00 mmol) and *t*-butyl acrylate (**45e**) (128 mg, 1.00 mmol). Purification by column chromatography (*n*-hexane/EtOAc: 10/1) yielded **97ce** (135 mg, 58%) as a colorless oil.

¹H-NMR (400 MHz, CDCl₃): δ = 7.45 (d, J = 15.9, Hz, 1H), 7.18 (dd, J = 8.2, 7.7 Hz, 1H), 7.00 (ddd, J = 7.7, 1.5, 0.9 Hz, 1H), 6.95–6.90 (m, 1H), 6.81 (ddd, J = 8.2, 2.6, 0.9 Hz, 1H), 7.25 (dd, J = 16.0, 0.4 Hz, 1H), 3.73 (s, 3H), 1.44 (s, 9H).

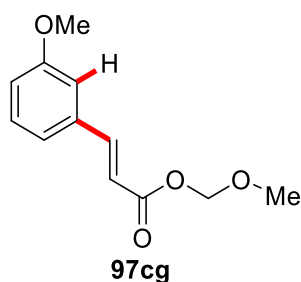
¹³C-NMR (101 MHz, CDCl₃): δ = 166.4 (C_q), 160.0 (C_q), 143.6 (CH), 136.2 (C_q), 129.9 (CH), 120.9 (CH), 120.6 (CH), 116.0 (CH), 112.9 (CH), 80.7 (C_q), 55.4 (CH₃), 28.4 (CH₃).

IR (ATR): 2976, 2935, 1703, 1636, 1580, 1143, 1041, 978, 849, 679 cm⁻¹.

MS (EI) m/z (relative intensity): 234 (30) [M]⁺, 178 (100), 161 (40), 147 (15), 133 (10), 118 (10), 77 (10), 57 (25), 43 (25).

HR-MS (EI) m/z calcd for C₁₄H₁₈O₃, [M]⁺ 234.1256, found 234.1245.

The analytical data are in accordance with those reported in the literature. ^[131]

**2-Methoxyethyl-(*E*)-3-(3-methoxyphenyl)acrylate (97cg):**

The general procedure **C** was followed using 2-methoxybenzoic acid (**21c**) (456 mg, 3.00 mmol) and 2-methoxyethyl acrylate (**45g**) (130 mg, 1.00 mmol). Purification by column chromatography (*n*-hexane/EtOAc: 3/1) yielded **97cg** (147 mg, 62%) as a colorless oil.

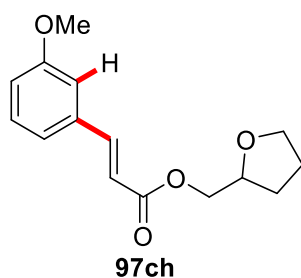
$^1\text{H-NMR}$ (400 MHz, CDCl_3): δ = 7.68 (d, J = 16.0 Hz, 1H), 7.29 (dd, J = 8.2, 7.7 Hz, 1H), 7.11 (ddd, J = 7.7, 1.5, 0.9 Hz, 1H), 7.05–7.03 (m, 1H), 6.93 (ddd, J = 8.2, 2.6, 1.0 Hz, 1H), 6.48 (d, J = 16.0 Hz, 1H), 4.42–4.25 (m, 2H), 3.82 (s, 3H), 3.71–3.61 (m, 2H), 3.42 (s, 3H).

$^{13}\text{C-NMR}$ (101 MHz, CDCl_3): δ = 167.0 (C_q), 160.1 (C_q), 145.2 (CH), 135.9 (C_q), 130.0 (CH), 121.0 (CH), 118.3 (CH), 116.5 (CH), 113.0 (CH), 70.7 (CH_2), 63.7 (CH_2), 59.2 (CH_3), 55.4 (CH_3).

IR (ATR): 2944, 2837, 1708, 1637, 1246, 1165, 1038, 850, 782, 679 cm^{-1} .

MS (EI) m/z (relative intensity): 236 (15) $[\text{M}]^+$, 178 (85), 161 (100), 133 (30), 118 (25), 90 (15), 77 (10), 58 (10), 43 (15).

HR-MS (EI) m/z calcd for $\text{C}_{13}\text{H}_{16}\text{O}_4$, $[\text{M}]^+$ 236.1049, found 236.1041.



(Tetrahydrofuran-2-yl)methyl-(*E*)-3-(3-methoxyphenyl)acrylate (97ch):

The general procedure **C** was followed using 2-methoxybenzoic acid (**21c**) (456 mg, 3.00 mmol) and tetrahydrofurfuryl acrylate (**45h**) (156 mg, 1.00 mmol). Purification by column chromatography (*n*-hexane/EtOAc: 3/1) yielded **97ch** (184 mg, 70%) as a colorless oil.

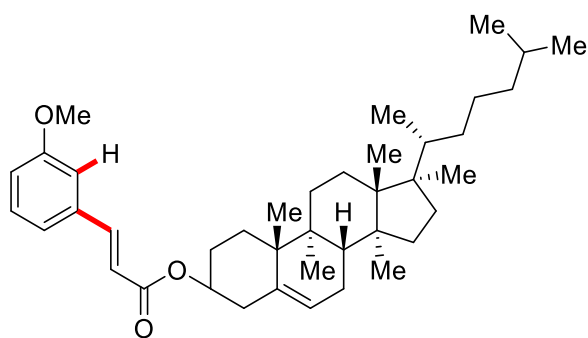
$^1\text{H-NMR}$ (400 MHz, CDCl_3): δ = 7.68 (d, J = 15.9 Hz, 1H), 7.29 (dd, J = 8.1, 7.7 Hz, 1H), 7.11 (ddd, J = 7.5, 1.5, 0.9 Hz, 1H), 7.05–7.03 (m, 1H), 6.93 (ddd, J = 8.2, 2.6, 0.9 Hz, 1H), 6.48 (d, J = 15.9 Hz, 1H), 4.31 (dd, J = 11.2, 3.3 Hz, 1H), 4.20 (ddd, J = 7.1, 7.0, 3.2 Hz, 1H), 4.13 (dd, J = 11.1, 7.0 Hz, 1H), 3.93 (ddd, J = 8.3, 7.0, 6.4 Hz, 1H), 3.87–3.78 (m, 1H), 3.83 (s, 3H), 2.10–1.87 (m, 3H), 1.72–1.61 (m, 1H).

$^{13}\text{C-NMR}$ (101 MHz, CDCl_3): δ = 167.0 (C_q), 160.1 (C_q), 145.2 (CH), 136.0 (C_q), 130.0 (CH), 121.0 (CH), 118.4 (CH), 116.5 (CH), 113.0 (CH), 76.8 (CH), 68.6 (CH_2), 66.8 (CH_2), 55.5 (CH_3), 28.2 (CH_2), 25.9 (CH_2).

IR (ATR): 2949, 2873, 1637, 1579, 1247, 1162, 1025, 855, 782, 679 cm^{-1} .

MS (EI) m/z (relative intensity): 262 (5) $[\text{M}]^+$, 178 (35), 161 (40), 133 (105), 118 (15), 84 (50), 71 (100), 58 (10), 43 (35).

HR-MS (EI) m/z calcd for $\text{C}_{15}\text{H}_{18}\text{O}_4$, $[\text{M}]^+$ 262.1205, found 262.1206.

**97cl****Cholesteryl-(*E*)-3-(3-methoxyphenyl)acrylate (97cl):**

The general procedure **C** was followed using 2-methoxybenzoic acid (**21c**) (228 mg, 1.50 mmol) and cholesteryl acrylate (**45l**) (202 mg, 0.50 mmol). Purification by column chromatography (*n*-hexane/EtOAc: 15/1) yielded **97cl** (210 mg, 77%) as a white solid.

M. p. = 119–120 °C.

¹H-NMR (400 MHz, CDCl₃): δ = 7.64 (d, *J* = 16.0 Hz, 1H), 7.34–7.27 (dd, *J* = 8.0, 7.9 Hz 1H), 7.11 (ddd, *J* = 8.1, 1.5, 0.8 Hz, 1H), 7.04 (dd, *J* = 2.7, 1.5 Hz, 1H), 6.93 (ddd, *J* = 8.2, 2.6, 1.0 Hz, 1H), 6.41 (d, *J* = 15.9 Hz, 1H), 5.41 (d, *J* = 3.5 Hz, 1H), 4.75 (ddt, *J* = 14.3, 7.4, 4.3 Hz, 1H), 3.83 (s, 3H), 2.54–2.28 (m, 2H), 2.06–0.95 (m, 29H), 0.92 (d, *J* = 6.5 Hz, 3H), 0.87 (dd, *J* = 6.6, 1.9 Hz, 6H), 0.69 (s, 3H).

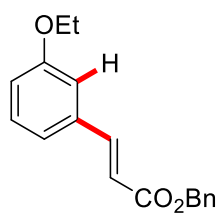
¹³C-NMR (101 MHz, CDCl₃): δ = 166.5 (C_q), 160.0 (C_q), 144.5 (CH), 139.8 (C_q), 136.0 (C_q), 130.0 (CH), 122.9 (CH), 120.9 (CH), 119.1 (CH), 116.2 (CH), 112.9 (CH), 74.3 (CH), 56.8 (CH), 56.3 (CH), 55.4 (CH₃), 50.2 (CH), 42.5 (C_q), 39.9 (CH₂), 39.7 (CH₂), 38.4 (CH₂), 37.2 (CH₂), 36.8 (C_q), 36.3 (CH₂), 36.0 (CH), 32.1 (CH₂), 32.0 (CH), 28.4 (CH₂), 28.2 (CH), 28.0 (CH₂), 24.4 (CH₂), 24.0 (CH₂), 23.0 (CH₃), 22.7 (CH₃), 21.2 (CH₂), 19.5 (CH₃), 18.9 (CH₃), 12.0 (CH₃).

IR (ATR): 2931, 2864, 1706, 1637, 1578, 1261, 1168, 1001, 736, 455 cm⁻¹.

MS (EI) *m/z* (relative intensity): 546 (0.2) [M]⁺, 386 (0.2), 368 (100), 353 (20), 260 (25), 247 (20), 213 (15), 161 (40), 147 (30), 43 (30).

HR-MS (ESI) *m/z* calcd for C₃₇H₅₄O₃Na, [M+Na]⁺ 569.3965, found 569.3938.

The analytical data are in accordance with those reported in the literature. ^[132]

**97dd****Benzyl-(*E*)-3-(3-ethoxyphenyl)acrylate (97dd):**

The general procedure **C** was followed using 2-ethoxybenzoic acid (**21d**) (499 mg, 3.00 mmol) and benzyl acrylate (**45d**) (162 mg, 1.00 mmol). Purification by column chromatography (*n*-hexane/EtOAc: 10/1) yielded **97dd** (194 mg, 69%) as a colorless oil.

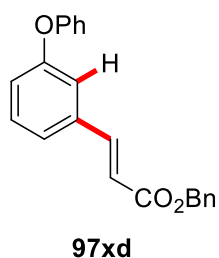
¹H-NMR (300 MHz, CDCl₃): δ = 7.70 (d, *J* = 16.0 Hz, 1H), 7.48–7.27 (m, 6H), 7.16 (ddd, *J* = 7.6, 1.5, 1.5 Hz, 1H), 7.04 (d, *J* = 2.1 Hz, 1H), 6.92 (ddd, *J* = 8.3, 2.6, 1.1 Hz, 1H), 6.47 (d, *J* = 16.1 Hz, 1H), 5.26 (s, 2H), 4.05 (q, *J* = 7.0 Hz, 2H), 1.42 (t, *J* = 7.0 Hz, 3H).

¹³C-NMR (75 MHz, CDCl₃): δ = 166.9 (C_q), 159.4 (C_q), 145.3 (CH), 136.2 (C_q), 135.8 (C_q), 130.0 (CH), 128.7 (CH), 128.4 (CH), 128.4 (CH), 120.8 (CH), 118.2 (CH), 117.0 (CH), 113.6 (CH), 66.5 (CH₂), 63.7 (CH₂), 14.9 (CH₃).

IR (ATR): 3034, 2980, 2937, 1708, 1636, 1226, 1154, 979, 696, 678 cm⁻¹.

MS (EI) *m/z* (relative intensity): 282 (35) [M]⁺, 236 (20), 191 (15), 163 (30), 147 (30), 91 (100), 65 (25), 43 (15).

HR-MS (ESI) *m/z* calcd for C₁₈H₁₈O₃Na, [M+Na]⁺ 305.1148, found 305.1149.

**Benzyl-(*E*)-3-(3-phenoxyphenyl)acrylate (3xd):**

The general procedure C was followed using 2-phenoxybenzoic acid (**21x**) (643 mg, 3.00 mmol) and benzyl acrylate (**45d**) (162 mg, 1.00 mmol). Purification by column chromatography (*n*-hexane/EtOAc: 10/1) yielded **97xd** (191 mg, 58%) as a white solid.

M. p. = 54–57 °C.

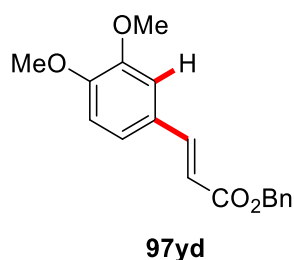
¹H-NMR (500 MHz, CDCl₃): δ = 7.64 (d, *J* = 16.0 Hz, 1H), 7.41–7.28 (m, 8H), 7.24–7.20 (m, 1H), 7.16–7.08 (m, 2H), 7.04–6.96 (m, 3H), 6.40 (d, *J* = 16.0 Hz, 1H), 5.22 (s, 2H).

¹³C-NMR (126 MHz, CDCl₃): δ = 166.7 (C_q), 158.1 (C_q), 156.8 (C_q), 144.6 (CH), 136.3 (C_q), 136.1 (C_q), 130.4 (CH), 130.1 (CH), 128.8 (CH), 128.5 (CH), 128.4 (CH), 123.9 (CH), 123.2 (CH), 120.7 (CH), 119.3 (CH), 118.8 (CH), 117.7 (CH), 66.6 (CH₂).

IR (ATR): 3033, 2970, 1703, 1637, 1487, 1234, 1153, 980, 784, 692 cm⁻¹.

MS (EI) *m/z* (relative intensity): 330 (40) [M]⁺, 284 (25), 223 (30), 199 (20), 165 (15), 131 (15), 91 (100), 77 (25), 65 (55), 51 (15).

HR-MS (ESI) *m/z* calcd for C₂₂H₁₈O₃Na, [M+Na]⁺ 353.1148, found 353.1139.

**Benzyl-(*E*)-3-(3,4-dimethoxyphenyl)acrylate (97yd):**

The general procedure C was followed using 2,3-dimethoxybenzoic acid (**21y**) (547 mg, 3.00 mmol) and benzyl acrylate (**45d**) (162 mg, 1.00 mmol). Purification by column chromatography (*n*-hexane/EtOAc: 4/1) yielded **97yd** (156 mg, 52%) as a colorless oil.

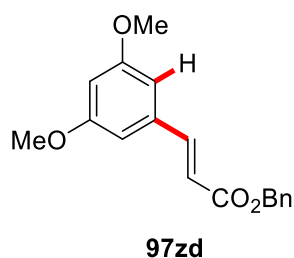
¹H-NMR (500 MHz, CDCl₃): δ = 7.67 (d, *J* = 15.9 Hz, 1H), 7.45–7.31 (m, 5H), 7.10 (dd, *J* = 8.3, 2.1 Hz, 1H), 7.05 (d, *J* = 2.0 Hz, 1H), 6.86 (d, *J* = 8.3 Hz, 1H), 6.36 (d, *J* = 15.9 Hz, 1H), 5.25 (s, 2H), 3.91 (s, 3H), 3.90 (s, 3H).

¹³C-NMR (126 MHz, CDCl₃): δ = 167.2 (C_q), 151.3 (C_q), 149.3 (C_q), 145.2 (CH), 136.3 (C_q), 128.7 (CH), 128.4 (CH), 128.4 (CH), 127.5 (C_q), 122.9 (CH), 115.7 (CH), 111.1 (CH), 109.7 (CH), 66.4 (CH₂), 56.1 (CH₃), 56.0 (CH₃).

IR (ATR): 2934, 2838, 1703, 1510, 1254, 1136, 845, 806, 733, 696 cm⁻¹.

MS (EI) *m/z* (relative intensity): 298 (100) [M]⁺, 253 (15), 207 (15), 191 (35), 164 (50), 91 (75), 84 (25), 77 (20), 65 (15), 43 (35).

HR-MS (EI) *m/z* calcd for C₁₈H₁₈O₄, [M]⁺ 298.1205, found 298.1206.

**Benzyl-(*E*)-3-(3,5-dimethoxyphenyl)acrylate (97zd):**

The general procedure **C** was followed using 2,4-dimethoxybenzoic acid (**21z**) (547 mg, 3.00 mmol) and benzyl acrylate (**45d**) (162 mg, 1.00 mmol). Purification by column chromatography (*n*-hexane/EtOAc: 10/1) yielded **97zd** (212 mg, 71%) as a white solid.

M. p. = 51-53 °C.

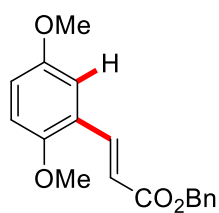
¹H-NMR (300 MHz, CDCl₃): δ = 7.65 (d, *J* = 16.0 Hz, 1H), 7.47–7.30 (m, 5H), 6.66 (d, *J* = 2.3 Hz, 2H), 6.50 (t, *J* = 2.3 Hz, 1H), 6.46 (d, *J* = 16.0 Hz, 1H), 5.25 (s, 2H), 3.81 (s, 6H).

¹³C-NMR (126 MHz, CDCl₃): δ = 166.6 (C_q), 161.0 (C_q), 145.2 (CH), 136.3 (C_q), 136.1 (C_q), 128.7 (CH), 128.3 (CH), 128.3 (CH), 118.5 (CH), 106.1 (CH), 102.8 (CH), 66.5 (CH₂), 55.6 (CH₃).

IR (ATR): 2838, 1709, 1637, 1589, 1455, 1277, 1043, 1004, 860, 696 cm⁻¹.

MS (EI) *m/z* (relative intensity): 298 (80) [M]⁺, 253 (40), 207 (60), 191 (50), 164 (45), 148 (30), 91 (100), 77 (20), 65 (20), 43 (15).

HR-MS (EI) *m/z* calcd for C₁₈H₁₈O₄, [M]⁺ 298.1205, found 298.1204.

**97aad****Benzyl-(*E*)-3-(3,6-dimethoxyphenyl)acrylate (97aad):**

The general procedure **C** was followed using 2,5-dimethoxybenzoic acid (**21aa**) (547 mg, 3.00 mmol) and benzyl acrylate (**45d**) (162 mg, 1.00 mmol). Purification by column chromatography (*n*-hexane/EtOAc: 10/1) yielded **97aad** (240 mg, 81%) as a colorless oil.

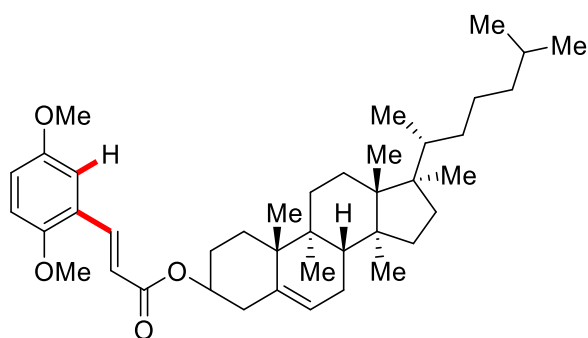
¹H-NMR (400 MHz, CDCl₃): δ = 8.02 (d, J = 16.2 Hz, 1H), 7.48–7.30 (m, 5H), 7.04 (d, J = 3.0 Hz, 1H), 6.91 (dd, J = 8.9, 3.0 Hz, 1H), 6.85 (d, J = 8.9 Hz, 1H), 6.56 (d, J = 16.2 Hz, 1H), 5.26 (s, 2H), 3.84 (s, 3H), 3.78 (s, 3H).

¹³C-NMR (101 MHz, CDCl₃): δ = 167.3 (C_q), 153.7 (C_q), 153.1 (C_q), 140.6 (CH), 136.4 (C_q), 128.7 (CH), 128.4 (CH), 128.3 (CH), 124.1 (C_q), 118.7 (CH), 117.4 (CH), 113.5 (CH), 112.6 (CH), 66.4 (CH₂), 56.2 (CH₃), 55.9 (CH₃).

IR (ATR): 2949, 2834, 1709, 1630, 1494, 1217, 1152, 860, 803, 695 cm⁻¹.

MS (EI) m/z (relative intensity): 298 (80) [M]⁺, 237 (10), 207 (25), 191 (15), 176 (20), 148 (15), 91 (100), 77 (20), 65 (15), 51 (10).

HR-MS (EI) m/z calcd for C₁₈H₁₈O₄, [M]⁺ 298.1205, found 298.1197.

**97aal****Cholesteryl-(*E*)-3-(3,6-dimethoxyphenyl)acrylate (97aal):**

The general procedure **C** was followed using 2,5-dimethoxybenzoic acid (**21aa**) (273 mg, 1.50 mmol) and cholesteryl acrylate (**451**) (202 mg, 0.50 mmol). Purification by column chromatography (*n*-hexane/EtOAc: 10/1) yielded **97aal** (280 mg, 97%) as a viscous oil.

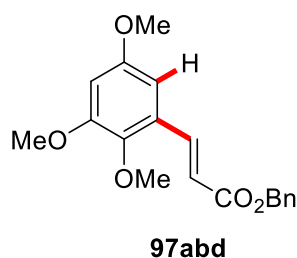
¹H-NMR (300 MHz, CDCl₃): δ = 7.93 (dd, *J* = 16.1, 0.5 Hz, 1H), 7.02 (d, *J* = 2.9 Hz, 1H), 6.88 (dd, *J* = 9.0, 2.9 Hz, 1H), 6.82 (d, *J* = 9.0 Hz, 1H), 6.46 (d, *J* = 16.1 Hz, 1H), 5.40–5.35 (d, *J* = 5.1 Hz, 1H), 4.85–4.61 (m, 1H), 3.82 (s, 3H), 3.77 (s, 3H), 2.41–2.36 (d, *J* = 8.0 Hz, 2H), 2.09–0.97 (m, 29H), 0.90 (d, *J* = 6.5 Hz, 3H), 0.85 (dd, *J* = 6.6, 1.4 Hz, 6H), 0.67 (s, 3H).

¹³C-NMR (101 MHz, CDCl₃): δ = 166.9 (C_q), 153.6 (C_q), 153.0 (C_q), 139.9 (C_q), 139.7 (CH), 124.2 (C_q), 122.8 (CH), 119.6 (CH), 117.2 (CH), 113.4 (CH), 112.6 (CH), 74.1 (CH), 56.9 (CH), 56.3 (CH), 56.2 (CH₃), 55.9 (CH₃), 50.2 (CH), 42.5 (C_q), 39.9 (CH₂), 39.7 (CH₂), 38.4 (CH₂), 37.2 (CH₂), 36.8 (C_q), 36.4 (CH₂), 36.0 (CH), 32.1 (CH₂), 32.1 (CH), 28.4 (CH₂), 28.2 (CH), 28.1 (CH₂), 24.5 (CH₂), 24.0 (CH₂), 23.0 (CH₃), 22.7 (CH₃), 21.2 (CH₂), 19.5 (CH₃), 18.9 (CH₃), 12.0 (CH₃).

IR (ATR): 2935, 2867, 1706, 1630, 1495, 1254, 1219, 1163, 1027, 800 cm⁻¹.

MS (EI) *m/z* (relative intensity): 577 (0.6) [M]⁺, 368 (30), 353 (10), 208 (100), 191 (15), 147 (10), 105 (10), 81 (10), 55 (10), 43 (20).

HR-MS (ESI) *m/z* calcd for C₃₈H₅₆O₄Na, [M+Na]⁺ 599.4071, found 599.4067.

**Benzyl-(*E*)-3-(3,5,6-trimethoxyphenyl)acrylate (97abd):**

The general procedure **C** was followed using 2,4,5-trimethoxybenzoic acid (**21ab**) (637 mg, 3.00 mmol) and benzyl acrylate (**45d**) (162 mg, 1.00 mmol). Purification by column chromatography (*n*-hexane/EtOAc: 4/1 + 5% NEt₃) yielded **97abd** (247 mg, 75%) as a colorless oil.

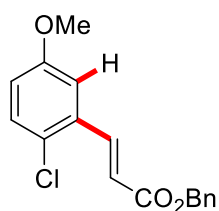
¹H-NMR (400 MHz, CDCl₃): δ = 8.03 (dd, J = 16.1, 0.6 Hz, 1H), 7.49–7.30 (m, 5H), 6.59 (d, J = 2.8 Hz, 1H), 6.54 (d, J = 2.8 Hz, 1H), 6.51 (d, J = 16.1 Hz, 1H), 5.26 (s, 2H), 3.85 (s, 3H), 3.80 (s, 3H), 3.79 (s, 3H).

¹³C-NMR (101 MHz, CDCl₃): δ = 167.0 (C_q), 156.2 (C_q), 154.0 (C_q), 143.2 (C_q), 140.1 (CH), 136.3 (C_q), 128.7 (CH), 128.4 (CH), 128.4 (CH), 128.4 (C_q), 119.3 (CH), 102.9 (CH), 101.0 (CH), 66.4 (CH₂), 61.8 (CH₃), 56.0 (CH₃), 55.7 (CH₃).

IR (ATR): 2940, 2837, 1710, 1632, 1585, 1279, 1152, 1054, 738, 696 cm⁻¹.

MS (EI) m/z (relative intensity): 328 (55) [M]⁺, 237 (30), 206 (25), 178 (10), 135 (10), 91 (100), 77 (5), 65 (10), 43 (5).

HR-MS (EI) m/z calcd for C₁₉H₂₀O₅, [M]⁺ 328.1311, found 328.1305.

**97acd****Benzyl-(*E*)-3-(2-chloro-5-methoxyphenyl)acrylate (97acd):**

The general procedure **C** was followed using 5-chloro-2-methoxybenzoic acid (**21ac**) (279 mg, 1.50 mmol) and benzyl acrylate (**45d**) (81 mg, 0.50 mmol) at 100 °C. Purification by column chromatography (*n*-hexane/EtOAc: 15/1) yielded **97acd** (122 mg, 81%) as a colorless oil.

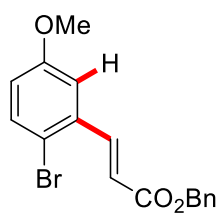
¹H-NMR (500 MHz, CDCl₃): δ = 8.10 (d, J = 16.0 Hz, 1H), 7.45–7.33 (m, 5H), 7.31 (d, J = 8.8 Hz, 1H), 7.10 (d, J = 3.0 Hz, 1H), 6.87 (dd, J = 8.8, 3.0 Hz, 1H), 6.46 (d, J = 16.0 Hz, 1H), 5.27 (s, 2H), 3.81 (s, 3H).

¹³C-NMR (126 MHz, CDCl₃): δ = 166.4 (C_q), 158.5 (C_q), 141.2 (CH), 136.0 (C_q), 133.3 (C_q), 131.0 (CH), 128.8 (CH), 128.4 (CH), 128.4 (CH), 126.8 (C_q), 120.7 (CH), 117.7 (CH), 112.2 (CH), 66.7 (CH₂), 55.7 (CH₃).

IR (ATR): 2940, 2836, 1711, 1467, 1288, 1266, 1227, 1159, 695, 451 cm⁻¹.

MS (EI) m/z (relative intensity): 302 (10) [M]⁺, 267 (20), 195 (15), 161 (10), 132 (10), 91 (100), 84 (15), 77 (10), 65 (10), 43 (35).

HR-MS (EI) m/z calcd for C₁₇H₁₅ClO₃, [M]⁺ 302.0710, found 302.0706.

**97add****Benzyl-(*E*)-3-(2-bromo-5-methoxyphenyl)acrylate (97add):**

The general procedure **C** was followed using 5-bromo-2-methoxybenzoic acid (**21ad**) (346 mg, 1.50 mmol) and benzyl acrylate (**45d**) (81 mg, 0.50 mmol) at 100 °C. Purification by column chromatography (*n*-hexane/EtOAc: 15/1) yielded **97add** (138 mg, 83%) as a colorless oil.

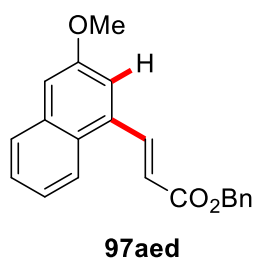
¹H-NMR (500 MHz, CDCl₃): δ = 8.04 (d, *J* = 15.9 Hz, 1H), 7.47 (d, *J* = 8.8 Hz, 1H), 7.44–7.30 (m, 5H), 7.08 (d, *J* = 3.1 Hz, 1H), 6.79 (dd, *J* = 8.8, 3.1 Hz, 1H), 6.40 (d, *J* = 15.8 Hz, 1H), 5.25 (s, 2H), 3.79 (s, 3H).

¹³C-NMR (126 MHz, CDCl₃): δ = 166.3 (C_q), 159.1 (C_q), 143.8 (CH), 136.1 (C_q), 135.2 (C_q), 134.2 (CH), 128.8 (CH), 128.5 (CH), 128.4 (CH), 120.9 (CH), 118.0 (CH), 116.2 (C_q), 112.6 (CH), 66.7 (CH₂), 55.7 (CH₃).

IR (ATR): 3031, 2937, 2836, 1710, 1463, 1287, 1225, 1159, 601, 448 cm⁻¹.

MS (EI) *m/z* (relative intensity): 348 (10) [M(⁸¹Br)⁺], 346 (10) [M(⁷⁹Br)⁺], 267 (20), 239 (5), 221 (10), 160 (15), 132 (10), 117 (5), 91 (100).

HR-MS (ESI) *m/z* calcd for C₁₇H₁₅⁷⁹BrO₃Na, [M+Na]⁺ 369.0097, found 369.0086.

**Benzyl-(*E*)-3-(2-bromo-5-methoxyphenyl)acrylate (97aed):**

The general procedure **A** was followed using 2-methoxy-3-naphtoic acid (**21ae**) (477 mg, 1.50 mmol) and benzyl acrylate (**45d**) (81 mg, 0.50 mmol). Purification by column chromatography (*n*-hexane/EtOAc: 15/1) yielded **97aed** (83 mg, 52%) as a yellow solid.

M. p. = 60-63 °C.

¹H-NMR (300 MHz, CDCl₃): δ = 8.52 (dd, *J* = 15.7, 0.6 Hz, 1H), 8.09 (d, *J* = 8.2 Hz, 1H), 7.84–7.73 (m, 1H), 7.55–7.30 (m, 8H), 7.21 (d, *J* = 2.7 Hz, 1H), 6.57 (d, *J* = 15.7 Hz, 1H), 5.32 (s, 2H), 3.94 (s, 3H).

¹³C-NMR (126 MHz, CDCl₃): δ = 166.5 (C_q), 156.9 (C_q), 141.8 (CH), 136.1 (C_q), 135.2 (C_q), 133.4 (C_q), 128.7 (CH), 128.4 (CH), 128.3 (CH), 127.6 (CH), 127.2 (C_q), 126.8 (CH), 124.6 (CH), 123.4 (CH), 121.1 (CH), 117.4 (CH), 108.8 (CH), 66.6 (CH₂), 55.6 (CH₃).

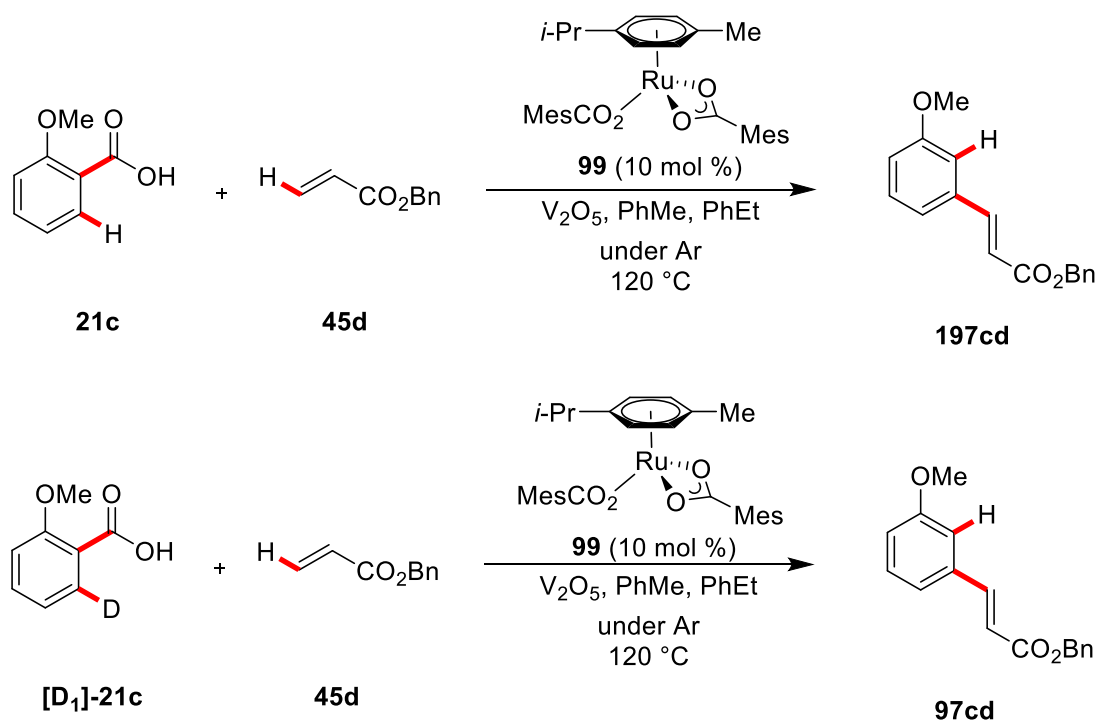
IR (ATR): 2940, 2829, 1708, 1628, 1304, 1167, 855, 730, 695, 431 cm⁻¹.

MS (EI) *m/z* (relative intensity): 318 (100) [M]⁺, 273 (10), 227 (45), 183 (55), 168 (40), 139 (40), 91 (100), 77 (15), 65 (15), 58 (10), 43 (25).

HR-MS (EI) *m/z* calcd for C₂₁H₁₈O₃, [M]⁺ 318.1256, found 318.1267.

5.3.2.2 Additional Studies for the Decarboxylative Alkenylation of Benzoic Acids

Kinetic Isotope Effect Measurement:



Two parallel reactions of benzyl acrylate (**45d**) with 2-methoxybenzoic acid (**21c**) or [D₁]-**21c** were performed to determine the KIE value by comparison of the initial rates for the formation of **97cd**. The kinetic data was determined by ¹H-NMR spectroscopy of the crude reaction mixtures using ethyl benzene as an internal standard.

2-Methoxybenzoic acid (**21c**) (228 mg, 1.50 mmol) or [D₁]-**21c** (230 mg, 1.50 mmol), [Ru(O₂CMe)₂(*p*-cymene)] (**99**) (28.1 mg, 0.05 mmol, 10.0 mol %) and V₂O₅ (91.0 mg, 0.50 mmol, 1.0 equiv) were placed in a pre-dried Schlenk-tube. The tubes were evacuated and refilled with Argon three times. PhMe (3.0 mL), benzyl acrylate (**45d**) (81.1 mg, 0.50 mmol) and ethyl benzene (53.1 mg, 0.5 mmol) were added. The reaction mixtures were heated to 120 °C and aliquots (~0.05 mL) were removed every 5 min. The aliquots were filtered over a short pad of silica (eluent: CDCl₃) and analyzed by ¹H-NMR spectroscopy. The product formation was determined by the comparison of the intensities of the methoxy-group signal of **97cd** and the aliphatic CH₃-group of ethyl benzene in the ¹H-NMR spectra (Figure 29, Table 41).

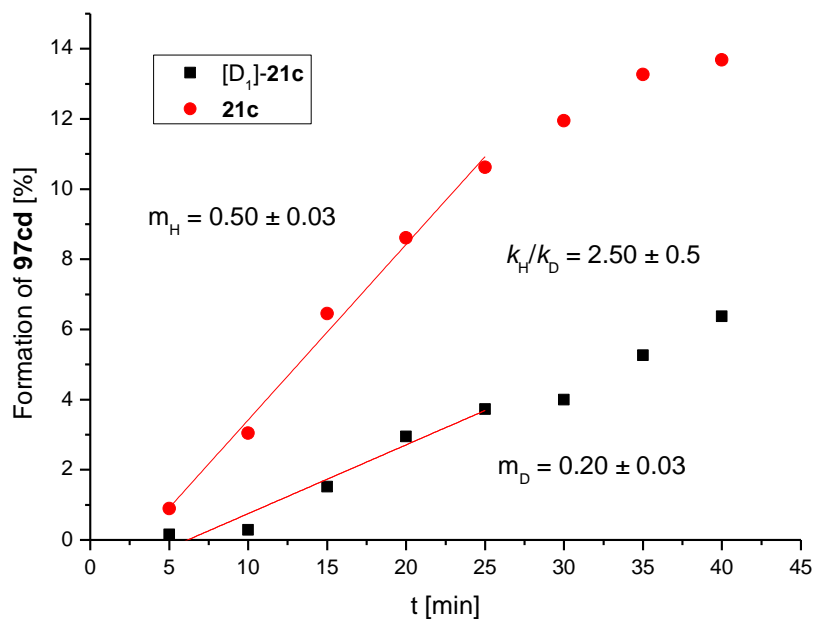
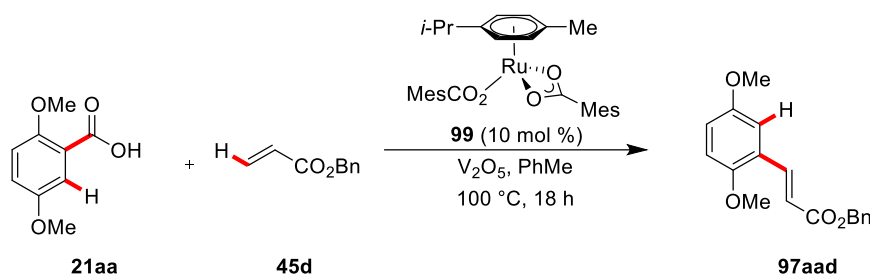


Figure 29: Graphical representation of the kinetic isotope effect measurement for the decarboxylative alkenylation.

Table 41: Data for the kinetic isotope effect measurement for the decarboxylative alkenylation.

Time [min]	Product formation with 21a [%]	Product formation with [D ₁]- 21a [%]
5	0.9	0.2
10	3.0	0.3
15	6.5	1.5
20	8.6	3.0
25	10.6	3.8
30	12.0	4.0
35	13.3	5.3
40	13.7	6.4

CO₂-Evolution Study:


2,5-Dimethoxybenzoic acid (**21a**) (405 mg, 2.25 mmol) and [Ru(O₂CMes)₂(*p*-cymene)] (**99**) (42 mg, 0.075 mmol, 10 mol %) were placed in a pre-dried 10 mL Schlenk-tube and connected over a three-way-cock to a burette with a reservoir filled with CO₂-saturated water. The flask was evacuated and refilled with Argon three times, while the three-way-cock was closed. PhMe (3.0 mL) was added and the reaction mixture was heated to 100 °C, while the three-way-cock connects the flask and the burette. After the gas equilibrium was reached, the three-way-cock was shortly opened to the atmosphere to remove unneeded gas volume and tare the water level of the burette. Then benzyl acrylate (**45d**) (122 mg, 0.75 mmol, 1.0 equiv) was added to the reaction mixture and the changes in the volume were recorded (Figure 30, Table 42). After 18 h the reaction was stopped by removal of the solvent *in vacuo*. Purification by column chromatography (*n*-hexane/EtOAc: 10/1) yielded **97aad** (181 mg, 81%) as a colorless oil.

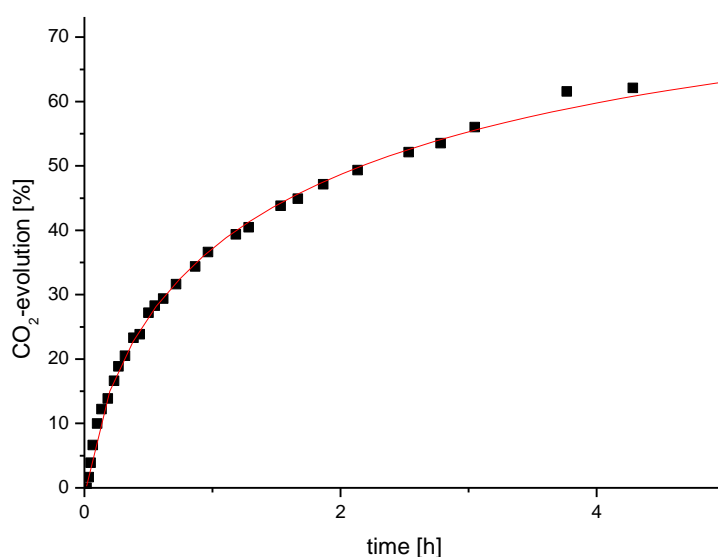


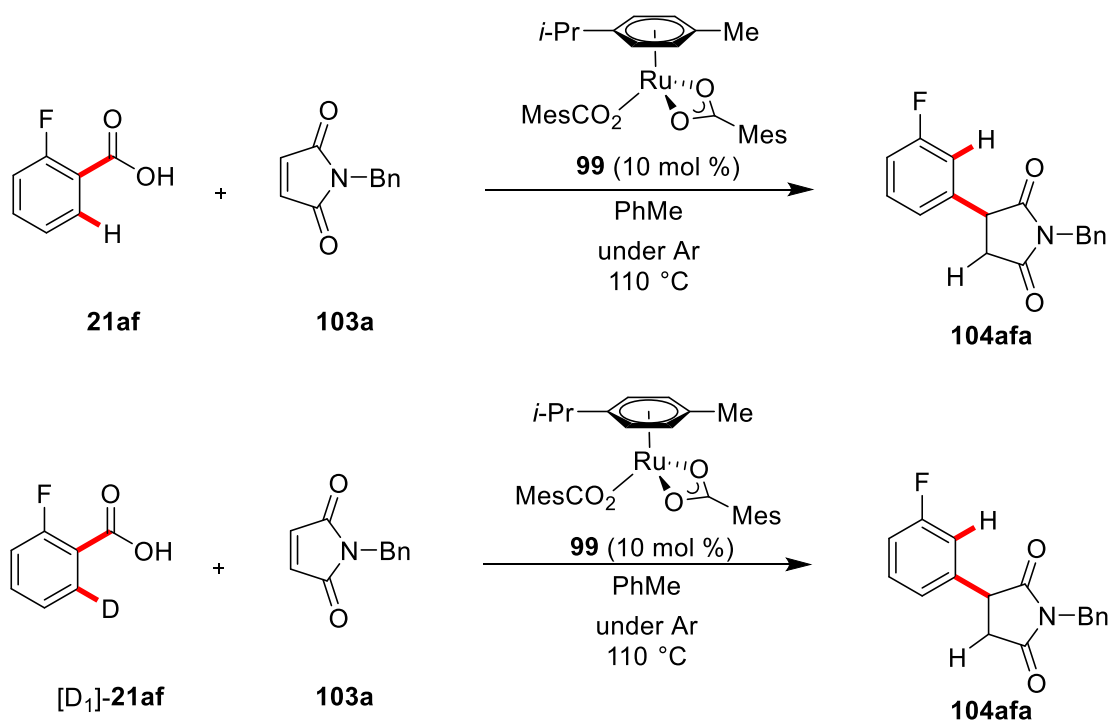
Figure 30: Graphical representation of the time dependant CO₂-evolution.

Table 42: CO₂-Evolution study for the decarboxylative alkenylation.

Time [min]	Volume[mL]	Time [min]	Volume [mL]
1	0.0	43	5.7
2	0.3	52	6.2
3	0.7	58	6.6
4	1.2	71	7.1
6	1.8	77	7.3
8	2.2	92	7.9
11	2.5	100	8.1
14	3.0	112	8.5
16	3.4	128	8.9
19	3.7	152	9.4
23	4.2	167	9.7
26	4.3	183	10.1
30	4.9	226	11.1
33	5.1	257	11.2
37	5.3	1080	13.9

5.3.2.3 Studies for the Decarboxylative Alkylation of Benzoic Acids

Kinetic Isotope Effect Measurement:



Two parallel reactions of *N*-benzyl maleimide (**103a**) with 2-fluorobenzoic acid (**21af**) or [D_1]-**21af** were performed to determine the KIE value by comparison of the initial rates for the formation of **104afa**. The kinetic data was determined by ^{19}F -NMR spectroscopy of the crude reaction mixtures using 2-fluoronaphthalene as an internal standard. The ^{19}F -NMR spectroscopic data was further confirmed GC measurement.

2-Fluorobenzoic acid (**21f**) (70 mg, 0.50 mmol) or [D_1]-**21af** (71 mg, 0.50 mmol), *N*-benzyl maleimide (**103a**) (45 mg, 0.25 mmol), 2-fluoronaphthalene (73 mg, 0.50 mmol) and $[\text{Ru}(\text{O}_2\text{CMes})_2(p\text{-cymene})]$ (**99**) (14.1 mg, 0.03 mmol, 10.0 mol %) were placed in a pre-dried Schlenk-tube. The reaction tubes were evacuated and backfilled with Ar three times. Toluene- d_8 (2.0 mL) was added, the reaction mixtures were heated to 110 $^\circ\text{C}$ and aliquots (~0.05 mL) were removed periodically. The aliquots were filtered over a short pad of silica (eluent: CDCl_3) and analyzed by ^{19}F -NMR spectroscopy. The product formation was determined, as shown in Figure 31, Table 43, by the comparison of the intensities of the product signal of **104afa** and the 2-fluoronaphthalene signal in the ^{19}F -NMR spectrum.

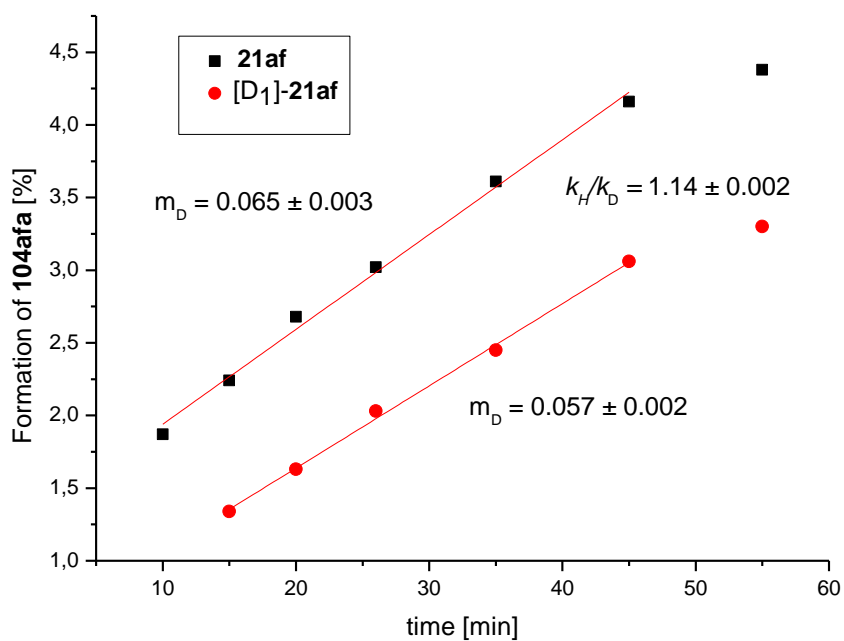
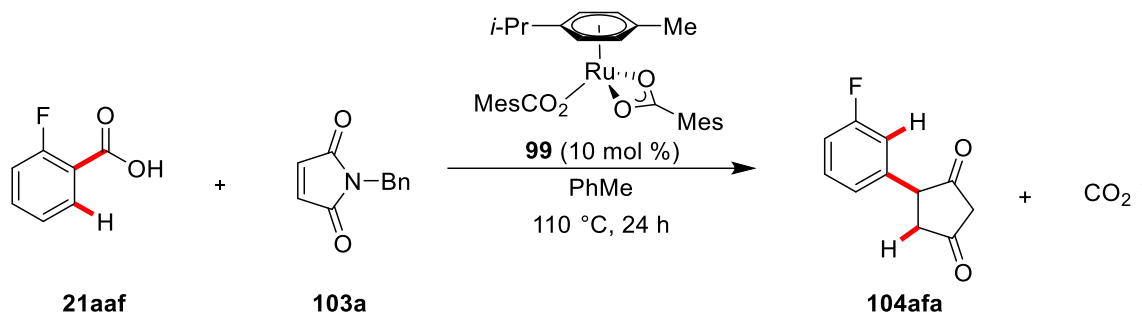


Figure 31: Graphical representation of the kinetic isotope effect measurement by ¹⁹F-NMR.

Table 43: Data for the kinetic isotope effect measurement by ¹⁹F-NMR.

t / min	Product formation with 21af [%]	Product formation with [D ₁]- 21af [%]
10	1.87	-
15	2.24	1.34
20	2.68	1.63
26	3.02	2.03
35	3.61	2.45
45	4.16	3.06
55	4.38	3.30

CO₂-Evolution Study:

2-Fluorobenzoic acid (**21af**) (280 mg, 2.0 mmol, 2.0 equiv), *N*-benzyl maleimide (**103a**) (187 mg, 1.0 mmol, 1.0 equiv) and [Ru(O₂CMes)₂(*p*-cymene)] (**99**) (56 mg, 0.1 mmol, 10 mol %) were placed in a pre-dried 10 mL Schlenk-tube and connected over a three-way-cock to a burette with a reservoir filled with CO₂-saturated water. The flask was evacuated and backfilled with Ar three times. The three-way-cock was adjusted to connect the reaction flask and the burette, the reaction flask was heated to 110 °C and PhMe (4.0 mL, CO₂ saturated, 105 °C) was added. The three-way-cock was opened shortly to the atmosphere to remove unneeded gas volume and tare the water level and the changes in the volume were recorded (Figure 32, Table 44). After 24 h the reaction mixture was poured into saturated NaHCO₃ solution and extracted with CH₂Cl₂ (3·20 mL). The combined organic layers were washed with brine (20 mL) and dried over anhydrous NaSO₄. Purification by column chromatography on silica gel (*n*-hexane/EtOAc: 4/1) yielded **104afa** (223 mg, 79%) as a colorless oil.

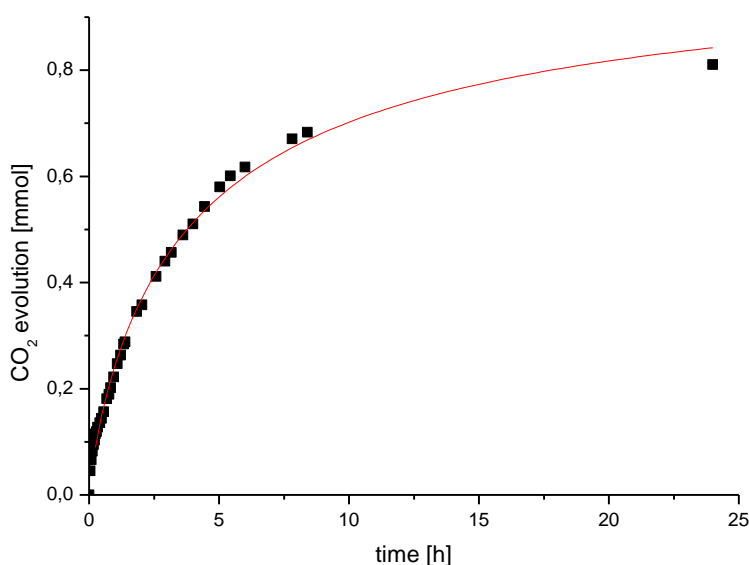
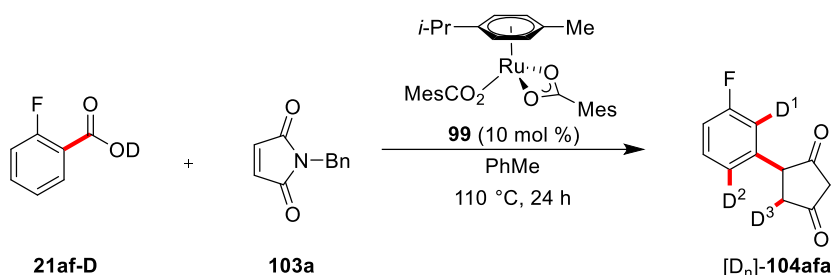


Figure 32: Graphical representation of the CO₂-evolution measurement.

Experimental Section

Table 44: Data for the CO₂-evolution study for the decarboxylatove alkylation.

<i>t</i> / min	<i>V</i> / mL	<i>t</i> / min	<i>V</i> / mL
0	0.0	73	6.4
2.5	1.1	80	6.9
5	1.6	83	7.0
7.5	2.0	110	8.4
10	2.3	122	8.7
12.5	2.5	155	10
15	2.8	175	10.7
17.5	2.9	190	11.1
20	3.1	217	11.9
25	3.3	240	12.4
29	3.5	267	13.2
34	3.8	302	14.1
41	4.4	326	14.6
46	4.6	360	15.0
50	4.9	469	16.3
57	5.4	504	16.6
65	6.0	1440	19.7

Decarboxylative Alkylation with Labeled Benzoic Acids:


2-Fluoro-deuterobenzoic acid (**21af-D**) (70 mg, 0.50 mmol, 2.0 equiv), *N*-benzyl maleimide (**45a**) (45 mg, 0.25 mmol, 1.0 equiv) and [Ru(O₂CMes)₂(*p*-cymene)] (**99**) (14.0 mg, 0.025 mmol, 10 mol %) were placed in a pre-dried pressure tube equipped with a rubber septum. The tube was evacuated and filled with N₂ or Ar three times, and then PhMe (1.0 mL) was added. The rubber septum was replaced by the pressure tube screw cap and the reaction mixture was stirred in a preheated oil bath at 110 °C for 24 h. At ambient temperature, all volatiles were removed *in vacuo* and saturated aq. NaHCO₃ solution (55 mL) was added. The resulting mixture was extracted with CH₂Cl₂ (3-45 mL). The combined organic layers were dried over Na₂SO₄, filtered and concentrated *in vacuo*. Column chromatography on silica gel (*n*-hexane/EtOAc: 4/1) and further purification by GPC yielded [D_n]-**104afa** (44mg, 62%) as a colorless oil. The deuterium incorporation was determined by ¹H-NMR spectroscopy, showing 45% deuterium in D¹-position, 38% in the D²-position and 28%/7% in D³/D^{3'}-position.

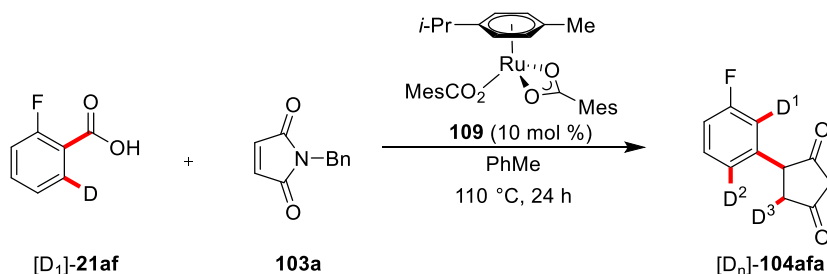
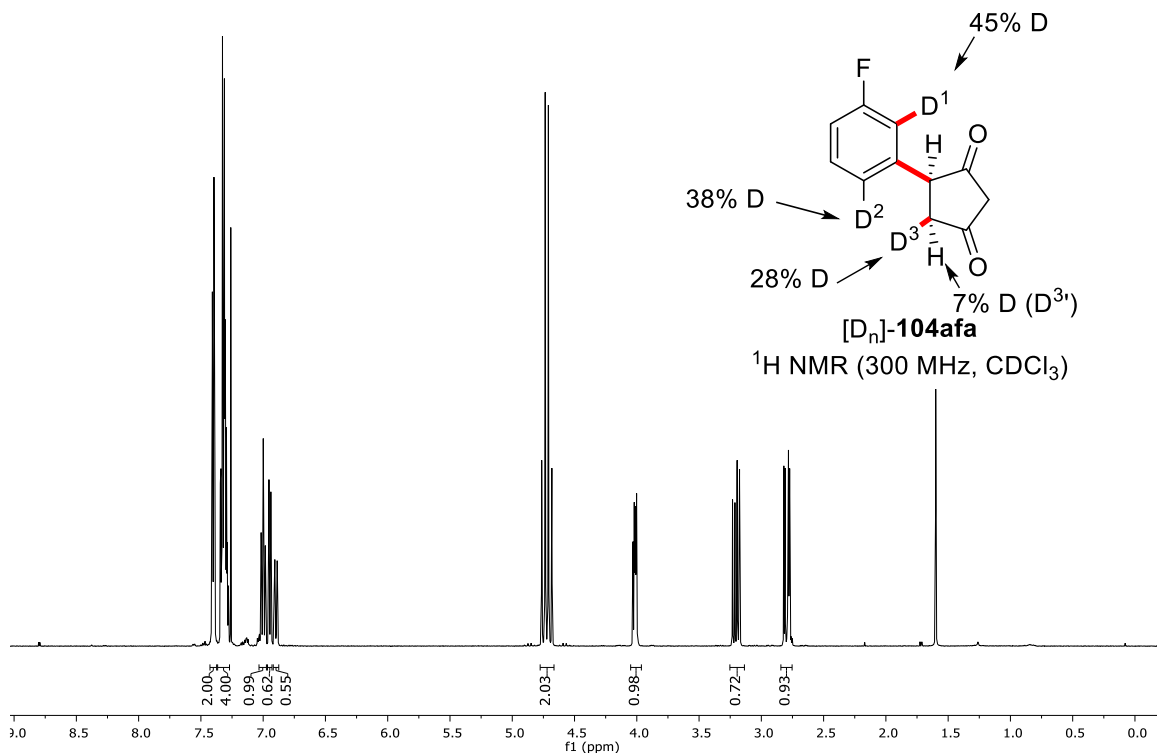
HR-MS (ESI): *m/z* calcd for C₁₇H₁₄FNO₂ [M+H]⁺ 284.1081, found 284.1080. Intensity: 60%.

m/z calcd for C₁₇H₁₃FNO₂D₁ [M+H]⁺ 285.1144, found 285.1140. Intensity: 100%.

m/z calcd for C₁₇H₁₂FNO₂D₂ [M+H]⁺ 286.1207, found 285.1196. Intensity: 72%.

m/z calcd for C₁₇H₁₁FNO₂D₃ [M+H]⁺ 287.1270, found 287.1252. Intensity: 30%.^[129]

Experimental Section



2-Fluoro-6-deuterobenzoic acid (**[D₁]-21af**) (70 mg, 0.50 mmol, 2.0 equiv), *N*-benzyl maleimide (**45a**) (45 mg, 0.25 mmol), and [Ru(O₂CMe)₂(*p*-cymene)] (**99**) (14.0 mg, 0.025 mmol, 10 mol %) were placed in a pre-dried pressure tube equipped with a rubber septum. The tube was evacuated and filled with N₂ or Ar three times and then PhMe (1.0 mL) was added. The rubber septum was replaced by the pressure tube screw cap and the reaction mixture was stirred in a preheated oil bath at 110 °C for 24 h. At ambient temperature, all volatiles were removed *in vacuo* and saturated aq. NaHCO₃ solution (55 mL) was added. The resulting mixture was extracted with CH₂Cl₂ (3 × 45 mL). The combined organic layers were dried over Na₂SO₄, filtered and concentrated *in vacuo*. Column chromatography on silica gel (*n*-hexane/EtOAc: 4/1) and further purification by GPC yielded **[D_n]-104afa** (40 mg, 56%) as a

Experimental Section

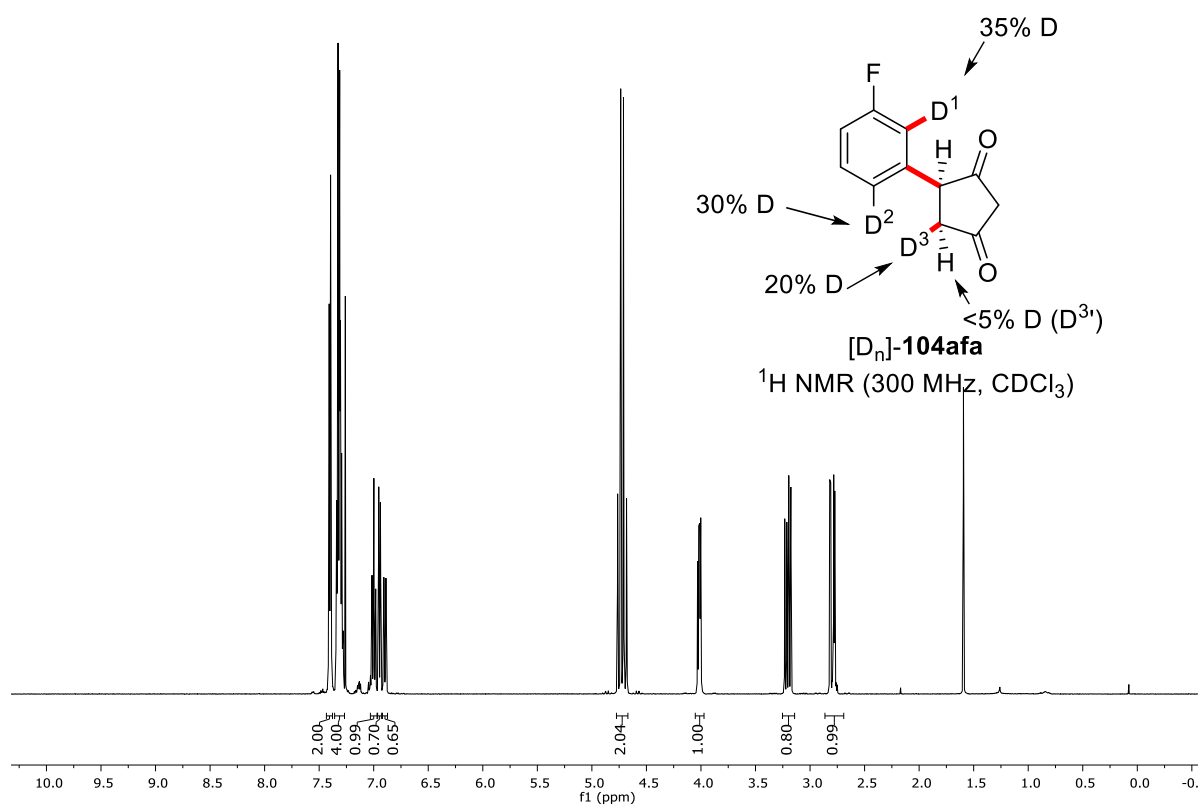
colorless oil. The deuterium incorporation was determined by ^1H -NMR spectroscopy, giving 35% deuterium in D^1 -Position, 30% in the D^2 -position and 20% in D^3 -position.

HR-MS (ESI): m/z calcd for $\text{C}_{17}\text{H}_{14}\text{FNO}_2$ $[\text{M}+\text{H}]^+$ 284.1081, found 284.1077. Intensity: 71%

m/z calcd for $\text{C}_{17}\text{H}_{13}\text{FNO}_2\text{D}_1$ $[\text{M}+\text{H}]^+$ 285.1144, found 285.1135. Intensity: 100%.

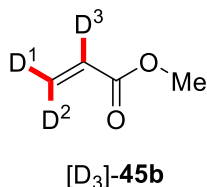
m/z calcd for $\text{C}_{17}\text{H}_{12}\text{FNO}_2\text{D}_2$ $[\text{M}+\text{H}]^+$ 286.1207, found 285.1170. Intensity: 57%.

m/z calcd for $\text{C}_{17}\text{H}_{11}\text{FNO}_2\text{D}_3$ $[\text{M}+\text{H}]^+$ 287.1270, found 287.1236. Intensity: 20%.^[129]



5.3.3 Data for the Ruthenium(II)-Catalyzed Deuteration of Acrylic Esters

5.3.3.1 Data of Deuterium Labeled Compounds



[D₃]-Methyl acrylate ([D₃]-**45b**):

a) The general procedure **E** was followed using methyl acrylate (**45b**) (86.1 mg, 1.00 mmol). After the reaction was finished, EtOAc (36.0 mg, 0.41 mmol) was added as the internal standard.

NMR conversion vs. internal standard: >95%.

Degree of Deuteration: D¹ = 95%; D² = 95%; D³ = 95%.

¹H-NMR (500 MHz, C₆D₆): δ = 6.37–6.35 (m, 0.05H), 6.11–6.08 (m, 0.05H), 5.81–5.77 (m, 0.05H), 3.73 (s, 3H).

²H-NMR (77 MHz, C₆D₆): δ = 6.41 (s, 1D), 6.14 (s, 1D), 5.84 (s, 1D).

¹³C-NMR (126 MHz, C₆D₆): δ = 166.8 (C_q), 130.16 (p, *J* = 24.6 Hz, CD₂), 127.83 (t, *J* = 25.3 Hz, CD), 51.7 (CH₃).

[D₃]-**45b** was not detectable *via* ESI-MS.

b) [RuCl₂(*p*-cymene)]₂ (**30**) (67.6 mg, 0.11 mmol, 0.2 mol %), *m*-CF₃-benzoic acid (104.9 mg, 0.55 mmol, 1.0 mol %) and potassium *m*-CF₃-benzoate (125.9 mg, 0.55 mmol, 1.0 mol %) were placed in a pre-dried 25 mL Schlenk-tube equipped with a rubber septum. The tube was evacuated and refilled with Ar three times. Methyl acrylate (**45b**) (4.75 g, 55.0 mmol, 1.0 equiv) was added and the mixture was stirred for 5 min, before D₂O (4.5 mL, 248.0 mmol, 4.5 equiv) was added and the mixture was heated to 80°C for 18 h. At ambient temperature a second Schlenk-tube was connected, cooled with liquid N₂ and passive vacuum (100–300 mbar) was applied until deuterated methyl acrylate was condensed to the second flask (4.31 g, 48.4 mmol, 88%).

Degree of Deuteration: D¹ = 75%; D² = 75%; D³ = 75%.



[D₃]-**45c**

[D₃]-Ethyl acrylate ([D₃]-45c):

The general procedure **E** was followed using ethyl acrylate (**45c**) (100 mg, 1.00 mmol) After the reaction was finished, CH₂Cl₂ (19.7 mg, 0.23 mmol) was added as the internal standard.

NMR conversion vs. internal standard: >95%.

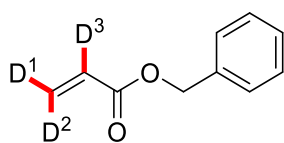
Degree of Deuteration: D¹ = 96%; D² = 96%; D³ = 96%.

¹H-NMR (500 MHz, C₆D₆): δ = 6.30–6.24 (m, 0.04H), 5.99–5.94 (m, 0.04H), 5.26–5.22 (m, 0.04H), 3.96 (q, *J* = 7.1 Hz, 1H), 0.93 (t, *J* = 7.2 Hz, 1H).

²H-NMR (77 MHz, C₆D₆): δ = 6.27 (s, 1D), 5.95 (s, 1D), 5.23 (s, 1D).

¹³C-NMR (126 MHz, C₆D₆): δ = 165.7 (C_q), 129.27 (p, *J* = 24.8 Hz, CD₂), 128.43 (t, *J* = 25.1 Hz, CD), 60.2 (CH₂), 14.1 (CH₃).

[D₃]-**2c** was not detectable *via* ESI-MS.



[D₃]-**45d**

[D₃]-Benzyl acrylate ([D₃]-45d):

The general procedure **D** was followed using benzyl acrylate (**45d**) (162 mg, 1.00 mmol). After the reaction was finished, C₆F₅H (16.8 mg, 0.10 mmol) was added as the internal standard.

NMR conversion vs. internal standard: 90%.

Degree of Deuteration: D¹ = 96%; D² = 96%; D³ = 96%

Experimental Section

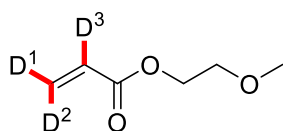
^1H NMR (500 MHz, Chloroform-*d*): δ = 7.43 – 7.30 (m, 5H), 6.50 – 6.35 (m, 0.04 H), 6.23 – 6.15 (m, 0.04 H), 5.88 – 5.82 (m, 0.04 H), 5.22 (s, 2H).

^2H NMR (77 MHz, Chloroform-*d*): δ = 6.50 (s, 1D), 6.22 (s, 1D), 5.89 (s, 1D).

^{13}C NMR (126 MHz, Chloroform-*d*): δ = 166.1 (C_q), 135.9(C_q), 130.5 (p, J = 24.6 Hz, CD₂), 128.6 (CH), 128.3 (CH), 128.3 (CH), 127.9 (t, J = 24.5 Hz, CD), 66.4 (CH₂).

HR-MS (ESI) m/z calcd for C₁₀H₇O₂D₃Na, [M+Na]⁺ 188.0761, found 188.0765; Intensity: 100%

HR-MS (ESI) m/z calcd for C₁₀H₈O₂D₂Na, [M+Na]⁺ 187.0699, found 187.0703; Intensity: 10%.^[129]



[D₃]-45g

[D₃]-2-Methoxyethyl acrylate ([D₃]-45g):

The general procedure **D** was followed using 2-methoxyethyl acrylate (**45g**) (130 mg, 1.00 mmol). After the reaction was finished, C₆F₅H (22.8 mg, 0.14 mmol) was added as the internal standard.

NMR conversion vs. internal standard: 75%.

Degree of Deuteration: D¹ = 95%; D² = 95%; D³ = 95%.

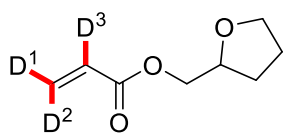
^1H -NMR (500 MHz, CDCl₃): δ = 6.47–6.34 (m, 0.05H), 6.18–6.09 (m, 0.05H), 5.87–5.75 (m, 0.05H), 4.38–4.22 (m, 2H), 3.69–3.56 (m, 2H), 3.38 (s, 3H).

^2H -NMR (77 MHz, CDCl₃): δ = 6.44 (s, 1D), 6.18 (s, 1D), 5.85 (s, 1D).

^{13}C -NMR (126 MHz, CDCl₃) δ = 166.3 (C_q), 130.5 (p, J = 24.6 Hz, CD₂), 127.8 (t, J = 25.3 Hz, CD), 70.5 (CH₂), 63.7 (CH₂), 59.1 (CH₃).

HR-MS (ESI) m/z calcd for C₆H₇O₃D₃Na, [M+Na]⁺ 156.0710, found 156.0709; Intensity: 100%.

HR-MS (ESI) m/z calcd for C₆H₈O₃D₂Na, [M+Na]⁺ 155.0648, found 155.0645; Intensity: 15%.^[129]



[D₃]-45h

[D₃]-Tetrahydrofurfuryl acrylate ([D₃]-45h):

The general procedure **D** was followed using tetrahydrofurfuryl acrylate (**45h**) (156 mg, 1.00 mmol). After the reaction was finished, C₆F₅H (17.0 mg, 0.10 mmol) was added as the internal standard.

NMR conversion vs. internal standard: 91%.

Degree of Deuteration: D¹ = 95%; D² = 95%; D³ = 94%.

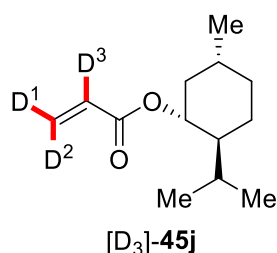
¹H-NMR (500 MHz, CDCl₃): δ = 6.41–6.37 (m, 0.05H), 6.15–6.10 (m, 0.06H), 5.83–5.78 (m, 0.05H), 4.22 (dd, *J* = 11.3, 3.5 Hz, 1H), 4.15 (qd, *J* = 7.0, 3.5 Hz, 1H), 4.07 (dd, *J* = 11.3, 6.8 Hz, 1H), 3.88 (dt, *J* = 8.3, 6.7 Hz, 1H), 3.79 (ddd, *J* = 8.3, 7.3, 6.1 Hz, 1H), 2.00 (dddd, *J* = 12.1, 8.4, 7.0, 5.3 Hz, 1H), 1.94–1.83 (m, 2H), 1.61 (ddt, *J* = 12.1, 8.4, 7.1 Hz, 1H).

²H-NMR (77 MHz, CDCl₃): δ = 6.44 (s, 1D), 6.18 (s, 1D), 5.85 (s, 1D).

¹³C-NMR (126 MHz, CDCl₃): δ = 166.3 (C_q), 130.5 (p, *J* = 24.6 Hz, CD₂), 127.8 (t, *J* = 25.2 Hz, CD), 76.6 (CH), 68.6 (CH₂), 66.6 (CH₂), 28.1 (CH₂), 25.8 (CH₂).

HR-MS (ESI) *m/z* calcd for C₈H₉O₃D₃Na, [M+Na]⁺ 182.0867, found 182.0869; Intensity: 100%.

HR-MS (ESI) *m/z* calcd for C₈H₁₀O₃D₂Na, [M+Na]⁺ 181.0804, found 181.0803; Intensity: 15%.^[129]



[D₃]-(-)-Menthyl acrylate ([D₃]- 45j):

The general procedure **D** was followed using (-)-menthyl acrylate (**45a**) (201 mg, 1.00 mmol). After the reaction was finished, C₆F₅H (20.3 mg, 0.12 mmol) was added as the internal standard.

NMR conversion vs. internal standard: >95%.

Degree of Deuteration: D¹ = 98%; D² = 98%; D³ = 98%.

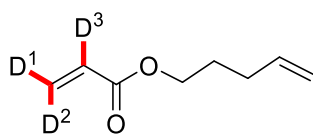
¹H-NMR (500 MHz, CDCl₃): δ = 6.36–6.34 (m, 0.02H), 6.11–6.06 (m, 0.02H), 5.80–5.76 (m, 0.02H), 4.76 (td, *J* = 10.9, 4.5 Hz, 1H), 2.05–1.99 (m, 1H), 1.87 (pd, *J* = 7.0, 2.7 Hz, 1H), 1.72–1.64 (m, 2H), 1.56–1.45 (m, 1H), 1.41 (ddt, *J* = 12.4, 10.8, 3.3 Hz, 1H), 1.04 (dtd, *J* = 36.7, 12.6, 10.4 Hz, 3H), 0.89 (t, *J* = 7.0 Hz, 6H), 0.76 (d, *J* = 7.0 Hz, 3H).

²H-NMR (77 MHz, CDCl₃): δ = 6.30 (s, 1D), 6.06 (s, 1D), 5.73 (s, 1D).

¹³C-NMR (126 MHz, CDCl₃): δ = 166.0 (C_q), 129.7 (p, *J* = 24.4 Hz, CD₂), 128.70 (t, *J* = 25.1 Hz, CD), 74.4 (CH), 47.2 (CH), 41.0 (CH₂), 34.4 (CH₂), 31.5 (CH), 26.5 (CH), 23.7 (CH₂), 22.2 (CH₃), 20.9 (CH₃), 16.6 (CH₃).

HR-MS (ESI) *m/z* calcd for C₁₃H₁₉O₂D₃Na, [M+Na]⁺ 236.1700, found 236.1700; Intensity: 100%.

HR-MS (ESI) *m/z* calcd for C₁₃H₂₀O₂D₂Na, [M+Na]⁺ 235.1638, found 235.1629; Intensity: 10%.^[129]

[D₃]-45k**[D₃]-Pent-4-enyl acrylate ([D₃]-45k):**

The general procedure **E** was followed using pent-4-enyl acrylate (**45k**) (193 mg, 1.00 mmol). After the reaction was finished, CH₂Cl₂ (21.1 mg, 0.25 mmol) was added as the internal standard.

NMR conversion vs. internal standard: >95%.

Degree of Deuteration: D¹ = 96%; D² = 96%; D³ = 96%.

¹H-NMR (500 MHz, C₆D₆): δ = 6.29–6.25 (m, 0.04H), 5.98–5.95 (m, 0.04H), 5.66–5.54 (m, 1H), 5.28–5.20 (m, 0.04H), 5.00–4.83 (m, 2H), 3.99 (t, *J* = 6.7 Hz, 2H), 1.87 (tdt, *J* = 7.9, 6.7, 1.4 Hz, 2H), 1.46 (ddt, *J* = 8.4, 7.5, 6.7 Hz, 2H).

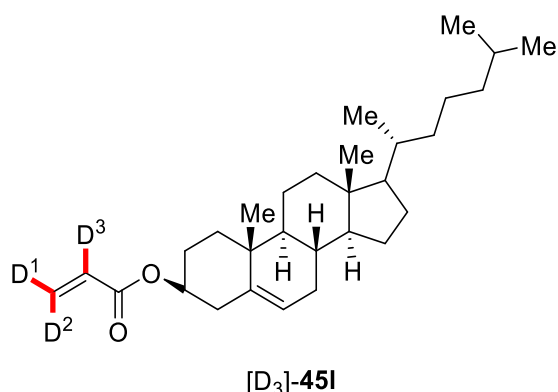
²H-NMR (77 MHz, C₆D₆): δ = 6.26 (s, 1D), 5.95 (s, 1D, partly overlaid by C₆D₆ spinning side-band), 5.25 (s, 1D).

¹³C-NMR (126 MHz, C₆D₆): δ = 165.8 (C_q), 137.7 (CH), 129.4 (p, *J* = 24.5 Hz, CD₂), 128.1 (t, *J* = 24.4 Hz, CD, overlapped by C₆D₆ signal), 115.3 (CH₂), 63.9 (CH₂), 30.3 (CH₂), 28.1 (CH₂).

HR-MS (ESI) *m/z* calcd for C₈H₉O₂D₄Na, [M+Na]⁺ 167.0981, found 167.0963; Intensity: 20%.

HR-MS (ESI) *m/z* calcd for C₈H₉O₂D₃Na, [M+Na]⁺ 166.0918, found 166.0913; Intensity: 100%.

HR-MS (ESI) *m/z* calcd for C₈H₁₀O₂D₂Na, [M+Na]⁺ 165.0855, found 165.0850; Intensity: 20%.^[129]



[D₃]-Cholesteryl acrylate ([D₃]-451):

The general procedure **E** was followed using cholesteryl acrylate (**451**) (440 mg, 1.00 mmol). After the reaction was finished, CH₂Cl₂ (19.9 mg, 0.24 mmol) was added as the internal standard.

NMR conversion vs. internal standard: >95%.

Degree of Deuteration: D¹ = 99%; D² = 99%; D³ = 98%.

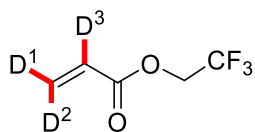
¹H-NMR (500 MHz, C₆D₆): δ = 7.08–6.97 (m, 0.01H), 6.36–6.30 (m, 0.02H), 6.09–6.00 (m, 0.01H), 5.36–5.29 (m, 1H), 4.86 (tt, *J* = 11.4, 4.9 Hz, 1H), 2.46 (ddd, *J* = 13.2, 5.1, 2.3 Hz, 1H), 2.38 (ddt, *J* = 13.4, 10.1, 2.3 Hz, 1H), 1.99 (dt, *J* = 12.5, 3.5 Hz, 1H), 1.93–1.78 (m, 3H), 1.69–0.85 (m, 23H), 0.99 (d, *J* = 6.7 Hz, 3H), 0.93 (d, *J* = 1.7 Hz, 3H), 0.91 (d, *J* = 1.7 Hz, 6H), 0.65 (s, 3H).

²H-NMR (77 MHz, C₆D₆): δ = 6.95 (s, 1D, partly overlaid by C₆D₆ spinning side-band), 6.32 (s, 1D), 6.02 (s, 1D).

¹³C-NMR (126 MHz, C₆D₆): δ = 165.2 (C_q), 139.8 (C_q), 129.01 (t, *J* = 24.6 Hz, CD), 128.41–127.70 (m, CD₂, overlapped by C₆D₆ signal), 123.0 (CH), 74.2 (CH), 57.0 (CH), 56.6 (CH), 50.4 (CH), 42.6 (C_q), 40.2 (CH₂), 40.0 (CH₂), 38.7 (CH₂), 37.3 (CH₂), 36.9 (C_q), 36.7 (CH₂), 36.3 (CH), 32.3 (CH₂), 32.2 (CH), 28.7 (CH₂), 28.5 (CH), 28.3 (CH₂), 24.7 (CH₂), 24.5 (CH₂), 23.1 (CH₃), 22.9 (CH₃), 21.4 (CH₂), 19.5 (CH₃), 19.1 (CH₃), 12.2 (CH₃).

HR-MS (ESI) *m/z* calcd for C₃₀H₄₅O₂D₃Na, [M+Na]⁺ 466.3765, found 466.3718; Intensity: 100%.

HR-MS (ESI) *m/z* calcd for C₃₀H₄₆O₂D₂Na, [M+Na]⁺ 465.3672, found 465.3658; Intensity: 10%.^[129]



[D₃]-45m

[D₃]-2,2,2-Trifluoroethyl acrylate ([D₃]-45m):

The general procedure **D** was followed using 2,2,2-trifluoroethyl acrylate (**45m**) (154 mg, 1.00 mmol). After the reaction was finished, CH₂Cl₂ (27.1 mg, 0.32 mmol) was added as the internal standard.

NMR conversion vs. internal standard: >95%.

Degree of Deuteration: D¹ = 96%; D² = 96%; D³ = 94%.

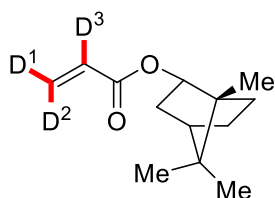
¹H-NMR (500 MHz, CDCl₃): δ = 6.52–6.49 (m, 0.04H), 6.19–6.16 (m, 0.06H), 5.97–5.95 (m, 0.04H), 4.54 (q, *J* = 8.4 Hz, 2H).

²H-NMR (77 MHz, CDCl₃): δ = 6.55 (s, 1D), 6.22 (s, 1D), 6.01 (s, 1D).

¹³C-NMR (126 MHz, CDCl₃): δ = 164.3 (C_q), 132.5 (p, *J* = 24.6 Hz, CD₂), 126.2 (t, *J* = 25.4 Hz, CD₂), 122.94 (q, *J* = 277.2 Hz, CF₃), 60.35 (q, *J* = 36.9 Hz, CH₂).

¹⁹F-NMR (376 MHz, CDCl₃): δ = -73.86 (t, *J* = 8.2 Hz).

[D₃]-**2m** was not detectable *via* ESI-MS.



[D₃]-45n

[D₃]-(-)-Bornyl acrylate ([D₃]-45n):

The general procedure **D** was followed using (-)-bornyl acrylate (**45n**) (193 mg, 1.00 mmol). After the reaction was finished, C₆F₅H (35.4 mg, 0.21 mmol) was added as the internal standard.

NMR conversion vs. internal standard: >95%.

Degree of Deuteration: $D^1 = 97\%$; $D^2 = 97\%$; $D^3 = 97\%$.

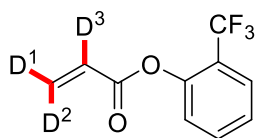
$^1\text{H-NMR}$ (500 MHz, CDCl_3): $\delta = 6.38\text{--}6.33$ (m, 0.03H), 6.14–6.10 (m, 0.03H), 5.79–5.76 (m, 0.03H), 4.95 (ddd, $J = 9.9, 3.5, 2.2$ Hz, 1H), 2.37 (dddd, $J = 13.5, 9.9, 4.8, 3.3$ Hz, 1H), 1.97 (ddd, $J = 12.6, 9.4, 4.5$ Hz, 1H), 1.75 (ttt, $J = 12.2, 4.6, 3.0$ Hz, 1H), 1.68 (t, $J = 4.5$ Hz, 1H), 1.36–1.19 (m, 2H), 1.00 (dd, $J = 13.7, 3.6$ Hz, 1H), 0.91 (s, 3H), 0.87 (s, 3H), 0.84 (s, 3H).

$^2\text{H-NMR}$ (77 MHz, CDCl_3): $\delta = 6.40$ (s, 1D), 6.16 (s, 1D), 5.83 (s, 1D).

$^{13}\text{C-NMR}$ (126 MHz, CDCl_3): $\delta = 166.7$ (C_q), 129.5 (p, $J = 24.5$ Hz), 128.7 (t, $J = 25.3$ Hz), 80.1 (CH), 49.0 (C_q), 47.9 (C_q), 45.0 (CH), 36.9 (CH_2), 28.1 (CH_2), 27.3 (CH_2), 19.8 (CH_3), 19.0 (CH_3), 13.6 (CH_3).

HR-MS (ESI) m/z calcd for $\text{C}_{13}\text{H}_{17}\text{O}_2\text{D}_3\text{Na}$, $[\text{M}+\text{Na}]^+$ 234.1544, found 234.1546; Intensity: 100%.

HR-MS (ESI) m/z calcd for $\text{C}_{13}\text{H}_{18}\text{O}_2\text{D}_2\text{Na}$, $[\text{M}+\text{Na}]^+$ 233.1481, found 233.1482; Intensity: 10%.^[129]



[D₃]-45o

[D₃]-2-Trifluorophenyl acrylate ([D₃]-45o):

The general procedure **D** was followed using 2-trifluoromethylphenyl acrylate (**45o**). After the reaction was finished, $\text{C}_6\text{F}_5\text{H}$ (22.1 mg, 0.13 mmol) was added as the internal standard.

NMR conversion vs. internal standard: >95%.

Degree of Deuteration: $D^1 = 95\%$; $D^2 = 95\%$; $D^3 = 84\%$

$^1\text{H-NMR}$ (500 MHz, CDCl_3): $\delta = 7.69$ (dd, $J = 7.8, 2.0$ Hz, 1H), 7.59 (ddd, $J = 7.8, 7.8, 1.8$ Hz, 1H), 7.35 (ddd, $J = 8.7, 7.2, 1.0$ Hz, 1H), 7.30 (d, $J = 8.1$ Hz, 1H), 6.68–6.61 (m, 0.05H), 6.38–6.30 (m, 0.16H), 6.10–6.04 (m, 0.05H).

Experimental Section

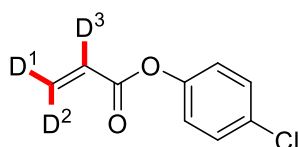
^2H -NMR (77 MHz, CDCl_3): $\delta = 6.66$ (s, 1D), 6.35 (s, 1D), 6.09 (s, 1D).

^{13}C -NMR (126 MHz, CDCl_3): $\delta = 163.8$ (C_q), 148.0 (q, $J = 2.1$ Hz, C_q), 133.0 (CH), 132.9 (p, $J = 25.1$ Hz, CD_2), 126.9 (q, $J = 4.9$ Hz, CH), 126.5 (t, $J = 25.5$ Hz, CD), 125.9 (CH), 124.2 (CH), 122.9 (q, $J = 277.7$ Hz, CF_3), 122.9 (q, $J = 31.7$ Hz, C_q).

^{19}F -NMR (283 MHz, CDCl_3): $\delta = -61.90$.

HR-MS (ESI) m/z calcd for $\text{C}_{10}\text{H}_4\text{O}_2\text{D}_3\text{F}_3\text{Na}$, $[\text{M}+\text{Na}]^+$ 242.0479, found 242.0480; Intensity: 100%.

HR-MS (ESI) m/z calcd for $\text{C}_{10}\text{H}_5\text{O}_2\text{D}_2\text{F}_3\text{Na}$, $[\text{M}+\text{Na}]^+$ 241.0416, found 241.0409; Intensity: 25%.^[129]



[D₃]-45p

[D₃]-4-Chlorophenyl acrylate ([D₃]-45p):

The general procedure **D** was followed using 4-chlorophenyl acrylate (**45p**) (182 mg, 1.00 mmol). After the reaction was finished, EtOAc (22.1 mg, 0.25 mmol) was added as the internal standard.

NMR conversion vs. internal standard: 80%.

Degree of Deuteration: $\text{D}^1 = 96\%$; $\text{D}^2 = 96\%$; $\text{D}^3 = 96\%$

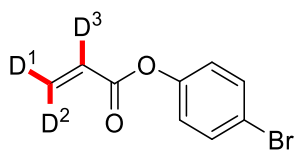
^1H -NMR (500 MHz, CDCl_3): $\delta = 7.37$ – 7.33 (m, 2H), 7.11– 7.04 (m, 2H), 6.61– 6.56 (m, 0.04H), 6.31– 6.27 (m, 0.04H), 6.03– 5.99 (m, 0.04H).

^2H -NMR (77 MHz, CDCl_3): $\delta = 6.63$ (s, 1D), 6.34 (s, 1D), 6.06 (s, 1D).

^{13}C -NMR (126 MHz, CDCl_3): $\delta = 164.5$ (C_q), 149.1 (C_q), 132.47 (p, $J = 24.7$ Hz), 129.6 (CH), 127.22 (t, $J = 25.5$ Hz), 123.0 (CH), 116.7 (C_q).

HR-MS (ESI) m/z calcd for $\text{C}_9\text{H}_4\text{O}_2\text{D}_3\text{ClNa}$, $[\text{M}+\text{Na}]^+$ 208.0215, found 208.0218; Intensity: 100%.

HR-MS (ESI) m/z calcd for $\text{C}_9\text{H}_5\text{O}_2\text{D}_2\text{ClNa}$, $[\text{M}+\text{Na}]^+$ 241.0152, found 207.0128; Intensity: 10%.^[129]



[D₃]-45q

[D₃]-4-Bromophenyl acrylate ([D₃]-45q):

The general procedure **D** was followed using 4-bromophenyl acrylate (**45q**) (226 mg, 1.00 mmol). After the reaction was finished, EtOAc (20.7 mg, 0.24 mmol) was added as the internal standard.

NMR conversion vs. internal standard: >95%.

Degree of Deuteration: D¹ = 95%; D² = 95%; D³ = 95%

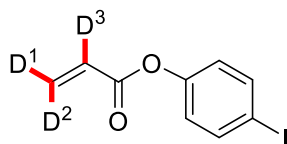
¹H-NMR (500 MHz, CDCl₃): δ = 7.52–7.47 (m, 2H), 7.06–7.00 (m, 2H), 6.61–6.55 (m, 0.05H), 6.34–6.26 (m, 0.05H), 6.04–5.96 (m, 0.05H).

²H-NMR (77 MHz, CDCl₃): δ = 6.63 (s, 1D), 6.34 (s, 1D), 6.06 (s, 1D).

¹³C-NMR (126 MHz, CDCl₃): δ = 164.2 (C_q), 149.5 (C_q), 132.4 (C_q), 132.3 (p, *J* = 24.5 Hz, CD₂), 127.0 (t, *J* = 25.1 Hz), 123.3 (CH), 118.9 (CH).

HR-MS (ESI) *m/z* calcd for C₉H₄O₂D₃⁷⁹BrNa, [M+Na]⁺ 251.9710, found 251.9707; Intensity: 100%.

HR-MS (ESI) *m/z* calcd for C₉H₅O₂D₂⁷⁹BrNa, [M+Na]⁺ 250.9647, found 250.9662; Intensity: 15%.^[129]



[D₃]-45r

[D₃]-4-Iodophenyl acrylate ([D₃]-45r):

The general procedure **D** was followed using 4-iodophenyl acrylate (**45r**) (273 mg, 1.00 mmol). After the reaction was finished, EtOAc (31.7 mg, 0.36 mmol) was added as the internal standard.

NMR conversion vs. internal standard: 85%.

Degree of Deuteration: $D^1 = 92\%$; $D^2 = 92\%$; $D^3 = 92\%$

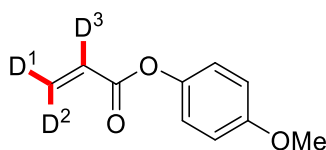
$^1\text{H-NMR}$ (500 MHz, CDCl_3): $\delta = 7.75\text{--}7.66$ (m, 2H), 6.94–6.88 (m, 2H), 6.60–6.57 (m, 0.08H), 6.32–6.27 (m, 0.08H), 6.03–5.99 (m, 0.08H).

$^2\text{H-NMR}$ (77 MHz, CDCl_3): $\delta = 6.63$ (s, 1D), 6.33 (s, 1D), 6.06 (s, 1D).

$^{13}\text{C-NMR}$ (126 MHz, CDCl_3): $\delta = 164.3$ (C_q), 150.5 (C_q), 138.6 (CH), 132.5 (p, $J = 24.7$ Hz), 127.2 (t, $J = 25.6$ Hz), 123.9 (CH), 90.0 (C_q).

HR-MS (ESI) m/z calcd for $\text{C}_9\text{H}_4\text{O}_2\text{D}_3\text{INa}$, $[\text{M}+\text{Na}]^+$ 299.9571, found 299.9570; Intensity: 100.

HR-MS (ESI) m/z calcd for $\text{C}_9\text{H}_5\text{O}_2\text{D}_2\text{INa}$, $[\text{M}+\text{Na}]^+$ 298.9508, found 298.9486; Intensity: 15%.^[129]



[D₃]-45s

[D₃]-4-Methoxyphenyl acrylate ([D₃]-45s):

The general procedure **D** was followed using 4-methoxyphenyl acrylate (**45s**) (178 mg, 1.00 mmol). After the reaction was finished, EtOAc (20.9 mg, 0.24 mmol) was added as the internal standard.

NMR conversion vs. internal standard: >95%.

Degree of Deuteration: $D^1 = 97\%$; $D^2 = 97\%$; $D^3 = 97\%$

$^1\text{H-NMR}$ (500 MHz, CDCl_3): $\delta = 7.05$ (d, $J = 9.2$ Hz, 2H), 6.90 (d, $J = 9.2$ Hz, 2H), 6.59–6.53 (m, 0.03H), 6.32–6.28 (m, 0.03H), 6.01–5.95 (m, 0.03H), 3.80 (s, 3H).

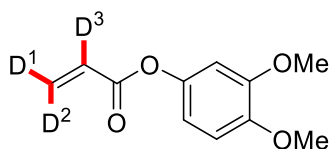
$^2\text{H-NMR}$ (77 MHz, CDCl_3): $\delta = 6.61$ (s, 1D), 6.34 (s, 1D), 6.02 (s, 1D).

$^{13}\text{C-NMR}$ (126 MHz, CDCl_3): $\delta = 165.1$ (C_q), 157.4 (C_q), 144.1 (C_q), 131.8 (p, $J = 24.7$ Hz, CD_2), 127.6 (t, $J = 25.3$ Hz, CD), 122.4 (CH), 114.5 (CH), 55.7 (CH_3).

Experimental Section

HR-MS (ESI) m/z calcd for $C_{10}H_7O_3D_3Na$, $[M+Na]^+$ 204.0710, found 204.0713; Intensity: 100%.

HR-MS (ESI) m/z calcd for $C_{10}H_8O_3D_2Na$, $[M+Na]^+$ 203.0648, found 203.0648; Intensity: 10%.^[129]



[D₃]-45t

[D₃]-3,4-Dimethoxyphenyl acrylate ([D₃]-45t):

The general procedure **D** was followed using 3,4-dimethoxyphenyl acrylate (**45t**) (208 mg, 1.00 mmol). After the reaction was finished, EtOAc (17.8 mg, 0.20 mmol) was added as the internal standard.

NMR conversion vs. internal standard: >95%.

Degree of Deuteration: D¹ = 94%; D² = 94%; D³ = 94%

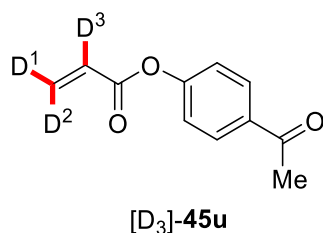
¹H-NMR (500 MHz, CDCl₃): δ = 6.84–6.80 (m, 1H), 6.68–6.64 (m, 2H), 6.55–6.53 (m, 0.06H), 6.29–6.24 (m, 0.06H), 5.98–5.93 (m, 0.06H), 3.84 (s, 3H), 3.83 (s, 3H).

²H-NMR (77 MHz, CDCl₃): δ = 6.57 (s, 1D), 6.29 (s, 1D), 5.98 (s, 1D).

¹³C-NMR (126 MHz, CDCl₃): δ = 164.9 (C_q), 149.4 (C_q), 146.9 (C_q), 144.2 (C_q), 131.8 (p, J = 24.6 Hz, CD₂), 127.4 (t, J = 24.9 Hz, CD), 112.8 (CH), 111.2 (CH), 105.7 (CH), 56.2 (CH₃), 56.0 (CH₃).

HR-MS (ESI) m/z calcd for $C_{11}H_9O_4D_3Na$, $[M+Na]^+$ 234.0816, found 234.0819; Intensity: 100%.

HR-MS (ESI) m/z calcd for $C_{11}H_{10}O_4D_2Na$, $[M+Na]^+$ 233.0753, found 233.0753; Intensity: 20%.^[129]



[D₃]-4-Acetylphenyl acrylate ([D₃]-45u):

The general procedure **E** was followed using 4-acetylphenyl acrylate (**45u**) (190 mg, 1.00 mmol). After the reaction was finished, EtOAc (16.0 mg, 0.18 mmol) was added as the internal standard.

NMR conversion vs. internal standard: >95%.

Degree of Deuteration: D¹ = 96%; D² = 96%; D³ = 70%; acetyl group: 17%.

¹H-NMR (500 MHz, C₆D₆): δ = 7.73–7.66 (m, 2H), 6.99–6.93 (m, 2H), 6.38–6.31 (m, 0.04H), 6.08–6.00 (m, 0.30 H), 5.46–5.41 (m, 0.04H), 2.14–2.07 (s and t, 2.48H).

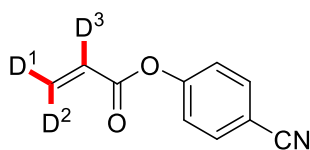
²H-NMR (77 MHz, C₆D₆): δ = 6.32 (s, 1D), 6.02 (s, 1D), 5.43 (s, 1D), 2.08 (t, *J* = 2.3 Hz).

¹³C-NMR (126 MHz, C₆D₆): δ = 196.1 (C_q), 163.4 (C_q), 154.5 (C_q), 135.0 (C_q), 132.18 (p, *J* = 25.3 Hz, CD₂), 130.1 (CH), 127.21 (t, *J* = 25.8 Hz, CD), 121.9 (CH), 26.2 (CH₃).

HR-MS (ESI) *m/z* calcd for C₁₁H₆O₃D₄Na, [M+Na]⁺ 217.0773, found 217.0768; Intensity: 35%.

HR-MS (ESI) *m/z* calcd for C₁₁H₇O₃D₃Na, [M+Na]⁺ 216.0710, found 216.0711; Intensity: 100%.

HR-MS (ESI) *m/z* calcd for C₁₁H₈O₃D₂Na, [M+Na]⁺ 215.0648, found 215.0648; Intensity: 30%.^[129]



[D₃]-45v

[D₃]-4-Cyanophenyl acrylate ([D₃]-45v):

The general procedure **E** was followed using 4-cyanophenyl acrylate (**45v**) (173 mg, 1.00 mmol). After the reaction was finished, EtOAc (25.0 mg, 0.28 mmol) was added as the internal standard.

NMR conversion vs. internal standard: 89%.

Degree of Deuteration: D¹ = 85%; D² = 85%; D³ = 52%

¹H-NMR (500 MHz, C₆D₆): δ = 6.94–6.90 (m, 2H), 6.65–6.61 (m, 2H), 6.33–6.23 (m, 0.15H), 5.97–5.87 (m, 0.48H), 5.40–5.33 (m, 0.15H).

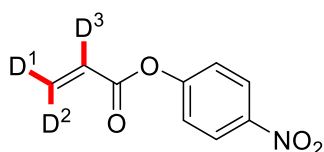
²H-NMR (77 MHz, C₆D₆): δ = 6.26 (s, 1D), 5.91 (s, 1D), 5.34 (s, 1D).

¹³C-NMR (126 MHz, C₆D₆): δ = 163.3 (C_q), 160.9 (C_q), 153.8 (C_q), 134.2 (C_q), 133.5 (CH), 133.23–132.16 (m, CD₂), 127.25–126.96 (m, CD), 122.6 (CH).

HR-MS (ESI) *m/z* calcd for C₁₀H₄NO₂D₃Na, [M+Na]⁺ 199.0557, found 199.0552; Intensity: 100%.

HR-MS (ESI) *m/z* calcd for C₁₀H₅NO₂D₂Na, [M+Na]⁺ 198.0495, found 198.0495; Intensity: 90%.

HR-MS (ESI) *m/z* calcd for C₁₀H₆NO₂D₁Na, [M+Na]⁺ 197.0432, found 197.0433; Intensity: 20%.^[129]



[D₃]-45w

[D₃]-4-Nitrophenyl acrylate ([D₃]-45w):

The general procedure **E** was followed using 4-nitrophenyl acrylate (**45w**) (193 mg, 1.00 mmol). After the reaction was finished, EtOAc (13.0 mg, 0.15 mmol) was added as the internal standard.

Experimental Section

NMR conversion vs. internal standard: >95%.

Degree of Deuteration: $D^1 = 95\%$; $D^2 = 95\%$; $D^3 = 36\%$.

$^1\text{H-NMR}$ (500 MHz, C_6D_6): $\delta = 7.78\text{--}7.69$ (m, 2H), 6.68–6.62 (m, 2H), 6.33–6.23 (m, 0.05H), 5.97–5.89 (m, 0.64H), 5.41–5.34 (m, 0.05H).

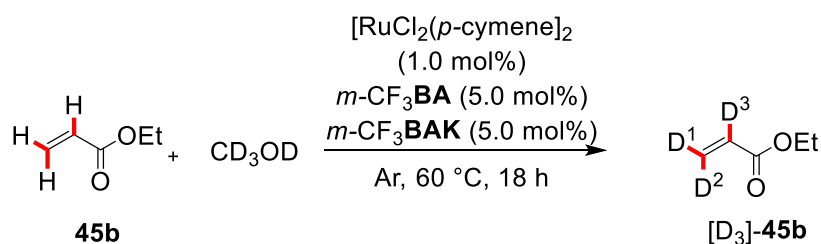
$^2\text{H-NMR}$ (77 MHz, C_6D_6): $\delta = 6.28$ (s at 6.30 and s at 6.27, 1D), 5.92 (s, 1D), 5.37 (s, 1D).

$^{13}\text{C-NMR}$ (126 MHz, C_6D_6): $\delta = 163.2$ (C_q), 155.2 (C_q), 145.5 (C_q), 132.8 (p, $J = 24.6$ Hz, CD_2), 127.0 (s, $\underline{\text{CH}}/\text{CD}$) & 126.7 (t, $J = 25.0$ Hz, $\text{CH}/\underline{\text{CD}}$), 125.1 (CH), 122.3 (CH).

HR-MS (ESI) m/z calcd for $\text{C}_9\text{H}_4\text{O}_4\text{D}_3\text{Na}$, $[\text{M}+\text{Na}]^+$ 219.0456, found 219.0442; Intensity: 70%.

HR-MS (ESI) m/z calcd for $\text{C}_9\text{H}_5\text{O}_4\text{D}_2\text{Na}$, $[\text{M}+\text{Na}]^+$ 218.0393, found 216.0393; Intensity: 100%.^[129]

5.3.3.2 Kinetic Study for the Deuterium Labelling Reaction



$[\text{RuCl}_2(p\text{-cymene})_2]$ (**30**) (6.1 mg, 0.01 mmol, 1.0 mol %), *m*-CF₃-benzoic acid (9.5 mg, 0.05 mmol, 5.0 mol %), potassium *m*-CF₃-benzoate (11.5 mg, 0.05 mmol, 5.0 mol %) and 1,3,5-trichlorobenzene (36.2 mg, 0.2 mmol, 0.2 equiv) as the internal standard, were placed in a pre-dried 25 mL Schlenk-tube. The tube was evacuated and refilled with Ar three times. Ethyl acrylate (**45b**) (100.1 mg, 1.00 mmol, 1.0 equiv) and d³-MeOD (1.0 mL, 24.7 mmol, 24.7 equiv) were added and the mixture was stirred for 10 minutes, before 0.6 ml were transferred into an argon filled NMR tube. The kinetic of the deuterium incorporation was determined by periodical ¹H-NMR measurement at a Bruker Avance 300 with temperature unit at 60°C (Figure 33, Table 45).

NMR conversion vs. internal standard: >95%.

Degree of Deuteration: D¹ = 83%; D² = 83%; D³ = 68%.

Experimental Section

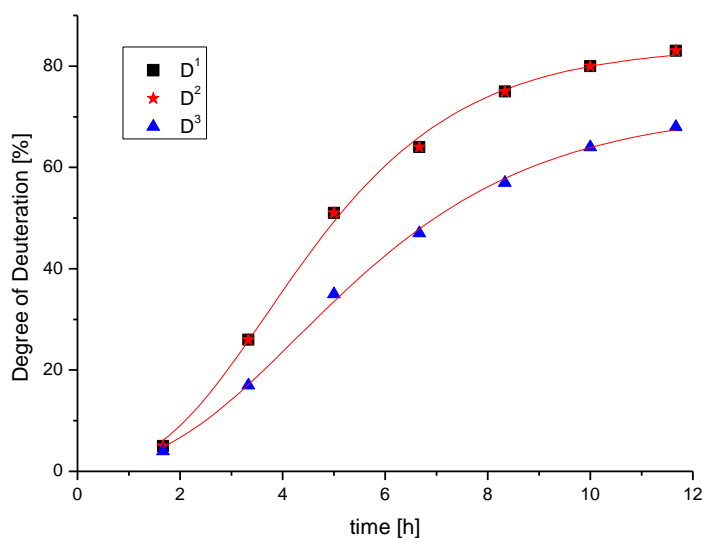
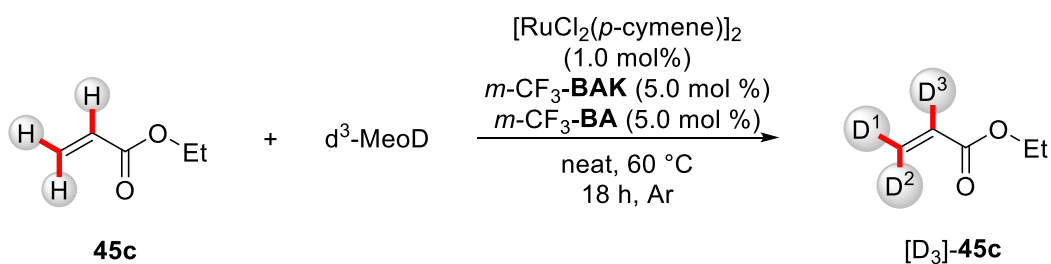


Figure 33: Data of the *in-operando* NMR study of the deuteration of ethyl acrylate.

Table 45: Data of the *in-operando* NMR study of the deuteration of ethyl acrylate.

Time [min]	D ¹ [%D]	D ² [%D]	D ³ [%D]
0	0	0	0
100	5	5	4
200	26	26	17
300	51	51	35
400	64	64	47
500	75	75	57
600	80	80	64
700	83	83	68

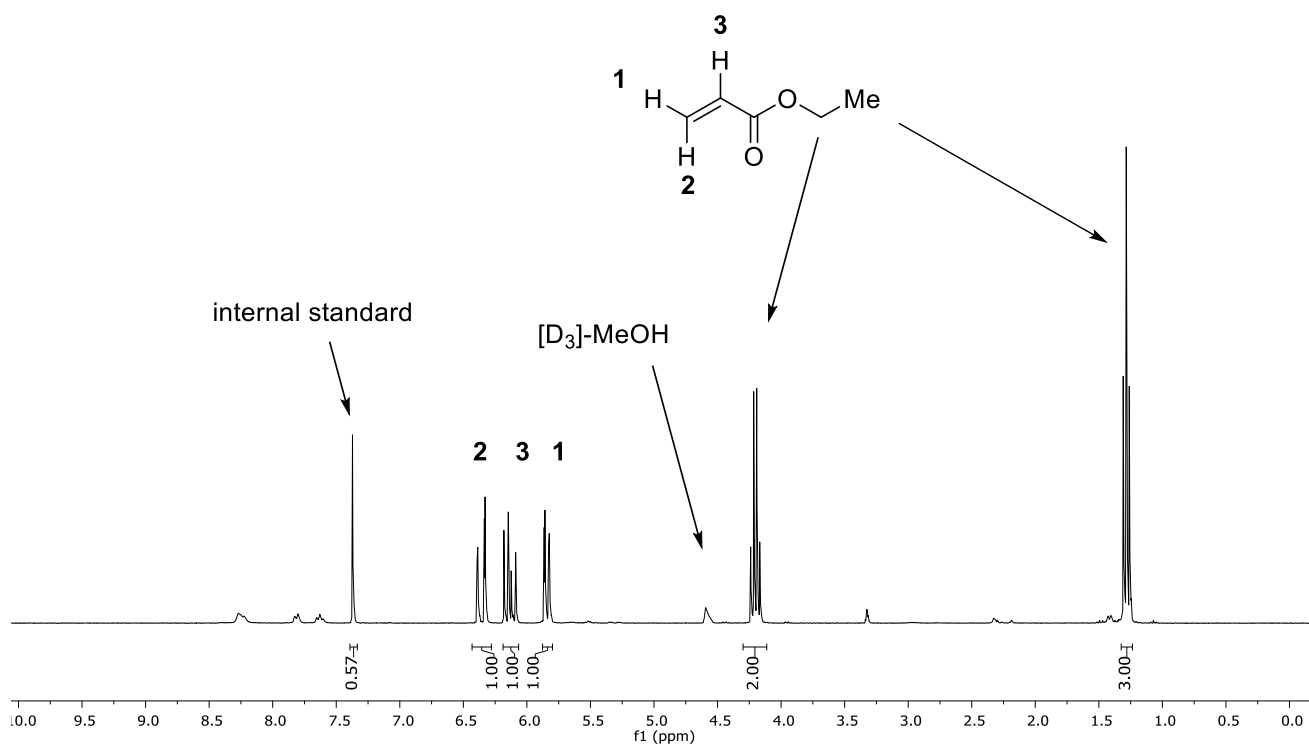


Figure 34: $^1\text{H-NMR}$ -Spectrum after 0 minutes of the *in-operando* NMR study of the deuteration of ethyl acrylate.

Experimental Section

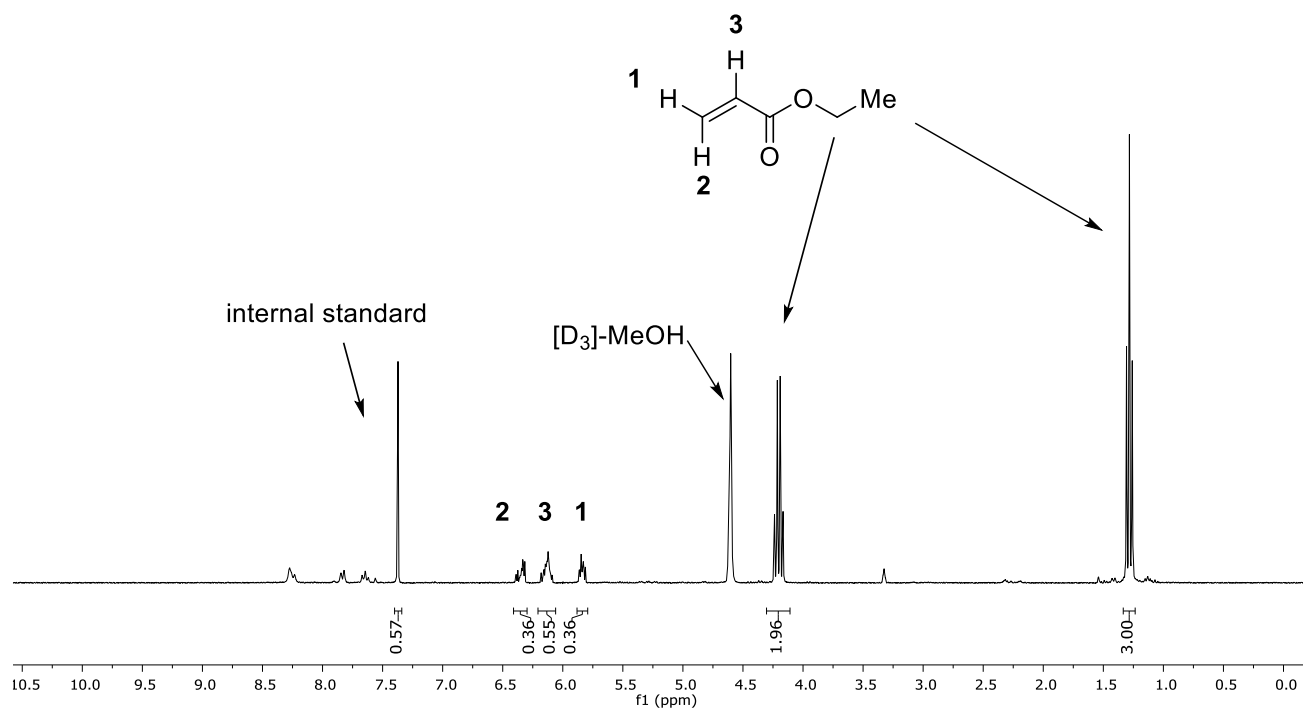


Figure 35: $^1\text{H-NMR}$ -Spectrum after 400 minutes of the *in-operando* NMR study of the deuteration of ethyl acrylate.

Experimental Section

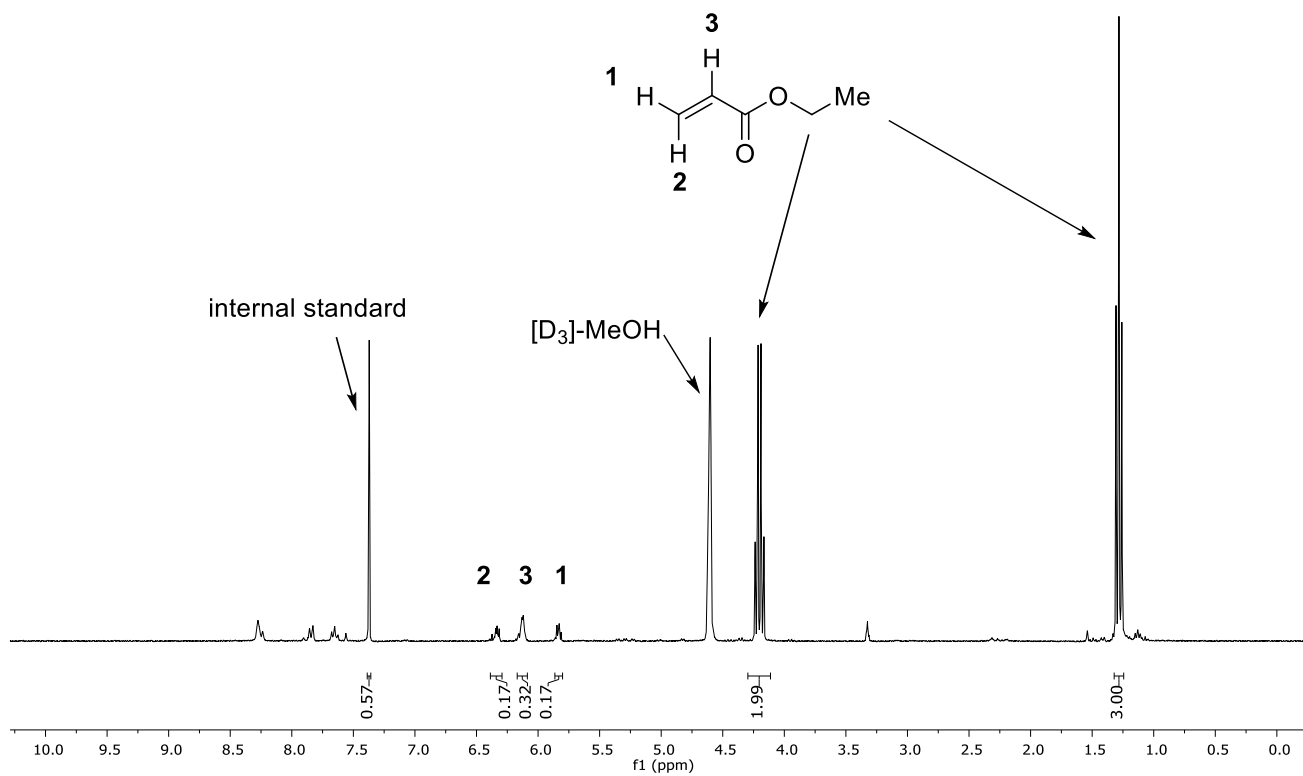
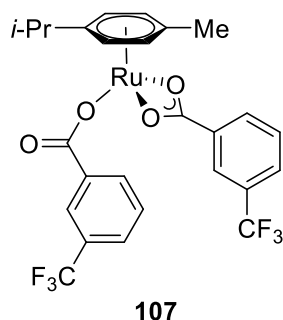


Figure 36: $^1\text{H-NMR}$ -Spectrum after 700 minutes of the *in-operando* NMR study of the deuteration of ethyl acrylate.

5.3.3.3 Synthesis of **107**

[RuCl₂(*p*-cymene)]₂ (**30**) (306 mg, 0.5 mmol, 1.0 equiv), *m*-CF₃-benzoic acid (380 mg, 2.0 mmol, 4.0 equiv) and K₂CO₃ (138 mg, 1.0 mmol, 2.0 equiv) were suspended in PhMe (30 mL) and stirred for 16 h. All volatiles were removed *in vacuo* and the residue was solved in CH₂Cl₂ (20 mL). Filtration over Celite, followed by evaporation of the solvent delivered **107** as an orange oil (617 mg, 1.0 mol, >99%).

X-ray suitable single crystals were obtained by overlaying a concentrated solution of **107** in CH₂Cl₂ solution in *n*-hexane and storing it at -30 °C.

¹H-NMR (300 MHz, CDCl₃): δ = 8.08 (s, 2H), 8.02 (d, *J* = 8.0 Hz, 2H), 7.63 (d, *J* = 7.6 Hz, 2H), 7.40 (dd, *J* = 8.0, 7.6 Hz, 2H), 6.02 (d, *J* = 6.1 Hz, 2H), 5.80 (d, *J* = 6.2 Hz, 2H), 2.37 (s, 3H), 1.43 (d, *J* = 7.0 Hz, 6H).

¹³C-NMR (126 MHz, CDCl₃): δ = 177.6 (C_q), 134.4 (C_q), 132.3 (CH), 130.5 (q, ²*J*_{C-F} = 32.7 Hz, C_q), 128.5 (CH), 128.1 (CH), 126.2 (CH), 126.1 (C_q), 123.9 (q, ¹*J*_{C-F} = 272.5 Hz, C_q), 98.7 (CH), 79.3 (C_q), 78.0 (CH), 31.7 (CH), 22.7 (CH₃), 18.8 (CH₃).

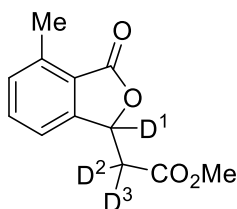
¹⁹F-NMR (282 MHz, CDCl₃): δ = -62.87.

IR (ATR): 2281, 1617, 1576, 1320, 1278, 1122, 1069, 789, 696, 496 cm⁻¹.

MS (EI) *m/z* (relative Intensity): 614 (1) [M]⁺, 595 (1), 551 (1), 460 (1), 424 (55), 381 (40), 173 (100), 145 (85).

107 could not be detected by ESI-MS.

5.3.3.4 Synthesis of Deuterium Labeled Compounds

[D₃]-47ab**[D₃]-Methyl 2-(4-methyl-3-oxo-1,3-dihydroisobenzofuran-1-yl-1-d)acetate ([D₃]-47ab):**

2-Methyl-6-deuterobenzoic acid-D ([D₁]-**21a-D**) (138 mg, 1.00 mmol, 2.0 equiv), [RuCl₂(*p*-cymene)]₂ (**30**) (15 mg, 0.03 mmol, 5.0 mol %) and KOAc (49 mg, 0.50 mmol, 1.0 equiv) were placed in a pre-dried 25 mL Schlenk-tube. The tube was evacuated and refilled with O₂ 3 times. Methyl acrylate-*d*₃ [D₃]-**45b** (45 g, 0.50 mmol, 1.0 equiv, 93% D) and CD₃OD (1.0 mL, 55 mmol, 55.0 equiv) were added and the mixture was heated to 80 °C for 18 h. The crude reaction mixture was absorbed on silica and purified by column chromatography (*n*-hexane/EtOAc: 4/1 + 5% NEt₃) to yield [D₃]-**47ab** as a white solid (88 mg, 40 μmol, 79%).

Degree of Deuteration: D¹ = 93%; D² = 93%; D³ = 93%. D² and D³ are overlapping in the ¹H-NMR spectra, their deuteration value is given as the average.

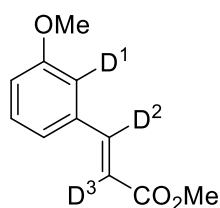
¹H-NMR (500 MHz, CDCl₃): δ = 7.52 (t, *J* = 7.6 Hz, 1H), 7.29–7.24 (m, 2H), 5.83–5.74 (m, 0.07H), 3.74 (s, 3H), 2.90–2.75 (m, 0.14H), 2.67 (d, *J* = 0.8 Hz, 3H).

²H-NMR (77 MHz, CDCl₃): δ = 5.79 (s, 1D), 2.84 (s, 2D).

¹³C-NMR (126 MHz, CDCl₃): δ = 170.1 (C_q), 169.9 (C_q), 149.2 (C_q), 140.0 (C_q), 134.1 (CH), 131.3 (CH), 123.4 (C_q), 119.4 (CH), 75.7 (t, *J* = 24.0 Hz, CD), 52.3 (CH₃), 39.0 (p, *J* = 19.9 Hz, CD₂), 17.4 (CH₃).

HR-MS (ESI) *m/z* calcd for C₁₂H₉O₄D₃Na, [M+Na]⁺ 246.0816, found 246.0814; Intensity: 100%.

HR-MS (ESI) *m/z* calcd for C₁₂H₁₀O₄D₂Na, [M+Na]⁺ 245.0753, found 245.0759; Intensity: 20%.^[129]



[D₃]-**97cb**

[D₃]-Methyl (E)-3-(3-methoxyphenyl-2-d)acrylate ([D₃]-97cb**):**

2-Methoxy-6-deuterobenzoic acid-D ([D₁]-**21c-D**) (231 mg, 1.50 mmol, 3.0 equiv), [Ru(CO₂Mes)₂(*p*-cymene)] (**99**) (28 mg, 0.05 mmol, 10 mol %) and V₂O₅ (91 mg, 0.50 mmol, 1.0 equiv) were placed in a pre-dried 25 mL pressure tube equipped with a rubber septum. The tube was evacuated and refilled with Argon three times. Methyl acrylate-*d*₃ [D₃]-**45b** (45 g, 0.50 mmol, 1.0 equiv, 93% D) and PhMe (1.0 mL) were added. The pressure tube was sealed and the mixture was heated to 120°C for 18 h. The crude reaction mixture was absorbed on silica and purified by column chromatography (*n*-hexane/EtOAc: 20/1) to yield [D₃]-**97cb** as a colorless oil (72 mg, 36 mmol, 54%).

Degree of Deuteration: D¹ = 82%; D² = 89%; D³ = 89%.

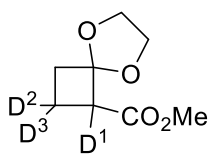
¹H-NMR (500 MHz, CDCl₃): δ = 7.68–7.60 (m, 0.11H), 7.30 (t, *J* = 7.9 Hz, 1H), 7.12 (dd, *J* = 7.6, 1.1 Hz, 1H), 7.04 (t, *J* = 2.1 Hz, 0.18H), 6.94 (dd, *J* = 8.3, 1.0 Hz, 1H), 6.47–6.35 (m, 0.11H), 3.83 (s, 3H), 3.81 (s, 3H).

²H-NMR (77 MHz, CDCl₃): δ = 7.71 (s, 1D), 7.09 (s, 1D), 6.46 (s, 1D).

¹³C-NMR (126 MHz, CDCl₃): δ = 167.5 (C_q), 160.0 (C_q), 144.5 (t, *J* = 24.3 Hz, CD), 135.7 (C_q), 130.0 (CH), 120.9 (CH), 117.8 (t, *J* = 25.3 Hz, CD), 116.3 (CH), 112.76 (t, *J* = 24.1 Hz, CD), 55.5 (CH₃), 51.9 (CH₃).

HR-MS (ESI) *m/z* calcd for C₁₁H₁₀O₃D₃, [M+H]⁺ 196.1048, found 196.1050; Intensity: 100%.

HR-MS (ESI) *m/z* calcd for C₁₁H₁₁O₃D₂, [M+H]⁺ 195.0985, found 195.0990; Intensity: 35%.^[129]



[D₃]-109

1,2,2-[D₃]-Methyl-5,8-dioxaspiro[3.4]octane-1-carboxylate ([D₃]-109):

A KO^tBu solution in *t*-butanol was freshly prepared, by dissolving potassium (2.5 g, 63 mmol, 3.1 equiv) was in *t*-BuOH (70 mL). At 100 °C 2-bromomethyl-1,3-dioxolan (**108**) (6.3 g, 38 mmol, 1.9 equiv) was added and the mixture was stirred at 85 °C for 2 h. All volatiles were transferred by distillation and then by condensation with passiv high vaccum and heating to 100°C of the reaction flask and cooling the receiving flask to -196 °C. [D₃]-Methyl acrylate (1.8 g, 20 mmol, 1.0 equiv, 93% D) and MEHQ (100 mg) were added and the mixture was stirred at 90 °C for 72 h. The solvent was distilled off and the residue was purified by column chromatography (*n*-hexane/EtOAc 20/1 → 10/1) to yield compound [D₃]-109 as a colorless oil (2.25 g, 12.8 mmol, 64%).

[D₃]-109 shows minor impurities. The purity is estimated to be >90%.

Degree of Deuteration: D¹ = 67%; D^{2/3} = 93%.

¹H-NMR (400 MHz, CDCl₃): δ = 4.06–3.94 (m, 2H), 3.92–3.86 (m, 2H), 3.71 (s, 3H), 3.42–3.35 (m, 0.33H), 2.39 (tt, *J* = 2.6, 1.1 Hz, 2H), 2.11–2.07 (m, 0.07H), 1.86–1.78 (m, 0.07H).

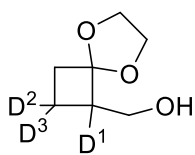
²H-NMR (61 MHz, CDCl₃): δ = 3.40 (s, 1D), 2.10 (s, 1D), 1.83 (s, 1D).

¹³C-NMR (126 MHz, CDCl₃): δ = 171.4 (C_q), 109.1 & 109.0 (C_q), 65.0 (CH₂), 64.7 (CH₂), 52.5 (s, CH/CD), 52.19 (t, *J* = 21.5 Hz, CH/CD), 51.9 (CH₃), 33.7 (CH₂), 13.38 (p, *J* = 21.4 Hz, CD₂).

HR-MS (ESI) *m/z* calcd for C₈H₉O₂D₃Na, [M+Na]⁺ 198.0816, found 198.0817; Intensity: 100%.

HR-MS (ESI) *m/z* calcd for C₈H₁₀O₂D₂Na, [M+Na]⁺ 197.0753, found 197.0754; Intensity: 60%.

HR-MS (ESI) *m/z* calcd for C₈H₁₁O₂DNa, [M+Na]⁺ 196.0691, found 197.0680; Intensity: 5%.^[129]

[D₃]-110**1,2,2-[D₃]- (5,8-dioxaspiro[3.4]octan-1-yl-1,2,2-*d*3)methanol ([D₃]-110):**

LiAlH₄ was suspended in Et₂O and [D₃]-109 (2.5 g, 63 mmol, 3.1 equiv) in Et₂O (10 mL) was slowly added at 0 °C over a period of 20 minutes. After the mixture was stirred at 30 °C for 3 h, H₂O (10 mL) was added and the white precipitate extracted with Et₂O (5-50 mL). The combined organic phases were washed with H₂O (50 mL) dried over MgSO₄ and filtered through a short plug of silica (3 cm). Removal of the solvent yielded [D₃]-110 as a colorless oil (1.12 g, 8.7 mmol, 79%).

[D₃]-110 shows minor impurities. The purity is estimated to be >90%.

Degree of Deuteration: D¹ = 67%; D^{2/3} = 90%.

¹H-NMR (500 MHz, CDCl₃): δ = 3.96–3.85 (m, 4H), 3.80–3.64 (m, 2H), 2.81–2.66 (m, 0.33H), 2.29–2.19 (m, 2H), 1.79–1.72 (m, 0.10H), 1.58–1.52 (m, 0.10H).

²H-NMR (77 MHz, CDCl₃): δ = 2.74 (s, 1D), 1.76 (s, 1D), 1.57 (s, 1D).

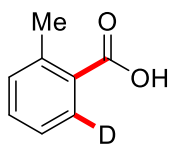
¹³C-NMR (126 MHz, CDCl₃): δ = 110.1 & 110.1 (C_q), 64.5 (CH₂), 64.0 (CH₂), 62.1 (d, *J* = 8.7 Hz, CH₂OH), 48.5 (CH/CD), 48.1 (t, *J* = 21.2, CH/CD), 33.5 (CH), 13.3 (p, *J* = 21.6, 21.1, 20.7 Hz, CD₂).

HR-MS (ESI) *m/z* calcd for C₇H₉O₃D₃Na, [M+Na]⁺ 170.0867, found 170.0868; Intensity: 100%.

HR-MS (ESI) *m/z* calcd for C₈H₁₀O₂D₂Na, [M+Na]⁺ 169.0804, found 169.0805; Intensity: 70%.

HR-MS (ESI) *m/z* calcd for C₈H₁₁O₂D Na, [M+Na]⁺ 168.0741, found 168.0739; Intensity: 10%.^[129]

5.3.4 Synthesis of Deuterated Benzoic Acids

[D₁]-**21a**

2-Methyl-6-deuterobenzoic acid ([D₁]-**21a**):

2-Methyl-benzoic acid (**21a**) (1.36 g, 10.0 mmol, 1.0 equiv), [RuCl₂(*p*-cymene)]₂ (**30**) (122 mg, 0.20 mmol, 2.0 mol %) and K₂CO₃ (55 mg, 0.40 mmol, 0.2 equiv) were placed in a pre-dried Schlenk-tube. The tube was evacuated and refilled with Ar three times. D₂O (4.0 mL, 220 mmol, 22.0 equiv) was added and the reaction mixture was stirred at 100 °C for 18 h. The solvent was removed under reduced pressure and additional D₂O (2.0 mL, 110 mmol, 11.0 equiv) was added. The reaction mixture was stirred at 100 °C for 16 h. At ambient temperature, the mixture was extracted with EtOAc (2·50 mL). The combined organic phases were washed with aqueous NaOH (2.0 M, 50 mL) and then both phases were acidified to pH = 1 with aqueous HCl (conc.). The organic phase was separated, dried over anhydrous Na₂SO₄ and the solvent was removed under reduced pressure. Purification by column chromatography (Et₂O) and Kugelrohr-distillation yielded [D₁]-**21a** (1.01 g, 7.4 mmol, 74%) as a white solid.

Degree of Deuteration: >98%.

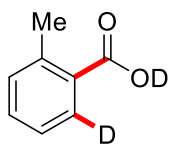
¹H NMR (300 MHz, CDCl₃): δ = 12.46 (s, 1H), 7.47 (dd, *J* = 7.5, 7.5 Hz, 1H), 7.34–7.27 (m, 2H), 2.68 (s, 3H).

¹³C NMR (75 MHz, CDCl₃): δ = 173.5 (C_q), 141.5 (C_q), 133.1 (CH), 132.1 (CH), 131.5 (t, *J* = 24.6 Hz, CD), 128.4 (C_q), 125.9 (CH), 22.3 (CH₃).

IR (ATR): 2645, 1672, 1451, 1267, 1109, 699, 651, 565, 480, 401 cm⁻¹.

MS (EI) *m/z* (relative intensity): 137 (90) [M]⁺, 129 (10), 119 (100), 105 (5), 92 (100), 78 (10), 66 (30), 63 (20).

HR-MS (ESI) *m/z* calcd for C₈H₆O₃D, [M-H]⁻ 136.0514, found 136.0515.

[D₂]-**21a****2-Methyl-6-deuterobenzoic acid-D ([D₂]-**21a**):**

2-Methyl-benzoic acid (**21a**) (0.68 g, 5.00 mmol, 1.0 equiv), [RuCl₂(*p*-cymene)]₂ (**30**) (31 mg, 0.05 mmol, 1.0 mol %) and K₂CO₃ (14 mg, 0.10 mmol, 2.0 mol %) were placed in a pre-dried Schlenk-tube. The tube was evacuated and refilled with Ar three times. D₂O (1.0 mL, 55 mmol, 11.0 equiv) and PhMe (1.0 mL) were added and the reaction mixture was stirred at 80 °C for 24 h. The solvent was removed under reduced pressure and additional D₂O (1.0 mL, 55 mmol, 11.0 equiv) and PhMe (1.0 mL) were added. The reaction mixture was stirred at 80 °C for 24 h. All volatiles were removed and the residue was purified by column chromatography (*n*-hexane/Et₂O: 1/1) and Kugelrohr-distillation to yield [D₂]-**21a** (643 mg, 4.17 mmol, 83%) as a white solid.

Degree of Deuteration: >98%.

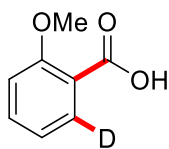
¹H NMR (300 MHz, CDCl₃): δ = 7.44 (dd, *J* = 7.5, 7.5 Hz, 1H), 7.29 (m, 2H), 2.67 (s, 3H).

¹³C NMR (75 MHz, CDCl₃): δ = 173.0 (C_q), 141.5 (C_q), 133.1 (CH), 132.1 (CH), 131.4 (m, CD), 128.4 (C_q), 125.9 (CH), 22.2 (CH₃).

IR (ATR): 2639, 1672, 1268, 921, 819, 803, 698, 650, 527, 401 cm⁻¹.

MS (EI) *m/z* (relative intensity): 137 (80) [M]⁺, 124 (5), 119 (95), 106 (5), 92 (100), 78 (10), 66 (25), 63 (15).

HR-MS (ESI) *m/z* calcd for C₈H₆O₂D, [M-D]⁻ 136.0514, found 136.0514.

[D₁]-**21c****2-Methoxy-6-deuterobenzoic acid ([D₁]-**21c**):**

2-Methoxybenzoic acid (**21c**) (2.50 g, 16.0 mmol, 1.0 equiv), [RuCl₂(*p*-cymene)]₂ (**30**) (200 mg, 0.30 mmol, 2.0 mol %) and KOAc (160 mg, 1.60 mmol, 0.1 equiv) were placed in a pre-dried Schlenk-tube. The tube was evacuated and refilled with argon three times. D₂O (3.0 mL, 165 mmol, 10.3 equiv) was added and the reaction mixture was stirred at 80 °C for 16 h. The solvent was removed under reduced pressure and additional D₂O (3.0 mL, 165 mmol, 10.3 equiv) was added. The reaction mixture was stirred at 80 °C for 16 h. At ambient temperature, the mixture was extracted with EtOAc (2·50 mL). The combined organic phases were washed with aqueous NaOH (2.0 M, 50 mL) and then both phases were acidified to pH = 1 with aqueous HCl (conc.). The organic phase was separated, dried over anhydrous Na₂SO₄ and the solvent was removed under reduced pressure. Purification by column chromatography (Et₂O) and Kugelrohr-distillation yielded [D₁]-**21c** (2.39 g, 15.6 mmol, 95%) as a white solid.

Degree of Deuteration: >98%.

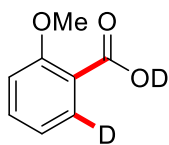
¹H NMR (300 MHz, CDCl₃): δ = 10.84 (s, 1H), 7.57 (dd, *J* = 8.3, 7.4 Hz, 1H), 7.13 (d, *J* = 7.4 Hz, 1H), 7.06 (dd, *J* = 8.3, 1.1 Hz, 1H), 4.07 (s, 3H).

¹³C NMR (126 MHz, CDCl₃): δ = 165.5 (C_q), 158.1 (C_q), 135.1 (CH), 133.5 (t, *J* = 25.0 Hz, CD), 122.1 (CH), 117.6 (C_q), 111.8 (CH), 56.8 (CH₃).

IR (ATR): 2843, 1662, 1642, 1253, 1117, 1011, 914, 823, 785, 702 cm⁻¹.

MS (EI) *m/z* (relative intensity): 153 (60) [M]⁺, 136 (45), 124 (70), 106 (100), 93 (33), 78 (60), 64 (25), 51 (20), 43 (50).

HR-MS (EI) *m/z* calcd for C₈H₇O₃D, [M]⁺ 153.0536, found 153.0536.

[D₂]-**21c****2-Methoxy-6-deuterobenzoic acid-D ([D₂]-**21c**):**

2-Methoxybenzoic acid (**21c**) (0.76 g, 5.00 mmol, 1.0 equiv), [RuCl₂(*p*-cymene)]₂ (**30**) (31 mg, 0.05 mmol, 1.0 mol %) and K₂CO₃ (14 mg, 0.10 mmol, 2.0 mol %) were placed in a pre-dried Schlenk-tube. The tube was evacuated and refilled with argon three times. D₂O (1.0 mL, 55 mmol, 11.0 equiv) and PhMe (1.0 mL) were added and the reaction mixture was stirred at 80 °C for 24 h. The solvent was removed under reduced pressure and additional D₂O (1.0 mL, 55 mmol, 11.0 equiv) and PhMe (1.0 mL) were added. The reaction mixture was stirred at 80 °C for 24 h. All Volatiles were removed and the residue was purified by column chromatography (*n*-hexane/Et₂O: 1/1) and Kugelrohr-distillation to yield [D₂]-**21c** (643 mg, 4.17 mmol, 83%) as a white solid.

Degree of Deuteration: >98%.

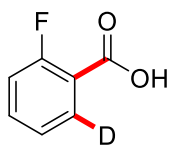
¹H NMR (300 MHz, CDCl₃): δ = 7.58 (dd, *J* = 8.4, 7.4 Hz, 1H), 7.15 (dd, *J* = 7.4, 1.1 Hz, 1H), 7.07 (dd, *J* = 8.4, 1.3 Hz, 1H), 4.08 (s, 3H).

¹³C NMR (75 MHz, CDCl₃): δ = 166.0 (C_q), 158.2 (C_q), 135.1 (CH), 133.1 (t, *J* = 25.0 Hz, CD), 121.7 (CH), 117.4 (C_q), 111.8 (CH), 56.6 (CH₃).

IR (ATR): 2950, 2634, 1662, 1462, 1117, 822, 702, 649, 424, 402 cm⁻¹.

MS (EI) *m/z* (relative intensity): 154 (20) [M]⁺, 153 (65), 136 (55), 124 (70), 106 (100), 93 (40), 78 (60), 64 (25), 51 (20), 43 (50).

HR-MS (ESI) *m/z* calcd for C₈H₆O₃D, [M-D]⁻ 152.0463, found 152.0465.

[D₁]-**21af****2-Fluoro-6-deuterobenzoic acid ([D₁]-**21af**):**

2-Fluorobenzoic acid (**21af**) (2.0 g, 14.2 mmol, 1.0 equiv), [RuCl₂(*p*-cymene)]₂ (**30**) (174 mg, 0.3 mmol, 2.0 mol %) and K₂CO₃ (96 g, 0.7 mmol, 5.0 mol %) was suspended in D₂O (3.0 mL, 165 mmol, 11.9 equiv) and stirred for 18 h at 90 °C. D₂O was evaporated first *in vacuo*, then by azeotropic distillation with PhMe (2·5mL). D₂O (1.5 mL, 83 mmol, 6.0 equiv) was added and the suspension was stirred for another 5 h at 90 °C. At ambient temperature the mixture was poured into Et₂O (120 mL) and was extracted with aq. NaOH (2 M, 30 mL). The inorganic phase was acidified to pH 1-2 using HCl (6 M, 150 mL) and extracted with Et₂O (2·30 mL). The combined organic layers were dried over anhydrous Na₂SO₄. Evaporation of the solvent, Kugelrohr-distillation (2 times) and recrystallisation from PhMe gave [D₁]-**21af** (1.1 g, 55%) as white crystals.

Degree of Deuteration: >98%.

M. p. = 124–126 °C.

¹H-NMR (300 MHz, CDCl₃): δ = 11.88 (s, 1H), 7.59 (ddd, *J* = 8.3, 7.4, 4.8 Hz, 1H), 7.28–7.14 (m, 2H).

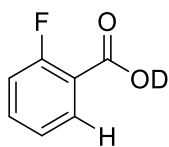
¹³C-NMR (75 MHz, CDCl₃): δ = 170.2 (C_q), 162.8 (d, ¹*J*_{C-F} = 262.3 Hz, C_q), 135.8 (d, ³*J*_{C-F} = 9.5 Hz, CH), 132.6 (t, *J* = 25.3 Hz, CD), 124.1 (d, ⁴*J*_{C-F} = 4.0 Hz, CH), 117.6 (d, ³*J*_{CF} = 8.8 Hz, C_q), 117.3 (d, ²*J*_{C-F} = 22.0 Hz, CH).

¹⁹F{¹H}-NMR (282 MHz, CDCl₃): δ = -108.17.

IR (ATR): 2652, 1682, 1606, 1458, 1282, 1245, 823, 695, 643, 402 cm⁻¹.

MS (EI) *m/z* (relative intensity): 141 (75), 124 (100), 113 (5), 96 (50), 91 (10), 85 (5), 76 (25), 69 (10), 58 (20), 51 (10).

HR-MS (ESI) *m/z* calcd for C₇H₅O₃FD [M+H]⁺ 142.0409, found 142.0410.

**21af-D****2-Fluoro-benzoic acid-D (21af-D):**

2-Fluorobenzoic acid (**21af**) (2.0 g, 14.2 mmol, 1.0 equiv) was suspended in D₂O (2.0 mL, 110 mmol, 7.9 equiv.) and stirred for 18 h at 90 °C. D₂O was evaporated first *in vacuo*, then by azeotropic distillation with PhMe (2 x 5 mL). D₂O (1.0 mL, 55 mmol, 3.9 equiv) was added and the suspension was stirred for another 5 h at 90 °C. Evaporation of D₂O and recrystallisation from PhMe gave **21af-D** (1.9 g, 95%) as white crystals.

Degree of Deuteration: >98%.

M. p. =122-124 °C.

¹H NMR (300 MHz, CDCl₃): δ = 12.10 (s, 0.01H), 8.06 (ddd, *J* = 7.5, 7.5, 1.9 Hz, 1H), 7.60 (ddd, *J* = 8.3, 7.4, 1.9 Hz, 1H), 7.33–7.12 (m, 2H).

¹³C-NMR (75 MHz, CDCl₃): δ = 169.9 (C_q), 162.8 (d, ¹*J*_{C-F} = 262.3 Hz, C_q), 135.8 (d, ³*J*_{C-F} = 9.2 Hz, CH), 132.9 (CH), 124.2 (d, ⁴*J*_{C-F} = 3.7 Hz, CH), 117.7 (d, ³*J*_{C-F} = 8.8 Hz, C^q), 117.3 (d, ²*J*_{C-F} = 22.4 Hz, CH).

¹⁹F{¹H}-NMR (282 MHz, CDCl₃): δ = -108.08.

IR (ATR): 2653, 2227, 1682, 1613, 1455, 1360, 1045, 748, 421 cm⁻¹.

MS (EI) *m/z* (relative intensity): 140 (80), 123 (100), 112 (5), 95 (55), 75 (35), 69 (10), 63 (5), 50 (15), 45 (10), 43 (5).

HR-MS (ESI) *m/z* calcd for C₇H₄O₃F [M-D]⁻ 140.0264, found 140.0263.

5.4 Data for X-Ray Diffraction Measurements

Crystal data for the x-ray structure of 47ad	
Identification code	mo_0240_CG_0m
Empirical formula	C ₁₈ H ₁₆ O ₄
Formula weight	296.31
Temperature/K	100.0
Crystal system	monoclinic
Space group	P2 ₁ /c
<i>a</i> /Å	9.8143(14)
<i>b</i> /Å	10.7707(13)
<i>c</i> /Å	27.914(4)
α /°	90
β /°	96.322(5)
γ /°	90
Volume/Å ³	2932.7(7)
<i>Z</i>	8
ρ_{calc} /cm ³	1.342
μ /mm ⁻¹	0.095
F(000)	1248.0
Crystal size/mm ³	0.447 × 0.308 × 0.028
Radiation	MoK α (λ = 0.71073)
2 Θ range for data collection/°	4.788 to 63.098
Index ranges	-11 ≤ <i>h</i> ≤ 14, -15 ≤ <i>k</i> ≤ 15, -41 ≤ <i>l</i> ≤ 41
Reflections collected	40426
Independent reflections	9781 [R _{int} = 0.0347, R _{sigma} = 0.0351]
Data/restraints/parameters	9781/0/399
Goodness-of-fit on F ²	1.038
Final R indexes [<i>I</i> ≥ 2 σ (<i>I</i>)]	R ₁ = 0.0450, wR ₂ = 0.1036
Final R indexes [all data]	R ₁ = 0.0638, wR ₂ = 0.1126
Largest diff. peak/hole / e Å ⁻³	0.35/-0.25
Identification code	mo_0240_CG_0m
Empirical formula	C ₁₈ H ₁₆ O ₄

Experimental Section

Crystal data for the x-ray structure of 100

Identification code	final	
Empirical formula	$C_{57} H_{69.20} Cl_2 N_4 O_{7.60} Ru_2$	
Formula weight	1205.00	
Temperature	100(2) K	
Wavelength	0.71073 Å	
Crystal system	Monoclinic	
Space group	Cc	
Unit cell dimensions	a = 18.844(2) Å	$\alpha = 90^\circ$.
	b = 15.919(2) Å	$\beta = 97.84(2)^\circ$.
	c = 18.261(3) Å	$\gamma = 90^\circ$.
Volume	5426.7(13) Å ³	
Z	4	
Density (calculated)	1.475 Mg/m ³	
Absorption coefficient	0.712 mm ⁻¹	
F(000)	2488	
Crystal size	0.200 x 0.200 x 0.100 mm ³	
Theta range for data collection	1.681 to 26.365°.	
Index ranges	-23<=h<=23, -19<=k<=19, -22<=l<=22	
Reflections collected	65303	
Independent reflections	11082 [R(int) = 0.0436]	
Completeness to theta = 19.546°	100.0%	
Absorption correction	Semi-empirical from equivalents	
Max. and min. transmission	0.4296 and 0.3924	
Refinement method	Full-matrix least-squares on F ²	
Data / restraints / parameters	11082 / 110 / 724	
Goodness-of-fit on F ²	1.050	
Final R indices [I>2sigma(I)]	R1 = 0.0249, wR2 = 0.0556	
R indices (all data)	R1 = 0.0267, wR2 = 0.0567	
Extinction coefficient	-0.021(7)	
Largest diff. peak and hole	n/a	

Experimental Section

Crystal data for the x-ray structure of 101

Identification code	final	
Empirical formula	C ₂₅ H ₂₆ O ₄ Ru	
Formula weight	491.53	
Temperature	100(2) K	
Wavelength	0.56086 Å	
Crystal system	Monoclinic	
Space group	P2 ₁ /c	
Unit cell dimensions	a = 8.793(2) Å b = 15.639(2) Å c = 15.581(3) Å	a = 90°. b = 95.500(3)°. g = 90°.
Volume	2132.7(7) Å ³	
Z	4	
Density (calculated)	1.531 Mg/m ³	
Absorption coefficient	0.412 mm ⁻¹	
F(000)	1008	
Crystal size	0.200 x 0.200 x 0.100 mm ³	
Theta range for data collection	1.836 to 19.546°.	
Index ranges	-10 ≤ h ≤ 10, -18 ≤ k ≤ 18, -18 ≤ l ≤ 18	
Reflections collected	49643	
Independent reflections	3797 [R(int) = 0.0688]	
Completeness to theta = 19.546°	99.9%	
Absorption correction	Semi-empirical from equivalents	
Max. and min. transmission	0.4247 and 0.3804	
Refinement method	Full-matrix least-squares on F ²	
Data / restraints / parameters	3797 / 0 / 275	
Goodness-of-fit on F ²	1.020	
Final R indices [I > 2σ(I)]	R1 = 0.0272, wR2 = 0.0578	
R indices (all data)	R1 = 0.0405, wR2 = 0.0626	
Extinction coefficient	n/a	
Largest diff. peak and hole	0.381 and -0.328 e.Å ⁻³	

Experimental Section

Crystal data for the x-ray structure of 107

Identification code	mo_0072_CG_0m_4
Empirical formula	C ₂₆ H ₂₂ F ₆ O ₄ Ru
Formula weight	613.50
Temperature/K	99.99
Crystal system	triclinic
Space group	P-1
a/Å	10.0251(8)
b/Å	10.6393(7)
c/Å	12.5733(8)
α/°	72.541(2)
β/°	79.432(2)
γ/°	85.085(2)
Volume/Å ³	1256.92(15)
Z	2
ρ _{calc} /cm ³	1.621
μ/mm ⁻¹	0.699
F(000)	616.0
Crystal size/mm ³	0.292 × 0.101 × 0.073
Radiation	MoKα (λ = 0.71073)
2θ range for data collection/°	4.924 to 57.998
Index ranges	-13 ≤ h ≤ 13, -13 ≤ k ≤ 14, 0 ≤ l ≤ 17
Reflections collected	6582
Independent reflections	6582 [R _{int} = ?, R _{sigma} = 0.0304]
Data/restraints/parameters	6582/0/338
Goodness-of-fit on F ²	1.075
Final R indexes [I >= 2σ (I)]	R ₁ = 0.0500, wR ₂ = 0.1119
Final R indexes [all data]	R ₁ = 0.0604, wR ₂ = 0.1187
Largest diff. peak/hole / e Å ⁻³	3.81/-1.26
Identification code	mo_0072_CG_0m_4
Empirical formula	C ₂₆ H ₂₂ F ₆ O ₄ Ru

6 References

- [1] C. C. C. Johansson Seechurn, M. O. Kitching, T. J. Colacot, V. Snieckus, *Angew. Chem. Int. Ed.* **2012**, *51*, 5062-5085.
- [2] a) I. Maluenda, O. Navarro, *Molecules* **2015**, *20*, 7528-7557; b) F.-S. Han, *Chem. Soc. Rev.* **2013**, *42*, 5270-5298; c) N. Miyaura, K. Yamada, A. Suzuki, *Tetrahedron Lett.* **1979**, *20*, 3437-3440; d) N. Miyaura, A. Suzuki, *J. Chem. Soc. Chem. Commun.* **1979**, *0*, 866-867; e) R. J. P. Corriu, J. P. Masse, *J. Chem. Soc. Chem. Commun.* **1972**, *0*, 144a-144a.
- [3] a) D. Haas, J. M. Hammann, R. Greiner, P. Knochel, *ACS Catal.* **2016**, *6*, 1540-1552; b) A. O. King, N. Okukado, E.-i. Negishi, *J. Chem. Soc. Chem. Commun.* **1977**, *0*, 683-684.
- [4] a) M. M. Heravi, P. Hajiabbasi, *Monatsh. Chem.* **2012**, *143*, 1575-1592; b) K. Tamao, K. Sumitani, M. Kumada, *J. Am. Chem. Soc.* **1972**, *94*, 4374-4376.
- [5] D. Milstein, J. K. Stille, *J. Am. Chem. Soc.* **1978**, *100*, 3636-3638.
- [6] R. F. Heck, J. P. Nolley, *J. Org. Chem.* **1972**, *37*, 2320-2322.
- [7] K. Sonogashira, Y. Tohda, N. Hagihara, *Tetrahedron Lett.* **1975**, *16*, 4467-4470.
- [8] For further information, see:
https://www.nobelprize.org/nobel_prizes/chemistry/laureates/2010/
- [9] D. Roy, Y. Uozumi, *Adv. Synth. Catal.* **2018**, *360*, 602-625.
- [10] L. Ackermann, *Chem. Rev.* **2011**, *111*, 1315-1345.
- [11] a) Y. Fujiwara, R. Asano, I. Moritani, S. Teranishi, *J. Org. Chem.* **1976**, *41*, 1681-1683; b) Y. Fujiwara, I. Moritani, S. Danno, R. Asano, S. Teranishi, *J. Am. Chem. Soc.* **1969**, *91*, 7166-7169; c) Y. Fujiwara, I. Moritani, M. Matsuda, S. Teranishi, *Tetrahedron Lett.* **1968**, *9*, 633-636; d) I. Moritani, Y. Fujiwara, *Tetrahedron Lett.* **1967**, *8*, 1119-1122.
- [12] a) D. L. Davies, S. A. Macgregor, C. L. McMullin, *Chem. Rev.* **2017**, *117*, 8649-8709; b) D. Balcells, E. Clot, O. Eisenstein, *Chem. Rev.* **2010**, *110*, 749-823.
- [13] D. Lapointe, K. Fagnou, *Chem. Lett.* **2010**, *39*, 1118-1126.
- [14] a) Y. Boutadla, D. L. Davies, S. A. Macgregor, A. I. Poblador-Bahamonde, *Dalton Trans.* **2009**, 5820-5831; b) Y. Boutadla, D. L. Davies, S. A. Macgregor, A. I. Poblador-Bahamonde, *Dalton Trans.* **2009**, 5887-5893.
- [15] a) D. Zell, M. Bursch, V. Müller, S. Grimme, L. Ackermann, *Angew. Chem. Int. Ed.* **2017**, *56*, 10378-10382; b) W. Liu, S. C. Richter, Y. Zhang, L. Ackermann, *Angew. Chem. Int. Ed.* **2016**,

References

- 55, 7747-7750; c) R. Mei, J. Loup, L. Ackermann, *ACS Catal.* **2016**, *6*, 793-797; d) W. Ma, R. Mei, G. Tenti, L. Ackermann, *Chem. Eur. J.* **2014**, *20*, 15248-15251.
- [16] a) D. H. Ess, S. M. Bischof, J. Oxgaard, R. A. Periana, W. Goddard, *Organometallics* **2008**, *27*, 6440-6445; b) J. Oxgaard, W. J. Tenn, R. J. Nielsen, R. A. Periana, W. A. Goddard, *Organometallics* **2007**, *26*, 1565-1567.
- [17] S. R. Neufeldt, M. S. Sanford, *Acc. Chem. Res.* **2012**, *45*, 936-946.
- [18] K. Shen, Y. Fu, J.-N. Li, L. Liu, Q.-X. Guo, *Tetrahedron* **2007**, *63*, 1568-1576.
- [19] a) L. N. Lewis, J. F. Smith, *J. Am. Chem. Soc.* **1986**, *108*, 2728-2735; b) L. N. Lewis, *Inorg. Chem.* **1985**, *24*, 4433-4435.
- [20] G. W. Parshall, W. H. Knoth, R. A. Schunn, *J. Am. Chem. Soc.* **1969**, *91*, 4990-4995.
- [21] a) F. Kakiuchi, T. Sato, T. Tsujimoto, M. Yamauchi, N. Chatani, S. Murai, *Chem. Lett.* **1998**, *27*, 1053-1054; b) S. Murai, F. Kakiuchi, S. Sekine, Y. Tanaka, A. Kamatani, M. Sonoda, N. Chatani, *Nature* **1993**, *366*, 529.
- [22] a) S. De Sarkar, W. Liu, S. I. Kozhushkov, L. Ackermann, *Adv. Synth. Catal.* **2014**, *356*, 1461-1479; b) K. M. Engle, T.-S. Mei, M. Wasa, J.-Q. Yu, *Acc. Chem. Res.* **2012**, *45*, 788-802.
- [23] M. Corbet, F. De Campo, *Angew. Chem. Int. Ed.* **2013**, *52*, 9896-9898.
- [24] a) Q. Gu, H. H. Al Mamari, K. Graczyk, E. Diers, L. Ackermann, *Angew. Chem. Int. Ed.* **2014**, *53*, 3868-3871; b) H. H. Al Mamari, E. Diers, L. Ackermann, *Chem. Eur. J.* **2014**, *20*, 9739-9743.
- [25] M. Zhang, Y. Zhang, X. Jie, H. Zhao, G. Li, W. Su, *Org. Chem. Front.* **2014**, *1*, 843-895.
- [26] G. Cera, T. Haven, L. Ackermann, *Angew. Chem. Int. Ed.* **2016**, *128*, 1506-1510.
- [27] H. A. Chiong, Q.-N. Pham, O. Daugulis, *J. Am. Chem. Soc.* **2007**, *129*, 9879-9884.
- [28] L. Ackermann, J. Pospech, K. Graczyk, K. Rauch, *Org. Lett.* **2012**, *14*, 930-933.
- [29] a) L. Ackermann, R. Vicente, A. Althammer, *Org. Lett.* **2008**, *10*, 2299-2302; b) L. Ackermann, A. Althammer, R. Born, *Angew. Chem. Int. Ed.* **2006**, *45*, 2619-2622; c) L. Ackermann, *Org. Lett.* **2005**, *7*, 3123-3125; d) S. Oi, Y. Ogino, S. Fukita, Y. Inoue, *Org. Lett.* **2002**, *4*, 1783-1785; e) S. Oi, S. Fukita, N. Hirata, N. Watanuki, S. Miyano, Y. Inoue, *Org. Lett.* **2001**, *3*, 2579-2581.
- [30] a) T. Yoshino, S. Matsunaga, *Adv. Organomet. Chem.* **2017**, *68*, 197-247; b) M. Moselage, J. Li, L. Ackermann, *ACS Catalysis* **2016**, *6*, 498-525.
- [31] a) R. Shang, L. Ilies, E. Nakamura, *Chem. Rev.* **2017**, *117*, 9086-9139; b) G. Cera, L. Ackermann, *Top. Curr. Chem.* **2016**, *374*, 1-34.

References

- [32] a) R. Cano, K. Mackey, G. P. McGlacken, *Catal. Sci. Technol.* **2018**, *8*, 1251-1266; b) W. Liu, L. Ackermann, *ACS Catal.* **2016**, *6*, 3743-3752; c) Y. Hu, B. Zhou, C. Wang, *Acc. Chem. Res.* **2018**, *51*, 816-827.
- [33] Precious metal prices for the 06/04/2018 received from: <http://www.infomine.com/investment/>, retrieved on 06/04/2018.
- [34] a) C. Kornhaaß, J. Li, L. Ackermann, *J. Org. Chem.* **2012**, *77*, 9190-9198; b) L. Ackermann, R. Vicente, H. K. Potukuchi, V. Pirovano, *Org. Lett.* **2010**, *12*, 5032-5035.
- [35] P. B. Arockiam, C. Bruneau, P. H. Dixneuf, *Chem. Rev.* **2012**, *112*, 5879-5918.
- [36] a) A. Schischko, H. Ren, N. Kaplaneris, L. Ackermann, *Angew. Chem. Int. Ed.* **2017**, *56*, 1576-1580; b) P. Nareddy, F. Jordan, M. Szostak, *ACS Catal.* **2017**, *7*, 5721-5745; c) R. Mei, C. Zhu, L. Ackermann, *Chem. Commun.* **2016**, *52*, 13171-13174.
- [37] a) L. Ackermann, N. Hofmann, R. Vicente, *Org. Lett.* **2011**, *13*, 1875-1877; b) L. Ackermann, P. Novák, R. Vicente, N. Hofmann, *Angew. Chem. Int. Ed.* **2009**, *48*, 6045-6048.
- [38] R. Mei, S.-K. Zhang, L. Ackermann, *Org. Lett.* **2017**, *19*, 3171-3174.
- [39] a) K. Korvorapun, N. Kaplaneris, T. Rogge, S. Warratz, A. C. Stückl, L. Ackermann, *ACS Catal.* **2018**, *8*, 886-892; b) Z. Ruan, S. K. Zhang, C. Zhu, P. N. Ruth, D. Stalke, L. Ackermann, *Angew. Chem. Int. Ed.* **2017**, *56*, 2045-2049; c) J. Li, K. Korvorapun, S. De Sarkar, T. Rogge, D. J. Burns, S. Warratz, L. Ackermann, *Nat. Commun.* **2017**, *8*, 15430; d) J. Li, S. Warratz, D. Zell, S. De Sarkar, E. E. Ishikawa, L. Ackermann, *J. Am. Chem. Soc.* **2015**, *137*, 13894-13901; e) N. Hofmann, L. Ackermann, *J. Am. Chem. Soc.* **2013**, *135*, 5877-5884.
- [40] a) M. Schinkel, J. Wallbaum, S. I. Kozhushkov, I. Marek, L. Ackermann, *Org. Lett.* **2013**, *15*, 4482-4484; b) M. Schinkel, I. Marek, L. Ackermann, *Angew. Chem. Int. Ed.* **2013**, *52*, 3977-3980.
- [41] a) Q. Bu, T. Rogge, V. Kotek, L. Ackermann, *Angew. Chem. Int. Ed.* **2018**, *57*, 765-768; b) C. Bruneau, P. H. Dixneuf, in *C-H Bond Activation and Catalytic Functionalization I* (Eds.: P. H. Dixneuf, H. Doucet), Springer International Publishing, Cham, **2016**, pp. 137-188; c) S. Nakanowatari, L. Ackermann, *Chem. Eur. J.* **2015**, *21*, 16246-16251; d) S. Warratz, C. Kornhaaß, A. Cajaraville, B. Niepötter, D. Stalke, L. Ackermann, *Angew. Chem. Int. Ed.* **2015**, *54*, 5513-5517; e) S. I. Kozhushkov, L. Ackermann, *Chem. Sci.* **2013**, *4*, 886-896; f) L. Ackermann, A. V. Lygin, N. Hofmann, *Angew. Chem. Int. Ed.* **2011**, *50*, 6379-6382; g) L. Ackermann, J. Pospech, *Org. Lett.* **2011**, *13*, 4153-4155.

References

- [42] a) K. Raghuvanshi, K. Rauch, L. Ackermann, *Chem. Eur. J.* **2015**, *21*, 1790-1794; b) F. Yang, K. Rauch, K. Kettelhoit, L. Ackermann, *Angew. Chem. Int. Ed.* **2014**, *53*, 11285-11288.
- [43] K. Raghuvanshi, D. Zell, L. Ackermann, *Org. Lett.* **2017**, *19*, 1278-1281.
- [44] W. Ma, P. Gandeepan, J. Li, L. Ackermann, *Org. Chem. Front.* **2017**, *4*, 1435-1467.
- [45] M. Miura, T. Tsuda, T. Satoh, S. Pivsa-Art, M. Nomura, *J. Org. Chem.* **1998**, *63*, 5211-5215.
- [46] K. Ueura, T. Satoh, M. Miura, *Org. Lett.* **2007**, *9*, 1407-1409.
- [47] K. Ueura, T. Satoh, M. Miura, *J. Org. Chem.* **2007**, *72*, 5362-5367.
- [48] S. Mochida, K. Hirano, T. Satoh, M. Miura, *J. Org. Chem.* **2009**, *74*, 6295-6298.
- [49] A. Renzetti, H. Nakazawa, C.-J. Li, *RSC Adv.* **2016**, *6*, 40626-40630.
- [50] a) L. Ackermann, R. Vicente, *Org. Lett.* **2009**, *11*, 4922-4925; b) D. E. Bergbreiter, J. Tian, C. Hongfa, *Chem. Rev.* **2009**, *109*, 530-582.
- [51] H. Zhao, T. Zhang, T. Yan, M. Cai, *J. Org. Chem.* **2015**, *80*, 8849-8855.
- [52] Q. Jiang, C. Zhu, H. Zhao, W. Su, *Chem. Asian J.* **2016**, *11*, 356-359.
- [53] a) Y. Qiu, C. Tian, L. Massignan, T. Rogge, L. Ackermann, *Angew. Chem. Int. Ed.* **2018**, *57*, 5818-5822; b) Y. Qiu, W. J. Kong, J. Struwe, N. Sauermann, T. Rogge, A. Scheremetjew, L. Ackermann, *Angew. Chem. Int. Ed.* **2018**, *57*, 5828-5832.
- [54] L. J. Gooßen, N. Rodríguez, K. Gooßen, *Angew. Chem. Int. Ed.* **2008**, *47*, 3100-3120.
- [55] a) N. Rodriguez, L. J. Goossen, *Chem. Soc. Rev.* **2011**, *40*, 5030-5048; b) L. J. Gooßen, G. Deng, I. M. Levy, *Science* **2006**, *313*, 662-664.
- [56] a) M. Font, J. M. Quibell, G. J. P. Perry, I. Larrosa, *Chem. Comm.* **2017**, *53*, 5584-5597; b) M. P. Drapeau, L. J. Gooßen, *Chem. Eur. J.* **2016**, *22*, 18654-18677.
- [57] a) S. Mochida, K. Hirano, T. Satoh, M. Miura, *J. Org. Chem.* **2011**, *76*, 3024-3033; b) A. Maehara, H. Tsurugi, T. Satoh, M. Miura, *Org. Lett.* **2008**, *10*, 1159-1162.
- [58] I. Larrosa, J. Cornella, *Synthesis* **2012**, *44*, 653-676.
- [59] J. Luo, S. Preciado, I. Larrosa, *Chem. Commun.* **2015**, *51*, 3127-3130.
- [60] J. Luo, S. Preciado, I. Larrosa, *J. Am. Chem. Soc.* **2014**, *136*, 4109-4112.
- [61] D. Nandi, Y.-M. Jhou, J.-Y. Lee, B.-C. Kuo, C.-Y. Liu, P.-W. Huang, H. M. Lee, *J. Org. Chem.* **2012**, *77*, 9384-9390.
- [62] X.-Y. Shi, X.-F. Dong, J. Fan, K.-Y. Liu, J.-F. Wei, C.-J. Li, *Sci. China Chem.* **2015**, *58*, 1286-1291.
- [63] S. De Sarkar, L. Ackermann, *Chem. Eur. J.* **2014**, *20*, 13932-13936.

References

- [64] a) J. Atzrodt, V. Derdau, W. J. Kerr, M. Reid, *Angew. Chem. Int. Ed.* **2018**, *57*, 2-29; b) R. Pony Yu, D. Hesk, N. Rivera, I. Pelczer, P. J. Chirik, *Nature* **2016**, *529*, 195-199; c) J. Atzrodt, V. Derdau, T. Fey, J. Zimmermann, *Angew. Chem. Int. Ed.* **2007**, *46*, 7744-7765.
- [65] S. D. Nelson, W. F. Trager, *Drug Metab. Dispos.* **2003**, *31*, 1481-1497.
- [66] O. F. R. A. More, *J. Phys. Org. Chem.* **2010**, *23*, 572-579.
- [67] Based on a graphic created by Olaf Lenz, Rainald62 - created with Xmgrace by Olaf Lenz, manually modified by Rainald62, CC BY-SA 3.0, <https://commons.wikimedia.org/w/index.php?curid=1820269>.
- [68] K. W. Quasdorf, A. D. Hutters, M. W. Lodewyk, D. J. Tantillo, N. K. Garg, *J. Am. Chem. Soc.* **2012**, *134*, 1396-1399.
- [69] R. Voges, J. R. Heys, T. Moenius, in *Preparation of Compounds Labeled with Tritium and Carbon - 14*, Wiley, Chichester, **2009**, pp. 25-45.
- [70] a) J. Atzrodt, V. Derdau, W. J. Kerr, M. Reid, *Angew. Chem. Int. Ed.* **2018**, *57*, 3022-3047; b) W. J. S. Lockley, J. R. Heys, *J. Label. Compd. Rad.* **2010**, *53*, 635-644; c) W. J. S. Lockley, *J. Label. Compd. Rad.* **2007**, *50*, 779-788.
- [71] a) M. B. Skaddan, C. M. Yung, R. G. Bergman, *Org. Lett.* **2004**, *6*, 11-13; b) S. R. Klei, J. T. Golden, T. D. Tilley, R. G. Bergman, *J. Am. Chem. Soc.* **2002**, *124*, 2092-2093; c) S. R. Klei, T. D. Tilley, R. G. Bergman, *Organometallics* **2002**, *21*, 4905-4911; d) J. T. Golden, R. A. Andersen, R. G. Bergman, *J. Am. Chem. Soc.* **2001**, *123*, 5837-5838.
- [72] a) G. N. Nilsson, W. J. Kerr, *J. Label. Compd. Rad.* **2010**, *53*, 662-667; b) R. Crabtree., *Acc. Chem. Res.* **1979**, *12*, 331-337.
- [73] W. Chen, R. A. Mook, R. T. Premont, J. Wang, *Cell. Signal.* **2018**, *41*, 89-96.
- [74] J. Zhou, J. F. Hartwig, *Angew. Chem. Int. Ed.* **2008**, *47*, 5783-5787.
- [75] a) G. Erdogan, D. B. Grotjahn, *Top. Catal.* **2010**, *53*, 1055-1058; b) G. Erdogan, D. B. Grotjahn, *J. Am. Chem. Soc.* **2009**, *131*, 10354-10355.
- [76] a) M. Hatano, T. Nishimura, H. Yorimitsu, *Org. Lett.* **2016**, *18*, 3674-3677; b) S. K. S. Tse, P. Xue, Z. Lin, G. Jia, *Adv. Synth. Catal.* **2010**, *352*, 1512-1522.
- [77] a) A. Di Giuseppe, R. Castarlenas, J. J. Pérez-Torrente, F. J. Lahoz, L. A. Oro, *Chem. Eur. J.* **2014**, *20*, 8391-8403; b) A. Di Giuseppe, R. Castarlenas, J. J. Pérez-Torrente, F. J. Lahoz, V. Polo, L. A. Oro, *Angew. Chem. Int. Ed.* **2011**, *50*, 3938-3942.
- [78] P. T. Anastas, *Green Chem.* **2003**, *5*, G29-G34.

References

- [79] W. Keim, in *Methanol: The Basic Chemical and Energy Feedstock of the Future: Asinger's Vision Today* (Eds.: M. Bertau, H. Offermanns, L. Plass, F. Schmidt, H.-J. Wernicke), Springer Berlin Heidelberg, Berlin, Heidelberg, **2014**, pp. 23-37.
- [80] P. T. W. Anastas, J. C. , *Green Chemistry: Theory and Practice*, Oxford University Press, New York, **1998**.
- [81] B. Chen, Y. Tao, M. Wang, D. Cai, T. Tan, in *Sustainable Production of Bulk Chemicals: Integration of Bio - Chemo - Resources and Processes* (Ed.: M. Xian), Springer Netherlands, Dordrecht, **2015**, pp. 51-68.
- [82] A. Ignaciuk, F. Vöhringer, A. Ruijs, E. C. van Ierland, *Energy Policy* **2006**, *34*, 1127-1138.
- [83] J. ten Dam, U. Hanefeld, *ChemSusChem* **2011**, *4*, 1017-1034.
- [84] T. J. Farmer, M. Mascal, in *Introduction to Chemicals from Biomass*, 2nd ed. (Eds.: J. Clark, F. Dewarte), John Wiley & Sons, Ltd, Chichester, UK, **2015**, pp. 89-155.
- [85] a) V. Isoni, D. Kumbang, P. N. Sharratt, H. Khoo, *J. Environ. Manage.* **2018**, *214*, 267-275; b) D. W. Rackemann, W. O. Doherty, *Biofuels Bioprod. Biorefin.* **2011**, *5*, 198-214; c) J. J. Bozell, L. Moens, D. C. Elliott, Y. Wang, G. G. Neuenschwander, S. W. Fitzpatrick, R. J. Bilski, J. L. Jarnefeld, *Resour. Conserv. Recycl.* **2000**, *28*, 227-239.
- [86] a) A. Osatiashtiani, A. F. Lee, K. Wilson, *J. Chem. Technol. Biot.* **2017**, *92*, 1125-1135; b) J. Yuan, S.-S. Li, L. Yu, Y.-M. Liu, Y. Cao, H.-Y. He, K.-N. Fan, *Energy Environ. Sci.* **2013**, *6*, 3308-3313.
- [87] a) L. Hu, J. Xu, S. Zhou, A. He, X. Tang, L. Lin, J. Xu, Y. Zhao, *ACS Catal.* **2018**, *8*, 2959-2980; b) J. M. R. Gallo, D. M. Alonso, M. A. Mellmer, J. A. Dumesic, *Green Chem.* **2013**, *15*, 85-90.
- [88] X. Tang, X. Zeng, Z. Li, L. Hu, Y. Sun, S. Liu, T. Lei, L. Lin, *Renew. Sust. Energ. Rev.* **2014**, *40*, 608–620.
- [89] D. M. Alonso, S. G. Wettstein, J. A. Dumesic, *Green Chem.* **2013**, *15*, 584-595.
- [90] a) L. Soh, M. J. Eckelman, *ACS Sustain. Chem. Eng.* **2016**, *4*, 5821-5837; b) D. Cespi, E. S. Beach, T. E. Swarr, F. Passarini, I. Vassura, P. J. Dunn, P. T. Anastas, *Green Chem.* **2015**, *17*, 3390-3400; c) C. Jimenez-Gonzalez, C. S. Ponder, Q. B. Broxterman, J. B. Manley, *Org. Process Res. Dev.* **2011**, *15*, 912-917.
- [91] D. Prat, A. Wells, J. Hayler, H. Sneddon, C. R. McElroy, S. Abou-Shehada, P. J. Dunn, *Green Chem.* **2016**, *18*, 288-296.
- [92] C. J. Clarke, W.-C. Tu, O. Levers, A. Bröhl, J. P. Hallett, *Chem. Rev.* **2018**, *118*, 747-800.

References

- [93] a) J. Yamaguchi, K. Amaike, K. Itami, in *Transition Metal - Catalyzed Heterocycle Synthesis via C-H Activation* (Ed.: X. Wu), Wiley-VCH, Weinheim, **2016**, pp. 505-550; b) D. Y.-K. Chen, S. W. Younn, *Chem. Eur. J.* **2012**, *18*, 9452-9474; c) S. K. Sinha, G. Zanoni, D. Maiti, *Asian J. Org. Chem.* **2018**, 10.1002/ajoc.201800203.
- [94] D. Lee, S. Chang, *Chem. Eur. J.* **2015**, *21*, 5364-5368.
- [95] M. E. Baumert, Bachelor thesis, Georg-August-University Goettingen (Goettingen), **2017**.
- [96] a) R. Porta, M. Benaglia, A. Puglisi, *Org. Process Res. Dev.* **2016**, *20*, 2-25; b) C. Wiles, P. Watts, *Green Chem.* **2012**, *14*, 38-54.
- [97] a) L. Malet-Sanz, F. Susanne, *J. Med. Chem.* **2012**, *55*, 4062-4098; b) J. Wegner, S. Ceylan, A. Kirschning, *Chem. Commun.* **2011**, *47*, 4583-4592.
- [98] Based on a graphic created by Vapourtech. Graphic used with permission by Vapourtech. <https://www.vapourtec.com/wp-content/uploads/2015/05/GasReactor-Consumed.png>.
- [99] S. Warratz, Dissertation thesis, Georg-August University Goettingen (Goettingen), **2016**.
- [100] S. Ortgies, R. Rieger, K. Rode, K. Koszinowski, J. Kind, C. M. Thiele, J. Rehbein, A. Breder, *ACS Catal.* **2017**, *7*, 7578-7586.
- [101] a) N. V. Belkova, E. S. Shubina, L. M. Epstein, *Acc. Chem. Res.* **2005**, *38*, 624-631; b) O. A. Filippov, N. V. Belkova, L. M. Epstein, A. Lledos, E. S. Shubina, *Comput. Theor. Chem.* **2012**, *998*, 129-140.
- [102] T. Rogge, L. Ackermann, unpublished results.
- [103] Y. P. K. Nekkanti, Dissertation thesis, Georg-August University Goettingen (Goettingen), **2016**.
- [104] J.-L. Yu, S.-Q. Zhang, X. Hong, *J. Am. Chem. Soc.* **2017**, *139*, 7224-7243.
- [105] N. Y. P. Kumar, T. Rogge, S. R. Yetra, A. Bechtoldt, E. Clot, L. Ackermann, *Chem. Eur. J.* **2017**, *23*, 17449-17453.
- [106] React-IR measurements and DFT calculations were performed by Torben Rogge.
- [107] E. Kossoy, Y. Diskin-Posner, G. Leitus, D. Milstein, *Adv. Synth. Catal.* **2012**, *354*, 497-504.
- [108] a) M. Miesch, B. Ndiaye, C. Hasselmann, E. Marchioni, *Radiat. Phys. Chem.* **1999**, *55*, 337-344; b) B. Ndiaye, G. Jamet, M. Miesch, C. Hasselmann, E. Marchioni, *Radiat. Phys. Chem.* **1999**, *55*, 437-445.
- [109] a) M. Moselage, J. Li, L. Ackermann, *ACS Catal.* **2016**, *6*, 498-525; b) J. J. Topczewski, M. S. Sanford, *Chem. Sci.* **2015**, *6*, 70-76; c) X. Chen, K. M. Englel, D.-H. Wang, J.-Q. Yu, *Angew. Chem. Int. Ed.* **2009**, *48*, 5094-5115; d) D. J. Burns, S. I. Kozhushkov, L. Ackermann, in

- Catalytic Hydroarylation of Carbon - Carbon Multiple Bonds* (Ed.: L. Ackermann), Wiley - VCH Weinheim, **2017**, pp. 49-81; e) L. Ackermann, in *Modern Arylation Methods* (Ed.: L. Ackermann), Wiley-VCH Verlag GmbH & Co. KGaA, Weinheim, **2009**, pp. 1-23.
- [110] A. Bechtoldt, C. Tirlor, K. Raghuvanshi, S. Warratz, C. Kornhaab, L. Ackermann, *Angew. Chem. Int. Ed.* **2016**, *55*, 264-267.
- [111] A. Bechtoldt, M. E. Baumert, L. Vaccaro, L. Ackermann, *Green Chem.* **2018**, *20*, 398-402.
- [112] N. Y. P. Kumar, A. Bechtoldt, K. Raghuvanshi, L. Ackermann, *Angew. Chem. Int. Ed.* **2016**, *55*, 6929-6932.
- [113] L. Krause, R. Herbst-Irmer, G. M. Sheldrick, D. Stalke, *J. Appl. Crystallogr.* **2015**, *48*, 3-10.
- [114] G. Sheldrick, *Acta Crystallogr. A* **2008**, *64*, 112-122.
- [115] G. M. Sheldrick, *Acta Crystallogr. C* **2015**, *71*, 3-8.
- [116] C. B. Hubschle, G. M. Sheldrick, B. Dittrich, *J. Appl. Crystallogr.* **2011**, *44*, 1281-1284.
- [117] O. V. Dolomanov, L. J. Bourhis, R. J. Gildea, J. A. K. Howard, H. Puschmann, *J. Appl. Crystallogr.* **2009**, *42*, 339-341.
- [118] T. Kottke, D. Stalke, *J. Appl. Crystallogr.* **1993**, *26*, 615-619.
- [119] S. V. Luis, P. Ferrer, I. M. Burguete, *J. Org. Chem.* **1990**, *55*, 3808-3812.
- [120] V. S. Pilyugin, Y. E. Sapozhnikov, N. A. Sapozhnikova, *Russ. J. Gen. Chem.* **2004**, *74*, 738-743.
- [121] T. Oberhauser, *J. Org. Chem.* **1997**, *62*, 4504-4506.
- [122] W. A. Nugent, R. J. McKinney, *J. M. Catal.* **1985**, *29*, 65-76.
- [123] S. B. Evans., J. E. Mulvaney, H. K. Hall, *J. Polym. Sci. A Polym. Chem.* **1990**, *28*, 1073-1078.
- [124] N. K. Mishra, P. Jihye, C. Miji, S. Satyasheel, J. Hyeim, J. Taejoo, H. Sangil, K. Saegun, K. I. Su, *Eur. J. Org. Chem.* **2016**, *2016*, 3076-3083.
- [125] S. W. Youn, H. S. Song, J. H. Park, *Org. Biomol. Chem.* **2014**, *12*, 2388-2393.
- [126] L. Chen, H. Li, F. Yu, L. Wang, *Chem. Commun.* **2014**, *50*, 14866-14869.
- [127] W.-J. Han, F. Pu, J. Fan, Z.-W. Liu, X.-Y. Shi, *Adv. Synth. Catal.* **2017**, *359*, 3520-3525.
- [128] HPLC chromatograms were recorded on an Agilent 1290 Infinity using the column CHIRALPAK® ID-3 and hexane/i-PrOH (9:1, 1 mL/min, detection at 274 nm).
- [129] HR-MS (ESI) peaks with an intensity >5% of the base peak were reported. The intensities are uncorrected and overlap with the ¹³C-peak of the less deuterated compound.
- [130] H. Yan, P. Sun, X. Qu, L. Lu, Y. Zhu, H. Yang, J. Mao, *Synth. Commun.* **2013**, *43*, 2773-2783.

References

- [131] B. H. Lipshutz, S. Ghorai, W. W. Y. Leong, B. R. Taft, D. V. Krogstad, *J. Org. Chem.* **2011**, *76*, 5061-5073.
- [132] I. J. Elenkov, D. I. Todorova, V. S. Bankova, T. S. Milkova, *J. Nat. Prod.* **1995**, *58*, 280-283.

Acknowledgements

Einige wenige Zeilen werden dem Umfeld, welches ich in den letzten dreieinhalb Jahren erleben durfte wahrlich nicht gerecht, dennoch möchte ich an dieser Stelle die Gelegenheit nutzen und mich bei den Menschen die mich unterstützt haben persönlich bedanken:

Mein besonderer Dank gilt meinen Mentor und Doktorvater Professor Dr. Lutz Ackermann für die Aufnahme in seinen Arbeitskreis und die exzellenten Möglichkeiten, welche sich mir dort boten. Die Ausstattung, die Internationalität und der wissenschaftliche Output machen diesen Arbeitskreis zu etwas ganz Besonderem.

Bei Professor Dr. Konrad Koszinowski möchte ich mich für die interessanten und anregenden Evaluierungsgespräche, sein Engagement während unserer persönlichen Kooperation, sowie für sämtliche weitere Unterstützung bedanken.

Vielen Dank auch den Mitgliedern meiner Prüfungskommission, Prof. Dr. Dietmar Stalke, Prof. Dr. Manuel Alcarazo, Dr. Max Hansmann und Dr. Franziska Thomas.

Für die Vermessung meiner Kristalle möchte ich Frau Helena Keil, sowie Herrn Dr. Christopher Golz recht herzlich danken. Den analytischen Abteilungen des Instituts unter Leitung von Herrn Dr. Holm Frauendorf und Herrn Dr. Michael John gilt mein Dank für das schnelle und gewissenhafte Analysieren meiner Proben und kompetenten Ratschlägen bei Fragestellungen und Problemen jeglicher Art.

Für das gewissenhafte Korrekturlesen dieser Arbeit bedanke ich mich bei Isaac Choi, Korkit Korvorapun, Joachim Loup, Dr. Lars Finger, Leonardo Massignan, Nicolas Sauermann, Ralf Steinbock, Ruhuai Mei, Torben Rogge und Thomas Müller.

Dem gesamten Arbeitskreis danke ich sowohl für fachliche Anregungen und Hilfestellungen, als auch die vielen schönen Teambuildingfahrten, Kanuabenteuer, (manchmal ausufernden) Feiern und Fußballturniere, auch wenn uns der ChemCup-Stern auf der Doktorarbeit verwehrt blieb.

Acknowledgements

Mein besonderer Dank geht an Alexandra, Thomas, Marc, Darko, Alan, Torben und Daniel (our most beautiful Friend) für die vielen schönen Grillfeiern, Partyabende, Unternehmungen und generell dafür das ihr in den letzten dreieinhalb Jahren mein Leben bereichert habt!

Mein Dank geht auch an Marcel für sein großes fachliches als auch soziales Engagement, während und nach seiner Bachelorarbeit.

Bedanken möchte ich mich auch bei meinem Mentor Herrn Dr. Thomas Perkovic für die offenen Gespräche, die mich persönlich sehr viel weitergebracht haben. Mein Dank gilt auch Frau Dr. Vera Bissinger für die Leitung des KaWirMento-Programmes und dafür das Sie mich als Teilnehmer ausgewählt hat. Auch Carla, Jia-Pei, Hannah, Julia, Luisa, Heide, Jana, Armin, Martin und Georg möchte ich meinen Dank für das letzte Jahr aussprechen.

Das größte Dankeschön gebührt jedoch meiner Familie, die mich immer und bei allem unterstützt und mir immer den Rücken freigehalten haben. Euer Rückhalt, eure Ratschläge und eure generell Unterstützung hat all das erst möglich gemacht!

Göttingen, Juni 2018

Alexander Bechtoldt

Curriculum Vitae

Personal Information

Name: Alexander Bechtoldt
Date of Birth: October 18th, 1987
Place of Birth: Frankfurt am Main, Germany
Gender: Male
Nationality: German

Academic Education

01.2015–Present **PhD Candidate in Organic Chemistry**
Institut für Organische und Biomolekulare Chemie,
Georg-August-Universität Göttingen
Supervisor: Prof. Dr. Lutz Ackermann
Thesis: Aerobic Ruthenium-Catalyzed C–H Functionalizations

12.2012–09.2014 **M. Sc. in Chemistry**
Johann Wolfgang von Goethe-Universität, Frankfurt am Main
Final Grade: 1.3
Master Thesis (Supervisor Prof. Dr. Matthias Wagner):
Additionsreaktionen von Element-Wasserstoff-Verbindungen an ungesättigte Kohlenwasserstoffe.

Curriculum Vitae

10.2009–12.2012

B.Sc. in Chemistry

Johann Wolfgang von Goethe-Universität, Frankfurt am Main

Supervisor: Prof. Dr. Matthias Wagner

Final Grade: 1.7

Bachelor Thesis (Supervisor Prof. Dr. Matthias Wagner): *Synthese
neuartiger Dipyrazol-Derivate.*

School Education

01.2015–06.2008

Eichendorffschule mit Gymnasialer Oberstufe Immanuel Kant, Kelkheim
(Ts.)

02.1998–07.1998

Pestalozzi-Schule, Kelkheim (Ts.)

08.1995–02.1998

Adolf-Reichwein-Schule, Frankfurt-Zeilsheim

Teaching Experience

04.2018–07.2018

Assistant of the practical course: „Organisch Chemische
Grundpraktikum“

01.2018–03.2018

Supervision of the “MEMO-Internship” of Leonard Hartung

10.2017–02.2018

Assistant of the practical course: “Angewandte Organische Synthese”

04.2017–07.2017

Assistant of the practical course: „Organisch Chemische
Grundpraktikum“

11.2016–03.2017

Supervision of the bachelor thesis of Marcel Emir Baumert

Curriculum Vitae

- 10.2017–02.2018 Assistant of the practical course: “Organisch Chemisches Fortgeschrittenenpraktikum”
- 04.2016–07.2016 Assistant of the practical course: „Organisch Chemische Grundpraktikum“
- 10.2015–01.2016 Assistant of the practical course: „Chemie für Mediziner“
- 07.2015–08.2015 Assistant of the practical course: “Catalysis”
- 04.2015–07.2015 Lecture assistant of the course: “Experimentalchemie II: Organische Chemie”

Publications

- 6) F. Ferlin, L. Luciani, S. Santoro, A. Marrocchi, D. Lanari, A. Bechtoldt, L. Ackermann, L. Vaccaro, "A continuous flow approach for the C–H functionalization of 1,2,3-triazoles in γ -valerolactone as biomass-derived medium" *Green Chem.* **2018**, 20, 2888-2893.
- 5) A. Bechtoldt, M. E. Baumert, L. Vaccaro, L. Ackermann, "Ruthenium(II) oxidase catalysis for C–H alkenylations in biomass-derived γ -valerolactone" *Green Chem.* **2018**, 20, 398-402
- 4) N. Y. P. Kumar, T. Rogge, S. R. Yetra, A. Bechtoldt, E. Clot, L. Ackermann, "Mild Decarboxylative C–H Alkylation: Computational Insights for Solvent-Robust Ruthenium(II) Domino Manifold" *Chem. Eur. J.* **2017**, 23, 17449-17453.
- 3) N. Y. P. Kumar, A. Bechtoldt, K. Raghuvanshi, L. Ackermann, "Ruthenium(II)-Catalyzed Decarboxylative C–H Activation: Versatile Routes to meta-Alkenylated Arenes" *Angew. Chem. Int. Ed.* **2016**, 55, 6929-6932.

2) A. Bechtoldt, C. Tirlor, K. Raghuvanshi, S. Warratz, C. Kornhaaß, L. Ackermann, "Ruthenium Oxidase Catalysis for Site-Selective C–H Alkenylations with Ambient O₂ as the Sole Oxidant" *Angew. Chem. Int. Ed.* **2016**, *55*, 264-267.

1) A. Bechtoldt, H-W. Lerner, M Bolte, "The first example of a two-coordinated Au(I) atom bonded to an Fe(II) atom and an N-heterocyclic carbene (NHC) ligand", *Acta Cryst.*, **2015**, *C71*, 448-451.

Conferences

- | | |
|---------|---|
| 11.2017 | National Organic Symposium Trust for Research Scholars (J-NOST),
Varanasi (India)
Invited Oral Presentation |
| 09.2017 | ICASEC Summer School, Göttingen (Germany)
Poster Presentation |
| 09.2017 | Wissenschaftsforum 2017, Berlin (Germany)
Poster Presentation |
| 06.2017 | 20 th European Symposium on Organic Chemistry (ESOC), Cologne
(Germany)
Poster Presentation |
| 06.2016 | 8. Göttinger Chemieforum, Göttingen (Germany)
Poster Presentation |

Erklärung

Hiermit erkläre ich, dass die vorliegende Dissertation in dem Zeitraum

von Februar 2015 bis Juli 2018

am Institut für Organische und Biomolekulare Chemie der Georg-August-Universität

unter Anleitung von **Herrn Prof. Dr. Lutz Ackermann**

selbstständig durchgeführt und keine anderen als die angegebenen Hilfsmittel und Quellen verwendet habe.

Göttingen, den 09.07.2018

Alexander Bechtoldt